

**PHYSICOCHEMICAL AND CONDUCTOMETRIC STUDIES OF
SOME TRIAZOLIUM AND PYRROLIDINIUM BASED IONIC
LIQUIDS IN BINARY AQUEOUS AMINE FOR ENERGY
STORAGE APPLICATIONS**

Thesis Submitted for the Award of the Degree of

DOCTOR OF PHILOSOPHY

In

Chemistry

By

Nidhi

Registration Number: 11916781

Supervised By

Dr. Praveen Kumar Sharma (14155)

Department of Chemistry (Professor)

Lovely Professional University, Punjab

Co-Supervised By

Dr. Ramesh Chand Thakur

Department of Chemistry (Associate Professor)

Himachal Pradesh University, Shimla

Dr. Ashish Kumar

Department of Chemistry

(Professor)

NCE, Bihar Engineering University,

DSTTE, Government of Bihar,

Patna



**L OVELY
P ROFESSIONAL
U NIVERSITY**

Transforming Education Transforming India

LOVELY PROFESSIONAL UNIVERSITY, PUNJAB

2025

DECLARATION

I hereby declare that the presented work in the thesis entitled “**Physicochemical and Conductometric Studies of some Triazolium and Pyrrolidinium based Ionic liquids in binary aqueous amine for energy storage application**” In fulfilment of degree of Doctor of Philosophy (Ph.D.) is outcome of research work carried out by me under the supervision of my supervisor Dr. Praveen Kumar Sharma, Professor, Department of Chemistry, Lovely Professional University, Phagwara, Punjab and co-supervisor Dr. Ramesh Chand Thakur, Associate Professor, Department of Chemistry, Himachal Pradesh University, Summer Hill Shimla and Dr. Ashish Kumar, Professor, NCE, Department of Science and Technology, Government of Bihar, Patna.

In keeping with the general practice of reporting scientific observations, due acknowledgements have been made whenever work described here has been based on findings another investigator. According to the requirements for the Doctor of Philosophy (Ph.D.) in Chemistry degree, my dissertation is a complete and authentic account of my own research work, with all sources properly cited. This work has not been submitted in part or full to any other University or Institute for the award of any degree.

Nidhi

Reg. No- 11916781

Department of Chemistry,
Lovely Professional University,
Phagwara, Punjab, India.

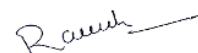
CERTIFICATE

This is to certify that the work reported in the Ph. D. thesis entitled “**Physicochemical and Conductometric Studies of some Triazolium and Pyrrolidinium based Ionic liquids in binary aqueous amine for energy storage applications**” submitted in fulfillment of the requirement for the award of degree of **Doctor of Philosophy (Ph.D.)** in the **Chemistry**, is a research work carried out by **Nidhi (11916781)**, is bonafide record of his/her original work carried out under my supervision and that no part of thesis has been submitted for any other degree, diploma or equivalent course.

Dr. Praveen Kumar Sharma
Professor,
Department of Chemistry,
Lovely Professional University,
Phagwara, Punjab,
India



Dr. Ashish Kumar
Professor,
Department of Science and Technology,
NCE, Bihar Engineering University
Government of Bihar, Patna
India
Date: 16/05/2024



Dr. Ramesh Chand Thakur
Associate Professor,
Department of Chemistry,
Himachal Pradesh University,
Summer Hill Shimla,
India

ABSTRACT

Efficient energy storage solutions are essential for the widespread implementation of renewable energy technologies. Ionic liquids (ILs) are being considered as very promising options for energy storage applications because of their distinctive physicochemical features and capacity to be customized for specific purposes. The main objective of this research is to investigate the physicochemical and conductometric characteristics of these systems consisting of ionic liquids and amine. The density, sound velocity and electrical conductivity of the binary solutions were measured and evaluated to obtain a deeper understanding of the interactions between the ionic liquids and the aqueous amine solvents. Conductometric investigations were conducted to comprehend the ion transport characteristics and the overall efficiency of these systems for energy storage purposes. The research results contribute to the advancement of energy storage systems by utilizing ionic liquids in conjunction with aqueous amine solvents. Comprehending the physicochemical features and ion transport pathways in these systems can assist in the development and enhancement of sophisticated energy storage devices, like supercapacitors and batteries. The information and analysis produced from this research can be used to further investigate the capabilities of ionic liquid-amine systems for other energy-related uses. The main goal is to acquire a more profound comprehension of the interactions between these ionic liquids and amine solvents, and to evaluate their potential for applications in energy storage. To accomplish this, we will be examining a range of physicochemical characteristics, including density, conductivity. These features will offer significant observations regarding the behavior and effectiveness of the ionic liquid-amine systems. Through the analysis of density, we may ascertain the arrangement of molecules and the interactions that occur between them in the solution. Conductivity investigations will enable us to assess the ion transportation and overall effectiveness of the systems. The primary goal of the research program is to investigate and implement the role that thermodynamic, acoustic, spectroscopic and conductometric investigation may play in determining the nature and comparative extent of molecular interactions, aggregation in ionic liquids, and their sensitivity to variations in concentration, temperature, and molecular structure.

The aims and objectives of the present investigations are:

1. Determination of density and sound velocity of some Triazolium and Pyrrolidinium based ionic liquids binary aqueous amine (Trihexylamine, Tributylamine, Benzylamine, Dibenzylamine) at different temperatures and concentrations.
2. Estimation of Partial molar volumes, Partial molar adiabatic compressibility of some Triazolium and Pyrrolidinium based ionic liquids in binary aqueous amine (Trihexylamine, Tributylamine, Benzylamine, Dibenzylamine) at different temperatures and concentrations.
3. Estimation of various conductance parameters to analyze various molecular interactions in the selected ternary systems.
4. Interpretation of various obtained parameters by using some spectroscopic and cyclic voltammetry techniques.

To illustrate the intermolecular interactions existing between Triazolium- and Pyrrolidinium- based ionic liquids and aqueous amine, different parameters were acquired using the following techniques:

- Density measurements
- Sound velocity measurements
- Conductivity measurements
- Cyclic Voltammetry measurements
- Spectroscopic measurements.

For the sake of clarity and convenience in presentation, the thesis is divided into six chapters as mentioned below:

Chapter 1: Introduction

In first chapter Ionic liquids and amines are introduced in detail. It offers an introduction to ionic liquids, as well as information about their classification, history, and uses in many industries. This chapter also includes a comprehensive explanation of the composition, categorization, and use of additives (aqueous amine). It includes an overview of FT-IR spectroscopy, conductance, thermodynamics, and cyclic voltammetry.

Chapter 2: Literature Review

This chapter presents a thorough review of the literature on the volumetric, acoustic, conductometric and spectroscopic studies of amines with various types of ionic liquids and other solvents, as well as the research of ionic liquids with various additions.

Chapter 3: Experimental

The specifics of the chemicals used to conduct the experimental study are described in this chapter. Synthesis of the ionic liquids (1-butyl-1-methyl pyrrolidinium and 1-ethyl-3-methylimidazolium iodide) that were utilized in the study is discussed along with the determination of their structural makeup using various spectroscopic methods. There has also been a quick summary of the amines employed in the study. The specifics of the tools utilized, including the conductivity meter, FT-IR spectrophotometer, and electrochemical workstation and Anton Paar DSA 5000 M have been covered in this chapter.

Chapter 4: Thermodynamic, conductometric and cyclic voltametric parameters

The framework of various parameters estimated for ionic liquids in aqueous amine is included in this chapter. Various thermodynamic properties of solutions like apparent molar volume (V_ϕ), limiting apparent molar volume (V_ϕ^0), standard partial molar volumes of transfer (ΔV_ϕ^0) of the ternary mixtures, apparent molar isentropic compression ($K_{\phi,s}$), limiting apparent molar adiabatic compressibility ($K_{\phi,s}^0$) and partial molar isentropic compression of transfer ($\Delta K_{\phi,s}^0$) have been discussed in this chapter along with their working equations.

Chapter 5: Result and discussion

This chapter includes the findings and discussion of the entire field of research. Four additional sections, numbered I to IV, make up this chapter.

In **Section I (Part A)** volumetric and acoustic studies for 1,4-dimethyl-4H-1,2,4-triazolium iodide in (0.01, 0.03 and 0.05) mol.kg⁻¹ of aqueous benzylamine and benzamide at T= (288.15 to 318.15) K are carried out to predict the interactions present in the ternary mixtures under study. Interaction coefficients are determined using McMillan–Mayer theory. Pair and triplet interaction coefficients are determined using the transfer volumes (ΔV_ϕ^0) values. Hepler constant is employed to predict the structure making/breaking behavior of solute.

Section I (Part B), density and sound velocity values of 1-butyl-1-methyl pyrrolidinium iodide in (0.01, 0.03 and 0.05) mol kg⁻¹ of aqueous benzylamine and benzamide at different working temperatures are obtained. The thermophysical parameters like partial molar volume, apparent molar volume, apparent molar isentropic compression, standard partial molar volume of transfer, and partial molar isentropic compression and isentropic compression of transfer are determined at various concentration and equidistant temperatures.

In **Section I (Part C)** volumetric and acoustic studies for 1-butyl-1-methyl pyrrolidinium tetrafluoroborate in (0.01, 0.03 and 0.05) mol.kg⁻¹ of aqueous benzylamine at equidistant temperature are carried out to predict the interactions present in the ternary mixtures under study. Thereafter, thermodynamic parameters for ternary system have been calculated from density and speed of sound values. For the prediction of structure maker or breaker behavior of solute, Hepler constant is used. The interaction coefficients have also been determined using the transfer volumes.

Section II (Part A) deals with conductometric studies 1-butyl-1-methyl pyrrolidinium tetrafluoroborate in aqueous benzylamine at various concentrations at (288.15, 298.15, 308.15 and, 318.15) K. Onsager equation is used to determine the limiting molar conductivities.

In **Section II (Part B)** the values of specific conductivity (κ) for aqueous benzylamine and benzamide in 1, 4-Dimethyl-4H-1, 2, 4-triazolium iodide are determined at (288.15, 298.15, 308.15 and, 318.15) K. Further, from specific conductivity, molar conductivities are calculated and limiting molar conductivities are in turn determined employing Onsager equation. Specific conductivity, molar conductance and Limiting molar conductance were also calculated using the experimental data.

In **Section II (Part C)** Conductometric studies of aqueous benzylamine and benzamide in 1-butyl-1-methyl pyrrolidinium iodide has been discussed at four equidistant temperatures (288.15 to 318.15 K).

In Section III (Part A) FT-IR spectroscopy for 1,4-dimethyl-4H-1,2,4-triazolium iodide in aqueous benzylamine and benzamide has been discussed. The theoretical and experimental results predict the nature of interactions present in ternary systems and effect of temperature on the structure is also analyzed on the measured parameters.

Section III (Part B) deals with the FT-IR data for aqueous benzylamine and benzamide in 1-butyl-1-methyl pyrrolidinium iodide has been discussed. The spectra obtained describes the change in wave number of the investigated ternary system which further helps in the elucidation of the different structural changes. Also, this data is used for the validation of the results obtained using the thermodynamic parameters.

Section IV (Part A) deals with the cyclic voltammetry studies of aqueous benzylamine and benzamide in the presence of 1-butyl-1-methyl pyrrolidinium iodide. The cyclic voltammograms of the ternary mixture as a function of concentration at temperature has been explained in this chapter.

Chapter 5: Summary and conclusion

The major conclusions, comparative analysis, and volumetric, acoustic, conductometric, spectroscopic and cyclic voltametric analyses of ILs in aqueous amine are included in this chapter. In this chapter, results derived from various thermodynamical properties are discussed. This chapter also contains information about the current thesis work's future prospectus.

ACKNOWLEDGEMENT

I would love to express my sincere gratitude to everyone who has supported and encouraged me throughout my research journey.

First and foremost, I would like to express my deep gratitude to Almighty God for His divine guidance and blessings throughout this thesis journey. I am grateful for the wisdom, clarity, and understanding that He has bestowed upon me, enabling me to navigate the challenges and complexities of my research. I acknowledge that without His grace and blessings, this achievement would not have been possible.

Firstly, I am profoundly grateful to my supervisor **Dr. Ramesh Chand Thakur**, for the vast amount of time and effort he has invested in my research. His immense knowledge, relentless pursuit of academic excellence and unwavering faith in me have been instrumental in shaping his work.

I want to convey my sincere appreciation to **Dr. Ashish Kumar**, whose expertise, understanding and patience, added considerably to my doctoral experience. Also, I am thankful to my current supervisor **Dr. Praveen Kumar Sharma** for his invaluable guidance, patience, and support throughout my research journey.

I owe a lot of gratitude to **Dr. Vishal Sharma**, who despite having a busy schedule, always took the time to carefully listen to my issues and offer helpful advice. I would also like to thank **Mr. Manoj** for providing the necessary laboratory facilities and chemicals throughout my doctoral degree. Also, I am thankful to **Dr. Rakesh Kumar Bhardwaj**, Principle, B.L.J.S College Tosham for his valuable insight and steadfast encouragement throughout my whole research journey. His passionate spirit and support have paved a path for me in the research field.

I am also grateful to my colleagues and my friends Dr. Harpreet Kaur, Nancy George, Kajal Verma and Diksha in university for their intellectual companionship, camaraderie, and the academic experiences we shared. I am deeply thankful to Chitra Sharma and Jay for the vast amount of time and effort they have invested in my research. Whether it was late-night study sessions or moments of doubt, they were always there to provide a listening ear and offer words of encouragement. Their positivity, sense of humor, and unwavering support have made this journey more enjoyable and memorable. Their affinity has made this

journey enjoyable and fulfilling. They have been a source of laughter in times of stress, a source of inspiration in times of doubt, and a source of comfort in times of difficulty. Their friendship is a gift I will always cherish. I sincerely thank **Shrutila Sharma** and **Ankita** from DAV College, Chandigarh for their help, cooperation, and guidance in difficult time whether it is professional or personal.

Lastly, I would like to express love and gratitude to my family throughout this thesis journey, especially my father **Mr. Jaswant Singh** for his constant encouragement, relentless patience, and immense belief in me. My father's wisdom, encouragement, and continuous motivation have been invaluable in keeping me focused and determined. His belief in my potential has been a driving force behind my accomplishments. I am deeply thankful to my mother, **Mrs. Shakuntala** whose unwavering support and guidance have been my pillar of strength in this journey. Her unconditional love, guidance, and belief in my abilities have been a constant source of inspiration. Her unwavering support and sacrifices have played a significant role in shaping my academic pursuits. I am also grateful to my brother, **Navdeep** for his constant support, understanding, and encouragement. His enthusiasm and belief in my abilities have been a source of strength throughout this journey. I am truly blessed to have such a loving and supportive family, and I am forever grateful for their presence in my life. This work is an embrace of the strength and inspiration he has imbued me with, and for that, I am eternally grateful. Their belief in my abilities and aspirations has been a driving force. Their love, encouragement, and understanding have been instrumental in helping me navigate the challenges and stay motivated. I am truly grateful for their sacrifices, patience, and belief in my abilities. I dedicate this thesis to my loving family.

Nidhi

Reg. No- 11916781

Department of Chemistry,
Lovely Professional University,
Phagwara, Punjab, India.

TABLE OF CONTENTS

CHAPTER 1. INTRODUCTION		
1	Introduction	2
1.1	Solution Chemistry	2
1.2	Introduction to Ionic Liquids (ILs)	3
1.2.1	Composition of ILs	3
1.2.2	Classification of ILs	4
1.2.2.1	Imidazolium Based-ILs	5
1.2.2.2	Pyrrolidinium based-ILs	6
1.2.2.3	Triazolium based-ILs	7
1.2.2.4	Phosphonium based- ILs	8
1.2.2.5	Ammonium based-ILs	8
1.3	Properties of Ionic liquids	9
1.3.1	Density	9
1.3.2	Viscosity	10
1.3.3	Vapour Pressure	10
1.3.4	Melting Point	11
1.3.5	Ionic Conductivity	11
1.3.6	Electrochemical Properties	11
1.3.7	Thermal Stability	12
1.3.8	Toxicity	12
1.3.9	Biodegradability	12
1.3.10	Solubility	13
1.3.11	Scalability	13
1.4	Applications of Ionic Liquids	13
1.5	Introduction to Amines	16
1.5.1	Primary amines	16
1.5.2	Secondary amines	17
1.5.3	Tertiary amines	17
1.5.4	Quaternary amines	17

1.6	Application of Amines	18
1.7	Energy Storage Devices (ESDs)	19
1.7.1	Fundamentals of Energy Storage	20
1.7.1.1	Electrical energy storage technology	20
1.7.1.2	Mechanical energy storage technology	20
1.7.1.3	Thermal energy storage technology	21
1.7.1.4	Chemical energy storage technology	21
1.7.1.5	Electrochemical energy storage technology	21
1.8	Energy storage with Ionic Liquids	21
1.8.1	Ionic liquid in ESDs	24
1.9	Energy storage with Amines	25
1.9.1	Amines in Energy Storage Devices	26
1.10	Composition of potential Electrolyte	27
1.10.1	Thermodynamic properties	27
1.10.2	Acoustical properties	27
1.10.3	Conductance studies	27
1.10.4	FT-IR spectral studies	28
1.10.5	Cyclic Voltammetry	28
CHAPTER 2. LITERATURE SURVEY		
2.1	Literature review	31
2.1.1	Physicochemical properties of ILs	31
2.1.2	Classification and applications of ILs	42
2.1.3	ILs in Energy storage devices	46
2.1.4	Amines in Energy storage devices	56
CHAPTER 3. EXPERIMENTAL		
3.1	Materials	60
3.2	Synthesis of Ionic Liquids	62
3.2.1	Synthesis of Pyrrolidinium based ionic liquid	62

3.2.1.1	Synthesis of 1-butyl-1-methyl pyrrolidinium iodide ([BMPyr ⁺] [I ⁻])	62
3.2.2	Synthesis of imidazolium based ionic liquids	65
3.2.2.1	Synthesis of 1-ethyl-3-methylimidazolium iodide	65
3.3	Purification of synthesized Ionic liquids and other chemicals	68
3.4	Brief overview of chemicals used in study	69
3.4.1	1,4-dimethyl-4H-1,2,4-triazolium iodide [DMTI]	69
3.4.2	1-butyl-1-methyl pyrrolidinium iodide [BMPyr ⁺] [I ⁻]	69
3.4.3	1-butyl-1-methyl pyrrolidinium tetrafluoroborate [BMPyr ⁺] [BF ₄ ⁻]	69
3.4.4	1-ethyl-3-methyl imidazolium iodide [Emim ⁺][I ⁻]	70
3.4.5	Benzylamine	70
3.4.6	Benzamide	70
3.5	Experimental Techniques	71
3.5.1	Density and sound velocity measurements	71
3.5.2	Conductivity measurements	72
3.5.3	FT-IR Spectroscopic studies	73
3.5.4	Cyclic Voltametric studies	74
CHAPTER 4. THERMODYNAMIC, CONDUCTOMETRIC AND CYCLIC VOLTAMMETRIC PARAMETERS		
4.1	Thermodynamics of Solutions	77
4.1.1	Parameters derived from density measurements	77
4.1.1.1	Apparent molar volume	77
4.1.1.2	Apparent molar volume at infinite dilution	79
4.1.1.3	Partial molar volume of transfer	80
4.1.1.4	Effect of Temperature on partial molar volume	80
4.1.2	Parameters derived from sound velocity measurements	81
4.1.2.1	Apparent molar isentropic compression	81
4.1.2.2	Partial molar isentropic compression	82
4.1.2.3	Partial molar isentropic compression of transfer	82
4.1.2.4	Pair and triplet interaction coefficients	82

4.2	Transport properties	83
4.2.1	Conductance studies	83
4.2.2.1	Specific Conductance	83
4.2.2.2	Molar Conductance	83
4.2.2.3	Limiting Molar Conductance	84
4.2.2.4	Effect of Temperature	84
4.3	Cyclic voltametric Properties	84
4.3.1	Cyclic Voltammetry	84
CHAPTER 5. RESULTS AND DISCUSSION		
SECTION-I		
(1,4-dimethyl-4H-1,2,4-triazolium iodide + benzylamine/benzamide)		
	Density measurements	88
	Apparent molar volume (V_ϕ)	88
	Partial molar volume (PMV)	88
	Partial molar volume of transfer	89
	Effect of Temperature on partial molar volume	90
	Sound velocity measurements	90
	Apparent molar isentropic compression	91
	Partial molar isentropic compression	91
	Pair triplet interaction coefficient	92
	Conductance Measurements	92
	FT-IR Studies	93
SECTION-II		
(1-butyl-1-methyl pyrrolidinium iodide + benzylamine/benzamide)		
	Density measurements	119
	Apparent molar volume (V_ϕ)	119
	Partial molar volume (PMV)	120
	Partial molar volume of transfer	120
	Effect of Temperature on partial molar volume	121

Sound velocity measurements	122
Apparent molar isentropic compression	122
Partial molar isentropic compression	123
Pair triplet interaction coefficient	123
Conductance Studies	124
FT-IR Spectroscopy	125
Cyclic Voltammetry	126
<p style="text-align: center;">SECTION-III (1-butyl-1-methyl pyrrolidinium tetrafluoroborate + benzylamine)</p>	
Density & Sound velocity data	155
Apparent molar volume and apparent molar isentropic compression	155
Partial molar volume and partial molar isentropic compression	156
Partial molar volume of transfer and partial molar isentropic compression of transfer	156
Dependence of partial molar volume on temperature	157
Pair and triplet interaction coefficients	158
Conductance Studies	158
<p style="text-align: center;">CHAPTER 6. SUMMARY AND CONCLUSION</p>	
Summary and Conclusion	178
Significance and Future scope of work	184
References	186
List of Publications	212
List of Conferences/Webinars/ Short term Courses attended	213

LIST OF FIGURES

CHAPTER 1. INTRODUCTION		
Figure 1.1	Commonly used cations and anions in ionic liquids	4
Figure 1.2	General structure of imidazolium cation.	6
Figure 1.3	General structure of Pyrrolidinium cation.	6
Figure 1.4	General structure of Triazolium cation.	7
Figure 1.5	General structure of Phosphonium cation.	8
Figure 1.6	General structure of Ammonium cation	9
Figure 1.7	General structure of Primary Amine	17
Figure 1.8	General structure of Secondary Amine	17
Figure 1.9	General structure of Tertiary Amine	17
Figure 1.10	General structure of Quaternary Amine	18
CHAPTER 3. EXPERIMENTAL		
Figure 3.1	¹ H-NMR spectrum for synthesized ionic liquid 1-butyl-1-methyl pyrrolidinium iodide [BMPyr ⁺] [I ⁻].	63
Figure 3.2	¹³ C-NMR spectrum for synthesized ionic liquid 1-butyl-1-methyl pyrrolidinium iodide [BMPyr ⁺] [I ⁻].	63
Figure 3.3	FT-IR spectrum of synthesized ionic liquid 1-butyl-1-methyl pyrrolidinium iodide.	64
Figure 3.4	¹ H-NMR spectrum for synthesized ionic liquid 1-ethyl-3-methylimidazolium iodide [EMIM ⁺] [I ⁻].	66
Figure 3.5	¹³ C- NMR spectrum for synthesized ionic liquid 1-ethyl-3-methylimidazolium iodide [EMIM ⁺] [I ⁻].	67
Figure 3.6	FT-IR spectrum for synthesized ionic liquid 1-ethyl-3-methylimidazolium iodide [EMIM ⁺] [I ⁻].	68
Figure 3.7	Structure of 1, 4-dimethyl-4H-1, 2, 4-triazolium iodide.	69
Figure 3.8	Structure of 1-butyl-1-methyl pyrrolidinium iodide.	69
Figure 3.9	Structure of 1-butyl-1-methyl pyrrolidinium tetrafluoroborate.	70
Figure 3.10	Structure of 1-ethyl-3-methyl imidazolium iodide.	70
Figure 3.11	Structure of Benzylamine.	70

Figure 3.12	Structure of Benzamide.	71
Figure 3.13	Anton Paar DSA 500M	72
Figure 3.14	Electrical Conductivity meter	73
Figure 3.15	Shimadzu FT-IR-8400S Spectrophotometer	74
Figure 3.16	Metrohm Auto lab PGSTAT204 multi-channel Potentiostat/galvanostat electrochemical workstation.	75
<p style="text-align: center;">5. RESULTS AND DISCUSSION</p> <p style="text-align: center;">SECTION-I</p>		
Figure 5.1	Plots of variation of apparent molar volume (V_ϕ) of 1,4-Dimethyl-4H-1,2,4 triazolium iodide in (a) 0.01 mol.kg ⁻¹ and (b) 0.05 mol.kg ⁻¹ of aqueous solutions of benzamide; (c) 0.01 mol.kg ⁻¹ and (d) 0.05 mol.kg ⁻¹ of aqueous solutions of benzylamine at T = (288.15, 298.15, 308.15 and 318.15) K	112
Figure 5.2	Plot of variation of partial molar volume (V_ϕ^0) of 1,4-Dimethyl-4H-1,2,4 triazolium iodide in various concentrations m = (0.01, 0.03 and 0.05) mol.kg ⁻¹ of benzamide (Red); benzylamine (Blue) at 288.15 K (■), 298.15 K (●), 308.15 K (▲) and 318.15 K (▼)	113
Figure 5.3	Plot of variation of apparent molar isentropic compression ($K_{\phi,s}$) of 1,4-Dimethyl-4H-1,2,4 triazolium iodide in (a) 0.01 mol.kg ⁻¹ (b) 0.05 mol.kg ⁻¹ aqueous solutions of benzamide (Red); benzylamine (Blue) at T = (288.15, 298.15, 308.15 and 318.15) K	114
Figure 5.4	Plots showing the variation of Λ_o with \sqrt{C} for 1,4-Dimethyl-4H-1,2,4-triazolium iodide in 0.01 mol.kg ⁻¹ aqueous benzylamine at T = (298.15, 303.15, 308.15 and 313.15) K.	115
Figure 5.5	Plots showing the variation of Λ_o with \sqrt{C} for 1,4-Dimethyl-4H-1,2,4-triazolium iodide in 0.05 mol.kg ⁻¹ aqueous benzylamine at T = (298.15, 303.15, 308.15 and 313.15) K.	116

Figure 5.6	Plots of FT-IR spectra for [DMTI] iodide in (0.01 to 0.05) mol.kg ⁻¹ of aqueous benzamide.	117
Figure 5.7	Plots of FT-IR spectra for [DMTI] in (0.01 to 0.05) mol.kg ⁻¹ of aqueous benzylamine	
SECTION-II		
Figure 5.8	Plots of variation of apparent molar volume (V_ϕ) of 1-butyl-1-methyl pyrrolidinium iodide in (a) 0.01 mol kg ⁻¹ and (b) 0.05 mol kg ⁻¹ of aqueous solutions of benzylamine ; (c) 0.01 mol kg ⁻¹ and (d) 0.05 mol kg ⁻¹ of aqueous solutions of benzamide at T = (288.15, 298.15, 308.15 and 318.15) K	141
Figure 5.9	Plot of variation of partial molar volume V_ϕ^0 of 1-butyl-1-methyl pyrrolidinium iodide in various concentrations $m = (0.01, 0.03 \text{ and } 0.05)$ mol kg ⁻¹ of (a) aqueous benzylamine; (b) aqueous benzamide at 288.15 K, 298.15 K, 308.15 K and 318.15 K.	142
Figure 5.10	Plot of variation of apparent molar isentropic compression ($K_{\phi,s}$) of 1-butyl-1-methyl pyrrolidinium iodide in (a) 0.01 mol kg ⁻¹ and 0.05 mol kg ⁻¹ aqueous solutions of benzamide; (b) 0.01 mol kg ⁻¹ and 0.05 mol kg ⁻¹ aqueous solutions of benzylamine at T = (288.15, 298.15, 308.15 and 318.15) K.	143
Figure 5.11	Plot of variation of Λ_m against \sqrt{c} for 1-butyl-1-methyl pyrrolidinium iodide in (a) 0.01 mol.kg ⁻¹ and 0.05 mol.kg ⁻¹ aqueous solutions of benzylamine.	144
Figure 5.12	Plot of variation of Λ_m against \sqrt{c} for 1-butyl-1-methyl pyrrolidinium iodide in 0.01 mol.kg ⁻¹ and 0.05 mol.kg ⁻¹ aqueous solutions of benzamide at T = (288.15 K to 318.15K).	145
Figure 5.13	Plots of FT-IR spectra for [BMPyr ⁺][I ⁻] (0.001 and 0.009) mol.kg ⁻¹ in aqueous benzylamine.	146

Figure 5.14	Plots of FT-IR spectra for [BMPyr ⁺][I ⁻] (0.001 and 0.009) mol.kg ⁻¹ in aqueous benzamide (0.01 (D), 0.03 (E) and 0.05 (F)) mol.kg ⁻¹ .	147
Figure 5.15	Plot of variation of Cyclic Voltammetry of 1-butyl-1-methyl pyrrolidinium iodide (0.01 and 0.05) mol kg ⁻¹ of benzylamine.	148
Figure 5.16	Plot of variation of Cyclic Voltammetry of 1-butyl-1-methyl pyrrolidinium iodide in (0.01 and 0.05) mol kg ⁻¹ of benzamide.	149
Figure 5.17 (a)	Comparison of CV area of [BMPyr ⁺][I ⁻] (0.001 and 0.009) mol kg ⁻¹ in 0.01 (A) of aqueous benzylamine.	150
Figure 5.17 (b)	Comparison of CV area of [BMPyr ⁺][I ⁻] (0.001 and 0.009) mol kg ⁻¹ in 0.05 (B) of aqueous benzylamine.	151
Figure 5.18 (a)	Comparison of CV area of [BMPyr ⁺][I ⁻] (0.001 and 0.009) mol kg ⁻¹ in 0.01 (C) of aqueous benzamide.	152
Figure 5.18 (b)	Comparison of CV area of [BMPyr ⁺][I ⁻] (0.001 and 0.009) mol kg ⁻¹ in 0.05 (D) of aqueous benzamide.	153
Section III		
Figure 5.19	Plot of apparent molar volume (V_{ϕ}) against molality (m) of 1-butyl-1-methyl pyrrolidinium tetrafluoroborate in 0.01 mol.kg ⁻¹ aqueous solution of benzylamine at different temperatures.	171
Figure 5.20	Plot of apparent molar volume (V_{ϕ}) against molality (m) of 1-butyl-1-methyl pyrrolidinium tetrafluoroborate in 0.05 mol.kg ⁻¹ aqueous solution of benzylamine at different temperatures.	172
Figure 5.21	Plot of variation of apparent molar isentropic compression against ($K_{\phi,s}^o$) molality of 1-butyl-1-methyl pyrrolidinium tetrafluoroborate in 0.01 and 0.05 mol.kg ⁻¹ of aqueous benzylamine at four equidistant temperatures.	173
Figure 5.22	Plot of variation of PMV of 1-butyl-1-methyl pyrrolidinium tetrafluoroborate in aqueous benzylamine at different temperatures (288.15 K to 318.15 K).	174

Figure 5.23	Plots showing the variation of Λ_o with \sqrt{C} for 1-butyl-1-methyl pyrrolidinium tetrafluoroborate in 0.01 mol.kg ⁻¹ aqueous benzylamine at T = (298.15, 303.15, 308.15 and 313.15) K.	175
Figure 5.24	Plots showing the variation of Λ_o with \sqrt{C} for 1-butyl-1-methyl pyrrolidinium tetrafluoroborate in 0.05 mol.kg ⁻¹ aqueous benzylamine at T = (298.15, 303.15, 308.15 and 313.15) K.	176

LIST OF TABLES

CHAPTER 1. INTRODUCTION		
Table 1.1	List of some of the Ionic liquids with high potential window	21
CHAPTER 3. EXPERIMENTAL		
Table 3.1	Details of chemicals used during experimental work	61
Chapter 4.		
THERMODYNAMIC, CONDUCTOMETRIC AND CYCLIC VOLTAMMETRIC PARAMETERS		
Table 4.1	Change in volume in accordance with different type of interactions	80
CHAPTER 5. RESULTS AND DISCUSSION		
SECTION-I		
Table 5.1	Value of densities (ρ), apparent molar volumes (V_ϕ) of [DMTI] in aqueous solutions of benzamide and benzylamine at different temperatures	95
Table 5.2	Value of densities ρ , and ultrasonic speed, u of 1,4-Dimethyl-4H-1,2,4-triazolium iodide in water at different temperatures	97
Table 5.3	Partial molar volumes (V_ϕ^0) and experimental slopes (S_v^*) of 1,4-Dimethyl-4H-1,2,4-triazolium iodide in binary aqueous solutions of benzamide and benzylamine at different temperatures	98
Table 5.4	Partial molar volumes of transfer (ΔV_ϕ^0) of 1,4-Dimethyl-4H-1,2,4-triazolium iodide in binary aqueous solutions of benzamide and benzylamine at temperatures 218.15 to 318.15K	99
Table 5.5	Values of empirical parameters of Eq. (4) for 1,4-Dimethyl-4H-1,2,4-triazolium iodide in aqueous benzamide and benzylamine solutions	100

Table 5.6	Limiting apparent molar expansibilities (ϕ_E^0) for 1,4-Dimethyl-4H-1,2,4-triazolium iodide in aqueous benzamide and benzylamine solutions at different temperatures	101
Table 5.7	Values of ultrasonic speed (u) and apparent molar isentropic compression ($K_{\phi,s}$) of Ionic liquid in aqueous solutions of benzamide and benzylamine at different temperatures	102
Table 5.8	Partial molar isentropic compression ($K_{\phi,s}^0$) and experimental slopes (S_K^*) for 1, 4-Dimethyl-4H-1,2,4-triazolium iodide in aqueous solutions of benzamide and benzylamine at different temperatures	104
Table 5.9	Partial molar isentropic compression of transfer ($\Delta K_{\phi,s}^0$) for 1,4-Dimethyl-4H-1,2,4-triazolium iodide in aqueous solutions of benzamide and benzylamine at temperature from 218.1K to 318.15K	105
Table 5.10	Pair and triplet interaction coefficients of ternary mixture of 1,4-Dimethyl-4H-1,2,4-triazolium iodide in aqueous benzamide and benzylamine at different temperatures	106
Table 5.11	Specific Conductivity (k , $\mu\text{S}\cdot\text{cm}^{-1}$) and molar conductivity (Λ_m , $\text{S}\cdot\text{cm}^2\text{mol}^{-1}$) of 1,4-Dimethyl-4H-1,2,4 triazolium iodide in aqueous solution of benzylamine and benzamide.	107
Table 5.12	Limiting molar conductivity (Λ_m , $\text{S}\cdot\text{cm}^2\text{mol}^{-1}$) of 1,4-Dimethyl-4H-1,2,4 triazolium iodide in aqueous solution of benzylamine and benzamide.	109
Table 5.13	Activation energy of 1,4-Dimethyl-4H-1,2,4 triazolium iodide in aqueous solution of benzylamine and benzamide.	110
Table 5.14	Wave numbers recorded from the FT-IR spectral studies of IL (0.01 to 0.05) mol kg^{-1} in aqueous solution of benzamide and benzylamine.	111
SECTION-II		

Table 5.15	Value of densities (ρ), apparent molar volumes (V_ϕ) of 1-butyl-1-methyl pyrrolidinium iodide in aqueous solutions of benzylamine and benzamide at different temperatures.	127
Table 5.16	Partial molar volumes (V_ϕ^0) and experimental slopes (S_v^*) of 1-butyl-1-methyl pyrrolidinium iodide in binary aqueous solutions of benzamide and benzylamine at different temperatures.	129
Table 5.17	Partial molar volume of transfer (ΔV_ϕ^0) of 1-butyl-1-methyl pyrrolidinium iodide in binary aqueous solutions of benzylamine and benzamide at different temperatures.	130
Table 5.18	Values of empirical parameters of Eq. (4.19) for 1-butyl-1-methyl pyrrolidinium iodide in aqueous benzylamine and benzamide solutions.	131
Table 5.19	Limiting apparent molar expansibilities (ϕ_E^0) for 1-butyl-1-methyl pyrrolidinium iodide in aqueous benzylamine and benzamide solutions at different temperatures.	132
Table 5.20	Values of ultrasonic speed (u) and apparent molar isentropic compression ($K_{\phi,s}$) of Ionic liquid in aqueous solutions of benzylamine and benzamide at different temperatures and experimental pressure = 0.01 Mpa.	133
Table 5.21	Partial molar isentropic compression ($K_{\phi,s}^0$) and experimental slopes (S_K^*) for 1-butyl-1-methyl pyrrolidinium iodide in aqueous solutions of benzylamine and benzamide at different temperatures.	135
Table 5.22	Partial molar isentropic compression of transfer ($\Delta K_{\phi,s}^0$) of 1-butyl-1-methyl pyrrolidinium iodide in aqueous solutions of benzylamine and benzamide at temperature from 218.15K to 318.15K and experimental pressure = 0.01 Mpa.	136
Table 5.23	Pair and triplet interaction coefficients of 1-butyl-1-methyl pyrrolidinium iodide in aqueous solutions of benzylamine and benzamide at different temperatures.	137

Table 5.24	Molar conductivity (Λ_m , S.cm ² mol ⁻¹) 1-butyl-1-methyl pyrrolidinium iodide in aqueous solution of benzylamine and benzamide.	138
Table 5.25	Limiting molar conductivity (Λ° , S.cm ² mol ⁻¹) and activation energy (E_A) of 1-butyl-1-methyl pyrrolidinium iodide in aqueous solution of benzylamine and benzamide.	140
SECTION-III		
Table 5.26	Value of densities, ρ and speed of sound, u values of ternary mixture of various molalities of 1-butyl-1-methyl pyrrolidinium tetrafluoroborate in aqueous solutions of benzylamine at different temperatures.	160
Table 5.27	Apparent molar volume, V_ϕ and apparent molar isentropic compression, $K_{\phi,s}$ values of ternary mixtures of various molalities, m of Ionic liquid in benzylamine at different temperatures.	162
Table 5.28	Values of partial molar volumes, V_ϕ^0 and experimental slope, S_v^* of ternary mixtures of Ionic liquid in various molalities of aqueous benzylamine at different temperatures.	163
Table 5.29	Values of limiting apparent molar isentropic compression, $K_{\phi,s}^0$ and experimental slopes, S_K^* of ternary mixtures of Ionic liquid in various molalities, m of aqueous benzylamine at different temperatures.	164
Table 5.30	Values of PMV of transfer, ΔV_ϕ^0 and limiting molar isentropic compression of transfer, $\Delta K_{\phi,s}^0$ of ternary mixtures of Ionic liquid in various concentration (molality, $m=0.01, 0.03$ and 0.05) mol.kg ⁻¹ of aqueous benzylamine.	165
Table 5.31	Values of empirical parameters (a , b and c) of ternary mixture of Ionic liquid in various molalities, m of aqueous benzylamine at various temperatures.	166

Table 5.32	Values of molar expansibilities, ϕ_E^0 of ternary mixture of Ionic liquid in different concentrations of aqueous benzylamine at different temperatures.	166
Table 5.33	Values of pair (V_{AB} and K_{AB}) and triplet interaction coefficients (V_{ABB} and K_{ABB}) of ternary mixtures of Ionic liquid in aqueous benzylamine at different temperatures.	167
Table 5.34	Specific Conductivity (k , $\mu\text{S}\cdot\text{cm}^{-1}$) and molar conductivity (Λ_m , $\text{S}\cdot\text{cm}^2\text{mol}^{-1}$) 1-butyl-1-methyl pyrrolidinium tetrafluoroborate in aqueous solution of benzylamine.	168
Table 5.35	Limiting molar conductivity (Λ° , $\text{S}\cdot\text{cm}^2\text{mol}^{-1}$) of 1-butyl-1-methyl pyrrolidinium tetrafluoroborate in aqueous solution of benzylamine.	169
Table 5.36	Activation energy of 1-butyl-1-methyl pyrrolidinium tetrafluoroborate in aqueous benzylamine.	170

LIST OF ABBREVIATIONS

A	Degree of ionization
a, b, c	Empirical constants
AlCl ₃	Aluminum chloride
ARD	Average Relative Deviation
AMV	Apparent Molar Volume
[BF ₄] ⁻	Tetrafluoroborate anion
[BMPyr ⁺] [I ⁻]	1-butyl-1-methyl pyrrolidinium iodide
[BMPyr ⁺] [BF ₄] ⁻	1-butyl-1-methyl pyrrolidinium tetrafluoroborate
Br ⁻	Bromide ion
⁰ C	Temperature in degree Celsius
Cl ⁻	Chloride ion
C	Carbon atom
C ₂ , C ₄ , C ₅	Carbon at second, fourth and fifth position of imidazolium ring
[CF ₃ CO ₂] ⁻	Trifluoroacetate anion
-COOH	Carboxylic acid
¹³ C NMR	Carbon Nuclear Magnetic Resonance
c	Molarity
cm/s	Centimeter per second
CV	Cyclic voltammetry
d	Derivative
DSA	Density and sound velocity analyzer
[DMTI]	1,4-dimethyl-4H-1,2,4-triazolium iodide
e.g.	Example
[EMIM ⁺] [I ⁻]	1-ethyl-3-methyl imidazolium iodide
ESD	Energy storage devices
FT-IR	Fourier transform infrared spectroscopy
g	Gram
¹ H NMR	Hydrogen Nuclear Magnetic Resonance

H	Planck's constant
ILs	Ionic Liquids
J	Joule
KCl	Potassium chloride
K	Kelvin
kg.m ⁻³	Kilogram per cube meter
K _{φ,s}	Apparent molar isentropic compression
κ _{S,0} , κ _S	Isentropic compressibility of pure solvent and solution
ΔK _{φ,s} ⁰	Partial molar isentropic compression of transfer
κ	Conductivity
K _m	Equilibrium constant
MPa.s	Milli Pascal seconds
mS/cm	Milli Siemens per centimeter
mM	Millimole
ml	Milliliter
M	Molality
MW	Molecular weight
ms ⁻¹	Meter per second
mol kg ⁻¹	Mole per kilogram
m ³ ·mol ⁻¹	Meter cube per mole
m _A	Molality of solute in solvent
m _B	Molality of stock solution
m ³ ·mol ⁻¹ ·K ⁻²	Cubic meter per mole per square kelvin
m ³ ·mol ⁻¹ ·GPa ⁻¹	Cubic meter per mole giga per pascal
N	Number of carbon atoms
N ₁ , N ₃	Nitrogen at first and third position of imidazolium ring
-NH ₂	Amine
η	Viscosity

n_1, n_2	Number of moles of constituent 1 and 2
N	Avogadro's number
Na^+, K^+	Sodium and potassium ion
η_r	Relative viscosity
$[\text{PF}_6]^-$	Hexafluorophosphate anion
P	Pressure
PMV	Partial Molar Volume
ρ	Density of solution
ρ_o	Density of pure solvent
P_2O_5	Phosphorus Pentoxide
ppm	Parts per million
RSD	Relative standard deviation
R	Gas constant
RBF	Round bottom flask
S_V^*, S_K^*	Experimental slope
T	Temperature
TLC	Thin Layer Chromatography
U	Speed of Sound
VOCs	Volatile organic compounds
V	Volume
V_ϕ	Apparent molar volume
V_ϕ^0	Limiting value of apparent molar volume
ΔV_ϕ^0	Partial molar volume of transfer
V_m	Molar volumes
w.r.t.	With respect to
X	Mole fraction
∂	Partial differential
ϕ_E^0	Limiting apparent molar expansivity
$(\partial\phi_E^0/\partial T)$	Hepler constant
σ	Standard deviation

Chapter 1

Introduction

1. Introduction

1.1.Solution Chemistry:

Solution Chemistry is one of the remarkable subfields of physical chemistry. Although combining solute and solvent components to make a solution may appear like a straightforward operation, the phenomenon is more complex and includes several interactions among the solute and solvent components.

Solvents are being used inadvertently in the chemical sector, which includes pharmaceutical, paint, furniture, dry cleaning, detergent, and perfume manufacturing. In industries, choosing a solvent is mostly based on economic considerations, but taking environmental concerns into account, it is necessary to evaluate the environmental performance of the solvent in addition to its safety and health implications (Tokuda et al., 2004)(Jenkins, 2011). Intentionally or unintentionally, many organic solvents, which have high vapour pressure and are volatile, are absorbed by human bodies and also escape into the Environment, where they have an adverse effect on flora and animals. Body exposure to solvents poses several health hazards, including cancer, bronchial irritation, nausea, headaches, and depression.

Global research has recently concentrated on compounds that are simple to synthesize with minimal resource consumption and, more importantly, do not affect the environment. Due to their illustrated potential as replacements, ILs are therefore attracting the attention of researchers. The use of an ionic liquid instead of a normal organic solvent can result in unexpected and uncommon reactions.

1.2. Introduction to Ionic Liquids:

In the 21st century, the concept of synthetic and applied material science may be altered by ionic liquids (ILs). One of the fields of chemical research on novel materials that has grown most quickly in the last ten years is ILs (Austen Angell et al., 2012). These are the organic, molten or liquid salts made up of ions that are non-molecular compounds, present in their liquid phase even at room temperature. Due to their tendency to have a very low vapour pressure owing to the fact that they are liquid or molten salts, they have recently received a lot of interest as prospective solvents to replace organic solvents. In the form of molten salt at ambient temperature, Paul Walden initially proposed the concept of ILs in 1914. The first known ionic liquid, ethyl ammonium nitrate $[\text{EtNH}_3][\text{NO}_3]$, was created by distilling water out of a solution of concentrated nitric acid and

ethylamine to create pure salt (Frade & Afonso, 2010). These salts are electrically neutral because the positive ions that make them match the liquid's negative ions precisely. They lack any molecular-level presentation, just as other solvents, which are identified by their polar or apolar character based on interactions between solvent molecules. The melting points of ILs are lower than the boiling points of water (Khupse & Kumar, 2010).

They are also referred to as designer solvents, remarkable magical fluids, liquid organic salts, fused salts, liquid electrolytes, and green solvents. Due to their unique qualities, including high electrical conductivity, high thermal and chemical stability, non-aqueous nature, immiscibility, low nucleophilicity, low melting point, viscosity, negligible vapor pressure, high solvating power, and a significant amount of electrochemical space, ILs have drawn a lot of attention (Ghandi, 2014).

1.2.1 Composition of ILs:

ILs are composed of cations and anions with low melting points. The anions are inorganic, but the cations might be either organic or inorganic. Conductivity, density, polarity, and viscosity are just a few examples of the physical characteristics that are specifically impacted by the choice of cations and anions that compose up an IL. Imidazolium, pyrrolidinium, sulfonium, triazolium, and ammonium are merely some of the numerous types of known common bulky organic cations that are present in ILs, alongside other organic and inorganic anions with various functional groups, including iodide, tetrafluoroborate, chloride, and a few others. ILs are often used in synthesis, material science, catalysis, biocatalysts, medicine, green chemistry, electrochemistry, and chemical engineering, among other inter-disciplinary study areas (Jenkins, 2011).

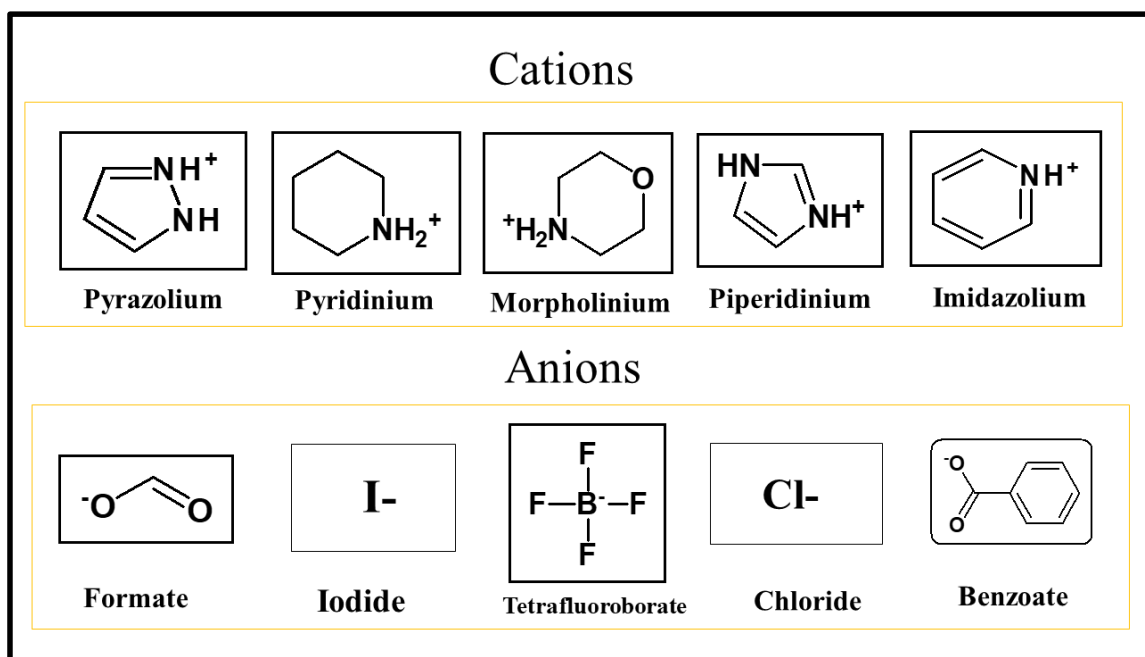


Figure 1.1: Commonly used cations and anions in ionic liquids.

1.2.2. Classification of ILs:

Considering that induced functionalities, cations, or anions are present, classifying ILs can be challenging. ILs can be categorized into different classes based on the variety of chemical structures they possess. The two most significant of them are the protic and aprotic ILs. Protic ionic liquids (PILs) and aprotic ionic liquids (AILs) are the proton-donating and the non-donating ILs, respectively. PILs are the most affordable and simple IL which have a high level of purity and are created by a straightforward proton exchange between equimolar base and Bronsted acid pairs (Marsh et al., 2004). In contrast to ordinary salts, protic ILs are thought to be a pure combination of ions with outstanding ionic behavior (Javed et al., 2018). As an outcome of proton transfer, which exhibits characteristics of hydrogen bonding in contrast to organic solvents, the particular sites for hydrogen bonding are produced in PILs. Due to which these ILs have extremely high levels of stability, conductivity, and thermal efficiency. PILs as neoteric electrolytes have great promise for battery design. PILs' high proton transfer energy contributes to their excellent conductivity (Stettner & Balducci, 2021).

In contrast, AILs lack distinguishing characteristics but can be found in a variety of cation and anion groups, either having or lacking the ability to form hydrogen bonds. These ILs are typically

created through a multi-step process involving the creation of a covalent connection between the designated anions (D. Macfarlane & Kar, 2017). Due to their strong covalent bonding, AILs are categorized as having stronger electrochemical and thermal properties than PILs. The high cohesive energy of aprotic ILs causes viscosities that obstruct ionic mobilities, making their conductivities troublesome for portable energy applications.

Hajipour and Rafiee divided ILs into 11 categories based on physical characteristics such viscosity, density, conductance, solubility, and the relative basicity or acidity qualities of its ions (Javed et al., 2018).

- a) Basic ILs**
- b) Acid ILs**
- c) Neutral ILs**
- d) Energetic ILs**
- e) Functionalized ILS**
- f) Chiral ILs**
- g) Bio-ILs**
- h) Protic Eutectic ILs**
- i) Supported ILs**
- j) Poly-ILs**
- k) ILs with amphoteric anions**

The allocation of anions and cations affects the characteristics of ILs. Since there are many different cations and anions that can be combined, ILs have very flexible characteristics. The anions represent the chemical properties and consequently the reactivity of ILs, whereas the cations regulate the physical qualities (Faunce et al., 2013). The composition of anions and cations has been used as a basis for investigating several different kinds of ILs. ILs are further divided into the following subcategories:

1.2.2.1. Imidazolium Based ILs

Imidazolium-based ILs have been one of the most investigated ILs during the past few decades. Low melting temperatures, good stability under oxidizing and reducing conditions, low viscosity, and ease of preparation are all characteristics of imidazolium-based ILs (Boruń, 2019; Burrell et al., 2007). These nitrogen-rich heteroatoms in ILs combine to produce an ionization product with great chemical stability. Both the counter anion and the imidazole ring cation are present in

imidazolium-based IL (Riyazuddeen & Afrin, 2012). The imidazolium cation ring typically consists of two nitrogen atoms linked by the methylene group.

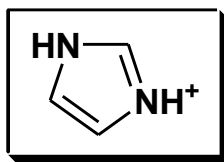


Figure 1.2: General structure of imidazolium cation.

Both nitrogen atoms in imidazole fall into the N₁ donor and N₃ acceptor categories. The amino nitrogen is N₁, while the imino nitrogen is N₃. Imidazolium-based ILs shows a wide range of advantages in sensors, adsorption, biomass pre-treatment, polymer production, and catalysts because of their unique composition and set of characteristics (Yahia et al., 2019). A computational analysis of a group of alkyl-methyl imidazolium-based ILs' electrochemical stability reveals that the anion structure has a significant impact on the electrochemical stability window while the imidazolium cation's alkyl side chain has little effect.

1.2.2.2. Pyrrolidinium based-ILs.

A cyclic amine with four carbon atoms in the cycle is pyrrolidine, also known as tetrahydropyrrole (C₄H₉N) (Anouti et al., 2010; Chaban, 2016; Yim et al., 2007). This liquid is clear and has an ammonia odor. Natural chemicals frequently contain the pyrrolidine component. In acidic conditions, pyrrolidine can be protonated to produce C₄H₁₀N⁺, a component of a new class of pyrrolidinium-based ILs. The creation of water- and air-stable, low-toxicity and low cost room temperature ILs is extremely desirable because the main drawbacks of some ILs are their relative high cost and their toxicity (Anouti et al., 2008). To satisfy these criteria, novel pyrrolidinium-based ILs with C₇H₁₅COO⁻, NO₃⁻, HCOO⁻, CF₃COO⁻, CH₃COO⁻ or HSO₄⁻ anions were created by neutralizing pyrrolidine with the relevant Bronsted acid (Pont et al., 2009).

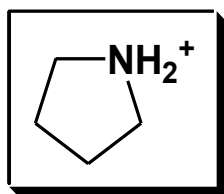


Figure 1.3: General structure of Pyrrolidinium cation.

Pyrrolidinium-based ILs were chosen for the experiment because they exhibit a higher electrochemical window and contain more locally charged aliphatic cations than delocalized aromatic cations like imidazolium (Asha et al., 2019a; Kumari et al., 2014). Pyrrolidinium-based ILs exhibit perceptible characteristics such as aliphaticity, localization of the positive charge, and better flexibilities as compared to imidazolium-based ILs.

1.2.2.3. Triazolium based-ILs.

In fact, ILs made of imidazolium are true ILs. Compared to triazolium ILs, a significant amount of research has been done in this area, and it is still expanding tremendously in both academic and industrial domains. The only structural difference between imidazolium and triazolium is a nitrogen atom. While the triazole group has three nitrogen atoms, the imidazole group only has two. Triazolium salts were not thought to have IL characteristics earlier in 1887 (Studies, 2022). By anion metathesis of a -amino acid ester, (S)-Proline, 4-hydroxy-L-Proline, and L-lysine were converted into the first triazolium-based IL. As an organo catalyst, triazolium ILs are used in a variety of asymmetric processes. Triazolium ILs were created and employed in a variety of chemical reactions as an efficient and environmentally acceptable alternative to traditional organic solvents.

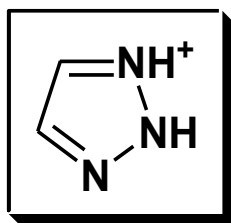


Figure 1.4: General structure of Triazolium cation.

Low melting points and high thermochemical stability at various temperatures, negligible vapour pressure, viscosity, and the capacity to solubilize solvents are only a few of the benefits of triazolium ILs (Studies, 2022; Yahia et al., 2019). Triazolium ILs can be alternate to very volatile and combustible organic solvents because to their intriguing and alluring properties. They have a variety of uses in organic synthesis as solvents/catalysts for asymmetric synthesis in addition to being "green" solvents.

1.2.2.4. Phosphonium based- ILs.

ILs based on phosphonium cations are a family of ILs that are easily accessible and, in some cases, have better qualities than ILs based on nitrogen cations. They have lately been studied for application as extraction solvents, corrosion inhibitors, chemical synthesis solvents, and electrolytes in batteries and super-capacitors (Tsunashima et al., 2014). Contrarily, despite significant benefits over their N-based counterparts, quaternary phosphonium-based (P-based) ILs have received significantly less study attention, because P-based ILs exhibit greater thermal stability, base stability, and ion conductivities. Since phosphonium salts are less vulnerable to both degradation pathways, they have better thermal stability.

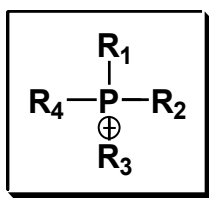


Figure 1.5: General structure of Phosphonium cation.

In conclusion, although receiving less attention than their ammonium analogues, P-based ILs exhibit considerable promise as novel electrolyte materials. ILs have a variety of applications, including gas separation, antimicrobial coatings, and gene transfer (Frade & Afonso, 2010).

1.2.2.5. Ammonium based-ILs.

In all the many families of ILs, ammonium based ILs are known to have a significant impact on chemical and biological processes. As a result of the expanding global need for ILs, ammonium-based ILs are drawing more and more attention as eco-friendly co-solvents in a variety of research domains (Asha et al., 2019b, 2019a). The distinctive and enticing characteristics of ammonium based ILs, which may offer certain advantages in numerous medicinal and therapeutic applications, drive their employment in batteries as electrolytes, fuel cells, polymerization processes, nanotechnology, and other commercial and scientific applications. In order to electrochemically intercalate lithium into a natural graphite anode, quaternary ammonium-based IL is utilized when trimethyl-n-hexylammonium cation is present, and these ammonium-based ILs are currently used in secondary batteries (Frade & Afonso, 2010; Neale, Murphy, et al., 2017).

Furthermore, because they alter the potential of biomolecules' intra- and intermolecular interactions, these ammoniums based ILs play a crucial and vital function in biomolecules and their activities. On the other hand, these ILs have clearly shown to be good biocompatible solvents for proteins, improving the stability and shelf life of a number of proteins as well as acting as stabilizing solvents for a number of amino acids and model protein complexes.

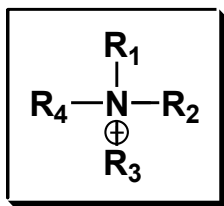


Figure 1.6: General structure of Ammonium cation.

With emphasis on their behavior in molecular solvents, we have examined numerous studies on the thermophysical characteristics of ammonium-based ILs in this aspect. Through intermolecular interactions, which have been discovered to be extremely sensitive to straightforward structural changes, the thermophysical characterization of ammonium-based ILs and molecular solvents has revealed their wide variety of uses.

1.3. Properties of Ionic liquids

In the thermophysical properties of ILs, the alkyl chain length of the cation, anions, and type of the solvent all play a significant role. With rising temperature, the impact of mixing various IL anions and cations along with the effect of alkyl chain on the characteristics of ILs has also been studied (Kennedy, 2009). The ILs' structure-based characteristics and the ions' structural configurations point to numerous further areas that could be investigated in a variety of scientific sectors. For extensive commercial applications and fundamental study, these thermophysical characteristics of ILs with molecular solvents will surely offer valuable and original knowledge on the molecular interactions and the structural arrangement of ILs' ions. Due to its numerous uses in different sectors of industry, there is currently a considerable deal of interest in studying the interactions and structures of binary mixes of IL with molecular solvents. To describe and comprehend the features of such systems, a thorough structural understanding of interactions is important (Yohannes et al., 2020). As a result, this viewpoint primarily focuses on recent

developments in the experimental thermophysical characteristics of ILs with molecular solvents. Some of the fundamental characteristics of the ionic liquids include the following:

1.3.1. Density

Ionic liquids typically have densities between 1.2 and 1.6 g cm⁻³. Compared to the advantages the anion's nature offers, the effect of the cation on the density of the ILs is less noticeable. The type of atomic interactions that a specific cation has with the counter anion is related to the way the cation affects density. The density falls for liquids containing the dicyanamide anion in the following order: pyrrolidinium > imidazolium > pyrrolidinium. The liquid density for substances containing thiocyanate as an anion falls as imidazolium > pyridinium > pyrrolidinium (Ben Ghanem et al., 2015; Galán Sánchez et al., 2009).

1.3.2. Viscosity

An ionic liquid's viscosity is an essential variable in electrochemical investigations due to its significant impact on the rate of mass movement within solutions. Ionic liquids typically have higher viscosities than ordinary molecular solvents. At room temperature, their viscosities do, in fact, normally vary from 30 cP to roughly 100 cP, but in exceptional instances, values as high as 500-600 cP are noted (Anouti et al., 2010). Often, the structure of the anion has a greater impact on viscosity than the structure of the cation. Water or other cosolvents reduce viscosity in ILs while chloride as a contaminant raises it. The ionic liquid's viscosity is greatly influenced by the characteristics of the anion and cation that make up the liquid. Higher basicity, size, and relative capacity to form hydrogen bonds in anionic species lead to more viscous ILs. Van der Waals forces, hydrogen bonds, and columbic forces appear to play a role in determining how viscous ILs are. Getting reduced viscosities is one of the pinnacles of IL research since it would allow for additional advancements in the performance of electrochemical devices through enhanced ion transport (Anouti et al., 2010; M. J. Lee et al., 1993).

1.3.3. Vapour pressure

The physical characteristic of ILs that is arguably most frequently cited as advantageous for application—yet one of the least studied—is their negligible vapour pressure. The vapour pressure

of ILs is quite low. The vapor pressure of ILs can be calculated at very low pressures and temperatures within 473.15 K to 573.15 K (Galiński et al., 2006; Z.I.Takai, 2018b).

1.3.4. Melting Point

The differential scanning calorimeter (DSC) is the method used to determine the melting point. Another attribute which is highly impacted by impurities in the IL is the capacity of many ILs to supercool and form glasses, which can confuse the measurement of melting point (Kuravi et al., 2013; Lierde et al., 1988; Neale, Schütter, et al., 2017). To put it another way, it will be claimed that any strongly ionic material that is fluid at ambient temperature will unavoidably show very low vapour pressures in close proximity of its triple point. The melting point of ILs is typically low—less than 100° C. The ILs have big ions and asymmetric cations, which lower the lattice energy and hence lower the melting point.

1.3.5. Ionic Conductivity

One of the most significant features of ILs recognized as electrolytes is ionic conductivity. In comparison to organic solvent/electrolyte systems, ionic liquids have reasonably good ionic conductivities (up to 10 mS cm⁻¹). The mobility of the charge carriers, which varies with the ion's molecular weight and size, determines the ionic conductivity. The dynamics of the ions, which are extremely crucial, have a significant impact on the way ILs work in an electrochemical device (Jónsson, 2020a). The amount of ion pairing or aggregation in the liquid can be determined by the conductivity of the liquid (Sharma et al., 2020). The ionic conductivity of ILs is frequently much lower than the anticipated if we were to only include the high ion concentrations; we would observe far stronger ionic conductivity if these ions were allowed to travel independently of one another. This ion aggregation is the reason for this. The term "ionicity" refers to the ion aggregation characteristic.

1.3.6. Electrochemical properties

Ionic liquids possess captivating electrochemical characteristics that render them appealing for diverse applications. Because of their distinctive ionic properties, they exhibit strong ionic conductivity, enabling efficient conduction of electric charge. The proper pairing of a cation and an anion appears to be fundamental in determining the anodic stability of the ILs (Farhadi &

Mohammed, 2016; Kuravi et al., 2013). Due to their electrochemical characteristics, ILs are generally used in supercapacitors, batteries, solar cells, fuel cells, electro winding, and other devices. These properties render them appropriate for utilization as electrolytes in batteries, supercapacitors, and fuel cells. In addition, ionic liquids possess a broad electrochemical stability range, enabling their utilization across a wider spectrum of voltages without experiencing breakdown. These properties make them highly useful in electrochemical operations, such as electrodeposition and electrochemical sensing. The adjustable characteristics of ionic liquids also allow for the creation of tailored electrolytes with precise electrochemical properties for various applications.

1.3.7. Thermal Stability

Thermal stability for ionic liquids is possible up to 450 °C. The binding force of the heteroatom-carbon and heteroatom-hydrogen bonds in ionic liquids determines their thermal stability, respectively. DSC measurements of specific heat capacity and storage densities are used to explore a variety of thermal characteristics crucial for IL applications (Chau et al., 2007; Jónsson, 2020a). Their thermal stability is vital to their applications and is the feature that is most frequently cited.

1.3.8. Toxicity

Ionic liquids are recognized for their comparatively lower toxicity in comparison to other solvents. Extensive research has been conducted on their prospective applications in many sectors such as drugs, energy, and materials. The safety profile of many ionic liquids is enhanced by their low volatility and non-flammability. Nevertheless, it is crucial to acknowledge that the toxicity of ionic liquids might still differ based on their composition and quantity. Adhering to appropriate safety protocols and conducting comprehensive risk evaluations are crucial when dealing with ionic liquids to guarantee secure handling and mitigate any potential hazards. Although some ILs are poisonous to aquatic life and may be harmful to human health, but recently they are frequently seen as more environmentally friendly substitutes for conventional solvents. Some of the anions and cations combinations which are utilized in ILs can lead to hazardous effect and may have negative impact on some of the ecosystems. This presents significant issues with the long-term environmental impacts and disposal of ILs, since inappropriate disposal may contaminate water supplies. Ionic liquid toxicity is a crucial topic given its potential application as novel materials

and environmentally friendly solvents for a broad number of potential applications (Javed et al., 2018)(Hartmann & Pereira, 2016).

1.3.9. Biodegradability

Although it is anticipated that ILs would biodegrade, but the extent of biodegradation depends on the IL's geometry and composition. Longer carbon chains have more oxidizable carbon atoms, which accelerate biodegradation. Ether added to IL's alkyl side chain decreases toxicity and increases biodegradability. Due to the fact that they don't contain a carbon source, ILs with halides as anions have a limited biodegradability (Marsh et al., 2004). For ILs containing formates, acetates, and simple carboxylates as anions, the biodegradation results are outstanding.

1.3.10. Solubility

In general, water is soluble in ionic liquids. The solubility and a few other characteristics of ILs are affected by the anions utilized in their composition. Ionic liquids that are very water soluble are produced by anions with high hydrophilicity. The hydrophobicity of IL is also influenced by the alkyl chain length of cations. ILs are very soluble in organic solvents in addition to water (Yahia et al., 2019; Zhao et al., 2013).

1.3.11. Scalability

The scalability of ionic liquid (IL) synthesis is essential for industrial applications, particularly in the context of the increasing demand for environmentally benign solvents. Common methods include direct synthesis, metathesis, and neutralization, each of which presents distinct environmental and cost-effectiveness challenges. Scalability is a critical component of purification and recovery processes, as it guarantees energy consumption and sustainability.

1.4. Applications of Ionic Liquids:

The advantageous relationships, structure, charge, immiscibility, and distinctive combination of the constituent ions being virtuous, non-coordinating, non-volatile, and highly polar are what give ILs their distinctive features (Vancov et al., 2012). It is helpful to go back to ILs' unique characteristics while thinking about all the various uses, which are continually expanding. Low

melting points, thermal stability and low vapor pressure are among the characteristics of ILs. The examples of specific qualities drawing applications are given below.

- a) Interest in using ILs as pharmaceutical salts, where the cation or anion constitutes an active medicinal element, is sparked by the low melting point of ILs.
- b) Because ILs are ionic, they also offer quite different solvation environments when compared to traditional molecular solvents. These environments are used in a variety of synthetic reactions as well as in the processing of materials, extraction, and gas separation.
- c) Both the breakdown of various biomaterials and their processing into higher-value products are being researched with ILs.
- d) The capacity of ILs to disintegrate and stabilize proteins, DNA, and RNA is also of great value for biotechnological applications.
- e) The utilization of ILs for processing and recycling rare earths is also based on their distinctive solubilizing capabilities, high electrochemical stability, and other factors. Two interesting approaches for the separation of rare-earth salts are the use of ILs as an ionic extract and as a substrate for the subsequent electrodeposition of pure rare-earth metal.
- f) Given that many ILs are used extensively in electrochemical devices for electro winning, water splitting, and other purposes, great electrochemical stability is perhaps the most significant properties of several ILs (Nicotera et al., 2005).
- g) Good water-splitting catalysts like $\text{MnOx}_{(1.5-2)}$, have been synthesized using ILs as a medium. One of the crucial characteristics of the IL in this case appears to be the structure, which imparts to the liquid phase throughout the reaction, which affects the thermodynamics of the reaction, even if these deposition and oxidation processes are still being investigated (Nidhi & Kaur, 2022).
- h) To examine the corrosion inhibition capabilities of the available ionic liquid chemicals that have been used as efficient and green (environmentally friendly) corrosion inhibitors in corrosive aqueous media over the past 20 years (Bashir et al., 2020; Parveen et al., 2019).
- i) ILs have been used in a variety of other synthetic processes, including those that are organic, inorganic, and biological.
- j) The advantages of IL's features are numerous. It is extremely helpful to be able to dissolve components that are intractable in typical organic solvents, and their ionic nature aids in stabilizing nanoparticle dispersion throughout synthesis (Bashir et al., 2020).

- k) Strong thermal stability and the low vapor pressure of ILs also offer an essential advantage because these reactions use temperatures up to 200 °C, necessitating the installation of an autoclave if water is used.
- l) A variety of nanoparticles are synthesized under the effect of the nature and structure of the IL. The structural organization of ILs and their effects on specific synthetic processes.
- m) Chiral ILs can also be used as the synthetic medium or as catalysts in stereoselective synthesis, which is another synthetic application for ILs.
- n) The capability to introduce a chirally pure moiety into the ionic configuration, from a natural or synthetic source, is the most significant and distinctive characteristic of the IL.
- o) ILs can be employed for biocatalysis, homogeneous and heterogeneous in addition to chiral catalysis. Two key material types are used in this application: supported ILs, which use a porous solid to support and immobilize catalysts containing ILs, and solid catalyst with IL layer, which coats a heterogeneous catalyst with an IL to enhance its capabilities.
- p) The application of ILs as heat transfer fluids, since this is an illustration of a use that benefits from the ILs' comparatively good thermal stability and heat capacity. To increase the IL's thermal conductivity and heat capacity, nanoparticles can also be added.
- q) The enormous structural variability of ILs, along with their wide liquid range, low pressure, and outstanding temperature stability, is a major benefit. Hypergolic ILs are ILs that are created to catch fire when in contact with an appropriate oxidant. These ILs are being developed to replace hydrazine, a hazardous and difficult-to-handle chemical, for use in propellants.
- r) The application of ILs as lubricants in tribology, or to reduce wear and friction between two moving parts, is principally benefited by their low vapor pressure, superior thermal stability, synthetic diversity, and capacity to interact strongly with various surfaces. This can sometimes include creating surface coatings made of IL degradation byproducts.
- s) Controlling the viscosity, which is a key factor in determining how well lubrication works, is another potential benefit of employing IL mixes. For this specific IL use, there is a sizable potential market for commercial products.
- t) ILs may also be combined with the base oils now in use; in this case, the IL takes the place of the customary additives.

- u) The use of ILs in sensors is yet another application with substantial commercial potential. Here, we're mostly talking about electrochemical sensors, where ILs' broad electrochemical window and non-volatility are a big plus. For this application, the IL is applied as a coating on a quartz crystal microbalance or utilized to alter the electrode surface.

1.5. Limitations of Ionic Liquids

Ionic liquids have several drawbacks despite they have many strengths which include minimal volatility and good thermal stability. High viscosity of ILs can hinder mass transfer in reactions and processes and lower efficiency in some applications, is a major disadvantage. Ionic liquids can also be expensive to produce because many of them are made from pricey raw ingredients, which makes them less practical for widespread use than conventional solvents. Some ionic liquids may be hazardous or detrimental to aquatic life, which make disposal more complex and raises worries about their overall effects on the environment. Furthermore, because not all cation and anion combinations are appropriate for applications, the small range of stable ionic liquid compositions limits their adaptability. Finally, there is still uncertainty regarding the performance of ionic liquids for different applications because understanding of their characteristics and behaviors is still evolving.

In the present study, a ternary system has been achieved by blending IL with appropriate aqueous solutions of benzylamine and benzamide. In the quest for green chemistry, utilization of aqueous medium has come to light, however the presence of water can alter the characteristics of the system like conductivity, viscosity, and electrochemical properties. Water, generally enhance the performance of ionic liquids as it has been suggested that addition of water can boost the conductivity, stability as well as system's electrochemical performance. In order to synthesize ILs with good physiochemical properties for potential energy applications, the impact of cation modification of IL with aqueous benzylamine and benzamide has been explored. The flexible organic compounds viz; benzylamine and benzamide are now recognized as promising materials in the field of energy storage devices (ESDs), leading to improvements in battery and super capacitor technology. benzylamine shows many industrial applications and are used as corrosion inhibitor, free-standing electrodes and is used in different ESDs. It is used as an electrolyte in lithium-ion batteries, resulting in increased battery capacity and cycle life. On the other hand, benzamide the amide derivative of benzoic acid has demonstrated potential as an electrode material

for supercapacitors, in which benzamide-derived carbon nano sheets demonstrated remarkable electrochemical performance. Furthermore, benzylamine has been investigated as redox-active materials in redox flow batteries while benzamide has been used as a binder material to increase the durability of battery electrode. Furthermore, benzylamine inclusion into supercapacitor electrolytes has shown promising improvement in supercapacitor performance. These facts demonstrate many uses of benzylamine and benzamide, emphasizing their importance in the continuous search for effective and environmentally friendly energy storage technologies.

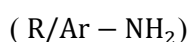
1.6. Introduction to Amines

Amines, the derivatives of ammonia are the most significant chemical molecules, which possess the property of having a nitrogen atom with a lone pair that is sp^3 hybridized with three single bonds to other elements. Amino acids, biogenic amines, trimethylamine (fish odor), and aniline are examples of significant amines with distinctively potent odors. A variety of biological processes break down amino acids to produce amines (G. Yang et al., 2020). Amines are present in a wide range of matrices, including environmental samples, industrial raw materials, finished goods, and waste. Due to the highly polar nature of these compounds, determining amines in these matrices is a difficult task. It is typically quite challenging to separate them from the matrix and then determine their final chromatographic composition (Tawalbeh et al., 2023).

Although there are many various forms of amine, they all have some characteristics since they all include an atom of nitrogen in their chemical structures (Eshetu et al., 2014). The simplest amine is ammonia (NH_3), which has three chemically equivalent hydrogen atoms linked to the central nitrogen atom. Inorganic amines, like trichloroamine, are created when hydrogen atoms in ammonia are swapped out for other elements (Truong et al., 2014). Organic amines are classed as follows when hydrogen atoms are replaced with different functional groups, such as alkyl or aryl groups:

1.6.1. Primary amines

Primary amines are the kind in which the alkyl (R) or aryl group (Ar) replaces the hydrogen atom.



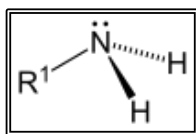


Figure 1.7: General structure of Primary Amine

Example: Methylamine, Aniline

1.6.2. Secondary amines

Secondary amines are the kind in which hydrogen atoms of ammonia molecules are substituted by two organic substituents.

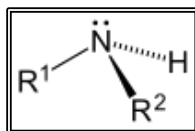


Figure 1.8: General structure of Secondary Amine

Example: Dimethylamine, Diphenylamine

1.6.3. Tertiary amines

Tertiary amines are the kind in which the 3 hydrogen atoms are displaced by the organic substituent.

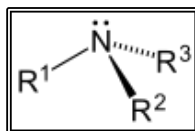
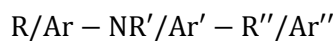
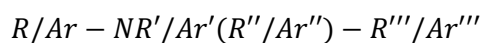


Figure 1.9: General structure of Tertiary Amine

Example: Trimethylamine, EDTA

1.6.4. Quaternary amines

Quaternary amines are the kind of amines in which all hydrogen atoms are replaced by alkyl or aryl groups.



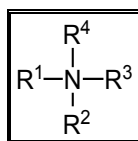


Figure 1.10: General structure of Quaternary Amine

Example: Benzalkonium chloride, Domiphen bromide

The hydrogen bonding has a major impact on the characteristics of amines, and as a result, they have high boiling points (Borch, 1969). The boiling point of amines is lower than that of comparable alcohols but significantly higher than that of phosphines. **Alkyl or aryl** amines are liquid by nature, have a high molecular weight, and are only marginally soluble in water (mainly aliphatic) (Hamdy et al., 2021). Aryl amines have their lone pair electron shared with the benzene ring, which reduces the tendency to form H-bonds. Aromatic amines have a substantially higher boiling point than aliphatic amines. Amides are substances with a nitrogen atom next to a carbonyl in the form of $R-C(=O)NR_2$, and they have various chemical characteristics.

1.7. Application of Amines

Amines and their derivatives are substances that are widely utilized in pharmaceuticals, cosmetics, rubber, polymers, insecticides, dyes, adhesives, solvents, corrosion inhibitors, pesticide production, and as intermediates in other synthetic processes (Mashtalir et al., 2015; Schon et al., 2016). Several of the significant uses for amines are given below:

- a)** Amines have important functions in the purification, manufacturing of amino acids, pharmaceutical, and energy storage industries (Roberts et al., 2009).
- b)** Amines are utilized as refrigerants and in the production of nitric acid, nylon, fertilizers, and other materials.
- c)** Because phenylethylamine is a natural component of cocoa beans, it can be found in chocolate, chocolate-based items, and confections.
- d)** Amines have been used as the reactive elements in a family of CO₂ adsorbents that is incredibly diverse and adaptable.
- e)** Amines and polyamines have been used to a variety of different solids to create unique and effective adsorbents. They have also been widely employed in combination with inorganic oxides as inexpensive and efficient support materials (Fekete et al., 2010).
- f)** They serve as emulsifying agents, surfactants, and parts of depilatory creams.

- g) Other applications include electroplating, textile production, accelerators for vulcanization, fuel additives, rocket fuels, etc. (Ge et al., 2000).
- h) Dioctadecyl amine has a significant deal of potential to function as organic PCMs for a variety of applications, including thermal or solar energy storage at room temperature (Powell & Whittaker-Brooks, 2022).
- i) A hybrid triarylamine-thiophene conducting polymer has also been created for charge storage.
- j) A new family of dendritic conducting polymers with a high specific capacitance in organic electrolytes is based on a bithiophene-triarylamine backbone (Song & Zhou, 2013).
- k) A universal method for creating O/N co-doped porous carbons has been established, based on benzoquinone and amines with various chemical structures.
- l) Quinone redox kinetics can be strengthened by amines with high electron-pair donicity, which can also include electroactive nitrogen molecules (Kwong et al., 1991).

1.8. Limitations of Amines

Although amines are significant chemical molecules with a wide range of uses, they have a number of drawbacks. Since many amines can irritate the skin, eyes, and respiratory system, providing health concerns while handling, their potential toxicity is a major worry. Furthermore, amines with a smaller molecular weight have a tendency to be volatile, which causes material to evaporate and be lost during processes, lowering efficiency. Because amines are susceptible to oxidation and degradation, which shortens their shelf life, stability can also be a problem. Additionally, they frequently have potent, disagreeable smells that need for extra ventilation or handling care in industrial environments. Their usage in watery contexts is complicated by their varying degrees of water solubility. Finally, the manufacturing of amines can be expensive and involve potentially dangerous chemicals, which raises questions about safety and the environment. Ultimately, even though amines have various uses, these drawbacks need to be carefully taken into account when choosing them for a given application.

1.9. Energy Storage Devices

Energy storage devices are one of the best alternatives to generate electricity and provide the stability and enormous amount of energy further looking towards the improvement in power systems as in their electrochemical and dynamic stability. With the rapid growth of the population, there is a huge need for energy storage devices that do not harm the environment. Speaking of energy storage devices, they are the ones that are used as an apparatus for storing electrical energy when needed and releasing it as needed. They are also a crucial component of the current energy supply chain (Nidhi & Kaur, 2022). The fundamental function that energy storage devices do for us is to convert one form of energy into another when necessary and then deliver that energy back to stored energy in a dependable and cost-effective manner. Along with all of these uses, these devices are crucial to our daily lives because they improve the grid's stability, increase the penetration of renewable resources, conserve fossil fuels, and lessen the environmental impact of energy production (Gonçalo A. O. Tiago 1 & 2, 2020). The decoupling of power generation from the load, which facilitates supply and also meets demand, is one further benefit these devices provide. Power systems, hybrid automobiles, and other telecommunication gadgets like cell phones and laptops all depend on energy storage devices. Along with storing and decoupling electricity for basic needs, these devices also increase grid security by allowing local and micro grids to store energy. These devices also play a crucial role in balancing the grid by increasing the adaptability and dependability of grid systems.

A few examples of energy storage technologies are batteries, capacitors, super capacitors, flow batteries, fuel cells, flywheels, and various pressurized gas storage systems. The China Energy Storage Alliance Global Project Database conducted a survey to learn more about the most popular and in-demand energy storage devices, and they discovered that pumped hydro storage makes up the majority of the world's storage technology. For electrochemical storage technologies, lithium-ion energy storage has the largest installed capacity, accounting for close to 65% of the total installed capacity.

1.9.1. Fundamentals of Energy Storage

The fundamental law which is considered as the backbone of all the energy conversions and storage devices is the First law of Thermodynamics i.e. which is Law of conservation of energy which stating that the energy can neither be created nor be destroyed but can be converted from one form to another form of energy (Wu et al., 2019, 2020).

All the electric storage technologies are categorized under different groups on the basis of kind of conversion they possess. These groups are mechanical, electrical, chemical and electrochemical (Kuravi et al., 2013; C. Liu et al., 2010).

1.9.1.1. Electrical energy storage technology

$$G=H-TS \quad (1.0)$$

Here, G is the Gibbs free energy.

H is Enthalpy

T is Temperature and S is Entropy.

This equation represents the maximum amount of electrical work that can be extracted from a storage system (Aricò et al., 2010).

1.9.1.2. Mechanical energy storage technology

$$E_{pot.} = f d \quad (1.1)$$

Where f denoting the force, m is the mass, d is the density and v is velocity (Hall & Bain, 2008).

Potential energy for all the mechanical devices. Kinetic energy is further represented as:

$$E_{kin.} = (1/2) m v^2 \quad (1.2)$$

1.9.1.3. Thermal energy storage technology

$$q = \rho C_p V \Delta T \quad (1.3)$$

Here q is the amount of heat which can be stored in the material with a specific volume represented by V, p is the specific heat (Sarkar & Bhattacharyya, 2012).

1.9.1.4. Chemical energy storage technology

The chemical storage is dependent on the energy associated in the chemical bonds of the fuels which are very strong and provides a high energy density (Hasnain, 1998a).

1.9.1.5. Electrochemical energy storage technology

The energy of the system depends on the charge storage at the electrodes in batteries and electrochemical interface in case of capacitors or super capacitors.

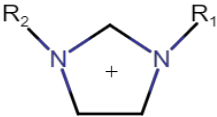
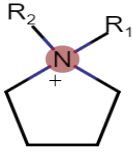
Mathematically, electrochemical conversion is defined as the ration of change in Gibbs free energy with respect to change in enthalpy ($\Delta G/\Delta H$) (Hasnain, 1998b; Ibrahim et al., 2008).

1.10. Energy storage with Ionic Liquids

The molten salts, often referred to as ILs, are composed of organic cations and have properties like ion conductivity, capacitance, a broad electrochemical window, non-flammability, etc. Additionally, it is recognized as a "green solvent" and is regarded as environmentally friendly. Ionic liquids have been utilized in numerous devices, such as fuel cells, super-capacitors, batteries, and dye-sensitive solar cells, to improve their performance. Ionic liquids are commercially viable for energy storage applications (Steinmann, 2017).

Regarding ionic liquids, preliminary characterization was done in order to determine the electrochemical window and stability (D. R. Macfarlane et al., 2014). The following table lists some ionic liquids with excellent stability and a wide potential window:

Table 1.1 : List of some of the Ionic liquids with high potential window.

Chemical Name	Structure
R,R'-Imidazolium	
R,R'-Pyrrolidinium	
Dicyanamide	PF_6^-
p-toluenesulphonate	$C_7H_7 - SO_3^-$
Bis(trifluoro-methane amide)Hexafluorophosphate sulphonyl	$(CF_3SO_2)_2N^-$

Due to specific set of properties including a great thermochemical stability, high potential and energy density they are now being considered as the best alternate in battery chemistries that are already been used like that of Li-ion batteries (Guo et al., 2019). And use of Ionic liquids as an electrolyte in batteries due to their energy capacitance is proven out to be game changing technology in the world of energy storage devices (Che et al., 1998).

One of the main research areas in ESDs is the contribution of ILs in the energy storage applications because of the constant demand of clean and sustainable energy (Plechko & Seddon, 2008). Due to their unique properties like no volatility, high conductance and high thermochemical stability. Ionic liquids almost meet the needs of the various energy storage appliances. So for diverse enhancement and improvements in the specific properties of ionic liquids which make them superior of other compounds to be used as electrolytes and electrodes must be explored (Radousky & Liang, 2012).

One of the main problems faced in case of some batteries now in trend is the explosion. So, this combination of IL and amines has one more advantage regarding this explosion issue. It is very much safe to handle as explosion rates are very low (Safa et al., 2016).

Applications of ILs as electrolytes in Li-ion cells appears to show their specific features, which no other material can easily adopt (Luntz & McCloskey, 2014). As ionic liquids have low coordinating properties, so for the Li-sulfur batteries these low coordinating features are exploited to minimize the dissolution of electroactive material into the electrolytes (Shah et al., 2017). It appears that the absence of electrolyte volatility is a need for Li-oxygen batteries that are exposed to oxygen (air) (Lu et al., 2010).

High stability, ionic conductivity, less toxicity and non-volatility has made the ionic liquids not only suitable for energy storage applications but also considered them on third number as the electrolytes (solvents) followed by water and some organic solvents (Holbrey & Rogers, 2002). Properties possessed by the ionic liquids are mainly because of their composition of cations and anions (Shah et al., 2017; Shi et al., 2016). Vander Wall forces of attraction, interaction and directionality of the cations and anions are the basic cause of the unique properties of these liquids. One of the main properties of ionic liquids which contributes a lot in their characteristic feature to be used in energy storage devices is their melting point (Farres-Antunez et al., 2018). A number of tests were carried out to completely understand the behavior of the ionic liquids, especially some

which have high melting point than the room temperature. One of the best example having melting point about 95°C is $P_{13}PTS$ (Wang et al., 2003).

To clarify, when it comes to ILs, it is important to keep in mind that not all of them have the aforementioned typical qualities. This means that there is room to create new ILs that are tailored to certain tasks (Y. Zhang et al., 2007).

One of the major factors is to look for a highly improved electrolyte as against the presently used electrolytes having certain limitations. IL based electrolytes are more chemically stable, have useable temperature range, high electrochemical stability window, safety and environmental friendly as compared to organic electrolytes (Zu & Li, 2011).

The large temperature windows and wide electrochemical window of ionic liquids makes them more environmental friendly (Dukhin & Goetz, 1996) as well as also enables the electrodeposition of the reducing metals or semiconductors which could not be deposited from the conventional water baths. Also the negligible vapour pressure of ionic liquids avoids the need to work with the autoclaves (Schmidt et al., 2017).

ILs due to their unique properties have the ability to substitute the organic electrolytes in applications where long lifetimes and increased thermal stability are considered as important, (Cui et al., 2020) such as large-scale stationary storage and in direct combination with renewable energy primary production devices.

Ionic liquids have been used for electrochemical applications involving CNT electrodes. CNT has been assembled and used for biosensors as they help in improving the kinetic transfer. The research work done by the Ajajan and his co-workers (Aricò et al., 2010) had found that the electron oxidation was more rapid on CNT electrode in comparison to the other electrodes. Talking about CNT, they have very good electrochemical properties with a high specific capacitance which makes it useful in sensors, super capacitors, electro catalysts and electrochemical actuators. In case of CNTs, the potential window available is limited by the electrolyte because of the inert nature of the carbon (Yu & Chen, 2019). The ability to store the charge determining the performance capabilities is mainly dependent on the inert electrochemical potential window. And recently, ionic liquids are considered as the highest effective electrolyte with a wide electrochemical potential window which makes them useful in photochemical cells and capacitors with a great environmental stability (Augustyn et al., 2013; Dukhin et al., 1996).

1.10.1. Ionic liquid in ESDs

- a) 1, 3-dialkylimidazolium increases the Li-salt stability in Li-ion batteries.
- b) 1-methyl-3-propylimidazolium iodide has the corrosion inhibiting property due to which it is being used for energy storage devices.
- c) N-methyl piperidinium-N-acetate bis (trifluoromethyl sulfonyl) imide is used as an additive for electrolytes in LiFePO₄ batteries.
- d) Bis (trifluoromethyl sulfonyl)imide is used for electric double layer capacitors and solar cells.
- e) 1-butyl-3-propylimidazolium bromide is used in batteries due to high stability and viscosity.
- f) A few protic ILs are used in Vanadium redox flow batteries.
- g) Imidazolium bromide is applicable in removal of micro contaminants to electro polishing of metals.

1.11. Energy storage with Amines

While discussing about amines, they also play an important role in energy storage applications. To examine the role of the amines we have had different groups of amines to specifically know about their merits and demerits of the use of amines in energy storage devices and also how they affect the physical and chemical properties of the energy storage devices (Guerfi et al., 2010; H. Liu & Yu, 2019). Firstly, talking about Tributylamine, this amine is used in energy storage devices as an electrolyte additive which improves the storage stability of the cell by the stabilization of the conductive salt and also is useful in trapping the water and HF in the storage devices (Mashtalir et al., 2015) benzylamine (primary), Dibenzylamine (secondary), Trihexylamine (tertiary) (Roberts et al., 2009) are used as thermal runaway retardants in the Li-ion batteries which are now in trend. They help the storage device to produce extra heat reducing the chances of self-destruction to a bit.

And while talking about these applications we will consider the work done by the S.K. Maritha (Nazir et al., 2019) and the team which identified dibenzylamine (DBA) as an efficient thermal runaway retardant candidate, which are basically embedded in the Lithium-ion batteries while using the thermally triggered thermal-runaway mitigation (TRM) methods. A lot of active TRM techniques and additives are used to increase the internal impedance were investigated while working on LIB got broken apart and released due to the exothermic reaction. And for this, DBA

has considered as an alternate solution and suitable candidate for TRM to stop the breakage (Shi et al., 2016; Song & Zhou, 2013). To completely understand the working mechanism of amine, along with DBA, benzylamine (BA) and trihexylamine (THA) were also examined and out of the two THA comes out to be more efficient than DBA.

Further to get to know about the effect caused by amines on a cell resistance, 2016 coin cells were made using the Nail penetration by using the LIR 2450 batteries which were firstly charged up to 4.3V and then disassembled and reassembled again with open cell cases with two holes which are used to inject the TRR and amines (BA, THA, DBA) and after injecting this a steel nail was penetrated through cell and then the temperature was recorded using the thermocouple and the distance between the nails. (Eftekhari et al., 2016; Eriksson et al., 1984; Ge et al., 2000).

The amines which are kept under considerations have different physical and chemical properties makes the different effect on the ΔT_{max} (Kono, 1978). So based on their properties it was observed that THA is not miscible with electrolyte because of which it forms a blockage in between the cathode- anode using a porous separator. And on the other hand, BA and DBA have the miscible nature with the electrolyte. And further coming to the miscible nature of BA and DBA, they do not block the Li^+ transport. So they decrease the electrolyte conductivity and out of these two DBA reduces conductivity more proficiently than BA (Fahys et al., 1994).

These amines are useful after the multiple charge/discharge cycles by improving the discharge retention.

1.11.1. Amines in Energy Storage Devices

- m)** Tributylamine is used as an electrolyte additive contributing to improvise the storage stability of cell by stabilizing the conductive salt.
- n)** Amines Dibutylamine are used as electrolyte component for Li-ion batteries.
- o)** Octadecylamine because of its corrosive nature are used in the treatment of iron as well as in storage devices.
- p)** Pyrrolidine, Piperidine, Dibutylamine are some of other amines which also have some great energy storage applications.
- q)** Dibenzylamine is used as an efficient thermal runaway retardant (TRR) candidate, which are basically embedded in the Lithium-ion batteries (Galiński et al., 2006; Mashtalir et al., 2015; Nazir et al., 2019).

1.12. Composition of potential Electrolyte

The mostly used batteries now-a-days are Li-ion batteries and the electrolyte for LIB is composed of two components mixture that are ethylene carbonate and dimethyl carbonate and $LiPF_6$ salt (Zhu et al., 2014). The use of this mixture in batteries is found out to be quite dangerous and self-destructive, also a few incidents of self-destructive laptops and mobile phones were witnessed. Also, the salt used gets hydrolyzed during the reaction in storage devices which further leads to the formation of a poisonous chemical HF which has very adverse effects on environment and also is unsafe. To overcome these limitations of the composition used in Li-ion batteries different ionic liquids has been tried as the electrolytes and luckily ionic liquids fulfill the requirement needed for a good battery including high electrochemical and thermal stability, potential and capacitance (Hallett & Welton, 2011).

While talking about the functioning of the batteries, the interaction between the electrodes, the charged molecules and applied electric potential are quite difficult to handle and these interactions plays a specific role in the manufacturing of good, designed electrolyte. Methodology/modelling allow us to study each of the parameter and components separately as well as in the combinations too (Dong et al., 2017; Earle et al., 2006). And to investigate their combination of ionic liquids and amines we also do thermal, transport, conductance and spectroscopic studies which will help us to measure the constants which are essential for the consideration of the suitable electrode material to be used in energy storage devices (F. Li et al., 2018).

1.12.1. Thermodynamic properties

Thermodynamic properties which are related to heat and other form of energy. The term thermodynamics suggests that flow of heat. This study subjects to energy changes that accompany physical and chemical processes. The several thermodynamic properties of a substance, such as its temperature, mass, pressure, thermal conductivity, etc., can be used to explain its state. Both extensive and intensive thermodynamic properties are possible. A system's extensive properties, such as mass, volume, and energy, depend on the quantity of a material being added, but its intensive properties, such as pressure, density, viscosity, etc., are independent of the quantity of a substance being present.

1.12.2. Acoustical properties

Acoustical properties are the properties controlling the response of materials to sound waves, which we further perceive as sound. The acoustic property also indicates the interactions among molecules providing the exact data for molecular interactions, specifically when conductometric data fails to provide the exact interpretation of the interactions.

1.12.3. Conductance studies

Ions can travel through cracks in the crystal lattice of a solid or an aqueous solution through a process known as ionic conduction. Ions are immobile because of their fixed position in the lattice of solid crystals. But ionic conduction rises with rising temperature. While anions, cations, and foreign ions like protons, impurity ions, and dopant ions are carriers of ionic charge, electrons carry the electronic charge. Electrolytic solutions have a particular feature called conductance that controls the type of solvent-solvent, ion-solvent and ion-ion synergies in mixed solvents. These research provide thermodynamic data in the form of association constants, as well as kinetic data in the type of ionic conductivities.

1.12.4. FT-IR spectral studies

A system's interactions can be evaluated with the aid of FT-IR spectral analyses. The vibrations of different atoms within a molecule, which modify the net dipole moment, result in the peak of the infrared spectrum. These spectral studies foretell the bond length change. To confirm the findings of thermodynamic parameters of the synergies present in the investigated systems at various concentrations of the IL and amine are employed, FT-IR spectroscopy has been conducted for investigated system.

1.12.5. Cyclic Voltammetry

Cyclic voltammetry is the method used to measure the current that emerges in an electrochemical cell when the voltage is excessive. Mainly this technique is used to predict the electrochemical properties of the electrode being used which further helps us to conclude whether the electrode being used has the effective electrochemical potential and then further to check the feasibility in the energy storage devices. Also, the cyclic voltammograms are helpful in describing the reduction

peaks to the reduction of the components. And mainly these components are oxygen and water which is already present in the ionic liquids. Not only to measure these electrochemical stabilities but also for the determination of the important data of the electrochemical reactions like locating the electroactive species redox potential voltammetry methods such as Linear sweep voltammetry (LSV) and cyclic voltammetry (CV) mainly used.

In short, understanding the physicochemical features of ionic liquids is essential to maximising their use and constructing appealing ionic liquids. A thorough grasp of the various physical and chemical properties is required before engaging in industrial applications. To predict the distinct parameters that indicate the various interactions, structure maker and structure breaker behaviour of solute in solvents, one can utilise the densities, acoustic, viscosity, and conductance values of the various systems. To determine the equilibrium properties of the mixes, classical and thermodynamic approaches can be combined.

In the investigated system, using various thermodynamic parameters (AMV, PMV, partial molar isentropic compression, partial molar volume of transfer, partial molar isentropic compression of transfer, pair and triplet interaction coefficients) are calculated using density and sound speed values at temperatures (288.15K to 318.15 K). While the concentration of IL is $m_{IL}=(0.001 \text{ to } 0.009) \text{ mol/kg}$, the concentration of benzylamine/ benzamide in range 0.01 mol/kg to 0.05 mol/kg . Additionally, conductivity data is used to look at the nature of a solute's ability to form and break structures in a specific solvent. Additionally, FT-IR spectrum analyses of the ternary mixes (IL + aqueous amine) at various concentrations have been carried out to validate the type of interactions (intermolecular and intramolecular) among the solute and solvent system expected from thermodynamic parameters determined. To investigate the electrochemical properties of the ternary systems, cyclic voltammetry studies has also been carried out.

Chapter 2

Literature Review

2.1. LITERATURE REVIEW

2.1.1. Physicochemical properties of Ionic Liquids

Industries are thriving to manufacture new items which are efficient as well as affordable. In accordance with the principle of green chemistry, it's critical to minimize the possibility for procedural hazards while designing and optimizing a product for technical quality. Green chemistry is a research area for designing novel environmentally friendly solvents to swap volatile organic solvent. ILs are designated as “green solvent “, because of its peculiar properties like reduced vapor pressure, low toxicity, biodegradability, zero flammability, stability, and recyclability. ILs consist of organic cations as well as inorganic anions. Some of the physical properties like chemical, biological and physical properties of ionic liquid can be customized according to the designated process. The provisional level of green solvent given to ILs is due to its low vapor pressure, nil flammability, and stable stability. Another predominance factor needed to be considered is atmospheric contamination (Costa et al., 2017). Dissipation in water raises concerns about its fate. Bioaccumulation, biotoxicity and ecotoxicity correlation of ILs are the areas which need to be investigated. A potential risk of these salts remaining in wastewater and subsequently contaminating aquatic and soil systems as well as live organisms due to lower mineralization of ILs by microbial communities. It has been found that unicellular organism shows different susceptibility and behavior in presence of ILs. It's the alkyl side chain length which affects the environment. Many strategies have been implemented to overcome the drawbacks. Photo electro chemical process methods, some strains like *Sphingomonas paucimobilis* and various chemical degradation processes and be used to improve degradability and removal from wastewater.

The purpose of this research by (Seddon et al., 2000) is to synthesize and characterize a variety of fatty acid-based ionic liquids by evaluating their densities and viscosities at a variety of temperatures. The thermal operating window and phase behavior are investigated, as well as the influence of branched and mono-unsaturated anion on physicochemical parameters. The density drops in the following order: methyl trioctylammonium 4-ethyloctanoate > methyl trioctylammoniumoleate > tetrahexylammonium oleate > tetraoctylammonium oleate, with no

dependence on the total amount of carbons in the IL. The experimental viscosity results reveal that molar volumes and alkane carbons have a linear relationship. The durability of ionic liquids over extended periods of time is seen to be significantly poorer compared to their short-term thermal stability, with a maximum temperature threshold of 363 K.

(Tokuda et al., 2004) prepared room-temperature ILs (RTILs) using 1-butyl-3-methylimidazolium and various fluorinated anions. Thermal behavior, ionic conductivity, density, self-diffusion coefficients and viscosity were observed over a long temperature range. The Vogel-Fulcher-Tamman equation fitted the self-diffusion coefficient, molar conductivity, ionic conductivity and viscosity. The self-diffusion coefficients showed higher values for cations over a wide temperature range.

(Matsumoto et al., 2005) measured vapor-liquid equilibria for binary systems methylcyclohexane–toluene and 1-octene–n-octane, as an entrainer. The addition of ionic liquid increased separation factors, and excess enthalpies were measured for methylcyclohexane and n-octane. Activity coefficients at constant dilution were determined for some solutes in various ILs.

(Anderson et al., 2005) synthesized and then further characterized 39 geminal dicationic ILs for refractive indices, density, viscosity, surface tensions, melting points, and miscibility. These compounds were paired with up to 4 anions and examined for their physicochemical properties. The liquid and thermal stability ranges exceeded conventional ILs, with one pyrrolidinium-based IL having a range of -4 to >400°C. X-ray crystallography showed relation between IL configurational degrees of freedom and melting points/glass transition temperatures. The solvation properties of these ILs were like monocationic analogues.

(Tokuda et al., 2005) Synthesized RTILs by adjusting the alkyl chain length of 1-alkyl-3-methylimidazolium bis(trifluoromethanesulfonyl)imide. Over a large temperature range, the thermal conductivity, thermal expansion coefficient, density, viscosity, and self-diffusion coefficients were all measured. Density decreases linearly with temperature, as do the viscosity,

self-diffusion coefficient, molar conductivity and ionic conductivity. Key physicochemical features of RTILs are determined by the ratio of molar conductivity to ionic diffusivity, which declines with more C-atoms in the alkyl chain.

(Deetlefs et al., 2006) reported a method is to predict ionic liquid densities and surface tensions using the parachor, a surface-tension-weighted molar volume. The parachors of ILs containing 1-alkyl-3-methylimidazolium cations were determined experimentally and calculated using existing parachor contribution data. The molar refractions were also determined experimentally and used to predict refractive indices. Although the errors were higher than parachor predictions, the method shows potential for developing parachor and molar refraction contribution data for ionic liquid physical properties.

(Greaves et al., 2006) The study reports the phase behavior and physicochemical parameters of 25 protic ionic liquids and fused salts, focusing on their properties and ionic behavior. These solvents can be made by combining primary amine with Bronsted acid in a stoichiometric ratio. Although they have inferior ionic behavior compared to aprotic ionic liquids, they offer interesting physicochemical features and could find applications beyond aprotic ionic liquids. The study aims to expand the number of known protic ionic liquids to include nonquaternary ammonium cations and simple organic or inorganic anions.

(Tokuda et al., 2006) discovered that the viscosity of room-temperature ILs is mostly determined by the mole fraction of additional molecular solvents and their identity, allowing them to anticipate viscosity changes during a process. Ionic liquid preparation produces chloride impurities, which dramatically enhance viscosity. The study emphasizes the significance of determining the purity of ionic liquids using methods such as the Volhard method or an ion-selective electrode for chloride and sodium measurement. Ionic solutions include water due to inadequate drying or absorption from ambient air. Water and chloride impurities both have a substantial impact on physical qualities, with chloride contamination increasing viscosity and water or other cosolvents decreasing it.

Purity measurements should always accompany reported physical data. The addition of cosolvents has been studied and fitted to equations for engineering design, with the effect being stronger for higher dielectric constants. Interesting water-ionic liquid interactions have been identified and discussed, and the structural change at the equimolar concentration of water and IL indicates the possible formation of a hydrogen-bonded complex with water.

(Pereiro et al., 2007) measured Density and Sound velocity, viscosity, refractive index, and surface tension of ILs at various temperatures. These parameters were predicted using the Parachor method, and at $T = 298.15$ K, a comparison was done among the experimental and predicted values. The results confirmed the good purity of the ILs synthesized in the laboratory. The dynamic viscosity and refractive index increased with increased alkyl chain of imidazolium cation. The density, speed of sound, and surface tension showed opposite behavior. The authors consider Parachor a reliable predictive method for [BMIM][PF₆] and [OMIM][PF₆] physical properties, but the largest differences were obtained for [HMIM][PF₆].

(Sharma et al., 2008) modified traditional ILs with tunable physicochemical properties, making them versatile and useful in various applications. These properties include viscosity, melting point, density, thermal stability, and miscibility with water and organic solvent. Multifunctional ILs, particularly dicationic and dianionic ILs, have a high range of properties than traditional, single-charged ILs, making them exceptional high temperature and selective gas chromatographic stationary phases.

Hydrophobic ionic liquids (ILs) containing 1-methyl-1-butyl, 1-methyl-1-propyl, 1-methyl-1-butyl, 1-methyl-1-propyl piperidinium, 1-methyl-1-octyl cations and 1-methyl-1-octyl are said to provide new alternatives to pyridinium and imidazolium ILs (Sharma et al., 2008). In applications such as electrochemical devices and rechargeable lithium-ion batteries, its superior heat stability enhances safety. These ILs are hygroscopic but only sporadically soluble in water. Relationships between structure and property may aid in the development of green solvents for certain uses.

(Sharma et al., 2008) examined the physical properties of systems involving imidazolium-based ionic liquids and water, measuring density, viscosity, specific conductance, and surface tension. It finds that solutions' properties change with ionic liquid and water association, alkyl length, and anion polarity.

(Jin et al., 2008) investigated the physical properties of four RTIL containing 1-butyl-3-methylimidazolium cations and bis (trifluoromethyl sulfonyl) imide (TF_2N^-) anions. Electronic structure methods are used for the calculation of properties. Experimental measurements are reported, and correlations are discussed for estimating Hildebrand solubility parameters.

A comparison has been carried out between the protic ILs and equivalent ILs (1R3HIm) that have the same radical in the cation structure and the same anion. It is believed that the weakening of the hydrogen bond and the ion-ion interaction is the cause of the lower melting temperatures of the ILs containing 1R3MeIm cations.

(Zhang et al., 2009) synthesized and characterized a new series of ionic liquids containing three cyclic sulfonium cations and four anions. These liquids exhibit various physicochemical properties, including spectroscopic characteristics, ion cluster behavior, surface properties, phase transitions, thermal stability, density, viscosity, refractive index, tribological properties, ion conductivity, and electrochemical window.

(Zhang et al., 2009) analyzed the structural and physical characteristics of 1-alkyl-3-methylimidazolium bis (trifluoro methane) amide ($[\text{CN}_1\text{C}_1\text{im}][\text{NTf}_2]$) for $N = 4, 6, 8,$ and 10 and contrasted them to those of 1,3-dialkylimidazolium bis(trifluoro methane) amide ($[(\text{CN}/_2)_2\text{im}][\text{NTf}_2]$). Asymmetric IL has greater molecular disparities than symmetric IL. The glass transition temperature changes inversely with the longest alkyl chain's length and the structural heterogeneities' correlation length. Investigations of viscosity demonstrate the even-odd effect and show that the asymmetric IL is more viscous than the symmetric IL.

Ionic liquids are crucial for electrochemical devices and green chemistry applications, often confined in polymer matrices or porous matrices. (Q. Zhang et al., 2009) discussed the science and technological applications of ionic liquids confined in nano-pores, including experimental studies on physicochemical properties, layering, and structural heterogeneity. Basic ideas about ionic liquids and confinement are briefly included.

(Endres, 2010) defined ionic liquids (ILs) as molten salts with low volatility, thermal stability, nonflammability, and high conductivity. Their ionic nature is crucial for characterizing their properties. This study discusses methodologies for assessing ILs' ionic nature, their dependence on polarity scales, structure and physicochemical characteristics, and the effects of different classes and binary systems on ionicity.

(Fumino et al., 2011) synthesized Lactam-based IL through an atom economization process among lactams and Brønsted acids. Density, sound velocity, viscosity was then measured at atmospheric pressure and temperature. Thermodynamic properties like isentropic compressibility and coefficient of thermal expansion were calculated. Lattice potential energy and standard entropy were estimated to assess fluid disorder.

The study by (Chhotaray et al., 2014) investigates the impact of temperature and water addition on physicochemical properties of liquid mixtures containing chromium chloride, choline chloride, and water in a 1:0.5:x ratio. Measurements show that increasing water content decreases density, surface tension and conductivity. The results are interpreted using hole theory, and uniform, grey Cr coatings with high current efficiency can be obtained at temperatures between 40-50°C.

(Rocha et al., 2016) Geminaldi cationic ILs exhibit potential properties compared to monocationic ILs. They can be tuned by structural modifications. 18 dications were synthesized using imidazolium, pyrrolidinium, and phosphonium cations, and 36 dications were synthesized with NTf₂⁻ and PFOS⁻ anions. The study evaluated the effect of structural moieties on physicochemical parameters like solubility, viscosity, thermal stability and melting points.

(Patil et al., 2016) DFT-based computational techniques are superior for discovering enhanced compounds for electrochemical purposes. This study introduces a workflow based on Density Functional Theory (DFT) for the prediction of physicochemical parameters of room-temperature ionic liquids. The workflow involves the screening of 48 pairs of ionic liquids and the subsequent analysis of the obtained data. This paper examines the dynamic features, anticipated electrochemical stabilities and charge in the context of practical applications.

(Karu et al., 2016) Ionic liquids properties are influenced by intermolecular interactions among anions and cations, with hydrogen bonds playing a crucial role in their structure and properties. This paper addresses three questions: whether hydrogen bonds existing in Coulomb fluids, how they contribute to overall interaction, and their importance for physical properties. Imidazolium-based ionic liquids, DSC, DFT computations, viscometry, and quartz-crystal microbalance measurements are some of the experimental and theoretical techniques used in this study. According to the research, hydrogen bonding has a substantial impact on the composition and characteristics of ionic liquids. This means that qualities can be adjusted to operate throughout a wider temperature range, which increases the range of possible uses.

(Bobrova et al., 2016) investigated the physical and electrochemical characteristics of RTILs based on asymmetric amide anions and aliphatic onium cations. The C_1C_2 salts have a lower melting point than TFSI salts but have twice the viscosity. Low viscosity RTILs can be prepared using TSAC anion and tetra-alkylammonium cation.

Highly hydrogen-dense metal borohydrides have been suggested as viable options for on-board hydrogen storage. But their potential for real-world use is limited by the high reaction temperature and slow kinetics. These must be overcome in order improvements have been made to the hydrogen storage qualities in both the thermodynamic and kinetic domains. The electronegativity of M can be used to anticipate and alter the thermodynamic stability of $M(BH_4)_n$. The creation of an intermediate molecule like $M(B_{12}H_{12})_{n/2}$ and the multistep reaction pathway may be responsible

for the high reaction temperature and delayed kinetics. The combination of $M(BH_4)_n$ with other hydrides or metals can be used to prevent the creation of $M(B_{12}H_{12})_{n/2}$. This strategy modifies the chemical route, which enhances the thermodynamic and kinetic aspects of hydrogen storage. It has been established that additives and nanoconfinement are essential for improving reaction kinetics. The requirements for on-board hydrogen storage for fuel cell vehicles cannot be met by any of the materials now available, hence ongoing attempts to create novel materials are necessary. Many $M(BH_4)_n$ have the capacity to release hydrogen at a moderate temperature, according to theoretical predictions, and the slow kinetics are thought to be mostly to blame for the high reaction temperature. In order to succeed practically with metal borohydrides, it will be vital to develop efficient methods to obtain fast reaction kinetics (Sagbas & Sahiner, 2018).

Ionic liquids (ILs) are unique ions-based materials with negligible volatility, a liquid state at various temperatures, and the ability to change based on anion and cation type. Understanding their nature and structure is crucial for successful sorption media use. (Yavir et al., 2020) discusses ILs' chemical and physical characteristics, their applications, and their combinations with various microextraction techniques.

ILs are increasingly being utilized in various chemical sectors as environmentally friendly surfactants, replacing petroleum industry surfactants. Poly-ionic liquids (PILs) are a mixture of polymers with ILs' properties, such as heat stability and salt tolerance. A study on PIL flooding found that it had a lower critical micellar concentration (CMC) than similar ILs, demonstrated good salt tolerance, and long-term thermal stability. PIL also showed low interfacial tension values at crude oil-aqueous interfaces. Core-flooding tests done by (Prathibha Pillai, 2020) showed that PIL increased viscosity with concentration, and after water flooding, 31.25% of the initial oil in place was recovered.

(Poole & Atapattu, 2021) studied room temperature ionic liquids as solvents with favorable environmental and technical features. Gas chromatography offers advantages such as low sample concentrations, high accuracy, faster measurements, and a wider temperature range. It also allows

for determining impure samples' physicochemical properties. Gas chromatography can measure gas-liquid proportion constants, infinite dilution activity coefficients, partial molar quantities, solubility parameters, solvation parameter models, thermal stability, transport properties, and surface properties.

(Chen et al., 2022) synthesized six hydroxy pyridine anion-based protic ionic liquids (PILs) using equimolar proton transfer with superbases DBU or TMG. The physicochemical properties of these PILs were measured, revealing stronger hydrogen bonding and electrostatic interaction in cyclic cations. The CO₂ absorption behavior of PILs was influenced by η , α_p , and alkalinity, with PILs with [2-OP][−] showing superior carbon capture performance. The absorption mechanism showed that CO₂ can combine with O[−] in an anion to create carbonate. By adjusting the structure, it is possible to control their physicochemical characteristics and CO₂ absorption behavior.

For thirteen distinct imidazolium-based ionic liquids, thermodynamic and acoustic parameters were discussed at atmospheric pressure and temperatures in range 293.15 to 343.15 K by the (Aljasmí et al., 2022). Viscosity is the attribute most affected by temperature change, with all other properties generally decreasing as expected as the temperature rises. The well-known Vogel–Flutcher–Tamman equation is used to correlate viscosity, whereas linear correlation is used to determine density. With the experimental density data, the associated coefficients of thermal expansion were computed. Moreover, the isentropic compressibility was computed using the Laplace–Newton equation. The empirical Guggenheim equation was used to calculate the critical and boiling temperatures. Additionally, the impact that the various ionic liquids' alkyl chains have on the thermophysical parameters that have been measured is examined.

(Igor Baskin & Alon Epshtein, 2022) aimed to determine the best machine learning techniques and molecular representations for QSPR models for predicting the properties of ionic liquids (ILs). The study included 407 to 1204 ILs with different organic and inorganic ions. The models were constructed using multitask learning and ranked based on properties. The results showed that

nonlinear ML techniques outperformed linear ones, neural networks outperformed classical ML techniques, and transformers outperformed other neural network types.

(Ohta et al., 2023) compared the physical properties of three synthesized ionic liquids (ILs). The results showed that $[P_{222}(2O_2)][NF_2]$ had the lowest glass transition temperature and viscosity, while $[P_{222}(2S_2)][NF_2]$ had the highest density and surface tension. The study suggests using both fs-RIKES and THz-TDS approach are for revealing molecular motions.

Surface active ionic liquids (SAILs) are intriguing options for a variety of applications because they combine the beneficial properties of both surfactants and ionic liquids (ILs). It is unclear how SAIL ionic topologies affect their physicochemical characteristics, which restricts their absorption. In this paper, to close this knowledge gap, (Ávila et al.,2023) examined the gas absorption and corresponding critical micelle concentration, density, viscosity and surface tension of SAILs with different cation and anion configurations in water. Because linear alkyl chains are more densely packed due to increased interdigitation, SAILs containing anions with linear alkyl chains have smaller molar volumes than those with branched alkyl chains. SAILs are also roughly two orders of magnitude more viscous than equivalent conventional ILs as a result of this interdigitation. Compared to traditional ILs, SAILs at the liquid–air interface cause low surface tensions by orienting alkyl chains toward the air. Surface tensions of all SAILs might be used to predict critical temperatures of approximately 900 K. Like traditional surfactants in water, SAILs dissolve in water and adsorb at the liquid-air interface, lowering the surface tension and causing micelles to form. The micelles are spherical, as demonstrated by molecular simulations, and aggregates containing more ion pairs form at lower critical micelle concentrations. After examining the absorption capacities of N₂ and CO₂, we find that ionic liquids with bigger non-polar domains may absorb more of both gases.

Over the past 20 years, extensive research has focused on ionic liquids (ILs) in various industries. (Albayrak, 2024) aimed to understand their physicochemical characteristics, specifically focusing on the antibacterial properties of o-phosphoric acid (PA) and N-methyl pyrrolidone (NMP). Using

FT-IR, ^1H NMR, ^{31}P NMR, and DSC analysis, the synthesized NMP-PA IL was found to have higher viscosity than imidazolium-based ILs.

Various thermodynamic parameters for $[\text{C}_n\text{mpyr}][[\text{NTf}_2]]$ ($n = 3, 4, 6, 8$), $[\text{C}_n\text{mpyr}][[\text{N}(\text{CN})_2]]$ ($n = 3, 4$), $[\text{C}_n\text{mim}][[\text{N}(\text{CN})_2]]$ ($n = 2, 4$), and $[\text{B}_n\text{zmim}][[\text{N}(\text{CN})_2]]$ were measured and discussed at temperatures 293.15 to 343.15 K by (Aljasmi et al., 2024). All parameters decrease with increasing temperature as predicted; the attribute most impacted by this change is dynamic viscosity. The density, sound speed, surface tension, and refractive index are determined using linear correlation as a function of temperature, whereas the dynamic viscosity is related using the well-known Vogel–Fulcher–Tamman equation. The physical properties of the ionic liquids under study are mostly influenced by the type of anions, variation in the alkyl chain having less of an impact, according to the findings.

Isoniazid, a medication used to treat tuberculosis, is susceptible to hydrolysis, leading to harmful hydrazine. To improve its stability and solubility, five choline ionic liquids (ILs) were used by (Carla Luzia et al., 2024). The powdered forms showed poor solubility, while the INH: $[\text{ChBenz}]$, INH: $[\text{ChBis}]$, and INH: $[\text{ChAc}]$ forms had minimal inhibitory concentrations. The ILs directly impacted isoniazid's solubility, conformational structure, and stability. This research is relevant to drug crystallization.

2.1.2. Classification and applications of Ionic Liquids

(Bradaric et al., 2003) has focused on imidazolium ionic liquids, but few investigations have been conducted on phosphonium ionic liquids. Patent literature claims the manufacture and use of phosphonium ionic liquids, but commercial applications have not yet materialized. This research aims to develop a large-scale producer of ionic liquids for industrial applications, discussing synthesis, physical characteristics, and comparing them to imidazolium systems.

(Paul et al., 2005) examined the suitability of RTIL based on substituted imidazolium cations for optical applications. These liquids exhibit fluorescence in the UV or early visible region, with excitation wavelength dependence. However, these liquids lack in a few optical studies.

(Paul et al., 2005) studied tetra-alkylphosphonium-based amino-acid ionic liquids (AAILs) which exhibit lower viscosities and higher decomposition temperatures compared to ammonium-based ILs. AAILs are halogen-free and designer ILs, with solubility and thermal properties influenced by side chains.

(Abbott et al., 2007) measured conductivity, viscosity, density, and surface tension in glycolic mixtures with choline chloride, fitting to hole theory. The dominant charge mobility mechanism is hole mobility at a ChCl mole fraction of approximately 0.2.

(Ribeiro et al., 2009) analyzed heat capacity and thermal conductivity of ionic liquids and MWCNTs-ionanofluids as a function of temperature. The thermal conductivity data are in good agreement with reported data, with an estimated uncertainty of 1%. Ionanofluids show moderate increases in thermal conductivity and a weak dependence on temperature. The specific heat capacity of ionic liquids is consistent with literature values. An enhancement of up to 8% was found for [C₄mim] [PF₆] with MWCNTs, a first for nanofluids. Further studies will explore nanocluster formation and preferred heat transfer and storage paths.

(Govinda et al., 2011) analyzed parameters of binary systems of dimethylsulfoxide (DMSO) with ionic liquids (ILs) at temperatures ranging from 298.15 to 328.15K under atmospheric pressure and then further predicted the parameters. The study uses the Redlich-Kister polynomial to correlate results. The intermolecular synergies and structural effects are observed, focusing on ion-pair interactions, ion-dipole and H- bonding between ILs and DMSO molecules.

(Qiao et al., 2012a) studied a new series of ionic liquids, consisting of alkyl(alkenyl)trifluoroborate and 1-ethyl-3-methylimidazolium anions with low-viscosity, hydrophilic nature and low-melting

were synthesized and characterized. These salts showed phase transition behavior and variation in thermodynamic parameters, which were influenced by structural variations, such as length and fluorination, influenced their properties.

(Qiao et al., 2012b) studied thermophysical and transport characteristics of IL which are crucial for process design, but experimental data is scarce and often contradictory. Group contribution methods were developed to estimate few parameters using literature data. These models provide accurate predictions of property values for ionic liquids and can be extended to new cations and anions groups.

(Govinda et al., 2013) thermophysical characteristics of ammonium cation with -OH anion and 1-alkyl-3-methyl imidazolium cation with various anions were assessed. Densities, ultrasonic sound velocities, and viscosities across the entire content range and across all four temperatures are measured. The Redlich-Kister polynomial equation is utilized to determine the relationship between the excess volume by mass and the divergence in viscosity.

(Singh et al., 2014) examined synergies among acetonitrile and imidazolium-based ionic liquids (ILs) using density and sound velocity data under various temperature and concentration. These results aid in understanding structure-property correlation between ILs and intermolecular interactions.

(Wojnarowska & Paluch, 2015) studied protic ionic liquids (PILs) are crucial materials for emerging technologies, particularly fuel cells. Recent research focuses on their dielectric properties at ambient and elevated pressure, using broadband dielectric spectroscopy to recognize conductivity mechanisms. This paper summarizes recent progress in this field.

(Chennuri et al., 2015) measured density and sound velocity data for binary solutions of protic ionic liquids (PILs) with water and ethanol. The Redlich-Mayer equation was used to calculate V_ϕ and K_ϕ values, indicating stronger ILs-ethanol synergies than IL-water synergies. The

thermodynamic properties of these mixtures were explained based on anion structural contribution of protic ionic liquids.

(Anvari et al., 2016) investigated the antimicrobial and anti-adhesive properties of various 1-Butyl-3-methylimidazolium ionic liquids (ILs) against various pathogenic bacteria. The ILs were evaluated using various techniques, including agar disk diffusion, agar well diffusion, and MIC analyses. The strongest antibacterial activity was found in [OMIM][NO₃], while HMIM[NO₃] showed the best antibacterial activity. HPY[NO₃] was the strongest growth inhibitor among pyridinium-based ILs. The study found that not all ionic liquids exhibit anti-adhesive activity.

(Gruzdev et al., 2017) thermophysical characteristics of ammonium and imidazolium cation with various anions were assessed. Ammonium-based ILs, 1-ethyl-3-methylimidazolium chloride, and triethanol ammonium-based protic ILs were used in their synthesis. The PILs were characterized using ¹H NMR, ¹³C NMR, ¹H/¹⁵N NMR, and FT-IR spectroscopic methods. The study also investigated the temperature dependence of conductivity and electrochemical window of each PIL.

(Boruń, 2019) analyzed conductometric studies on ionic association and solvation processes of imidazolium ionic liquids, focusing on 1-ethyl-3-methylimidazolium tetrafluoroborate and 1-butyl-3-methylimidazolium tetrafluoroborate. It examines temperature, solvent structure, cation and anion effects, ion transport processes, and thermodynamic properties.

According to (Nasirpour et al., 2020) Ionic liquids (ILs) have gained interest since their introduction in 1914 due to their unique properties. These organic salts are non-volatile and nonflammable and can be synthesized through the combination of anions and cations. ILs are suitable for various chemical processes and applications, including separation processes, lignocellulose pretreatment, enhanced oil recovery, biocatalytic reactions, lubrication, and electrochemistry.

Ionic liquids (ILs) are gaining attention as solvents in biochemistry due to their beneficial properties and availability in various variants. (Shukla & Mikkola, 2020) offer directional and non-directional forces towards solute molecules, allowing them to interact with polar/non-polar solutes like proteins and DNA. These interactions help understand their structure and functioning, which have implications in biomedical applications. ILs are hydrophilic and hydrophobic, maintaining their integrity over long-range temperatures. Their ability to stabilize protein or DNA structures depends on their ranking in the Hofmeister series. The ability of ionic liquids to promote DNA coiling and uncoiling depends on basicity, electrostatic interaction, and hydrophobicity. These changes in DNA structure have implications for biosensor design and targeted drug delivery in biomedical applications.

The chemical industry is increasingly seeking environmentally friendly alternatives to toxic and volatile solvents, such as supercritical carbon dioxide and ionic liquids. These compounds are used as green catalysts in chemical reactions and advanced material construction. (Ehsan Kianfar & Sajjad Mafi, 2020) discussed the structure, cation, anion types, and synthesis methods of IL, as well as their main application areas and basic applications.

Ionic liquids (ILs) have significantly impacted research and technology in the last 20 years, offering a clean, efficient, and environmentally friendly alternative to volatile organic solvents. They can change their properties based on usage, and standard synthesis techniques are needed for consistent reproducibility. However, the main challenges include large-scale industrial yields, toxicity, and environmental friendliness. (Tingting et al., 2022) explores recent research on homogeneous and heterogeneous ILs, their purity, environmental effects, and green characteristics. ILs have potential applications in electrochemistry, solvent engineering, catalysis, biological assistance, physical chemistry, and analytical chemistry.

(Yimei et al., 2023) examined the thermal stability, structural characteristics of ionic liquids based on active medicinal components. The first ionic liquids were lidocaine-based, with salicylate and ibuprofen as counterions. The structures were verified using infrared, mass, ^1H , and ^{13}C spectroscopy. DFT and MD calculations were performed to understand the structural organization.

2.1.3. Ionic Liquids in Energy storage devices:

(Cho et al., 2012) synthesized Graphene oxides using the modified Hummers method, resulting in fully exfoliated GOs dispersed in deionized water. Reduced GOs were reduced into reduced graphene oxide (RGO) using a hydrazine solution. IL-functionalized RGOs were prepared by mixing RGOs with ILs, and their electrochemical properties were measured using four ILs.

(Vatamanu et al., 2013) explored the Molecular dynamics simulations as potential pathways to increase energy storage in electric double-layer (EDL) supercapacitors using room-temperature ionic liquid electrolytes and carbon-based nanostructured electrodes. A comparison of capacitances shows that electrode curvature and surface roughness improve capacitive storage. Nanoconfinement in conductive electrode pores enhances capacitance due to mismatches in ion-electrode interactions. These nano-porous structures generate non-Faradic capacitance from 260 to 350 F/g, surpassing current nanostructured electrode performance.

(Eshetu et al., 2014) reviewed ionic liquids (ILs) as eco-friendly and promising reaction media for electrochemical energy storage. They are suitable for functional advanced materials, materials production, and preparing highly engineered functional products. This Review reviews IL-based green synthesis processes for batteries, supercapacitors, and green electrode processing, assessing the status of research and stimulating new ideas.

(Chakrabarti et al., 2014) Deep eutectic solvents (DESs) and ILs have been employed in a variety of applications, including lithium-ion batteries, electrodeposition, electropolishing, and fuel cells. Sandia National Laboratories recently suggested metal ion based ILs. This paper looks at the possible uses of DESs in renewable energy storage and utility-scale load levelling. It also highlights Sandia National Laboratories' findings on employing ILs as electrolytes for RFBs, as well as the viability of replacing ILs with DESs in the near future.

(Xue et al., 2015) discussed a novel energy storage approach utilizes ionic liquids as a joint ion-conducting medium and redox active catholyte material. Earth-abundant ferric ion is used as an oxidizing agent in a 1:1 mixture with ethyl methyl-imidazolium-tetrachloroaluminate. The cell's high voltage and cyclability are confirmed, and it achieves an unexpected energy efficiency of over 96% at 180°C. This cell is a promising area for future research in energy storage.

(Vatamanu et al., 2015) discussed the enhancement of non-Faradaic charge and energy density in nanostructured electrodes is crucial for energy storage in electric double layer capacitors. Molecular dynamics simulations reveal atomistic mechanisms and correlations between electrode/electrolyte structures, leading to capacitance enhancement. Symmetric electrode setups with smooth nanopores show up to 50% capacitance increase, while asymmetric electrodes and rough surfaces show substantial enhancement. Nano-porous electrodes can be increased through screening ionic interactions and optimizing nanopore structure to account for cation and anion chemical structures.

(Hernández et al., 2017) explored new polymeric materials like polymer electrolytes and redox polymers to enhance electrochemical energy storage devices like batteries. Redox-active counter anions, such as anthraquinone and nitroxide, can be incorporated into poly (ionic liquid)s, broadening their applications in various energy storage technologies. This simple anion exchange reaction enables the synthesis of these materials, which can be used in various electrochemical energy storage technologies, including lithium batteries, organic redox flow batteries, metal-air batteries and fuel cells.

(R. Singh et al., 2017) presents the synthesis, characterization, and dual electrochemical application of a new ionic liquid-based polymer electrolyte. The ionic liquid [DMPIm][TFSI] and polymer PVDF-HFP enhance electrical conductivity by several folds. The synthesized thin film and electrode show uniform surface morphology. The material is highly stable and reliable for long-term energy devices.

(Tsuda et al., 2017) reviewed the advancements in electrochemical technology using Lewis acidic halo-aluminate room-temperature ionic liquids (RTILs) and new chloroaluminate mixtures. The field has seen steady growth, with researchers now handling halo-aluminate RTILs and their mixtures more easily. Current research focuses on electroplating and energy storage, with new findings and insights gained through state-of-the-art technologies.

(Watanabe et al., 2017) discussed ILs as molten salts with melting points $< 100^{\circ}\text{C}$, with potential applications in conversion materials, energy storage and devices. They are used as electrolyte materials for Li-sulfur batteries, Li/Na ion batteries, non-humidified fuel cells and Li-oxygen batteries. ILs possess high ionic conductivity, nonvolatility and high thermal stability and making them suitable for various applications. However, further research is needed to explore unique applications that require ILs' unique properties.

(Martins & Torresi, 2018) reviewed ILs are liquids with low melting points and potential applications in electrochemical energy storage and conversion because of their high thermal stability and low vapor pressure.

(Stettner et al., 2018) electrolytes for electrochemical energy storage systems like supercapacitors and lithium-ion batteries, ionic liquids (ILs) have been given serious consideration. However, further research is required to fully comprehend their potential benefits and drawbacks. Mechanical and physical attributes of combinations of bis(2-methoxyethyl) ether diglyme (2G) and the ionic liquids $[\text{Pyr}_{14}] [\text{TFSI}]$ and $[\text{PyrH}_4] [\text{TFSI}]$ are investigated. The findings indicate that these combinations hold great potential for use in cutting-edge sodium-based electronics.

(Doherty, 2018) discussed the recent developments show the potential of incorporating redox functionality into IL structure for energy applications. This shift from pure materials to redox solutes in IL-based electrolytes and ionic conductive components in electrochemical devices opens up a wide range of potentially useful materials.

Ionic liquid electrolytes, paired with target ion salts, have gained interest as advanced electrolytes for sodium chemistries. (Basile et al., 2018) examined their unique properties, structure-property relationships, salt addition effects, cation and anion functionalization, and their impact on physicochemical and thermal character. The authors discuss the use of ionic liquid electrolytes paired with organic solvents and the impact of water as an additive. The research focuses on super concentrated sodium electrolytes with higher Na^+ concentrations, improving device performance and target ion mobility.

The European Project RENAISSANCE-ITN aimed to develop innovative polyelectrolytes for energy and environmental applications. (Basile et al., 2018) synthesized various types of polyelectrolytes, including renewable or natural ions, thiazolium cations, catechol functionalities, and cheap deep-eutectic monomers. The project led to significant advances in energy storage technologies, including carbonaceous materials, lignin/conducting polymer biopolymer electrodes, and ionicels for supercapacitors and batteries.

(Thangavel et al., 2018) discussed the development of high-energy, long-cycle supercapacitors using sustainable materials is crucial for next-generation applications. Watermelon rind, a bio-waste from watermelons, can be used to create ultra-stable high temperature green supercapacitors with a high-voltage ionic liquid electrolyte. These supercapacitors exhibit remarkable performance at room and high temperatures, with maximum energy densities of 174 Wh kg^{-1} and 177 Wh kg^{-1} at 60°C . These results show the potential for eco-friendly, high-performing, green energy storage devices for electric vehicles and other advanced energy storage systems.

(Yan et al., 2018) used salt-templated carbons with altered pore structures and nitrogen-doped analogues as model systems to study ion migration dynamics and energy storage in hierarchical pore structures in electric double-layer capacitors. Structural changes in the ionic liquid electrolyte strengthen charge storage beyond expectations. A quantitative model of the structure-dynamics relationship is proposed, with an optimal ratio of mesopores to micropores of 3:1 in pore volume. Nitrogen doping improves rate capability rather than energy storage.

(Wu et al., 2019) explored absorption thermal energy storage (ATES) systems utilizing H₂O/ionic liquid (IL) mixtures as novel working fluids to neglect the problems related to crystallization. ILs are compared for dynamic charging or discharging features and whole cycle performance. The best-performing IL is [DMIM][DMP], with the highest COP and ESD of 149.5 kW h/m³ in the investigated operating conditions.

Due to excellent optical qualities and extremely biocompatible makeup, carbon dots CDs have proven to be more advantageous materials than the hazardous metal-based quantum dots, making them essential materials, particularly for biological environments and living beings. The effects of the synthesis procedure, precursors, and the use of hetero atoms on the characteristics and uses of CDs were exposed. The hydrothermal and microwave treatments were discovered to be the most widely used CD synthesis processes due to their usefulness, affordability, and ability to generally produce nontoxic byproducts and uniform particle sizes while providing CDs with excellent optical properties and high quantum yields. Additionally, by altering the reaction conditions, such as the reaction time, reaction temperature, and the types and concentrations of precursor molecules in these procedures, it is possible to influence the PL behavior of the CDs (Guo et al., 2019).

(Kar et al., 2019) studied the development of alternative, cost-effective, dependable, and sustainable renewable energy storage technologies is necessary to cut down on the world's consumption of fossil fuels. Many energy storage applications, including electric vehicles (EV), have shown a great deal of interest in high-energy density devices such rechargeable lithium and magnesium batteries. However, using standard high-flammability electrolytes poses a safety risk to batteries and restricts the use of several high-voltage cathodic and low-voltage anodic materials. Therefore, for the next generation of high-energy density batteries, the demonstration of nonflammable and thermally stable electrolytes with large electrochemical windows is important.

(Stettner et al., 2019) investigated the properties of water-in-PIL (protic ionic liquid) electrolytes, specifically 1-butylpyrrolidinium bis (trifluoromethane sulfonyl) imide (PyrH₄TFSI). The amount

of water inside the electrolyte significantly impacts its properties, including viscosity, conductivity, density, cation-anion interaction, and electrochemical stability. Water improves transport properties and capacitance retention in EDLCs but reduces operative voltage and affects inactive components. To achieve high stability, inactive components in an aqueous environment is necessary.

(Wu et al., 2020) explored ATES utilizing ionic liquids (ILs) for renewable/waste energy utilization in buildings. 7 ILs are feasible for ATES working fluids, while 4 ILs (DMIM, EIM, DEP, and EtSO₄) are selected for detailed comparisons. Results show that LiBr's operating temperatures are constrained by limiting COPs, crystallization, and ESDs under lower condensation temperatures and higher generation.

Promising anode candidates for energy storage technologies include liquid metal and alloy systems at room temperature. When compared to solid state electrodes, the LM anodes are innately dendrite free or exhibit self-healing qualities because of the fluidic and malleable characteristics of liquid metals. The well-known Na-K and Ga-based fusible alloys might offer low reduction potential for high battery voltage, high battery capacity, and high energy density, and the quick mass/charge transit in the liquid anodes would help achieve high power. Fusible alloys don't require as much energy to maintain the molten state as high-temperature liquid metal anodes, which helps to reduce costs, increase energy transfer efficiency, reduce the risk of corrosion from high temperatures, and improve battery safety. We can build the substrate using the distinctive wetting behavior of the liquid metal, which varies depending on whether an oxidation layer is present or not, and the induction of the conversion reaction. The liquid metal's flexibility and fluidity may also make it possible to use LM anodes in stationary flow batteries and flexible batteries. The LM anode-based anodes may satisfy diverse requirements by constructing various battery types, including alkali-alloy-based batteries (Na-K), ga-alloy-based alkali ion batteries, supercapacitors, and hybrid-cation batteries (Gonçalo A. O. Tiago 1 & 2, 2020).

(Karuppasamy, Vikraman, et al., 2020) Ion exchange condensation was used to create a brand-new, large, fluorinated anion-based ionic liquid called 1-ethyl-3-methylimidazolium bis (nonafluorobutane-1-sulfonyl imidate) ($\text{Im}_1, {}_3\text{BNFSI}$). This liquid is used to prepare electrolytes. Lithium bis (nonafluorobutane-1-sulfonyl imidate) salt, propylene carbonate, and dimethoxy ethane solvents were used to generate non aqueous liquid electrolytes, which were then taken into consideration for use in lithium-ion batteries. For the produced electrolytes, the highest electrical conductivity of 2.21 mS/cm^1 and the widest electrochemical stability window (4.3V) were achieved. LiFePO_4 / ionic liquid electrolytes/Li coin cell achieved the highest specific capacity ($132.75 \text{ mA h.g.}^{-1}$), indicating that they are a promising candidate for high performance lithium-ion batteries.

ILs have potential as green solvents and liquid electrolytes for renewable energy storage devices like lithium ion batteries (LIBs) and supercapacitors (SCs). (Karuppasamy et al., 2020) presents the state-of-the-art electrochemical, cycling, and physicochemical properties of ILs, as well as their potential as designer solvents for replacing flammable organic carbonates and improving energy storage performance. It highlights emerging challenges and opportunities for IL-based energy devices and the design of new structures for energy and environmental applications.

(Jónsson, 2020b) discussed IL as electrolytes for energy storage devices. This text discusses various modeling approaches, experimental results, theoretical developments, molecular dynamics simulation options, and initial work on ionic liquids and electrolyte formulations.

(Stettner et al., 2020) investigated aprotic and protic ionic liquid (IL)-based electrolytes for calcium-based energy storage systems. They show good transport properties and electrochemical stabilities, comparable to IL-based electrolytes for lithium and sodium-based systems. They are used in electrochemical double layer capacitors for high reversibility and stability.

Electrolytes and electrodes have improved over time, leading to the development of electrochemical energy storage devices. The interaction between electrodes and electrolytes

determines energy storage ability and safety.(Kim et al., 2021) reviews the electrochemical and physicochemical characteristics of Li-ion batteries and supercapacitors using ILs and introduces recent energy storage device ILs.

Ionic liquids (ILs)-based gels have become a research hotspot, combining gel properties with intrinsic ILs properties. (Gao et al., 2021) divided into three types: ILs hydrogels, ionic gels synthesized by high-molecular organic polymers, and ILs acting as both the continuous and dispersed phases. These gels have applications in energy storage, sensing, electrochemical devices, antibacterial, and gas capture. Different synthesis methods have different performance and applications. This review provides the latest developments on ILs-based gels, perspectives on various applications, and challenges to be aware of in this field.

(Miao et al., 2021) reviewed ionic liquids (ILs) as widely used in energy storage systems, particularly supercapacitors, due to their high-rate energy harvesting and long-term durability. ILs offer low vapor pressure, molecular designability, and features like ionized environments, thermal/chemical stability, and universal solubility/affinity. Three types of IL-based electrolyte components are used, including neat IL electrolytes, mixtures, and quasi-solid-state electrolytes. ILs also play a role in material science as microstructure-directing agents, heteroatom dopants, and carbon precursors, enhancing interfacial physicochemical interactions and addressing challenges for next-generation supercapacitor applications.

(Stettner & Balducci, 2021) discussed the development of safer electrolytes for modern electrochemical energy storage devices, focusing on protic ionic liquids (PILs). It compares their characteristics, syntheses, benefits, and drawbacks to aprotic ionic liquids. The article analyzes PILs' use in supercapacitors and batteries and presents challenges for improving and expanding their use in energy storage devices.

(Xu et al., 2021) considered ionic liquids are promising electrolyte solvents or additives for rechargeable batteries and supercapacitors due to their superior physical and electrochemical

properties. A roadmap is needed to discuss progress, techniques, opportunities, and challenges in ionic liquid electrolytes for rechargeable batteries and supercapacitors. Optimizing these electrolytes for energy storage requires considering native chemical/physical properties and roles. This roadmap will guide future research in ionic liquid electrolytes for rechargeable batteries and supercapacitors.

2.1.4. Amines in Energy Storage Devices

(Chen et al., 2020) introduces a novel arylamine connection for covalent organic frameworks (COFs), leading to the creation of two new arylamine-linked COFs (AAM-TPB and AAM-Py). These COFs, which have a similar appearance to polyaniline, have excellent performance in storing pseudocapacitive energy. They have a high capacitance of 271 F/g when tested using a three-electrode setup at a discharge rate of 1 A g^{-1} .

(Kaiqi Jiang & Hanming Liu, 2023) demonstrated the utilization of fatty amines (FAs) as innovative organic materials that undergo phase change (PCMs) for the creation of composites with high energy density, known as FSPCM. The composites, known as FAs/GS, exhibit a high latent heat and a low supercooling degree, with a loading rate ranging from 7063 to 10660 wt%. GS, or graphene sheets, increase thermal conductivity, and even after 200 cycles, the amount of stored heat remains high. This research presents new possibilities for utilizing FAs as efficient organic phase change materials (PCMs) and showcasing their promise for energy-conserving applications.

(Song & Zhou, 2013) introduces an innovative thermal energy storage system called amine-based thermal energy storage (ATES). This system utilizes a thermally reversible reaction between amine and CO_2 to generate thermal energy of superior quality. The ATES system surpasses water-based sensible thermal storage technology in terms of heat output, conversion efficiency, energy density, and long-term storage capacity. It is economically feasible and has potential uses in heating buildings and storing waste heat from industries.

Organic electrode materials provide a sustainable and flexible option as a substitute for inorganic intercalation electrodes. These materials possess excellent electrochemical properties, flexibility, processability, and a wide range of structures, making them highly suitable for various ESDs such as supercapacitors, rechargeable lithium/sodium batteries, aqueous rechargeable batteries, thin film batteries, all-organic batteries and redox flow batteries. (Dubois, 2014) presents a comprehensive review of the historical progression and practical uses of organic electrode materials.

Molecular electrocatalysts play a vital role in storing and utilizing energy from intermittent renewable energy sources. The development of these themes involves three key aspects: the categorization of catalysts into first, second, and outer coordination spheres based on their conceptual partitioning, the creation of thermodynamic models to prevent the formation of high- and low-energy intermediates, and the regulation of proton movement during electrochemical fuel generation and utilization reactions. (Xiaoyin Cao et al;2020) involved the inclusion of pendant amines in the second coordination sphere, which enables the breaking and creation of H–H bonds, as well as the combination of proton and electron transfer processes. Comprehending the mechanisms of these proton-transfer processes and the obstacles they encounter is crucial in order to develop molecular electrocatalysts that are both faster and more effective for the purpose of energy storage.

(Z. Yang et al., 2021) introduced a novel composite phase change materials (CPCMs) device has been created by depositing ZnO nanorods on indium tin oxide glass and filling it with fatty amines. The gadget demonstrates exceptional efficiency in converting light energy into heat energy, reaching a peak of 90.2% at an intensity of 1 sun. The nanorod structure, which is aligned vertically, minimizes both tortuosity and heat reaction time in a unique way. The device has a high electro-to-thermal conversion efficiency, achieving a maximum of 69.8% at low voltage. This platform has the potential to be an optimal solution for applications involving the storage and conversion of solar energy.

A new MOF has been synthesized by (Jia Zhang et al; 2023) utilizing a manganese-based compound, specifically $\{\text{Mn-Ni-NH}_2(\text{h}_2\text{fipbb})\}$ MOF. The material has a distinct hierarchical topology that facilitates effective penetration of electrolytes and transmission of electrons. With a specific capacitance of 711.60 Fg^{-1} and high-power and energy density of 743.99 Wkg^{-1} and 20.49 Wh kg^{-1} , respectively, this material shows great potential for use in electrochemical energy storage applications.

(Jun Yang et al; 2023) has created a novel composite phase change material (PCM) called CuOHS-PCMs, which is designed for energy storage and conversion. The material achieves this by absorbing fatty amines from multishell metal oxide hollow microspheres (CuOHS). The composite phase change materials (PCMs) possess latent heats of 198.8, 192.6, and $196.0 \text{ J}\cdot\text{g}^{-1}$. These PCMs demonstrate favorable thermal characteristics and achieve photothermal conversion efficiencies of 84.0, 81.4, and 78.0% when exposed to light. As a result, they hold promise for applications in photothermal conversion, solar energy harvesting, and storage.

The objective of this study by (Hartani Mohamed et al; 2023) is to enhance the solubility, restricted capacity, and lifespan of tiny organic compounds in aqueous proton batteries (APBs). Quinone-amine polymer nanospheres (PQANS) were created by combining 3,3'-diaminobenzidine with benzoquinone. This process led to an enhancement in both the ability to store and release energy and the long-term stability of the nanospheres. The anode of the PQANS exhibited a specific capacity of 50.6 milliampere-hours per gram at an applied current density of 1 ampere per gram, over the course of 600 cycles. This finding serves as a benchmark for the development of superior polymer-based electrode materials in aqueous batteries.

Chapter 3

Experimental

3.1. MATERIALS

In this chapter, complete details of the experimental work including chemicals used, synthesis of the ILs, purification and characterization of the synthesized IL along with the various techniques used to carry out the experimental work has been discussed.

Table 3.1 Details of chemical used during experimental work.

S.No.	Chemicals	Molecular Formula	Provenance	CAS number	Molecular Mass	Mass fraction purity ^a
1	1-butyl-1-methyl pyrrolidinium iodide	C ₉ H ₂₀ IN	Synthesized in Laboratory	5611-17-2	269.17	≥0.92 ^b
2	1-butyl-1-methyl pyrrolidinium tetrafluoroborate	C ₉ H ₂₀ BF ₄ N	Sigma Aldrich	345984-11-4	229.07	≥0.99 ^a
3	1,4-dimethyl-4H-1,2,4-triazolium iodide	C ₄ H ₈ IN ₃	Sigma Aldrich	120317-69-3	225.03	≥0.99 ^a
4	1,4- dibromobutane	Br (CH ₂) ₄ Br	Sigma Aldrich	110-52-1	215.91	≥0.99 ^a
5	1-ethyl-3-methyl-imidazolium iodide.	C ₆ H ₁₁ IN ₂	Synthesized in Laboratory	35935-34-3	238.07	≥0.95 ^b
6	1-methylimidazole	C ₄ H ₆ N ₂	Sigma Aldrich	616-47-7	82.10	≥0.99 ^a
7	Acetonitrile	CH ₃ CN	HIMEDIA Laboratories Pvt. Ltd. India	75-05-8	41.05	≥0.99 ^a

8	Benzamide	$\text{C}_6\text{H}_5\text{CONH}_2$	HIMEDIA Laboratories Pvt. Ltd. India	55-21-0	121.14	$\geq 0.99^a$
9	Benzylamine	$\text{C}_6\text{H}_5\text{CH}_2\text{NH}_2$	HIMEDIA Laboratories Pvt. Ltd. India	100-46-9	107.15	$\geq 0.98^a$
10	Diethyl ether	$(\text{CH}_3\text{CH}_2)_2\text{O}$	Sigma Aldrich	200-467-2	74.12	$> 0.98^a$
11	Ethyl iodide	$\text{C}_2\text{H}_5\text{I}$	Sigma Aldrich	75-03-6	156.97	$\geq 0.99^a$
12	Pyrrolidine	$\text{C}_4\text{H}_9\text{N}$	Sigma Aldrich	123-75-1	71.12	$\geq 0.99^a$
13	Potassium carbonate	K_2CO_3	Sigma Aldrich	584-08-7	138.21	$\geq 0.98^a$
14	Sodium iodide	NaI	Sigma Aldrich	7681-82-5	149.85	$\geq 0.98^a$

^a According to the supplier's statement.

^b as per ^1H NMR, ^{13}C NMR or mass spectroscopy.

3.2 SYNTHESIS OF IONIC LIQUIDS

Some of the Ionic liquids used in our experimental work were synthesized in our laboratory and their synthesis procedure along with their characterization are discussed below:

3.2.1. Synthesis of Pyrrolidinium based ionic liquid.

1-butyl-1-methyl pyrrolidinium iodide was synthesized using the following method described in the literature (Yim et al., 2007) and then further characterized for the structural elucidation and purity analysis.

3.2.1.1. Synthesis of 1-butyl-1-methyl pyrrolidinium iodide ([BMPyr⁺] [I⁻])

To synthesize [BMPyr⁺] [I⁻], 1,4-dibromobutane was dissolved in acetonitrile in RBF (500 ml) followed by the addition of potassium carbonate and pyrrolidine. After addition, the solution prepared was then heated overnight at a constant temperature of 353 K. Thin layer Chromatography (TLC) was carried out for the establishment of the results of the reaction. The reaction mixture was then set aside to cool it down until its temperature reaches to 298 K and after cooling, a celite pad in 100 ml RBF was used to keep the extracted solid from the reaction mixture. Using magnetic stirrer, the liquid left was constantly mixed and stirred followed by the addition of sodium iodide. Once again, celite pad was used for the filtration of the solid mass and the solvent was drawn out using a vacuum. By using the minimum amount of acetonitrile, the residue was reconstituted followed by the addition of diethyl ether to obtain the product. Then it was kept in vacuum to produce the desired product, i.e. an off white solid with an estimated yield of 79%.

On the basis of ¹H NMR, ¹³C NMR and mass spectroscopy the purity of the synthesized ionic liquid was found to be 94%. The product synthesized was characterized by:

¹H NMR (500 MHz, DMSO-d₆) δ (ppm): 3.47 (s, 1H), 3.40 – 3.29 (m, 1H), 3.01 (s, 2H), 2.51 (s, 0H), 2.08 (s, 3H), 1.67 (d, J = 8.2 Hz, 1H), 1.39 – 1.25 (m, 1H), 0.92 (t, J = 7.4 Hz, 2H)] (Fig 3.1)

¹³C NMR (126 MHz, DMSO-d₆) δ (ppm) 63.28, 62.61, 47.47, 39.42 (dp, J = 42.0, 21.0 Hz), 24.77, 20.76, 19.08, 13.33 (Fig. 3.2).

FT-IR (cm⁻¹): 3500.45cm⁻¹ (N-H Stretching), 2957.15cm⁻¹ (C-H Stretching), 2872.38cm⁻¹ (C-H Stretching), 1460.34cm⁻¹ (=CH Stretching), 925.55cm⁻¹ (O-H Stretching), 734.89cm⁻¹ (C-H Stretching) (Fig. 3.3).

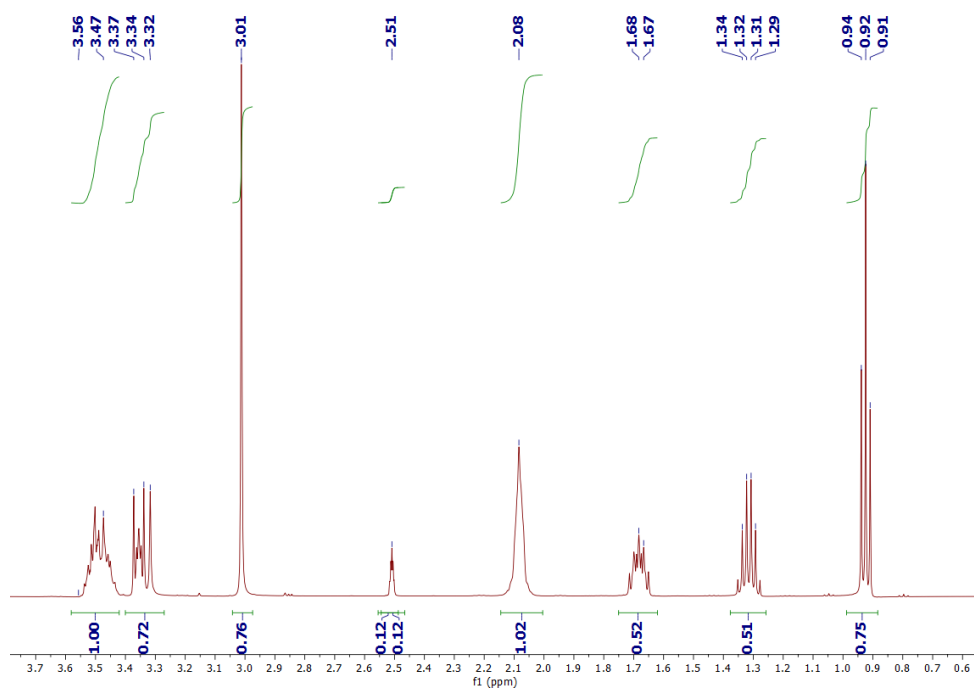


Figure 3.1: ^1H -NMR spectrum for synthesized $[\text{BMPyr}^+][\text{I}^-]$.

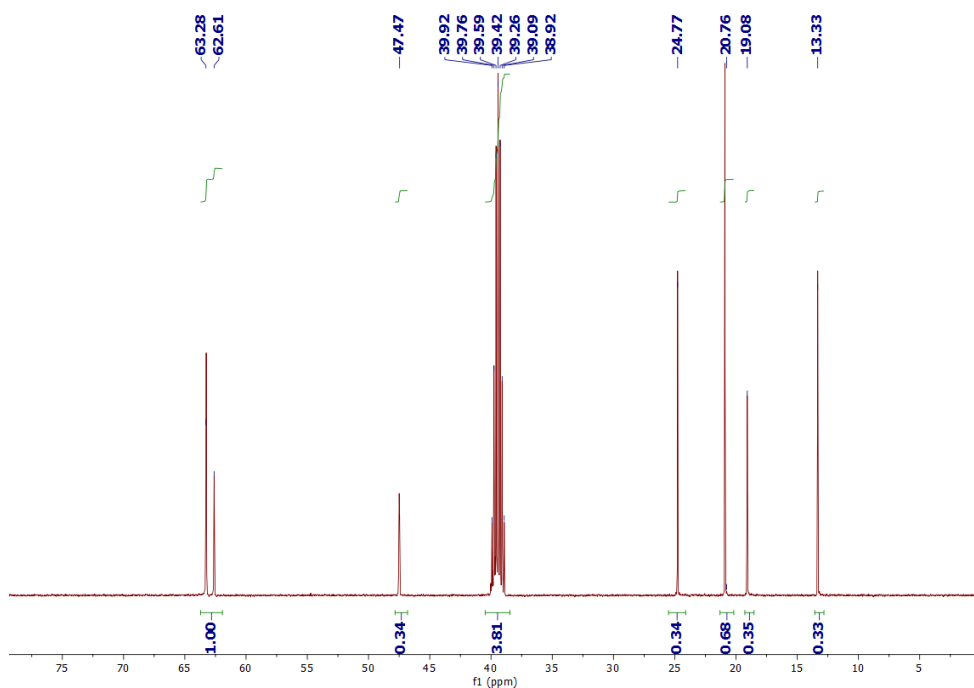


Figure 3.2: ^{13}C -NMR spectrum for synthesized $[\text{BMPyr}^+][\text{I}^-]$.

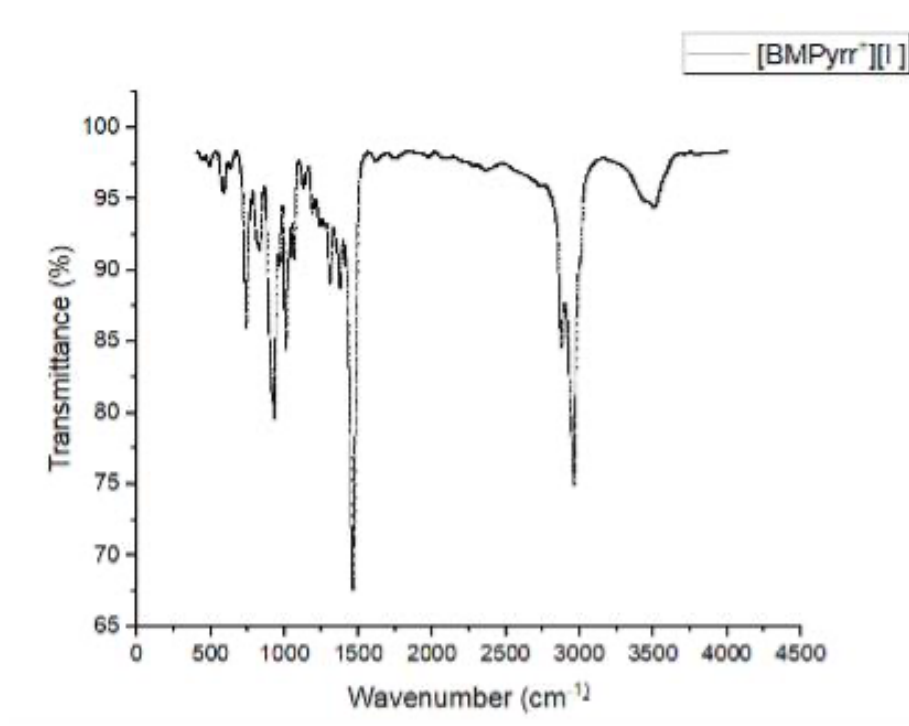


Figure 3.3: FT-IR spectrum of synthesized ($[BMPyr^+][I^-]$).

3.2.2. Synthesis of imidazolium based ionic liquids:

Synthesis of 1-ethyl-3-methylimidazolium iodide [EMIM⁺][I⁻] was carried out using the following method discussed in the literature (Haddad et al., 2020; Zhao et al., 2013). Basically, [EMIM⁺][I⁻] was obtained by the quaternization of 1-methyl imidazole and ethyl iodide under the exposure in microwave. After synthesizing, for the structural elucidation and to analyze the purity characterization was done.

3.2.2.1 Synthesis of 1-ethyl-3-methyl imidazolium iodide.

For the synthesis of IL, a mixture of 1-methylimidazole and ethyl iodide was heated under microwave exposure at 120 °C. For about 3 minutes. After heating the reaction mixture was then evaporated at a low pressure followed by continuous washing using diethyl ether for the removal of excess ethyl iodide. After washing, the solvent was removed, and the obtained product was dried under the vacuum for continuously 8 hours to obtain a high purity product. 1-ethyl-3-methylimidazolium iodide was obtained, a yellowish viscous liquid. The yield of the synthesis was about 89%. The purity of the synthesized ionic liquid was determined on the basis of ¹HNMR that was found to be 96%.

For the characterization of the product ¹HNMR, ¹³CNMR and FT-IR spectroscopy were done:

¹H-NMR: ¹H NMR (500 MHz, DMSO-*d*₆) δ 9.21 (s, 1H), 7.83 (s, 1H), 7.73 (s, 1H), 4.21 (d, *J* = 7.3 Hz, 2H), 3.86 (s, 3H), 1.40 (t, *J* = 7.3 Hz, 4H).

¹³C-NMR: ¹³C NMR (126 MHz, DMSO-*d*₆) δ 135.99, 123.27, 121.72, 43.98, 14.97.

FT-IR spectrum: 3788.48 cm⁻¹, 3164.43 cm⁻¹, 2984.78 cm⁻¹, and 1573.65 cm⁻¹, 1462.28 cm⁻¹, 1020.89 cm⁻¹, 846.82 cm⁻¹, 647.67 cm⁻¹, 586.19 cm⁻¹

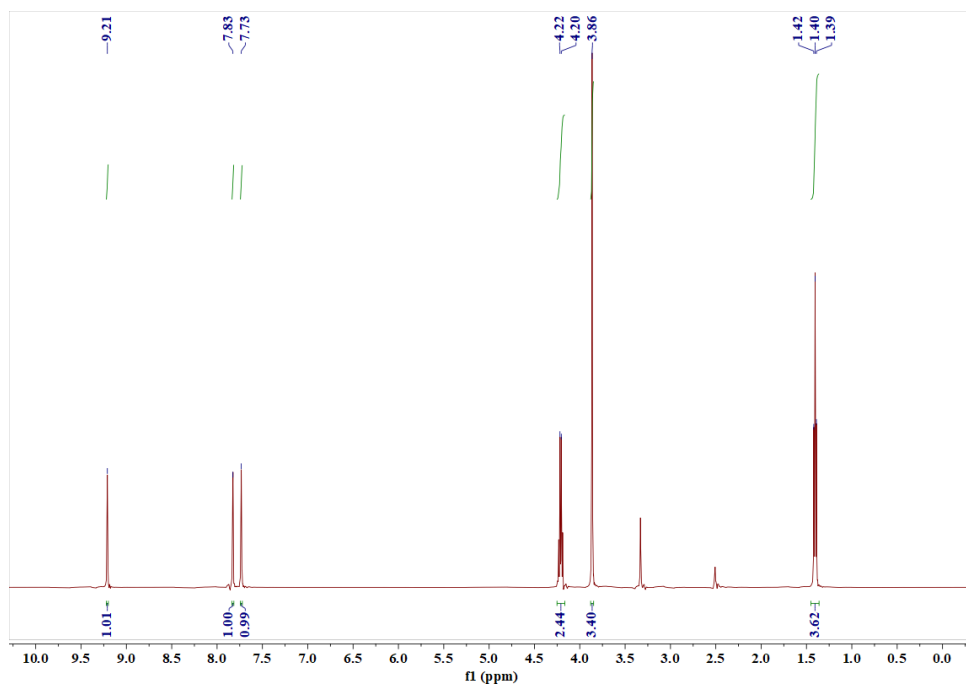


Figure 3.4: ¹H-NMR spectrum for synthesized [EMIM⁺] [I⁻].

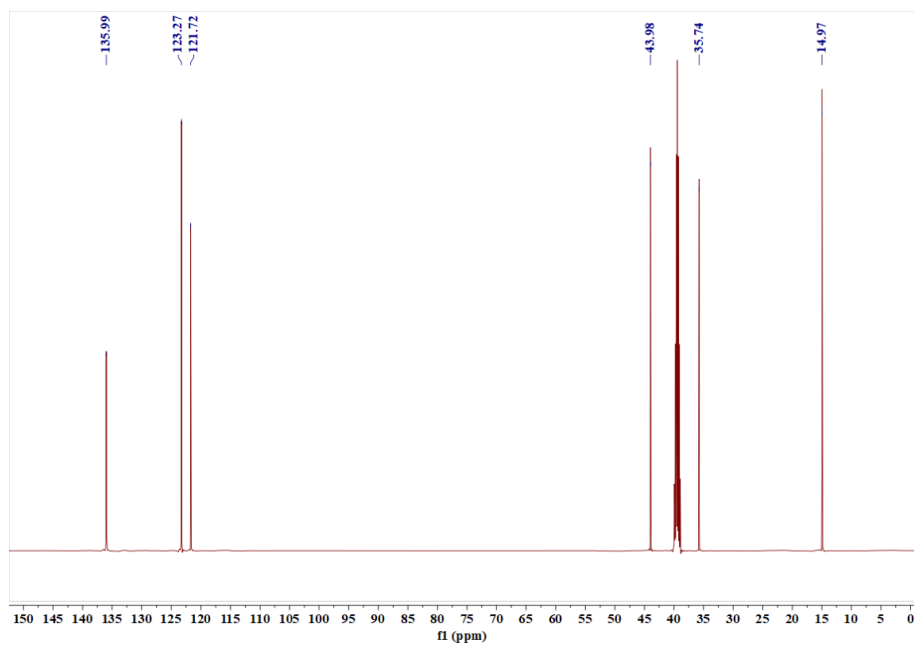


Figure 3.5: ¹³C- NMR spectrum for synthesized [EMIM⁺] [I⁻].

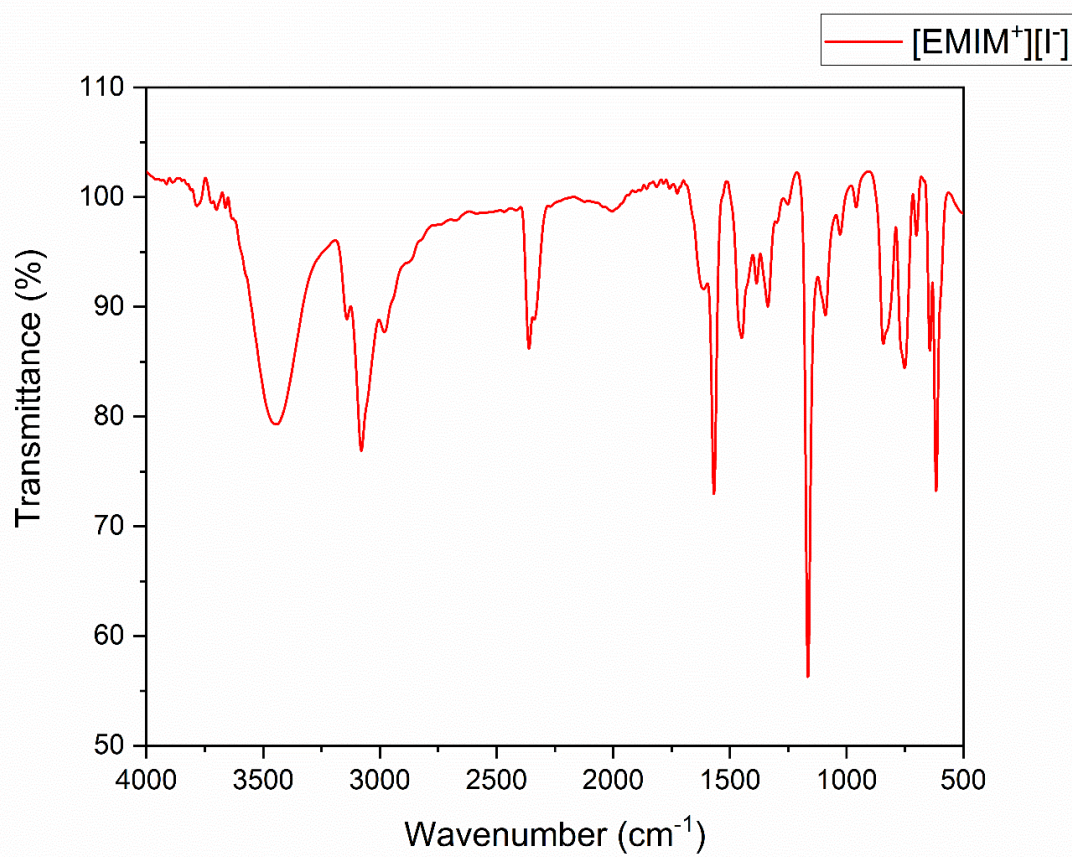


Figure 3.6: FT-IR spectrum for synthesized [EMIM⁺][I⁻].

3.3. PURIFICATION OF SYNTHESIZED IONIC LIQUIDS AND OTHER CHEMICALS

Table 3.1 tabulates the mass fraction purity of all the procured chemicals. All the ionic liquids along with other chemicals like Benzylamine, Benzamide, 1,4-dibromobutane, Potassium carbonate, Pyrrolidine, Sodium iodide, 1-methylimidazole, Ethyl iodide, diethyl ether, Acetonitrile were used as procured, without any further purification. For the synthesized ionic liquids, purification methods were stated along with the synthesis process. For the making of the solutions, triply distilled water was used, and the samples were kept in the glass apparatus sealed using parafilm to prevent the moisture absorption in the sample.

3.4. BRIEF OVERVIEW OF CHEMICALS USED IN STUDY

3.4.1. 1,4-dimethyl-4H-1,2,4-triazolium iodide [DMTI]:

The triazolium based ionic liquids shows a versatile nature with a very low vapour pressure along with high thermal stability, non- flammability, high solubility, and high potential.

[DMTI] shows a great application in different synthesis processes, in capillary electrophoresis, as antifungal and anti-microbials. They also have a very low cytotoxicity and shows a great application in ESDs.

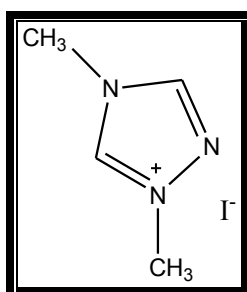


Figure 3.7: Structure of [DMTI]

3.4.2. 1-butyl-1-methyl pyrrolidinium iodide [BMPyrr⁺] [I⁻]:

The pyrrolidinium class of ionic liquids consist of more localised aliphatic cations, because of which they have a very high electrochemical window.

1-butyl-1-methyl pyrrolidinium iodide possess properties like greater flexibility, aliphaticity and low toxicity making them more environment friendly. These ILs are mainly used as solid-state dye-sensitized solar cells, solvents for extraction and as catalysts.

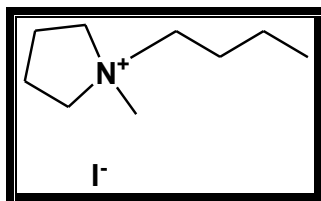


Figure 3.8: Structure of [BMPyrr⁺][I⁻].

3.4.3. 1-butyl-1-methyl pyrrolidinium tetrafluoroborate [BMPyrr⁺][BF₄⁻]:

The pyrrolidinium class of ionic liquids consist of more localised aliphatic cations making them more useful in energy devices due to their high chemical window and high electrochemical stability.

1-butyl-1-methyl pyrrolidinium tetrafluoroborate is mainly used in lubricants, catalytic properties and in storage devices like solar cells.

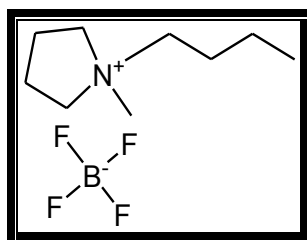


Figure 3.9: Structure of [BMPyrr⁺][BF₄⁻].

3.4.4. 1-ethyl-3-methylimidazolium iodide:

Imidazolium based Ionic liquids is one of the important types of ILs because of their specific set of properties like low cost, non-toxic, great solubility, safety and high adsorption on metal.

1-ethyl-3-methylimidazolium iodide is an IL that can be prepared by reacting methylimidazole with iodoethane. This ionic liquid in particular shows a very great application in Energy storage devices (ESDs).

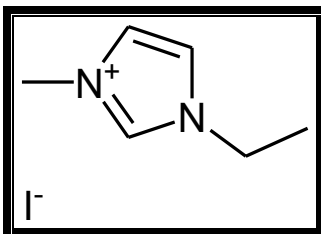


Figure 3.10: Structure of 1-ethyl-3-methyl imidazolium iodide.

3.4.5. Benzylamine:

Benzylamine is the organic chemical compound, primary amine consisting of one benzyl group attached to an amine functional group. It shows many applications like is used in the production of pesticides, pharmaceuticals and also in the synthesis of many organic compounds. It also acts as corrosion inhibitor.

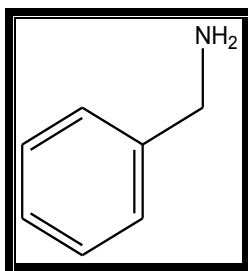


Figure 3.11: Structure of Benzylamine.

3.4.6. Benzamide:

Benzamide is the amide derivative of benzoic acid. It shows a great application as an enzyme and is also widely used in bio transformations and in energy storage applications.

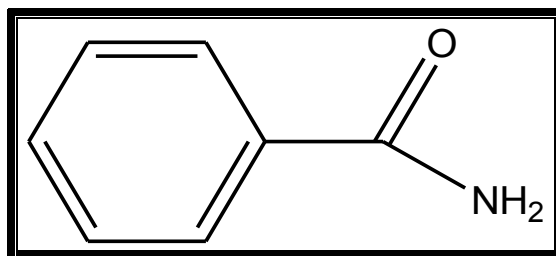


Figure 3.12: Structure of Benzamide.

3.5 EXPERIMENTAL TECHNIQUES:

To evaluate the interactions between the various Ionic liquids with benzylamine and benzamide in order to get the final findings multiple methodologies were employed.

The methodologies used to gather the experimental data are discussed below:

3.5.1. Density and sound velocity measurements

3.5.2. Conductivity measurements

3.5.3. FT-IR Spectroscopic studies

3.5.4. Cyclic Voltametric studies

Every solution was prepared by weight (molal), and a Sartorius CPA 225D balance was utilized to weigh the materials with an accuracy of ± 0.00001 gm. The solutions were prepared using triply distilled water, which has a specific conductance of less than $1.0 \times 10^{-6} \text{S.cm}^{-1}$.

3.5.1. Density and sound velocity measurements

The Anton Paar DSA 5000M was used for the calculation of the values for density and sound velocity. DSA determines two parameters that are physically separate i.e., density and sound velocity simultaneously in a single configuration that too with accuracy. Prior to each series of measurements in the experimental temperature range, the instrument was calibrated by determining the density and sound velocity of dried air and freshly generated triple distilled and deionized water at 293.15 K. The temperature range in which this instrument works is from 273.15 K to 345.15 K. Both the parameters density as well as sound velocity are temperature sensitive parameters, so the constant temperature was maintained using the internal Peltier module. The accuracy of sound measurements of density and speed was found to be $1 \times 10^{-3} \text{kg.m}^{-3}$ and $1 \times 10^{-2} \text{ms}$, respectively. The average level of uncertainty for sound speed and density was 0.15kg.m^{-3} and 1.0ms^{-1} , respectively. The molality of the solution has uncertainties within $2 \times 10^{-5} \text{mol.kg}^{-1}$. The provision of the most precise temperature control is facilitated by the utilization of two integrated Platinum 100 thermometers, which can be effectively tracked back to national standards. The DSA 5000 is capable of automatically correcting density measurement mistakes that arise from viscosity by monitoring the damping of oscillation in the filled-in sample.



Figure 3.13: AntonPaar DSA 500M

In order to carry out a measurement, the sample under investigation is filled in the measuring cells using a syringe. Once the measurement is complete, an acoustic signal informed. The outcomes are consequently transformed into concentration, specific gravity, or other density/velocity of sound-related units by the utilization of the integrated conversion tables and functions.

3.5.2. Conductivity measurements

For the conductivity measurements, a Digital conductivity meter supplied by Labrtronics Pvt. Ltd. was used. This instrument consists of two Platinum electrodes embedded in pyrex glass and dip type cell which has a cell constant equal to 1 cm^{-1} . The principle of the instrument is very simple, two plates/ electrodes are placed in the sample and the potential is applied across the plates which helps in the measurement of the current. The conductivity and the cell constant are displayed on the screen.

Before taking the measurements, the instrument has been calibrated properly because the user is not known of the accurate dimensions. For our studies, the conductivity meter has been calibrated using 0.01 M KCl solution. After the calibration, the conductivity meter has been properly cleaned with distilled water and then rinsed with the solution under investigation. Then the solution is filled

in the vessel and placed in the thermostat at least for 10-15 minutes so that the solution can attain the desired constant temperature. Three consecutive readings were taken and then the average value has been considered as the final value.



Figure 3.14: Electrical Conductivity meter

3.5.3. FT-IR Spectroscopic Studies:

The spectroscopic studies help us to determine the chemical composition, structure of the compound and the interactions among the system at the molecular level. FT-IR spectra were recorded using the Shimadzu spectrometer 8400 S which can be operated using any laptop or simple desktop. The measurements done on this instrument are based on the amount of light absorbed by the sample at each wavelength.

The FT-IR spectrum for the pure Ionic liquid, benzylamine, benzamide and the ternary mixtures has been recorded in the wave region of 500 cm^{-1} to 4500 cm^{-1} .



Figure 3.15: Shimadzu FT-IR-8400S Spectrophotometer

3.5.2. Cyclic Voltametric studies:

Cyclic voltammetry helps us in the determination of the electrochemical properties of the electrode being used. To measure the electrochemical properties with the help of CV graphs, Metrohm Autolab PGSTAT204 multi- channel Potentiostat/ Galvanostat electrochemical workstation with a tightly closed three-electrode cell in an inert environment of argon flow was used. The cyclic voltammograms of the ternary mixtures (IL+ benzylamine/benzamide + water) as a function of concentration at room temperature in the potential range from -1.0 V to + 2.0 V demonstrates the correlation between the reduction and oxidation potential peaks and are graphically represented. For all the systems under investigation, Ag wire in 10 mM AgCl was taken as the reference electrolyte. Platinum wire worked as a counter electrode and Pt was used as a working electrode with a diameter of 3mm were used. The starting potential for these voltammograms was 0V, with no current flowing, and three cycles were recorded.

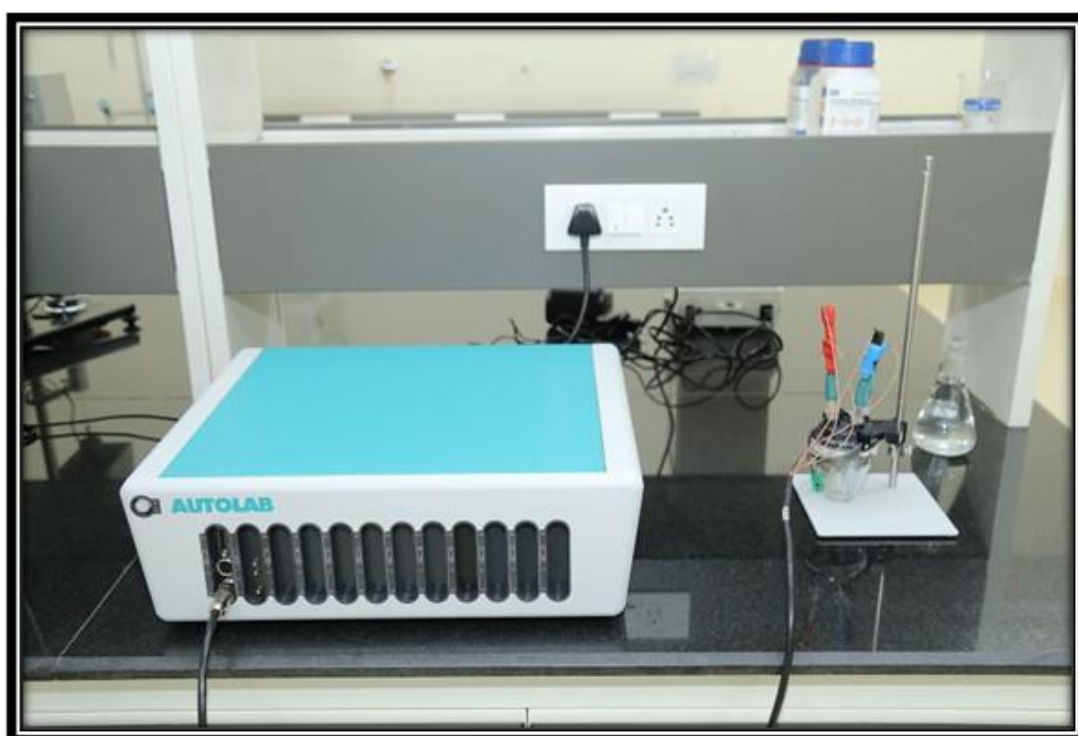


Figure 3.16: Metrohm Autolab PGSTAT204 multi-channel Potentiostat/galvanostat electrochemical workstation.

Chapter 4

Thermodynamic, Conductometric and Cyclic Voltametric parameters

4.1. THERMODYNAMICS OF SOLUTIONS

Thermodynamic properties are the properties which are related to heat and other form of energy. Mass, volume, temperature, and pressure are some of the thermodynamic parameters which are used for the evaluation of these properties. To properly understand the type and degree of molecular aggregation that occurs in these liquid mixtures, thermodynamic analysis is essential. The neighboring structure of a liquid mixture affects the qualities of the mixture, which in turn affects the forces that exist between the molecules and their structural forms as well as the volume of the molecules. When a mixture's composition changes, the local structure of the molecules also changes, which affects the thermodynamic properties of the mixture. Therefore, it is crucial to comprehend these features in order to foretell the numerous interactions that exist between the various solution components (Qiao et al., 2012b).

4.1.1. PARAMETERS DERIVED FROM DENSITY MEASUREMENTS

The volumetric features of the solution are considered a sensitive area for foreseeing the numerous interactions that are present. At various temperatures and solute/ solvent concentrations, the experimental density values are then utilized to determine important parameters which aid in deciphering the synergies present in the mixtures.

4.1.1.1. Apparent molar volume:

The AMV of a solute can be determined by sampling a substantial amount of the solution. The volume must be so high that the addition of more solute like one mole would not have any kind of effect on the solution's concentration (Fumino et al., 2011; Zheng et al., 2011).

The mathematical equation used for the calculation of AMV is as follows:

$$\bar{V}_2 = V_\phi^o = \left(\frac{\partial V}{\partial n_2}\right)_{T,P,n_i} \quad (4.1)$$

Here, n_i is the number of moles of all other constituents except i^{th} constituent. The factors like temperature, pressure and moles are kept constant.

For a solution composed of two constituent's equation, the partial molar volume becomes:

$$\bar{V}_2 = \left(\frac{\partial V}{\partial n_2}\right)_{T,P,n_1} \quad (4.2)$$

n_1 is the number of moles of the solvent. Whereas n_2 is the number of moles of the solute.

The volume of a solution is the function of temperature, pressure and amount of the components in the mixture i.e., $V(T, P, n_1, n_2, \dots)$.

In binary systems, the differential volumes on addition or removal of any component at constant temperature and pressure can be expressed as:

$$dV = \left(\frac{\partial V}{\partial n_1}\right)_{T,P,n_2} dn_1 + \left(\frac{\partial V}{\partial n_2}\right)_{T,P,n_1} dn_2 \quad (4.3)$$

The differential volume can be re-written as:

$$dV = \bar{V}_1 dn_1 + \bar{V}_2 dn_2 \quad (4.4)$$

Integrating the above equation:

$$V = n_1 \bar{V}_1 + n_2 \bar{V}_2 \quad (4.5)$$

Here, V is the total partial volume. \bar{V}_1 and \bar{V}_2 are the partial volumes for solvent and solute respectively.

AMVs (V_ϕ) are also used for the calculation of the Partial molar volume at constant temperature and pressure using the density measurements. The AMV is the final volume when n_2 moles of solute are added to the system with a fixed number of moles (n_1).

Mathematically this relation is represented as:

$$V_\phi = \frac{V - n_1 V_1^0}{n_2} \quad (4.6)$$

After the rearrangement of the above equation, the volume of solution at any particular added n_2 moles of solute, the equation becomes:

$$V = n_2 V_\phi + n_1 V_1^0 \quad (4.7)$$

Here n_1 is the number of moles of solvent and n_2 is the number of moles of solute. At the given temperature, V is the total volume of the solution and V_1^0 is the molar volume of solvent.

At constant Temperature, Pressure and n_1 , differentiating the above equation w.r.t n_2 , we get the following equation:

$$\left(\frac{\partial V}{\partial n_2}\right)_{T,P,n_1} = \bar{V}_2 = V_\phi + n_2 \left(\frac{\partial V_\phi}{\partial n_2}\right)_{T,P,n_1} \quad (4.8)$$

After rearranging the above equation, we get:

$$\bar{V}_1 = \left(\frac{V - n_2 \bar{V}_2}{n_1} \right) \quad (4.9)$$

Substituting equation (4.8) in the above equation:

$$\bar{V}_1 = 1/n_1 [n_1 V_1^o - n_2 (\partial V_\phi / \partial n_2)_{T,P,n_1}] \quad (4.10)$$

The apparent molar volume in terms of measured values of densities and the molecular weights of solvent (M_1) and solute (M_2) is given by:

$$V_\phi = 1/m [(n_1 M_1 + n_2 M_2)/(\rho - n_1 V_1^o)] \quad (4.11)$$

When the concentration is taken in liters, then $n_2 = m$ i.e. the molality of the solution and n_1 is equal to the number of moles of water in 1000g.

Which mathematically is represented as:

$$V_\phi = 1/m [(1000 + m M_2)/\rho - 1000/\rho_o] \quad (4.12)$$

The density of the solution is denoted by ρ , while the density of the pure solvent is denoted by ρ_o , and the molar mass of the solute is denoted by, M (kg. Mol⁻¹).

When the density is in g.cm⁻³ instead of kg.cm⁻³, the factor of 1000 appears. So, rearranging the equation, the equation for apparent molar volume used in our ternary mixtures is stated as below:

$$V_\phi = (M/\rho) - \{(\rho_o - \rho)/m_A \rho \rho_o\} \quad (4.13)$$

When molar concentration is used, then we use $n_2 = C$ i.e. the molarity of the solution, and then the above equation becomes:

$$V_\phi = (M/\rho) - \{(\rho_o - \rho)/C \rho_o\} \quad (4.14)$$

4.1.1.2. Apparent molar volume at infinite dilution:

AMV and molality are helpful in determining the solute-solute and solute-solvent synergies. This parameter helps to know the predominance of the specific type of interactions.

At high concentration, Masson (H. Kumar, Sheetal, & Behal, 2017) had proposed the linear relationship of the apparent molar volume and molality as:

$$V_{\phi} = V_{\phi}^o + S_V^* m_A \quad (4.15)$$

Here, V_{ϕ}^o is the partial molar volume (when infinite dilution $V_{\phi} = V_{\phi}^o$) and S_V^* (coefficient for non-ionic solutes) is the experimental slope which varies with the charge and type of ions and m_A is the molality of the solute. The plot of V_{ϕ}^o against m is undeviating. Using the least square fitting of the values, V_{ϕ}^o is collected from the above equation.

In the case of ionic solutes, the equation for apparent molar volumes becomes:

$$V_{\phi} = V_{\phi}^o + S_V^* C^{1/2} \quad (4.16)$$

S_V^* is the coefficient for non-ionic solutes, Similarly, S_V^* is the observed slope that changes along with the charge and type of the ions. Redlich and Meyer suggested the following extrapolation equation:

$$V_{\phi} = V_{\phi}^o + S_V^* C^{1/2} + b_v C \quad (4.17)$$

Where S_V^* the theoretical limiting slope is calculated from Debye –Huckel limiting law and b_v is an empirical constant determined from the experimental results (S. K. Sharma et al., 2016).

4.1.1.3. Partial molar volume of transfer:

The following equation utilizes the partial molar volumes to determine the amount of solute that would be transferred from water to aqueous ionic liquid at constant dilution:

$$\Delta V_{\phi}^o = V_{\phi}^o(\text{in aqueous IL solution}) - V_{\phi}^o(\text{in water}) \quad (4.18)$$

The values for the PMV of transfers are explained on behalf of the co-sphere model.

In accordance with the co-sphere model, when two hydration co-spheres overlap, the volume changes negatively as a result of the release of a small number of water molecules into the bulk. Two solute particles may reach sufficiently close to one another when there is displacement in the co-sphere materials, which causes the overlapping of the co-spheres leading to different changes in the thermodynamics parameters. In accordance with this model, the volume of water molecules in the solvate sphere is less for polar species than non-polar species due to electrostriction's action and a decline in the hydrogen-bonded network, which results in water molecules in the solvate sphere transferring to the bulk. Therefore, hydrophilic interactions result in positive values while

ion-hydrophobic and hydrophobic-hydrophobic synergies provide negative values (Juglan et al., 2020).

Due to various types of synergies in the molecule, the volume is also affected. Below table (Table 4.1) tabulates the volume change because of various interactions.

Table 4.1. Change in volume in accordance with different type of interactions.

S.No.	Interactions	Change in Volume
1.	Hydrophobic- hydrophobic	$\Delta V < 0$
2.	Ionic (dipolar)-Hydrophobic	$\Delta V < 0$
3.	Ionic-Ionic	$\Delta V > 0$

4.1.1.4. Influence of Temperature on PMV

At infinite temperature, the following polynomial equation describes the change in PMV:

$$V_{\phi}^o = a + b(T - T_{ref}) + c(T - T_{ref})^2 \quad (4.19)$$

In this equation, T is the temperature (in Kelvin), empirical constants are (a,b,c) and T_{ref} is 298.15 K. Conceptual and measured outcomes both show some variation in V_{ϕ}^o , termed as ARD (Average Relative Deviation) which is calculated by using the equation:

$$\sigma = (1/n) \sum [abs((Y_{exp.} - Y_{calc.})/Y_{exp.})] \quad (4.20)$$

Where, (Y= V_{ϕ}^o , PMV at constant dilution)

Further, Partial molar expansibilities (ϕ_E^o) represents the solute-solvent synergies and are mathematically represented by the following equations:

$$\phi_E^o = (\partial V_{\phi}^o / \partial T)_p = b + 2c(T - T_{ref}) \quad (4.21)$$

The resultant positive values of ϕ_E^o signifies the existence of solute-solvent interactions.

The ability of the solute to behave as structure promoter or destroyer in mixed solvents is represented by the equation stated by Hepler (Hepler, 1969) as follows:

$$(\partial\phi_E^o/\partial T)_p = (\partial^2 V_\phi^o/\partial T^2)_p = 2C \quad (4.22)$$

$(\partial\phi_E^o/\partial T)_p$ Discovers whether the solute may establish or demolish a framework in the solvent.

4.1.2: PARAMETERS DERIVED FROM SOUND VELOCITY MEASUREMENTS

Acoustical properties are those that govern way materials react to sound waves, which humans further interpret as sound. When conduct metric data is unable to provide an accurate interpretation of the interactions in some circumstances, the acoustic property also reveals the interactions between molecules and provides the exact data for molecular interactions (K. Kaur et al., 2018).

4.1.2.1. Apparent molar isentropic compression

The given equation is used to calculate the apparent molar isentropic compression of the ternary systems under investigation using the calculated density and sound velocity values:

$$K_{\phi,S} = [(M\kappa_S/\rho) - \{(\kappa_S, o\rho - \kappa_S\rho_o)/(m_A\rho\rho_o)\}] \quad (4.23)$$

Here, m_A and M is the molality and molar mass of the ionic liquid (solute) respectively, κ_S is the isentropic compressibility of the solution, $\kappa_S, o\rho$ is the isentropic compressibility of the pure solvent, ρ and ρ_o are the densities of solute (ionic liquid) and solvent (benzylamine or benzamide) respectively.

Further to calculate the coefficient of isentropic compressibility (κ_S), Laplace Newton's equation has been used:

$$\kappa_S = 1 / (u^2\rho) \quad (4.24)$$

Here, u is the sound velocity and ρ is the density of the solution.

4.1.2.2 Partial molar isentropic compression

The relation for the partial molar isentropic compression is given:

$$K_{\phi,S} = K_{\phi,S}^o + S_K^* m_A \quad (4.25)$$

In this equation, $K_{\phi,S}^o$ denotes limiting molar isentropic compression, S_K^* is the experimental slope showing solute-solute interactions, m_A is the molality of the Ionic liquid in aqueous solutions of benzylamine or benzamide.

Positive values of limiting molar isentropic compression ($K_{\phi,s}^o$) denotes strong solute-solvent interactions, small S_K^* values signify the weaker solute-solute interactions.

4.1.2.3. Partial molar isentropic compression of transfer

At infinite dilutions, for the calculation of partial molar isentropic compression of transfer ($\Delta K_{\phi,s}^o$) of solute from water to solutions below equation was used:

$$\Delta K_{\phi,s}^o = K_{\phi,s}(\text{in aqueous amine/amide solution}) - K_{\phi,s}^o(\text{in water}) \quad (4.26)$$

The values of partial molar isentropic compression of transfer ($\Delta K_{\phi,s}^o$) suggest that solvent and solute molecules are linked, which further enhances the interactions between the ions.

4.1.2.4. Pair and triplet interaction coefficients.

The theory by McMillan and Mayer (McMillan & Mayer, 1945) helped in the determination of the interaction coefficients of the interactions among two or more solutes which was further modified by Friedman and Krishanan (Millero et al., 1978). The following equation expresses the partial molar volume of transfer:

$$\Delta V_{\phi}^o(\text{water to aqueous amine/amide solution}) = 2V_{AB}m_B + 3V_{ABB}m_B^2 \quad (4.27)$$

Partial molar isentropic compression of transfer mathematically is expressed as:

$$\Delta K_{\phi,s}^o(\text{water to aqueous amine/amide solution}) = 2K_{AB}m_B + 3K_{ABB}m_B^2 \quad (4.28)$$

In the above equations, A is the Ionic liquid, B is the benzylamine or benzamide, m_B is the molality of aqueous solutions of benzylamine/benzamide.

V_{AB} and V_{ABB} are the volumes whereas K_{AB} and K_{ABB} are the isentropic compression symbolizing the pair and triplet interactions coefficients.

4.2 TRANSPORT PROPERTIES:

4.2.1. Conductance studies

Ionic conduction (λ -lambda) is mainly considered as the change in the position of an ion from one site to another of a solid or aqueous solution's crystal lattice through its defects. In solids, ions mainly stay at a fixed position in the crystal lattice without any movement and in case of liquids it is completely electrolytic.

Conductance is a distinctive characteristic of electrolytic solutions which is indirectly proportional to resistance i.e., it is the reciprocal of resistance, following Ohm's law and determining the nature of ion, solvent and also the interactions in mixed solvents. Conductance studies give a brief of the ionic conductivities and association constants, respectively, providing kinetic and thermodynamic information.

The Molar Conductivity, denoted by Λ_m is basically the theoretical conductivity of electrolytes and that too per mole and is also termed as the conducting power. Its primary definition is total conducting power of all the ions created when one mole of electrolyte dissolves in the solution. It gauges how well an electrolyte conducts electricity when dissolved in a solution.

$$\Lambda_m = \text{Specific conductance } (\kappa) \times 1/c \quad (4.29)$$

Where κ denotes specific conductance and c is the molar concentration of the electrolyte.

4.2.2.1. Specific Conductance

Specific conductance (denoted by κ) is further indirectly proportional to the specific resistance i.e equals to the reciprocal of the specific resistance and is the measure of the resistance of any component which has a length of 1 m with a cross sectional area equal to 1 m².

Mathematically,

$$\kappa = \frac{1}{\rho} = (1/a) \times \text{Conductance} \quad (4.30)$$

Here, ρ is the specific resistance and $(1/a)$ is the cell constant.

4.2.2.2. Molar Conductance

Molar conductance is mainly the ratio of the specific conductance and molar concentration and is the measure the rate of migration of anions and cations and also their number, both the cases in 1 mole of the solute. Molar conductance with dilution, its values increase.

Relation between molar conductivity and specific conductivity is given by:

$$\Lambda_m = \kappa \times 1000 N \quad (4.31)$$

N is the normality of the solution.

4.2.2.3. Limiting Molar Conductance

Limiting molar conductivity of the solution is calculated using the Onsager relation:

$$\Lambda_m = \Lambda_m^o - S\sqrt{C} \quad (4.32)$$

In the plots, Λ against \sqrt{C} , straight lines give the intercept which is equal to limiting molar conductance and slope is equal to the Onsager constant (denoted by S). These values obtained help in interpreting the ion-solvent interactions. Higher the values of limiting molar conductance, greater the ion-solvent interactions.

4.2.2.4. Effect of Temperature:

The below equation gives the effect of temperature, where E_A is the activation energy and gas constant are denoted by R. It is feasible to calculate E_A from the slope of the straight line generated by the plot of the $\log \Lambda_o$ versus $1/T$.

$$\Lambda = \Lambda_o e^{E_A/RT} \quad (4.33)$$

Graphically, if we plot graph between $\log \Lambda$ and $1/T$. It gives a straight line, and the slope is useful for the determination of E_A .

From the above values calculated, we can conclude that solubilization is favorable given that all activation energy values are positive.

4.3. CYCLIC VOLTAMMETRIC PROPERTIES

4.3.1. Cyclic Voltammetry

The cyclic voltammograms of the ternary mixtures (IL+ benzylamine/benzamide + water) as a function of concentration at room temperature in the potential range from -1.0 V to + 2.0 V demonstrates the correlation between the reduction and oxidation potential peaks.

Using the CV graphs obtained, we can also compare the specific capacitance of the mixture at concentrations (0.001 and 0.009) mol.kg⁻¹. The area under CV curve is directly proportional to the capacitance of the solution. Greater the area, the higher the capacitance will be.

From noticing the area under the curve, we can validate the data obtained for the capacitance of the mixture using the equation:

$$C_P = \frac{Area}{2mk (V_2 - V_1)} \quad (4.34)$$

Here, C_P is the specific capacitance, A (area) is the area under the CV curve, m denotes the active mass or molar concentration of the electrode, k is for scan rate of CV and $(V_2 - V_1)$ is the potential window obtained.

Chapter 5

Results and Discussion

SECTION-I

Volumetric, acoustic, conductometric and spectroscopic studies of 1,4.-Dimethyl-4H-1,2,4- triazolium iodide in binary aqueous benzylamine and benzamide at various temperatures.

Volumetric, acoustic, conductometric and spectroscopic studies of 1,4.-Dimethyl-4H-1,2,4-triazolium iodide in binary aqueous benzylamine and benzamide at various temperatures

Density measurements

In the present study, density of [DMTI] (0.001 to 0.009) mol kg^{-1} was measured in different concentrations of aqueous benzamide and benzylamine (0.01 , 0.03 and 0.05) mol.kg^{-1} at four various temperatures. The experimental data for density is represented in Table 5.1 and the density of IL+ Water is tabulated in Table 5.2. From the tabulated data it is clear that density of ionic liquid increases with the increasing concentration of IL as well as composition of benzamide/benzylamine and decreases as we raise the temperature. Using the observed values of density, below stated volumetric parameters were calculated to predict the interactions present in the investigated ternary system (benzamide/ benzylamine + water + IL).

Apparent molar volume

Equation (4.13) was used for the calculation of the apparent molar volume (AMV) of [DMTI] in (0.01 , 0.03 and 0.05) mol.kg^{-1} aqueous solution of benzamide and benzylamine (Zhou & Liu, 2009).

The calculated apparent molar volumes are represented in Table 5.1 and are graphically shown in Fig 5.1. Fig 5.1 (a) and Fig 5.1 (b) represents AMV of [DMTI] in (0.01 and 0.05) mol kg^{-1} of aqueous benzamide and benzylamine solutions respectively. From the calculated values of AMV, it is clear that the values of V_ϕ are positive at all temperatures and concentrations signifying the strong solute-solvent interactions present in the system which are further strengthened with the increase in the temperature. As we raise the temperature, thermal movement of the molecules also increases which further increases the volume. On contrary, the interactions among solute-solvent are weakened with the rise in the concentration of aqueous benzamide and benzylamine (H. Kumar & Katal, 2018).

Partial molar volume (PMV)

Partial molar volumes or limiting apparent molar volumes (V_ϕ^0) are calculated by using the least square fitting method to the equation (4.15) (Verma, et al., 2017):

The values of V_{ϕ}^o and S_V^* with standard errors are tabulated in Table 5.3. From the observed data, values of V_{ϕ}^o are positive which further increase with rising temperature and decreases with increasing concentration of [DMTI] in aqueous solutions of benzamide and benzylamine. Plots of variation of PMV of the ionic liquid in concentrations $m = (0.01, 0.03 \text{ and } 0.05) \text{ mol.kg}^{-1}$ of benzamide and benzylamine at four equidistant temperatures are shown in Fig.5.2. The positive values of V_{ϕ}^o depicts the prevalence of ion-hydrophilic interactions in the system over hydrophobic-hydrophobic and ion-hydrophobic interactions (H. Kumar. et al., 2017; H. Kumar & Katal, 2018). The electrostriction, which decreases with temperature, is responsible for the rising V_{ϕ}^o values with temperature. Additionally, when temperature rises, the amount of hydrogen bonds in the aqueous benzamide/benzylamine mixture decreases, increasing the amount of free solvent available for the solvation.

Instead, smaller and negative values of S_V^* confirm that interactions among solute-solute are weaker in comparison to the solute-solvent interactions (H. Kumar et al., 2020). The values of S_V^* follow no specific trend from which we can conclude that there are various factors which affect the solute-solute interaction (H. Kumar, Kumari, et al., 2018). The dominance of ion-hydrophilic interactions is supported by co-sphere overlap model according to which ionic or bipolar species overlap of co-spheres have positive values which further results in increasing volume (Pal & Kumar, 2005).

Partial molar volume of transfer

Equation (4.18) was used for calculating partial molar volumes of transfer [DMTI] from water to aqueous benzamide and benzylamine at constant dilution.

The calculated data of ΔV_{ϕ}^o is listed in Table 5.4. In the ternary mixtures (benzamide/benzylamine+ IL+ water), values of ΔV_{ϕ}^o are positive (except for 288.15K) indicating the significant interactions between [DMTI] and aqueous solutions of benzamide/benzylamine which are further strengthened with the increasing temperature. The values of ΔV_{ϕ}^o are also found in agreement with co sphere model (Y. Li et al., 2019), from which the information regarding the nature of the interactions among solute and the solvent can be obtained. The various possible interactions that can occur among [DMTI] and aqueous benzamide/benzylamine are as follows- (i) ion-ion interactions between ions of IL and benzamide/ benzylamine (ii) ion-hydrophobic

interactions among alkyl groups of IL and ions of benzamide/ benzylamine (iii) hydrophilic-hydrophilic interactions in polar groups of IL and benzamide/ benzylamine (iv) hydrophobic-hydrophobic interactions between non-polar groups of IL and studied benzamide/ benzylamine. In accordance to co-sphere overlap model, the negative values of ΔV_{ϕ}^o indicate the presence of ion-hydrophobic interactions and hydrophobic-hydrophobic interactions and the positive values indicates the ion-hydrophilic interactions and hydrophilic-hydrophilic interactions (H. Kaur et al., 2021; K. Kaur et al., 2017). In the present study, ion-hydrophilic interactions and hydrophilic-hydrophilic interactions dominate over hydrophobic-hydrophobic as well as ion-hydrophobic interactions.

Effect of Temperature on partial molar volume

Variation in the values of apparent molar volumes (V_{ϕ}^o) with temperature at infinite solution is given by using the polynomial equation (4.19)

The values (a,b,c) are calculated by using the least square fitting for V_{ϕ}^o in equation (4.19). Values of these empirical constants along with ARD (Average Relative Deviation) are listed in Table 4.5. Empirical constants for [DMTI] in aqueous benzamide and benzylamine solutions are found positive except values of c in both the binary aqueous mixtures of benzamide and benzylamine which have been found negative (Amirchand et al., 2021).

Further Partial molar expansibilities (ϕ_E^o) represent the interactions among solute-solvent represented using the equation (4.21)

The presence of interactions among solute-solvent is indicated by the positive values of partial molar expansibilities. The ability of the solute to act as structure breaker or maker in a mixed solvent system is further represented by the equation (4.22) stated by Hepler (Hepler, 1969):

The values of $(\partial\phi_E^o/\partial T)_p$ decides the structure making or breaking behavior of the solute in a particular solvent system (Romero et al., 2018) and are tabulated in Table 5.6. In the studied ternary solutions small and negative values of $(\partial\phi_E^o/\partial T)_p$ have been observed which confirms the structure breaking nature of [DMTI] in aqueous benzamide and benzylamine solutions.

Sound velocity measurements

Sound velocity values were measured for [DMTI] with concentration ranging from (0.001 to 0.009) mol kg⁻¹ in various concentrations of benzamide and benzylamine (0.01, 0.03 and 0.05)

mol.kg⁻¹ at (288.15, 298.15, 308.15, 318.15) K. The experimental data obtained for sound velocity are represented in Table 5.7 and the sound velocity of IL+ Water is tabulated in Table 5.2. Analyzing the data it has been noted that the sound velocity values of ionic liquid increase with increasing concentration as well as temperature.

Apparent molar isentropic compression

Apparent molar isentropic compression of ionic liquid in binary aqueous solutions of benzamide and benzylamine was calculated using Equation (4.23).

For the calculation of coefficient of isentropic compressibility κ_s , following Laplace Newton's equation (4.24) was used.

The values for $K_{\phi,s}$ are obtained from the equation (4.23) and are tabulated in Table 5.7 and visually represented in fig 5.3(a) and 5.3(b). From Table 5.7 it is clear that the values of $K_{\phi,s}$ (apparent molar compressibility) at all the concentrations and temperatures are negative and these values further increase as we increase both concentration and temperature. The negative values of $K_{\phi,s}$ indicate the less compression of water molecule surrounding the ionic charged groups of IL. With the decrease in negative value, the structural compressibility of water is also decreased which indicates the less ordering of IL on solvents.

Partial molar isentropic compression

Equation (4.25) was used to determine the alteration of apparent molar isentropic compression with molal concentration.

Values of $K_{\phi,s}^o$ and S_K^* are depicted in Table 5.8 with standard errors. The values of $K_{\phi,s}^o$ are found negative which indicate the strong interactions among solute and solvent and positive values of S_K^* indicate the solute – solute interactions. In the present investigation, solute–solvent interactions dominate over solute – solute interactions (Roy et al., 2007). At infinite dilution, the solvent molecules surround each other which led to negligible ion-ion interaction and stronger ion-solvent interaction or solute solvent interactions. It is also clear that with increasing temperature the values of $K_{\phi,s}^o$ turn into less negative signifying the reduced electrostriction with rising temperature and some of the H₂O molecules enter the bulk from the hydration sphere (H. Kumar et al., 2014).

In order to calculate partial molar isentropic compression $\Delta K_{\phi,s}^o$ of IL from water to aqueous solutions of benzamide and benzylamine at infinite dilution equation (4.26) has been used.

All the observed calculated values of $\Delta K_{\phi,s}^o$ are tabulated in Table 5.9. The negative values of $\Delta K_{\phi,s}^o$ indicate the structure breaking tendency of the ionic liquid in aqueous solutions of benzamide and benzylamine and behavior is found in good agreement with the findings of volumetric studies.

Pair triplet interaction coefficient

Friedman and Krishnan modified the theory given by McMillan and Mayer (McMillan & Mayer, 1945) which helps in identifying the interaction coefficients of the interactions between two or more than two solutes. Partial molar volume of transfer and partial molar isentropic compression of transfer is expressed by equations (4.21) and (4.22) respectively.

Values of V_{AB} , K_{AB} , V_{ABB} , K_{ABB} are listed in Table 5.10 and are calculated by using (4.21) and (4.22) equations. In case of IL + aqueous benzamide values of V_{AB} , K_{AB} are positive indicating the significant pair wise interaction between IL and aqueous benzamide. On the other hand, values of V_{ABB} , K_{ABB} are negative. In the above-mentioned formalism, H₂O molecules are liberated from the hydration co-sphere to the bulk due to the overlap when nonbonding favorable interactions are present (H. Kumar, et al., 2021; S. Sharma et al., 2020). Higher values of pair interaction coefficient than those of the triplet interaction coefficients signifies the predominance of pair wise interaction in the current system. In case of IL + aqueous benzylamine no specific trend has been found. The values of triplet coefficient K_{ABB} is inversely proportional to temperature for the first system and directly proportional to temperature for the second system.

Conductance measurements

Conductivity of all aqueous solutions of benzylamine in [DMTI] and aqueous benzamide in [DMTI] of various molal concentration ranging from 0.001 to 0.009 mmol/kg have been determined by using digital conductivity meter which was supplied by Labtronics Pvt. Ltd. (India). 0.01 M KCl solution was used for the calibration of conductivity cell with the determination of cell constant equal to 1cm⁻¹. Before every measurement the solution was gently stirred using the

magnetic stirrer before measuring conductance (Pathania, Sharma, Vermani, Vermani, & Grover, 2021).

The conductivity (k , $\mu\text{S}\cdot\text{cm}^{-1}$) of 1[DMTI] in 0.01 to 0.05 mol solutions of benzylamine and benzamide at temperatures varying from 288.15 K to 318.15 K are measured.

Equation (4.31) was used for the calculation of the molar conductivities (Λ_m , $\text{S}\cdot\text{cm}^2\text{mol}^{-1}$) of the ternary solutions,

Conductivity (k , $\mu\text{S}\cdot\text{cm}^{-1}$) and molar conductance (Λ_m , $\text{S}\cdot\text{cm}^2\text{mol}^{-1}$) measured at four different temperatures (288.15K to 318.15K) are recorded in Table 5.11. From the results we can conclude that with the increasing concentration of the solution molar conductivity decreases and with increase in temperature molar conductance increases. Higher the temperature, higher the frequency resulting in the breakage of the bond due to the increase in vibrational and translational degrees of freedom resulting in the increase in mobilities of the ions (Johansson et al., 2010).

Figure 5.4 and Figure 5.5, The plots of Λ_m vs. \sqrt{c} , where straight line gives intercept equal to limiting molar conductance and the slope is equal to Onsager constant (denoted by S) were found to be straight lines throughout the whole composition range which concludes the complete dissociation of the solution and reference electrode.

The values obtained of molar conductance were further used for the calculation of limiting molar conductance using the Onsager equation (Equation 4.32) which is tabulated in Table 5.12.

With increasing temperature, so does the value of limiting molar conductance, which is due to the increased mobility of ions. Also using these values, we can interpret the ion-solvent interactions. Higher the values of limiting molar conductance greater the ion-solvent interactions i.e. the increase in the values of limiting molar conductance indicates the increase in the ion-solvent interaction. Among both the systems, these have the higher ion-solvent interactions [30-31].

Equation (4.33) represents the impact of temperature on conductance where activation energy is represented by E_a . Table 5.13 tabulates the data obtained for activation energy obtained by the slope of the linear plot of $\log \Lambda$ versus $1/T$.

FT-IR Studies

For the final confirmation of intermolecular interaction, which are predicted by thermodynamic and acoustic parameters at different temperature and concentrations, FT-IR spectral studies were performed at room temperature using Shimadzu FT-IR 8400S spectrophotometer. In case of

mixture of IL and aqueous benzamide, the peaks in the range between 1600-1650 cm^{-1} are assigned to C=O stretching, while the peaks around 3200-3350 cm^{-1} is indicative for -OH vibration. The transmission band for pure compound are designated as 1639.55 cm^{-1} (C=O Str.), 3312.5 cm^{-1} (N-H Str.)

In case of mixture of IL and aqueous benzylamine, the peak in range 1400-1700 cm^{-1} are assigned to C=C stretching, while the peaks in range 3000-3400 cm^{-1} is for -OH stretching. The pure compound shows peaks at 696.33 cm^{-1} and 734.90 cm^{-1} (monosubstituted), 1391 cm^{-1} (C-N Str.), 1453 cm^{-1} and 1602-1649 cm^{-1} (C=C Str. of aromatic ring), 2870.17 cm^{-1} (-C-H str. sp^3), 3028.06 cm^{-1} (-C-H str. sp^2 aromatic), 3264.04-3300.30 cm^{-1} (O-H Str.). The wave-numbers obtained from the FT-IR spectral studies of aqueous mixtures are tabulated in Table 5.14 and visually represented in Figure 5.7 and 5.8. The bands for functional group in benzylamine and benzamide show same behavior as that of the pure compound with slight shifts in the position of band or intensity. The change in wave number shows the presence of intermolecular interactions, and the overlapping of peaks also signifies the strong behavior of the functional group. All the vibrations are sensitive, and these vibrations provide the structural information of the particular system as well as presence of intermolecular and intramolecular interactions (H. Kumar, Verma, & Chadha, 2017; H. Kumar & Katal, 2018). In the studied ternary systems, the shift in wavenumber corresponding to -OH group towards lower side confirms the presence of intermolecular interactions.

Table 5.1.

Value of densities (ρ), apparent molar volumes (V_ϕ) of [DMTI] in aqueous solutions of benzamide and benzylamine at different temperatures.

$^a m_A /$ (mol.kg ⁻¹)	$\rho \times 10^{-3} / (\text{kg m}^{-3})$				$V_\phi \times 10^6 / (\text{m}^3 \text{mol}^{-1})$			
	288.15 K	298.15 K	308.15 K	318.15 K	288.15 K	298.15 K	308.15 K	318.15 K
[DMTI] + 0.01 (mol. kg⁻¹) aqueous Benzamide								
0.00000	0.999315	0.997251	0.995215	0.993428				
0.00126	0.999479	0.997402	0.995353	0.993554	94.99	104.97	115.42	125.09
0.00253	0.999644	0.997555	0.995494	0.993681	94.97	104.96	114.83	125.24
0.00379	0.999808	0.997706	0.995632	0.993807	94.96	104.94	114.99	125.16
0.00633	1.000139	0.998012	0.995912	0.994062	94.93	104.91	115.02	125.10
0.00887	1.000468	0.998316	0.996191	0.994315	94.90	104.88	114.94	125.11
[DMTI] + 0.03 (mol. kg⁻¹) aqueous Benzamide								
0.00000	0.999531	0.997599	0.995642	0.993782				
0.00126	0.999698	0.997754	0.995794	0.993924	93.00	102.71	105.06	113.02
0.00253	0.999865	0.997908	0.995946	0.994065	92.98	102.85	104.80	113.17
0.00379	1.000032	0.998062	0.996097	0.994207	92.97	102.93	105.02	112.99
0.00634	1.000369	0.998373	0.996403	0.994493	92.93	102.91	104.94	112.89
0.00885	1.000700	0.998679	0.996705	0.994774	92.90	102.90	104.80	112.89
[DMTI] + 0.05 (mol. kg⁻¹) aqueous Benzamide								
0.00000	0.999802	0.997982	0.996017	0.994109				
0.00127	0.999975	0.998141	0.996173	0.994253	89.01	99.96	101.93	112.00
0.00253	1.000146	0.998298	0.996328	0.994395	88.99	99.95	101.91	111.99
0.00379	1.000317	0.998456	0.996483	0.994537	88.97	99.93	101.90	111.97
0.00632	1.000662	0.998772	0.996794	0.994823	88.94	99.90	101.86	111.94
0.00885	1.001006	0.999088	0.997106	0.995109	88.91	99.87	101.83	111.91
[DMTI] + 0.01 mol.kg⁻¹ aqueous Benzylamine								
0.00000	0.999311	0.997182	0.994537	0.992157				

0.00126	0.999474	0.997333	0.994676	0.992283	95.99	104.97	115.03	125.20
0.00253	0.999638	0.997486	0.994816	0.992411	95.97	104.95	115.02	125.18
0.00380	0.999802	0.997738	0.994956	0.992538	95.96	104.93	115.00	125.16
0.00632	1.000127	0.997941	0.995233	0.992790	95.92	104.90	114.97	125.14
0.00886	1.000454	0.998245	0.995512	0.993043	95.89	104.87	114.94	125.10
[DMTI] + 0.03 mol.kg⁻¹ aqueous Benzylamine								
0.00000	0.999522	0.997425	0.994901	0.992556				
0.00126	0.999688	0.997580	0.995049	0.992698	94.00	101.96	107.96	113.02
0.00253	0.999853	0.997736	0.995196	0.992839	93.98	101.94	107.95	113.00
0.00380	1.000020	0.997892	0.995346	0.992982	93.97	101.93	107.93	112.98
0.00631	1.000349	0.998201	0.995640	0.993263	93.93	101.90	107.90	112.95
0.00888	1.000685	0.998517	0.995939	0.993550	93.90	101.86	107.87	112.92
[DMTI] + 0.05 mol.kg⁻¹ aqueous Benzylamine								
0.00000	0.999838	0.997801	0.995172	0.992919				
0.00127	1.000010	0.997959	0.995323	0.993062	89.01	99.96	105.95	112.00
0.00253	1.000182	0.998118	0.995473	0.993205	88.99	99.94	105.93	111.99
0.00379	1.000354	0.998275	0.995623	0.993347	88.98	99.93	105.92	111.97
0.00632	1.000698	0.998592	0.995925	0.993634	88.95	99.90	105.88	111.94
0.00884	1.001040	0.998906	0.996224	0.993918	88.92	99.86	105.85	111.90

^am_A is the molal concentration of [DMTI] in aqueous benzamide / benzylamine mixtures.

Standard uncertainty in molality of acetamide $u_r(m_{\text{Benzamide/Benzylamine}})$ and IL $u_r(m_{\text{IL}})$ are 0.005 mol.kg⁻¹ and 0.004 mol.kg⁻¹ correspondingly. The values of standard uncertainty in density, AMV, temperature and pressure are $u(\delta\rho) = 0.3 \text{ kg}\cdot\text{m}^{-3}$, $u(\delta V_\phi) = \pm (0.01 - 0.10) \times 10^{-3} \text{ m}^3\cdot\text{mol}^{-1}$, $u(T) = 0.01 \text{ K}$ and $u(P) = 0.01 \text{ MPa}$ correspondingly.

Table 5.2.

Value of densities ρ , and ultrasonic speed, u of 1,4-Dimethyl-4H-1,2,4-triazolium iodide in water at different temperatures.

$a_{m_A}/$ (mol.kg ⁻¹)	$\rho \times 10^{-3} / (\text{kg m}^{-3})$				$u / (\text{ms}^{-1})$			
	288.15 K	298.15 K	308.15 K	318.15 K	288.15 K	298.15 K	308.15 K	318.15 K
1,4-Dimethyl-4H-1,2,4-triazolium iodide + Water								
0.001262	0.999270	0.997205	0.994157	0.990308	1477.07	1492.74	1507.45	1524.14
0.002516	0.999429	0.997361	0.994282	0.990475	1479.54	1495.49	1510.20	1526.97
0.003765	0.999588	0.997518	0.994407	0.990641	1482.01	1498.23	1512.93	1529.78
0.006312	0.999912	0.997837	0.994662	0.990980	1487.04	1503.81	1518.51	1535.52

Table 5.3.

Partial molar volumes (V_{ϕ}^o) and experimental slopes (S_v^*) of 1,4-Dimethyl-4H-1,2,4-triazolium iodide in binary aqueous solutions of benzamide and benzylamine at different temperatures.

$^a m_B$ (mol kg ⁻¹)	$V_{\phi}^o \times 10^6 / (\text{m}^3 \text{mol}^{-1})$				$S_v^* \times 10^6 / (\text{m}^3 \text{kg mol}^{-2})$			
	288.15 K	298.15 K	308.15 K	318.15 K	288.15 K	298.15 K	308.15 K	318.15 K
IL+ Water								
0.00	97.9039 (±0.0018)	99.7537 (±0.0018)	101.9001 (±0.0018)	103.9501 (±0.0018)				
Benzamide								
0.01	95.0165 (±0.0009)	104.9874 (±0.0009)	110.0082 (±0.0008)	115.0520 (±0.0008)	-2.9921 (±0.0045)	3.0214 (±0.0044)	5.0601 (±0.0043)	3.0574 (±0.0042)
0.03	93.0092 (±0.0009)	102.9824 (±0.0009)	104.9582 (±0.0009)	113.0264 (±0.0008)	-4.9915 (±0.0046)	1.0112 (±0.0045)	0.0366 (±0.0045)	1.0271 (±0.0043)
0.05	89.0214 (±0.0009)	99.9801 (±0.0009)	101.9425 (±0.0008)	112.0263 (±0.0008)	-8.9857 (±0.0045)	-1.9834 (±0.0044)	-2.9901 (±0.0043)	0.0124 (±0.0042)
Benzylamine								
0.01	96.0101 (±0.0009)	104.9861 (±0.0009)	115.0511 (±0.0008)	125.2201 (±0.0002)	-12.3809 (±0.0002)	-12.6157 (±0.0018)	-12.7165 (±0.0017)	-12.6194 (±0.0015)
0.03	94.0123 (±0.0009)	101.9761 (±0.0009)	107.9801 (±0.0008)	113.6914 (±0.0012)	-12.3111 (±0.0002)	-12.5584 (±0.0018)	-12.6872 (±0.0018)	-12.8137 (±0.0018)
0.05	89.0217 (±0.0009)	99.9721 (±0.0009)	101.9012 (±0.0001)	112.0211 (±0.0008)	-12.0923 (±0.0002)	-12.5061 (±0.0019)	-12.5893 (±0.0019)	-12.7332 (±0.0018)

^a m_B is the molal concentration of aqueous solution of benzamide /benzylamine.

Table 5.4.

Partial molar volumes of transfer (ΔV_{ϕ}^0) of 1,4-Dimethyl-4H-1,2,4-triazolium iodide in binary aqueous solutions of benzamide and benzylamine at temperatures 218.15 to 318.15K.

$^a m_B$ (mol kg ⁻¹)	$\Delta V_{\phi}^0 \times 10^6 / (\text{m}^3 \text{mol}^{-1})$			
	288.15 K	298.15 K	308.15 K	318.15 K
Benzamide				
0.01	4.07	3.28	2.16	1.23
0.03	5.19	4.45	3.28	2.35
0.05	6.31	5.57	4.57	3.47
Benzylamine				
0.01	-2.90	5.23	13.15	21.27
0.03	-3.89	2.22	6.08	9.74
0.05	-8.88	0.22	0.03	8.07 (Nidhi, et.al., 2024)

^a m_B is the molality of benzamide and benzylamine.

Table 5.5.

Values of empirical parameters of Eq. (4) for 1,4-Dimethyl-4H-1,2,4-triazolium iodide in aqueous benzamide and benzylamine solutions.

$^a m_B / (\text{mol kg}^{-1})$	$a \times 10^6 / (\text{mol kg}^{-1})$	$b \times 10^6 / (\text{m}^3 \text{mol}^{-1} \text{K})$	$c \times 10^6 / (\text{m}^3 \text{mol}^{-1} \text{K}^{-2})$	R^2	ARD(σ)
Benzamide					
0.01	104.237	0.7749	-0.0123	0.9989	0.01879
0.03	100.871	0.6679	-0.0047	0.9994	0.05445
0.05	97.413	0.7316	-0.0022	0.9999	0.06807
Benzylamine					
0.01	105.135	0.9474	0.0029	0.9984	0.00361
0.03	101.727	0.7067	-0.0056	0.9991	0.00635
0.05	97.403	0.7308	-0.0021	0.9998	0.06823

$^a m_B$ is molality of aqueous solutions of benzamide and benzylamine respectively.

Table 5.6.

Limiting apparent molar expansibilities (ϕ_E^0) for 1,4-Dimethyl-4H-1,2,4-triazolium iodide in aqueous benzamide and benzylamine solutions at different temperatures.

^a m _B / (mol kg ⁻¹)	$\phi_E^0 \times 10^6 / (\text{m}^3 \text{mol}^{-1} \text{K}^{-1})$				$(\partial \phi_E^0 / \partial T)$
	288.15 K	298.15 K	308.15 K	318.15 K	
Benzamide					
0.01	1.012	0.775	0.529	0.282	-0.0246
0.03	0.761	0.668	0.573	0.478	-0.0094
0.05	0.775	0.099	0.127	0.154	-0.0044
Benzylamine					
0.01	0.888	0.947	1.007	1.066	0.0058
0.03	0.820	0.707	0.594	0.481	-0.0112
0.05	0.774	0.731	0.688	0.645	-0.0042

^a m_B is the molality of aqueous mixtures of benzamide /benzylamine

Table 5.7.

Values of ultrasonic speed (u) and apparent molar isentropic compression ($K_{\phi,s}$) of Ionic liquid in aqueous solutions of benzamide and benzylamine at different temperatures.

$^a m_A /$ (mol kg ⁻¹)	$u / (\text{ms}^{-1})$				$K_{\phi,s} \times 10^6 (\text{m}^3 \text{mol}^{-1} \text{GPa}^{-1})$			
	288.15 K	298.15 K	308.15 K	318.15 K	288.15 K	298.15 K	308.15 K	318.15 K
[DMTI] + 0.01 mol.kg⁻¹ Benzamide								
0.00000	1477.87	1492.98	1509.11	1525.74				
0.00126	1480.50	1495.37	1511.70	1527.60	-13.09	-11.52	-12.04	-8.31
0.00253	1483.16	1497.79	1514.32	1529.49	-13.05	-11.50	-12.01	-8.32
0.00379	1485.79	1500.18	1516.92	1531.36	-13.02	-11.47	-12.00	-8.31
0.00634	1491.12	1505.02	1522.17	1535.14	-12.95	-11.41	-11.93	-8.28
0.00887	1496.41	1509.83	1527.39	1538.90	-12.88	-11.36	-11.87	-8.26
[DMTI] + 0.03 mol.kg⁻¹ Benzamide								
0.00000	1480.92	1497.14	1512.52	1528.35				
0.00126	1483.19	1499.27	1514.47	1530.13	-11.28	-10.19	-8.99	-8.14
0.00253	1485.45	1501.39	1516.42	1531.91	-11.26	-10.17	-8.97	-8.13
0.00379	1487.71	1503.51	1518.36	1533.69	-11.23	-10.14	-8.96	-8.11
0.00634	1492.28	1507.79	1522.29	1537.28	-11.18	-10.10	-8.92	-8.08
0.00885	1496.77	1512.01	1526.15	1520.81	-11.13	-10.06	-8.89	-8.06
[DMTI] + 0.05 mol.kg⁻¹ Benzamide								
0.00000	1483.15	1500.61	1515.89	1531.14				
0.00127	1485.44	1502.81	1517.94	1532.93	-11.39	-10.43	-9.36	-8.10
0.00253	1487.72	1505.00	1519.98	1534.70	-11.36	-10.41	-9.34	-8.09
0.00379	1490.00	1507.18	1522.02	1536.47	-11.34	-10.39	-9.32	-8.07
0.00632	1494.57	1511.57	1526.10	1540.03	-11.29	-10.35	-9.28	-8.01
0.00885	1499.13	1515.96	1530.19	1543.58	-11.23	-10.30	-9.24	-8.02
[DMTI] + 0.01 mol.kg⁻¹ Benzylamine								
0.00000	1478.01	1493.89	1510.04	1526.85				

0.00126	1481.23	1497.11	1513.28	1530.13	-15.89	-15.41	-15.01	-14.67
0.00254	1484.47	1500.36	1516.55	1533.44	-15.84	-15.36	-14.96	-14.63
0.00381	1487.71	1503.60	1519.81	1536.74	-15.79	-15.31	-14.91	-14.58
0.00633	1494.13	1510.03	1526.28	1543.28	-15.69	-15.21	-14.82	-14.49
0.00886	1500.59	1516.49	1532.79	1549.87	-15.59	-15.11	-14.73	-14.40
[DMTI] + 0.03 mol.kg⁻¹ Benzylamine								
0.00000	1481.55	1498.06	1513.36	1529.26				
0.00126	1484.62	1501.28	1516.60	1532.54	-15.63	-15.30	-14.96	-14.70
0.00253	1487.69	1504.50	1519.84	1535.82	-15.58	-15.25	-14.92	-14.65
0.00380	1490.79	1507.75	1523.12	1539.13	-15.53	-15.20	-14.87	-14.61
0.00631	1496.89	1514.16	1529.56	1545.66	-15.43	-15.10	-14.77	-14.51
0.00888	1503.12	1520.69	1536.14	1552.31	-15.34	-15.01	-14.68	-14.42
[DMTI] + 0.05 mol.kg⁻¹ Benzylamine								
0.00000	1484.16	1501.78	1516.41	1532.58				
0.00127	1487.34	1505.01	1519.66	1535.87	-15.52	-15.19	-14.88	-14.60
0.00253	1490.51	1508.23	1522.91	1539.16	-15.48	-15.14	-14.84	-14.56
0.00379	1493.67	1511.44	1526.14	1542.43	-15.43	-15.09	-14.79	-14.51
0.00632	1500.03	1517.91	1532.64	1549.01	-15.33	-15.00	-14.69	-14.42
0.00884	1506.34	1524.31	1539.09	1555.53	-15.23	-14.90	-14.60	-14.33

^am_A is the molal concentration of [DMTI] in aqueous benzamide / benzylamine mixtures.

Standard uncertainty in molality of acetamide $u_r(m_{Benzamide/Benzylamine})$ and IL $u_r(m_{IL})$ are 0.005 mol.kg⁻¹ and 0.004 mol.kg⁻¹ correspondingly. The values of standard uncertainty in density, apparent molar isentropic compression, temperature and pressure are $u(\delta\rho) = 0.3 \text{ kg}\cdot\text{m}^{-3}$, $u(\delta K\phi, s) = \pm (0.15-1.65) \times 10^{-6} \text{ m}^3\cdot\text{mol}^{-1}\cdot\text{GPa}^{-1}$, $u(T) = 0.01 \text{ K}$ and $u(P) = 0.01 \text{ MPa}$ correspondingly.

Table 5.8.

Partial molar isentropic compression ($K_{\phi,s}^0$) and experimental slopes (S_K^*) for 1, 4-Dimethyl-4H-1,2,4-triazolium iodide in aqueous solutions of benzamide and benzylamine at different temperatures.

$^a m_B /$ (mol kg ⁻¹)	$K_{\phi,s}^0 \times 10^6 / (\text{m}^3 \text{mol}^{-1} \text{GPa}^{-1})$				$S_K^* \times 10^6 / (\text{kg m}^3 \text{mol}^{-2} \text{GPa}^{-1})$			
	288.15 K	298.15 K	308.15 K	318.15 K	288.15 K	298.15 K	308.15 K	318.15 K
IL + Water								
0.00	-11.05 (±0.01)	-10.27 (±0.01)	-09.29 (±0.01)	-08.08 (±0.01)				
Benzamide								
0.01	-13.13 (±0.01)	-11.64 (±0.01)	-10.13 (±0.01)	-8.66 (±0.01)	27.10 (±0.06)	22.27 (±0.17)	17.13 (±0.06)	12.69 (±0.08)
0.03	-11.31 (±0.01)	-10.21 (±0.01)	-9.01 (±0.01)	-8.16 (±0.01)	20.68 (±0.17)	17.05 (±0.05)	13.27 (±0.07)	11.45 (±0.11)
0.05	-11.42 (±0.05)	-10.46 (±0.01)	-9.38 (±0.01)	-8.12 (±0.01)	20.38 (±0.89)	17.38 (±0.37)	14.80 (±0.04)	11.14 (±0.03)
Benzylamine								
0.01	-15.95 (±0.03)	-15.45 (±0.09)	-15.05 (±0.05)	-14.71 (±0.02)	40.02 (±0.06)	38.91 (±0.18)	37.46 (±0.10)	36.24 (±0.05)
0.03	-15.67 (±0.09)	-15.34 (±0.09)	-15.01 (±0.09)	-14.74 (±0.01)	38.06 (±0.17)	38.57 (±0.19)	37.52 (±0.17)	36.99 (±0.21)
0.05	-15.57 (±0.03)	-15.24 (±0.09)	-14.92 (±0.09)	-27.04 (±0.02)	38.42 (±0.06)	38.24 (±0.19)	37.02 (±0.09)	36.14 (±0.04)

^a m_B is the molality of binary aqueous mixtures of benzamide / benzylamine.

Table 5.9.

Partial molar isentropic compression of transfer ($\Delta K_{\phi,s}^0$) for 1,4-Dimethyl-4H-1,2,4-triazolium iodide in aqueous solutions of benzamide and benzylamine at temperature from 218.1K to 318.15K.

$a_{\text{mB}} /$ (mol kg ⁻¹)	$\Delta K_{\phi,s}^0 \times 10^6 / (\text{m}^3 \text{mol}^{-1} \text{GPa}^{-1})$			
	288.15 K	298.15 K	308.15 K	318.15 K
Benzamide				
0.01	0.53	-0.17	-0.37	-1.07
0.03	1.02	-0.92	-0.81	-0.74
0.05	1.06	-1.02	-1.05	-0.63
Benzylamine				
0.01	-3.90	-4.18	-4.76	-5.53
0.03	-3.62	-4.07	-4.71	-5.56
0.05	-3.52	-3.97	-4.63	-5.46

a_{mB} is the molal concentration of aqueous mixtures benzamide and benzylamine.

Table 5.10.

Pair and triplet interaction coefficients of ternary mixture of 1,4-Dimethyl-4H-1,2,4-triazolium iodide in aqueous benzamide and benzylamine at different temperatures.

T / (K)	$V_{AB} \times 10^6 /$ (m³ mol⁻² kg)	$V_{ABB} \times 10^6 /$ (m³ mol⁻³ kg²)	$K_{AB} \times 10^6 /$ (m³ mol⁻² kg GPa⁻¹)	$K_{ABB} \times 10^6 /$ (m³ mol⁻³ kg² GPa⁻¹)
Benzamide				
288.15	-103.67	210.86	-8.58	224.27
298.15	112.52	-1800.30	12.86	-47.11
308.15	138.27	-2322.51	29.31	-259.69
318.15	91.58	-1262.21	27.85	-230.47
Benzylamine				
288.15	-51.29	-480.94	-143.67	1485.15
298.15	167.95	-2278.17	-157.24	1607.96
308.15	441.79	-6050.72	-179.77	1824.91
318.15	624.54	-7546.18	-210.43	2129.69

Table 5.11.

Specific Conductivity (k , $\mu\text{S}\cdot\text{cm}^{-1}$) and molar conductivity (Λ_m , $\text{S}\cdot\text{cm}^2\text{mol}^{-1}$) of 1,4-Dimethyl-4H-1,2,4 triazolium iodide in aqueous solution of benzylamine and benzamide.

$a_{\text{MA}}/$ ($\text{mol}\cdot\text{kg}^{-1}$)	Specific Conductivity (k , $\mu\text{S}\cdot\text{cm}^{-1}$)				Molar Conductance (Λ_m , $\text{S}\cdot\text{cm}^2\text{mol}^{-1}$)			
	288.15	298.15	308.15	318.15	288.15	298.15	308.15	318.15
[DMTI]+ aqueous 0.01 mol kg⁻¹ Benzylamine								
0.00126	737.81	1127.00	1409.80	1608.60	2.89	3.95	4.94	5.64
0.00253	929.65	1090.60	170.40	1337.00	1.62	1.90	2.04	2.33
0.00380	981.48	1261.40	1544.20	1843.80	1.14	1.47	1.79	2.14
0.00632	996.86	1313.20	1694.00	2053.80	0.70	0.92	1.18	1.43
0.00886	1213.84	2185.40	2249.80	2504.60	0.61	1.09	1.12	1.25
[DMTI]+ aqueous 0.03 mol kg⁻¹ Benzylamine								
0.00126	546.00	861.24	1078.21	1328.67	1.92	3.02	3.79	4.67
0.00253	687.47	939.42	1136.89	1205.47	1.20	1.64	1.99	2.11
0.00380	781.24	1212.40	1416.86	1789.25	0.91	1.41	1.65	2.08
0.00631	844.21	1261.40	1534.43	1845.27	0.59	0.88	1.08	1.29
0.00888	1199.8	1993.60	2220.42	2429.01	0.60	0.99	1.11	1.21
[DMTI]+ aqueous 0.05 mol kg⁻¹ Benzylamine								
0.00127	400.4	602	950.6	1142.4	1.9	2.10	3.31	3.98
0.00253	421.4	715.4	893.2	1057	0.74	1.025	1.56	1.85
0.00379	617.4	939.4	1390.2	1488.2	0.72	1.10	1.62	1.74
0.00632	662.2	1062.6	1401.4	1541.4	0.46	0.74	0.98	1.08
0.00884	935.2	1727.60	1982.4	2291.8	0.47	0.86	0.99	1.15

[DMTI]+ aqueous 0.01 mol kg⁻¹ Benzamide								
0.00126	565.6	698.6	813.4	994	1.99	2.45	2.86	3.49
0.00253	702.8	858.2	1026.2	1191.4	1.23	1.50	1.79	2.08
0.00379	732.2	1044.4	1212.4	1341.2	0.85	1.22	1.41	1.57
0.00633	915.6	1121.4	1276.8	1435	0.64	0.78	0.89	1.00
0.00887	1138.2	1254.4	1377.6	1661.8	0.57	0.63	0.69	0.83
[DMTI]+ aqueous 0.03 mol kg⁻¹ Benzamide								
0.00126	460.6	574	697.2	911.4	1.61	2.00	2.43	3.18
0.00253	557.2	772.8	964.6	1073.8	0.97	1.35	1.69	1.88
0.00379	583.8	730.8	925.4	1115.8	0.68	0.85	1.08	1.30
0.00634	873.6	875	1117.2	1141	0.61	0.61	0.78	0.80
0.00885	995.4	1141	1255.8	1369.2	0.50	0.57	0.63	0.68
[DMTI]+ aqueous 0.05 mol kg⁻¹ Benzamide								
0.00127	295.4	523.6	567	820.4	1.03	1.82	1.98	2.86
0.00253	435.4	610.4	726.6	911.4	0.76	1.07	1.27	1.59
0.00379	516.6	687.4	746.2	947.8	0.60	0.80	0.87	1.11
0.00632	655.2	764.4	928.2	1052.8	0.46	0.54	0.65	0.74
0.00885	764.4	949.2	1071	1254.4	0.38	0.47	0.54	0.63

m_A is the molality of [DMTI] in aqueous benzamide and benzylamine solutions.

Table 5.12.

Limiting molar conductivity (Λ_m , S.cm²mol⁻¹) of 1,4-Dimethyl-4H-1,2,4 triazolium iodide in aqueous solution of benzylamine and benzamide.

^a m _B (mol kg ⁻¹)	Limiting Molar Conductance (Λ° , S.cm ² ·mol ⁻¹)			
	288.15	298.15	308.15	318.15
Benzylamine				
0.001	3.45	4.76	5.90	6.76
0.003	2.45	3.68	4.63	5.63
0.005	1.69	2.50	3.98	4.76
Benzamide				
0.001	3.04	3.82	4.52	5.48
0.003	1.99	2.63	3.27	4.20
0.005	1.34	2.34	2.57	3.69

^am_B is molality of aqueous solution of benzamide and benzylamine.

Table 5.13.

Activation energy of 1,4-Dimethyl-4H-1,2,4 triazolium iodide in aqueous solution of benzylamine and benzamide.

Concentration ^a m _A / (mol.kg ⁻¹)	Activation Energy $E_A \times 10^{-3}(\text{kJ.mol}^{-1})$		
	0.01	0.03	0.05
Benzylamine			
0.000983	0.0140	0.0057	0.0052
0.002989	0.0097	0.0069	0.0055
0.004996	0.0070	0.0061	0.0056
0.006971	0.0080	0.0065	0.0058
0.008964	0.0061	0.0064	0.0057
Benzamide			
0.000983	0.0072	0.0064	0.0053
0.002989	0.0075	0.0065	0.0062
0.004997	0.0068	0.0066	0.0069
0.006971	-0.0012	0.0014	0.0078
0.008965	0.0094	0.0105	0.0079

^am_A is the molality of [DMTI] in aqueous benzamide and benzylamine solutions.

Table 5.14.

Wave numbers recorded from the FT-IR spectral studies of IL (0.01 to 0.05) mol kg⁻¹ in aqueous solution of benzamide and benzylamine.

^a m _A /(mol.kg ⁻¹)	Wave number (cm ⁻¹)	
	-OH	C=C
0.01 mol/kg benzamide + IL		
0.00126	3334.07	1635.69
0.00379	3319.60	1637.62
0.00887	3325.39	1638.00
0.03 mol/kg benzamide + IL		
0.00126	3337.93	1635.69
0.00379	3333.01	1639.01
0.00885	3325.03	1638.21
0.05 mol/kg benzamide + IL		
0.00127	3321.53	1635.69
0.00379	3329.25	1637.62
0.00885	3335.03	1638.21
0.01 mol/kg benzylamine + IL		
0.00126	3328.54	1634.25
0.00381	3340.82	1637.01
0.00886	3361.07	1637.62
0.03 mol/kg benzylamine + IL		
0.00126	3333.68	1634.01
0.00381	3328.48	1635.69
0.00888	3314.78	1636.65
0.05 mol/kg benzylamine + IL		
0.00127	3321.53	1638.58
0.00380	3320.21	1637.62
0.00884	3328.28	1638.58

^am_A is the molality of [DMTI] in aqueous mixtures of benzamide and benzylamine.

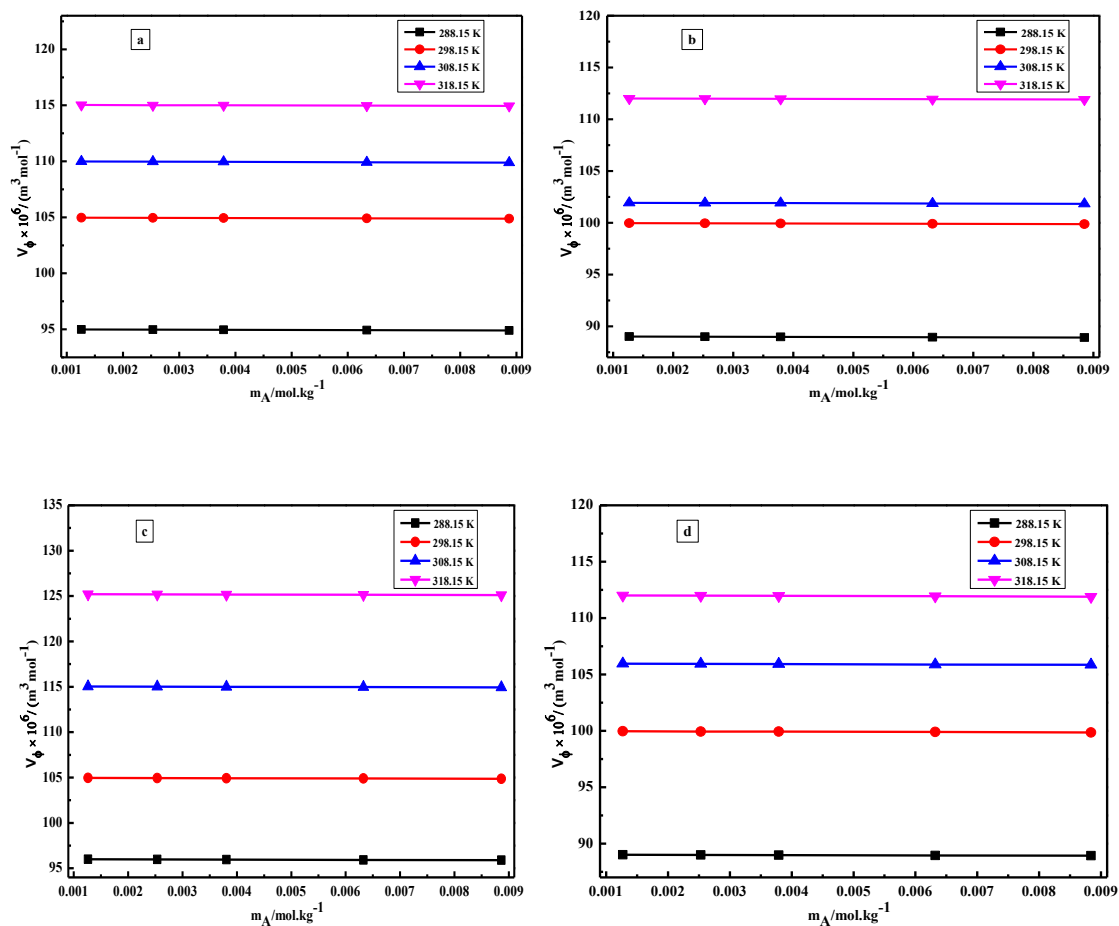


Figure 5.1.

Plots of variation of apparent molar volume (V_ϕ) of 1,4-Dimethyl-4H-1,2,4 triazolium iodide in (a) 0.01 mol kg⁻¹ and (b) 0.05 mol kg⁻¹ of aqueous solutions of benzamide; (c) 0.01 mol kg⁻¹ and (d) 0.05 mol kg⁻¹ of aqueous solutions of benzylamine at $T = (288.15, 298.15, 308.15 \text{ and } 318.15) \text{ K}$.

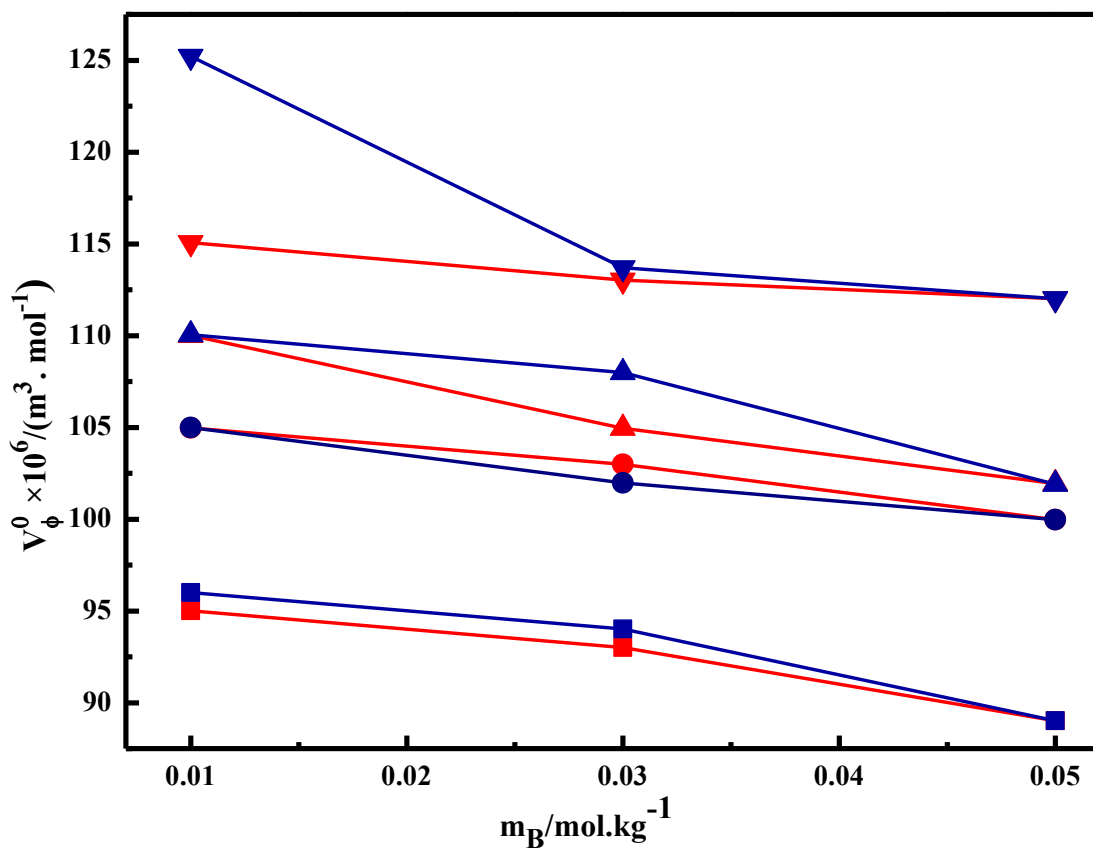


Figure 5.2.

Plot of variation of partial molar volume V_ϕ^0 of 1,4-Dimethyl-4H-1,2,4 triazolium iodide in various concentrations $m = (0.01, 0.03 \text{ and } 0.05) \text{ mol kg}^{-1}$ of benzamide (Red); benzylamine (Blue) at 288.15 K (■), 298.15 K (●), 308.15 K (▲) and 318.15 K (▼).

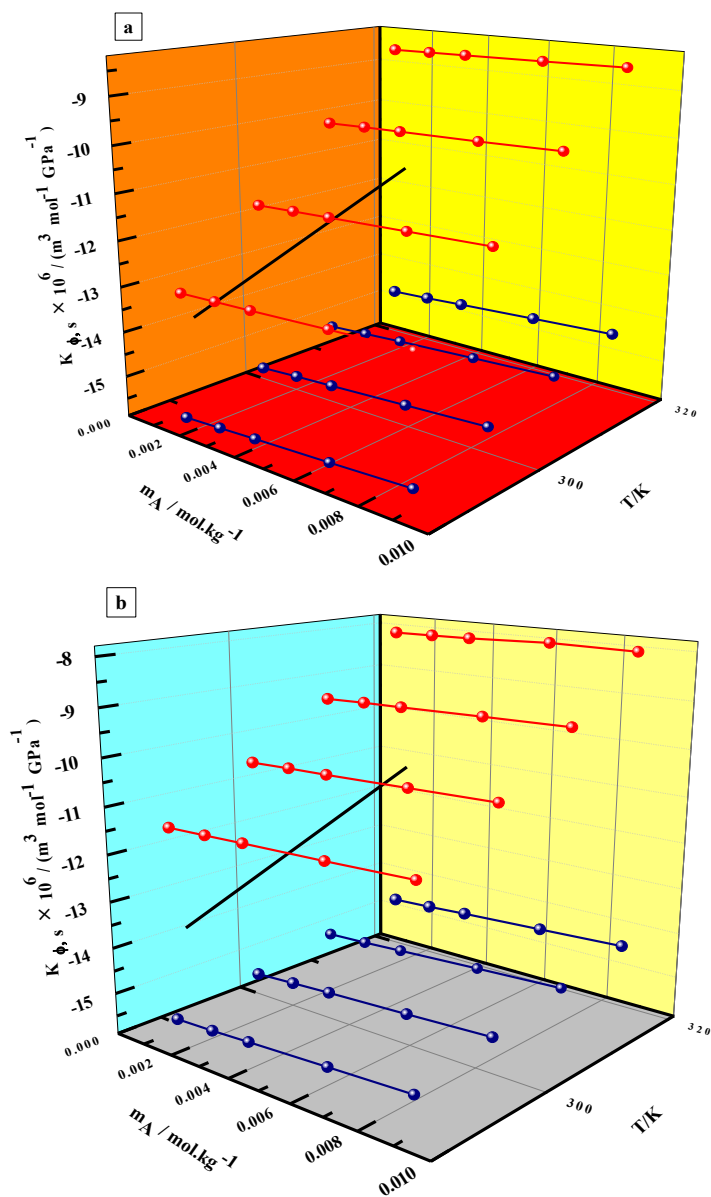


Figure 5.3.

Plot of variation of apparent molar isentropic compression ($K_{\phi,s}$) of 1,4-Dimethyl-4H-1,2,4 triazolium iodide in (a) 0.01 mol kg⁻¹ (b) 0.05 mol kg⁻¹ aqueous solutions of benzamide (Red); benzylamine (Blue) at T = (288.15, 298.15, 308.15 and 318.15).

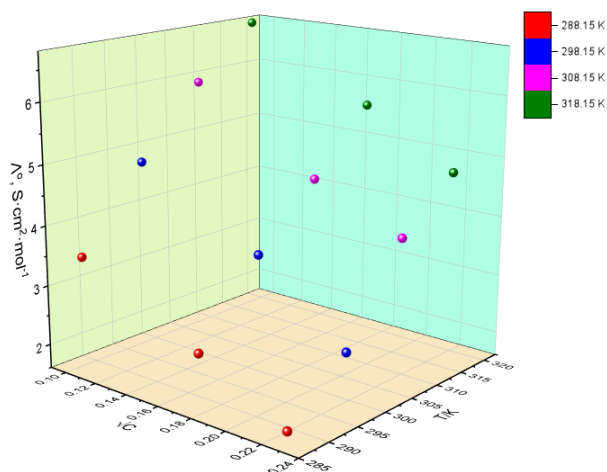


Figure 5.4

Plots showing the variation of Λ_o with \sqrt{C} for 1,4-Dimethyl-4H-1,2,4-triazolium iodide in 0.01 mol.kg⁻¹ aqueous benzylamine at T = (298.15, 303.15, 308.15 and 313.15) K.

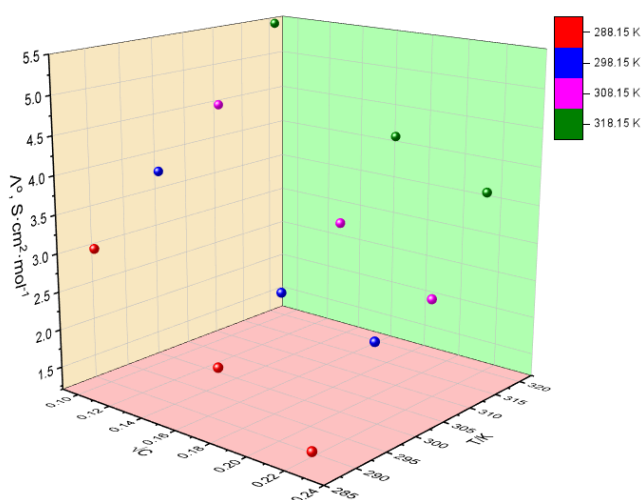


Figure 5.5

Plots showing the variation of Λ_o with \sqrt{C} for 1,4-Dimethyl-4H-1,2,4-triazolium iodide in 0.05 mol.kg⁻¹ aqueous benzylamine at T = (298.15, 303.15, 308.15 and 313.15) K.

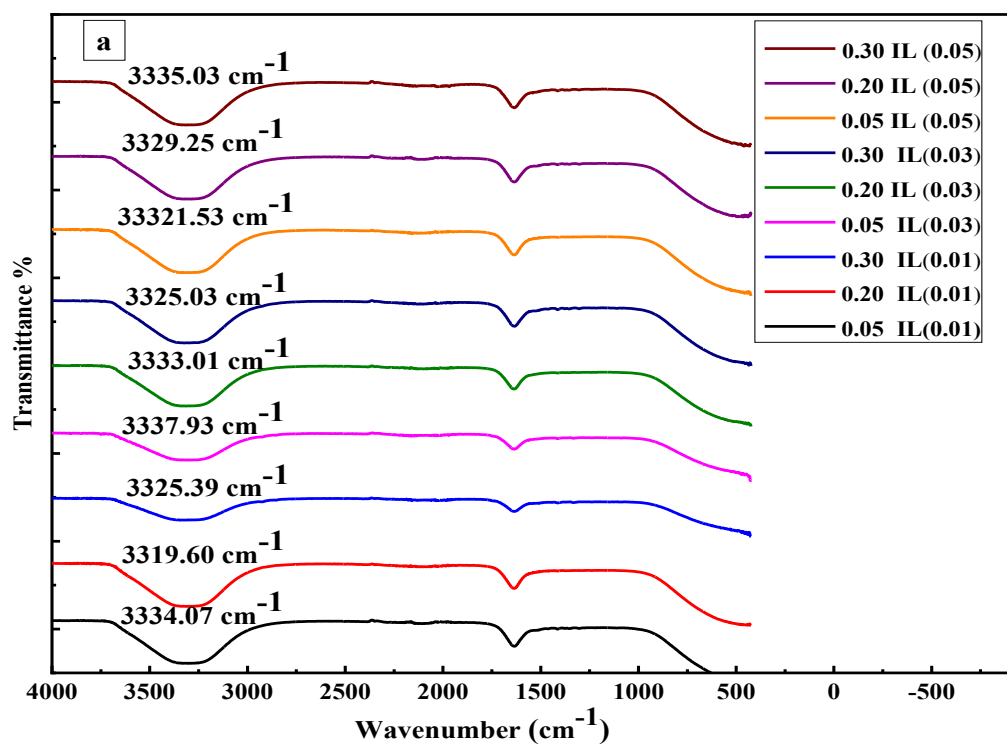


Figure 5.6

Plots of FT-IR spectra for [DMTI] iodide in (0.01 to 0.05) mol.kg⁻¹ of aqueous benzamide.

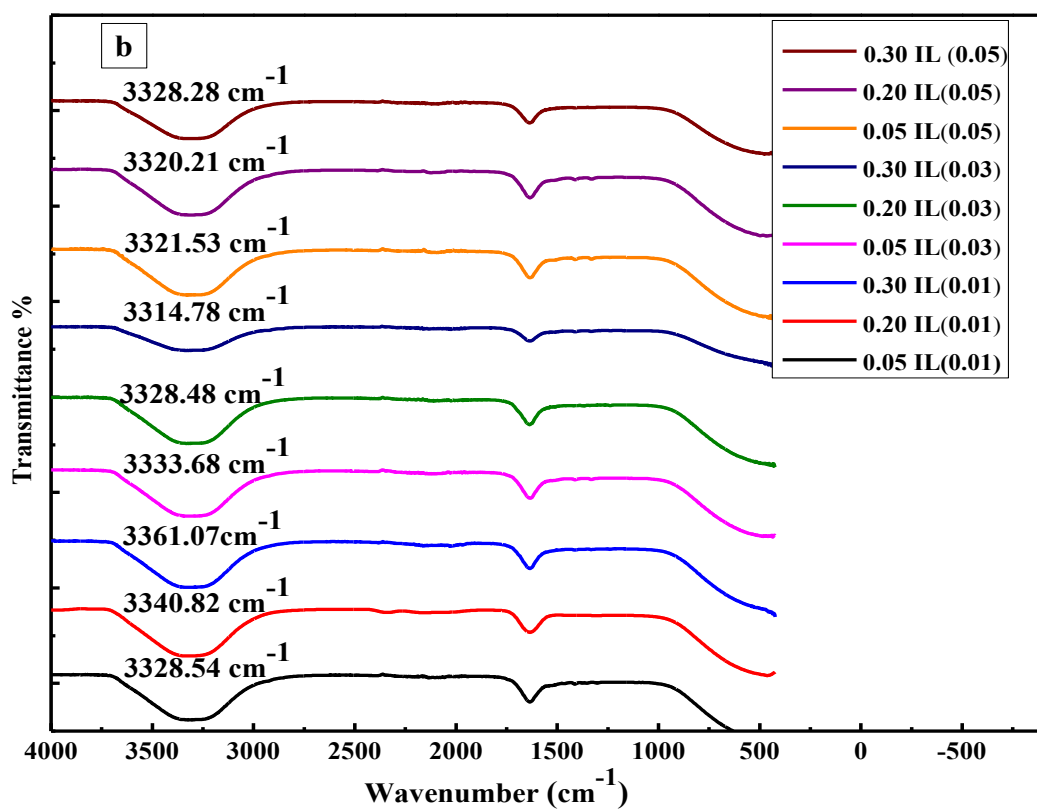


Figure 5.7

Plots of FT-IR spectra for [DMTI] in (0.01 to 0.05) mol.kg^{-1} of aqueous benzylamine

SECTION-II

Volumetric, acoustic, conductometric, spectroscopic and cyclic voltametric studies of 1-butyl-1-methyl Pyrrolidinium iodide in binary aqueous benzylamine and benzamide at various temperatures

Volumetric, acoustic, conductometric, spectroscopic and cyclic voltametric studies of 1-butyl-1-methyl Pyrrolidinium iodide in binary aqueous benzylamine and benzamide at various temperatures

Density measurements

In the current study, density (ρ) of [BMPyr⁺][I⁻] at different molal concentrations varying from 0.001 mol.kg⁻¹ to 0.009 mol.kg⁻¹ were measured in different concentrations of aqueous benzamide / benzylamine (0.0 to 0.05) mol.kg⁻¹ at a temperature range (288.15 K to 318.15 K). The experimental density values are tabulated in Table 5.15. From the measured data it is noted that density of ionic liquid (1-butyl-1-methyl pyrrolidinium iodide) escalates with increasing concentration of IL and benzamide/ benzylamine content in water. On the other hand, density values of [BMPyr⁺][I⁻] decrease as we increase the temperature. The density values are further used to calculate the various volumetric parameters to analyze the interaction occurring in the ternary mixture (IL + aqueous benzamide/ benzylamine).

Apparent molar volume (V_ϕ)

The AMV of 1-butyl-1-methyl pyrrolidinium iodide in three concentrations 0.01, 0.03, and 0.05 mol.kg⁻¹ of aqueous solutions of benzamide/ benzylamine are calculated by using equation (4.21) [32-33].

Table 5.15 tabulates the calculated V_ϕ as a function of molality and is also shown graphically. Fig.5.8.(a) and (b) represents AMV of [BMPyr⁺][I⁻] in (0.01 & 0.05) mol kg⁻¹ of aqueous benzamide and benzylamine solutions respectively. It is observed that V_ϕ values are positive which implies that the ternary mixtures of IL + aqueous benzylamine/benzamide exhibit strong solute-solvent interactions, which further intensify with increasing temperature. An increase in temperature causes a greater thermal movement of the molecules, which results in an increase in the volume (Chakraborty et al., 2019; Pal et al., 2015). In contrast, the solute-solvent interactions are weakened as the concentration of aqueous benzamide and benzylamine solution increases.

Partial molar volume (PMV)

PMV (V_{ϕ}^0), also known as limiting apparent molar volume is calculated by using least square fitting method to the equation (4.15) (H. Kumar, Chadha, Verma, et al., 2017).

Table 5.16 provides the data for V_{ϕ}^0 and S_v^* along with standard errors. In binary aqueous solutions of benzamide and benzylamine, it is duly noted from the observed data that the V_{ϕ}^0 values are positive and further increase with increase in temperature while decreases with increasing concentration of [BMPyr⁺][I⁻]. In Fig. 5.9, plots are illustrating the variation of the partial molar volume (V_{ϕ}^0) of 1-butyl-1-methyl pyrrolidinium iodide in various concentrations of benzamide and benzylamine $m = (0.01, 0.03 \text{ \& } 0.05) \text{ mol kg}^{-1}$ at four equidistant temperatures (288.15 K to 318.15 K) are shown. Positive and large values of V_{ϕ}^0 is an indicator of strong solute-solvent interactions. The electrostriction, which decreases with temperature, is responsible for the rising V_{ϕ}^0 values with temperature. Additionally, when temperature rises, the amount of hydrogen bonds in the aqueous benzamide/benzylamine mixture decreases, increasing the amount of free solvent available for the solvation.

As indicated by the positive values V_{ϕ}^0 , the system's ion-hydrophilic interactions are more prevalent than hydrophobic-hydrophobic and ion-hydrophobic interactions (H. Kumar et al., 2013; H. Kumar & Chadha, 2014). However, weaker solute-solute interactions than those between solutes and solvents are corroborated by smaller and negative values of S_v^* . Since there is no trend apparent from the values of S_v^* , it can be summarized that additional factors may also affect the interactions between the solutes (P. Kaur et al., 2022). The co-sphere overlap model, which states that the bipolar or ionic species overlap of co-spheres is always positive and leads to increase in volume, which validates the prevalence of ion-hydrophilic interactions (H. Kaur et al., 2020).

Partial molar volume of transfer

Equation (4.18) is used to calculate the partial molar volumes of transfer of 1-butyl-1-methyl pyrrolidinium iodide from water to aqueous benzamide and benzylamine at the infinite dilution.

Values of ΔV_{ϕ}^0 are recorded in the Table 5.17 and all the negative values of ΔV_{ϕ}^0 (except for the temperatures 308.15 K and 318.15 K) indicates the significant interactions between 1-butyl-1-methyl pyrrolidinium iodide and aqueous solutions of benzamide/ benzylamine and as the temperature rises, these interactions get stronger. The values of ΔV_{ϕ}^0 are in agreement with the co sphere model [39-

40], from which the information regarding nature of the solute and solvent interactions can be obtained. Also from Table 5.17, it is clear that ΔV_{ϕ}^0 escalates with increase in temperature as increased temperature leads to decrease in electrostriction.

Various types of interactions between 1-butyl-1-methyl pyrrolidinium iodide and aqueous solutions of benzamide/benzylamine are possible and can be mentioned as : (a) ion-ion interactions among ions of IL and benzamide/benzylamine (b) ion-hydrophobic interactions among alkyl groups of IL and ions of benzamide/benzylamine (c) hydrophilic-hydrophilic interactions among polar groups of IL and the benzamide/benzylamine; (d) hydrophobic-hydrophobic interactions among non-polar groups of IL and the benzamide/benzylamine. Ion-hydrophobic interactions and hydrophobic-hydrophobic interactions are represented by negative values of ΔV_{ϕ}^0 in accordance with the co-sphere overlap model, whereas positive values of ΔV_{ϕ}^0 indicates ion-hydrophilic interactions and hydrophilic-hydrophilic interactions.

Hydrophobic-hydrophobic and ion-hydrophobic interactions are pervasive in the current investigation compared to the ion-hydrophilic interactions and hydrophilic-hydrophilic interactions (H. Kumar et al, 2021; Sharma. P, et al., 2021).

Effect of Temperature on partial molar volume

The following polynomial Equation (4.19) gives the variation of PMV (V_{ϕ}^0) with temperature at infinite solution.

Least square fitting for V_{ϕ}^0 in equation (4.19) is used to determine the values of these empirical constants. The values of empirical constants (a,b,c) are positive for all the concentrations. There are the variations present in hypothetical a value of V_{ϕ}^0 , known as ARD (Average Relative Deviation). Values of these empirical constants along with the ARD are tabulated in Table 5.18. Empirical constants for 1-butyl-1-methyl pyrrolidinium iodide in aqueous benzamide and benzylamine solutions are found positive (H. Kumar et al., 2016; V. Singh et al., 2015; Thakur et al., 2020).

Further Partial molar expansibilities (ϕ_E^0) represent the solute-solvent interaction and are mathematically represented by the equation (4.21)

The resultant values of partial molar expansibilities are positive which indicates the dominance of strong solute–solvent interactions in the present systems. Also, with the increasing temperature, these

values increase which attributes to more hydrophobic character of the system. The ability of the solute to act as structure destroyer or promoter in a mixed solvent system is further represented by the equation (4.22) stated by Hepler (Hepler, 1969).

Here the values of $(\partial\phi_E^0/\partial T)_p$ are tabulated in Table 5.19 and in the present investigated ternary solutions, the positive and modest values of $(\partial\phi_E^0/\partial T)_p$ support the structure promoting function of [BMPyr⁺][I⁻] in aqueous benzamide and benzylamine solutions. The positive values of ϕ_E^0 can also be attributed to the packing effect phenomenon indicating the significant interactions which are prevalent in the investigated system. The positive values of ϕ_E^0 at all concentrations and temperatures promotes the solute-solvent interactions in the present system which were also confirmed by the AMV data.

Sound velocity measurements

The sound velocity values at four equidistant temperatures (288.15 K to 318.15) K were measured in various concentrations of benzylamine and benzamide (0.01 to 0.05) mol.kg⁻¹ and is recorded in Table 5.20. After analyzing the data, it was found that the sound velocity values of 1-butyl-1-methyl pyrrolidinium iodide increases with increasing concentration of IL as well as content of benzamide/benzylamine and temperature.

Apparent molar isentropic compression

Equation number (4.23) is used for the calculation of the apparent molar isentropic compression of the present ionic liquid in the binary aqueous solutions of benzyl amine and benzamide.

The Laplace Newton's equation (4.24) is used for calculation of the coefficient of isentropic compressibility K_S .

The values obtained for $K_{\phi,S}$ from the equation (4.24) are recorded in Table 5.20 and depicted in Fig 5.10 (a) and 5.10 (b). It is evident from Table 5.20; values of $K_{\phi,S}$ (apparent molar compressibility) are negative at all the concentrations and temperatures. These values further rise with rise in concentration of IL as well as temperature. Negative values of $K_{\phi,S}$, indicate the lower degree of water molecule compression around the ionic charged groups of IL (Shekaari et al., 2015) and negative values of $K_{\phi,S}$ further decreases, indicating the lowering in structural compressibility of water indicating the lesser ordering of IL on solvents. On the other hand, with rise in temperature,

again the values of $K_{\phi,s}$ becomes less negative indicating the reduction of electrostriction and promotes release of some water molecules in the bulk with increase in temperature. The lower degree of water molecule compression around the ionic charged groups of IL is shown by the negative value of $K_{\phi,s}$.

Partial molar isentropic compression

Equation (4.25) is used for the determination of the alteration of apparent molar isentropic compression with molal concentration.

Table 5.21 provides the values of $K_{\phi,s}^0$ and S_K^* along with standard errors. Strong solute-solvent interactions are indicated by negative values of $K_{\phi,s}^0$ while solute-solute interactions are indicated by positive values of S_K^* .

As a result, in the present investigation, interactions among solute-solvent are more prominent over solute-solute interactions (H. Kumar et al., 2019; H. Kumar & Behal, 2016). It is also obvious that values of $K_{\phi,s}^0$ decrease as the temperature rises i.e., lessens, indicating that electrostriction reduction occurs when temperature rises, and some water molecules diffuse into the bulk from the hydration sphere.

Equation (4.26) was used for the calculation of partial molar isentropic compression of transfer ($\Delta K_{\phi,s}^0$) of IL from water to aqueous solution of benzamide and benzylamine at infinite dilution.

Table 5.22 lists all the observed and calculated values of $\Delta K_{\phi,s}^0$. The positive and small negative values of $\Delta K_{\phi,s}^0$ signifies the structure promoting nature of the IL in aqueous solutions of benzamide and benzylamine.

Pair triplet interaction coefficient

The McMillan and Mayer theory (McMillan & Mayer, 1945) helped in determining the interaction coefficients of interactions among two or more solutes which was further modified by Friedman and Krishnan. Equation (4.27) expresses the Partial molar volume of transfer and equation (4.28) expresses partial molar isentropic compression of transfer.

Values of V_{AB} , V_{ABB} , K_{AB} and K_{ABB} are listed in Table 5.23. From the values of pair and triplet interactions, it is clear that in case of IL + aqueous benzamide, values of V_{AB} increases with increasing temperature and value of K_{AB} do not follow any trend. The positive values of V_{AB} except at

temperature 288.15K shows the presence of pair wise interactions. The value of triplet coefficient K_{ABB} is indirectly proportional to temperature for the first system and directly proportional to temperature for the second system.

From the proposed formalism, we can say that along with pair wise interactions, non-bonding favorable interactions are also present which are due to the overlap of hydration co-sphere (Naseem et al., 2016; Pal et al., 2014).

Conductance studies

The conductance of electrolytic solutions determines the character of interactions between solutes-solute, solvent-solvent, or solute-solvent. These investigations provide kinetic information in the form of ionic conductivities and thermodynamic information in the form of association constants.

Equation (4.31) was used for the calculation of molar conductivity ($\Lambda_m, S.cm^2.mol^{-1}$) of the ternary solution.

Molar conductivity ($\Lambda_m, S.cm^2.mol^{-1}$) were measured at four equidistant temperature (288.15 K to 318.15 K) and data for molar conductance is tabulated in Table 5.24. From the obtained data, we can conclude that in case of molar conductivity, it increases with rising temperature and decreases with increasing concentration.

Plots of Λ_m against \sqrt{c} (Figure 5.11 and 5.12) over the entire composition range within investigated concentration range were found to be straight lines at all temperatures under consideration, which demonstrates the complete dissociation of ionic liquid in the consideration solvent system. The values obtained of molar conductance were used for the calculation of limiting molar conductance using the Onsager relation (Equation 4.32).

In the plots, Λ_m against \sqrt{c} , straight lines give the intercept which is equal to limiting molar conductance and slope is equal to Onsager constant (denoted by S). Table 5.25 tabulates the resultant values of limiting molar conductivity. From the calculated data, it is noticed that the values of Limiting molar conductance increases as we increase the temperature at all concentrations which is due to the mobility of ions. Increase in the temperature results in higher frequency and bond breaking due to which translational and vibrational degrees of freedom increases, thus the mobility of ions increases (Sharma. P, et.al., 2021; Z.I.Takai, 2018a). These values obtained helps in interpreting the

ion-solvent interactions. Higher the values of limiting molar conductance, greater the ion-solvent interactions.

Equation 4.33 gives the effect of temperature, where E_A is the activation energy and gas constant are denoted by R . It is feasible to calculate E_A from the slope of the straight line generated by the plot of the $\log \Lambda_o$ versus $1/T$. The values of activation energy are tabulated in Table 5.25. We can conclude the favorable solubilization in system given that all activation energy values are positive (H. Kumar, et. al., 2021).

FT-IR Spectroscopy

It is the technique used for the final confirmation of intermolecular interaction as well as structure determination. FT-IR spectral studies have been performed at room temperature using Shimadzu FT-IR 8400S spectrophotometer. This instrument emits infrared radiation, some of which is reflected and some of which is absorbed by the molecules of the sample. Then the sample molecule, converts these radiations into rotational or vibrational energy. The spectra and molecular fingerprint of the material can be obtained by the resultant signal. In case of investigated ternary mixture of IL and aqueous benzylamine and benzamide, the peaks are recorded in the range between 5000-500 cm^{-1} . The major peak of aqueous solutions around 3200-3350 cm^{-1} is indicative for -OH stretching band for water. In addition to -OH stretch bands, some other bands appear at 2361.00 cm^{-1} , 3321.30 cm^{-1} , 1635.20 cm^{-1} and 589.09 cm^{-1} .

In case of ternary mixture of IL and aqueous benzylamine, the peak 1636.04 cm^{-1} are assigned to C=C stretching, the peaks in range 3300-3400 cm^{-1} indicates N-H stretching, peaks in range 550-600 cm^{-1} indicates C-I stretching and peaks in range 3000-3400 cm^{-1} is for -OH stretching. Similarly for ionic liquid and aqueous benzamide, the peak 1635.20 cm^{-1} is assigned to C=C stretching, 3321.30 cm^{-1} is assigned to N-H stretching, 2361.00 cm^{-1} is assigned to N=C=O stretching and 3783.88 to -OH stretching. With minor changes in band position or intensity, the bands for functional groups in benzylamine and benzamide behave in a manner similar to that of the pure molecule (Figure 5.13 and 5.14). Intermolecular interactions are shown by a change in wave number, and the overlap of peaks denotes a strong functional group behavior. All vibrations are sensitive, and these vibrations reflect the specific system's structural characteristics as well as the presence of both intra- and intermolecular interactions. The presence of intermolecular interactions is confirmed in the investigated ternary system by the change in wavenumber corresponding to the -OH group towards the lower side.

Cyclic Voltammetry

To acquire the electrochemical data of the system PC Metrohm Autolab PGSTAT204 multi-channel Potentiostat /galvanostat electrochemical workstation with a tightly closed three-electrode cell in an inert environment of argon flow was used. The cyclic voltammograms of the ternary mixtures (IL+ benzylamine/benzamide + water) as a function of concentration at room temperature in the potential range from -1.0 V to + 2.0 V demonstrates the correlation between the reduction and oxidation potential peaks and are visually represented in Figure 5.15 and Figure 5.16. For the present system under investigation, Ag wire in 10 mM AgCl was taken as reference electrolyte and Platinum wire working as counter electrode and Pt was used as working electrode with a diameter of 3mm were used (Buzzeo et al., 2003). The starting potential for these voltammograms was 0V, with no current flowing, and three cycles were recorded. The best suited results for the electrochemical window were attained in third cycle at 100 mVs⁻¹, which are shown in the figures so that the electrochemical data can be compared carefully.

In case of 0.01 mol kg⁻¹ of benzylamine, the oxidation and reduction peaks for concentration 0.001 and 0.009 were approx. 1.01 V and -0.09 V respectively which gives us an electrochemical window equal to 2.0V. Similarly, for all the concentrations, the electrochemical window was calculated and from the data obtained, we can interpret that at higher concentration, the potential window is greater. In both the systems, IL+ aqueous benzylamine shows a greater and higher potential window (Taylor et al., 2008; E. Zhang et al., 2019).

Using the CV graphs obtained, we can also compare the specific capacitance of the mixture at different concentration (0.001 and 0.009) mol kg⁻¹. Area of CV curve is directly proportional to the capacitance of the solution. Greater the area, higher the capacitance will be. From the Figure 5.17 and 5.18, it is observed that area of CV curve is greater in 0.001 mol kg⁻¹ of the aqueous benzylamine and in case of 0.05 mol kg⁻¹ of aqueous benzylamine, CV curve area is greater at 0.009 mol kg⁻¹ indicating that at higher concentration, specific capacitance is higher. Similar results were noted for the mixture in aqueous benzamide.

Table 5.15.

Value of densities (ρ), apparent molar volumes (V_ϕ) of 1-butyl-1-methyl pyrrolidinium iodide in aqueous solutions of benzylamine and benzamide at different temperatures.

^a m _A / (mol.kg- ¹)	$\rho \times 10^{-3} / (\text{kg m}^{-3})$				$V_\phi \times 10^6 / (\text{m}^3 \text{mol}^{-1})$			
	288.15 K	298.15 K	308.15 K	318.15 K	288.15 K	298.15 K	308.15 K	318.15 K
[BMPyrr⁺][I⁻] + 0.01 mol kg⁻¹ Benzylamine								
000000	0.99922	0.99805	0.99658	0.99501				
0.000983	0.99932	0.99815	0.99667	0.99510	164.40	168.99	172.31	177.48
0.002989	0.99953	0.99835	0.99687	0.99529	164.36	168.95	172.28	177.44
0.004997	0.99974	0.99855	0.99706	0.99547	164.33	168.92	172.24	177.41
0.006971	0.99995	0.99875	0.99726	0.99565	164.30	168.89	172.21	177.38
0.008965	1.00016	0.99895	0.99745	0.99584	164.26	168.85	172.18	177.35
[BMPyrr⁺][I⁻] + 0.03 mol kg⁻¹ Benzylamine								
000000	0.99929	0.99742	0.99562	0.99360				
0.000983	0.99941	0.99753	0.99572	0.99370	155.28	159.18	163.30	168.68
0.002951	0.99963	0.99774	0.99593	0.99395	155.24	159.14	163.27	168.65
0.004924	0.99985	0.99796	0.99614	0.99409	155.21	159.11	163.23	168.62
0.006893	1.00008	0.99818	0.99635	0.99429	155.17	159.07	163.20	168.58
0.008864	1.00030	0.99840	0.99656	0.99449	155.14	159.04	163.16	168.55
[BMPyrr⁺][I⁻] + 0.05 mol kg⁻¹ Benzylamine								
000000	0.99940	0.99745	0.99556	0.99337				
0.000982	0.99952	0.99756	0.99567	0.99347	150.77	154.65	159.27	163.43
0.002949	0.99975	0.99778	0.99589	0.99368	150.74	154.62	159.23	163.39

0.004928	0.99999	0.99801	0.99611	0.99389	150.70	154.58	159.20	163.36
0.006895	1.00022	0.99824	0.99632	0.99410	150.67	154.55	159.16	163.33
0.008859	1.00045	0.99846	0.99654	0.99431	150.63	154.51	159.13	163.29
[BMPyrr⁺][I⁻] + 0.01 mol kg⁻¹ Benzamide								
000000	0.99931	0.99725	0.99521	0.99342				
0.000983	0.99940	0.99732	0.99527	0.99346	173.61	189.56	208.78	232.38
0.002989	0.99960	0.99748	0.99539	0.99354	173.57	189.53	208.76	232.36
0.004997	0.99979	0.99765	0.99552	0.99361	173.54	189.50	208.73	232.34
0.006971	0.99998	0.99780	0.99564	0.99369	173.51	189.47	208.71	232.32
0.008965	1.00017	0.99796	0.99576	0.99376	173.47	189.43	208.68	232.31
[BMPyrr⁺][I⁻] + 0.03 mol kg⁻¹ Benzamide								
000000	0.99953	0.99759	0.99564	0.99378				
0.000983	0.99962	0.99768	0.99570	0.99381	169.09	184.29	205.87	230.55
0.002989	0.99983	0.99785	0.99583	0.99390	169.05	184.26	205.85	230.53
0.004997	1.00003	0.99802	0.99596	0.99398	169.02	184.23	205.82	230.51
0.006971	1.00022	0.99819	0.99608	0.99405	168.98	184.20	205.80	230.49
0.008965	1.00042	0.99836	0.99621	0.99413	168.95	184.17	205.77	230.47
[BMPyrr⁺][I⁻] + 0.05 mol kg⁻¹ Benzamide								
000000	0.99980	0.99798	0.99601	0.99410				
0.000983	0.99990	0.99807	0.99608	0.99415	165.57	179.23	203.00	227.14
0.002989	1.00011	0.99825	0.99621	0.99423	165.53	179.20	202.97	227.12
0.004997	1.00032	0.99843	0.99635	0.99432	165.50	179.17	202.94	227.10
0.006971	1.00052	0.99861	0.99648	0.99440	165.46	179.14	202.92	227.08
0.008965	1.00073	0.99879	0.99661	0.99449	165.43	179.10	202.89	227.06

Standard uncertainty of molality according to declared purity levels is $u(m) = 0.01 \text{ mol.kg}^{-1}$, $u(\rho)$ in measurement of density is 0.005 kg.m^{-3} , $u(u)$ in sound velocity measurement is 0.05 m.s^{-1} , in $u(T)$ in different temperatures is $1 \times 10^{-2} \text{ K}$ and in pressure $u(P)$ is 0.01 MPa .

Table 5.16.

Partial molar volumes (V_{ϕ}^o) and experimental slopes (S_v^*) of 1-butyl-1-methyl pyrrolidinium iodide in binary aqueous solutions of benzamide and benzylamine at different temperatures.

$^a m_B$ (mol kg ⁻¹)	$V_{\phi}^o \times 10^6 / (\text{m}^3 \text{mol}^{-1})$				$S_v^* \times 10^6 / (\text{m}^3 \text{kg mol}^{-2})$			
	288.15 K	298.15 K	308.15 K	318.15 K	288.15 K	298.15 K	308.15 K	318.15 K
1-butyl-1-methyl pyrrolidinium iodide + Water								
0.00	182.04 (±0.0001)	172.07 (±0.0001)	160.67 (±0.0001)	148.71 (±0.0001)				
Benzylamine								
0.01	164.45 (±0.0001)	169.03 (±0.0001)	172.33 (±0.0001)	177.43 (±0.0001)	-17.22 (±0.0001)	-16.96 (±0.0001)	-16.77 (±0.0002)	-16.41 (±0.0002)
0.03	155.29 (±0.0001)	159.19 (±0.0001)	161.95 (±0.0001)	166.31 (±0.0001)	-17.68 (±0.0001)	-17.55 (±0.0001)	-17.38 (±0.0002)	-17.11 (±0.0004)
0.05	150.78 (±0.0001)	154.67 (±0.0001)	159.28 (±0.0001)	163.44 (±0.0001)	-17.84 (±0.0002)	-17.75 (±0.0001)	-17.59 (±0.0001)	-17.43 (±0.0001)
Benzamide								
0.01	173.62 (±0.0001)	189.57 (±0.0001)	208.79 (±0.0001)	232.38 (±0.0001)	-16.59 (±0.0002)	-15.17 (±0.0001)	-12.80 (±0.0001)	-8.89 (±0.0001)
0.03	169.10 (±0.0001)	184.30 (±0.0001)	205.88 (±0.7108)	230.55 (±0.4132)	-16.91 (±0.0002)	-15.70 (±0.0001)	-13.20 (±0.0001)	-9.22 (±0.0001)
0.05	165.58 (±0.0001)	179.25 (±0.0001)	203.01 (±0.0001)	227.15 (±0.0001)	-17.14 (±0.0002)	-16.16 (±0.0002)	-13.58 (±0.0002)	-9.84 (±0.0001)

^a m_B is molality of aqueous solution of benzylamine and benzamide. Standard uncertainty of molality according to declared purity levels is $u(m) = 0.01 \text{ mol.kg}^{-1}$, $u(\rho)$ in measurement of density is 0.005 kg.m^{-3} , $u(u)$ in sound velocity measurement is 0.05 m.s^{-1} , in $u(T)$ in different temperatures is $1 \times 10^{-2} \text{ K}$ and in pressure $u(P)$ is 0.01 MPa .

Table 5.17.

Partial molar volume of transfer (ΔV_{ϕ}^0) of 1-butyl-1-methyl pyrrolidinium iodide in binary aqueous solutions of benzylamine and benzamide at different temperatures.

$^a m_B$ (mol kg ⁻¹)	$\Delta V_{\phi}^0 \times 10^6 / (\text{m}^3 \text{ mol}^{-1})$			
	288.15 K	298.15 K	308.15 K	318.15 K
Benzylamine				
0.01	-17.63	-03.00	11.65	28.79
0.03	-26.75	-12.81	02.64	19.99
0.05	-31.26	-17.34	-01.39	14.74
Benzamide				
0.01	-08.42	-04.88	03.58	12.95
0.03	-12.94	-10.14	00.68	11.12
0.05	-16.46	-15.20	-02.19	07.17

^a m_B is molality of benzylamine and benzamide respectively. The standard uncertainty in molality as per stated purities is $u(m) = 0.01$. Std. uncertainties in $u(\rho)$ in measurement of density are 0.005 kg.m^{-3} . Std. uncertainty $u(u)$ in sound velocity measurement is 0.05 m.s^{-1} . Std. uncertainty in $u(T)$ in different temperatures are $1 \times 10^{-2} \text{ K}$. Std. uncertainty in pressure $u(P)$ is 0.01 Mpa .

Table 5.18.

Values of empirical parameters of Eq. (4.19) for 1-butyl-1-methyl pyrrolidinium iodide in aqueous benzylamine and benzamide solutions.

$^a m_B / (\text{mol kg}^{-1})$	$a \times 10^6 / (\text{mol kg}^{-1})$	$b \times 10^6 / (\text{m}^3 \text{mol}^{-1} \text{K})$	$c \times 10^6 / (\text{m}^3 \text{mol}^{-1} \text{K}^{-2})$	R^2	ARD(σ)
Benzylamine					
0.01	168.53	0.4110	0.0014	0.9987	0.00729
0.03	159.04	0.4061	0.0037	0.9989	0.00256
0.05	154.84	0.4189	0.0006	0.9889	0.00303
Benzamide					
0.01	189.40	1.7640	0.0191	0.9994	0.00219
0.03	184.80	1.8228	0.0236	1.0000	0.00676
0.05	180.70	1.8229	0.0261	0.9966	0.02038

$^a m_B$ is molality of aqueous solutions of benzylamine and benzamide respectively. The standard uncertainty in molality as per stated purities is $u(m) = 0.01$. Std. uncertainties in $u(\rho)$ in measurement of density are 0.005 kg.m^{-3} . Std. uncertainty $u(u)$ in sound velocity measurement is 0.05 m.s^{-1} . Std. uncertainty in $u(T)$ in different temperatures are $1 \times 10^{-2} \text{ K}$. Std. uncertainty in pressure $u(P)$ is 0.01 Mpa .

Table 5.19.

Limiting apparent molar expansibilities (ϕ_E^0) for 1-butyl-1-methyl pyrrolidinium iodide in aqueous benzylamine and benzamide solutions at different temperatures.

^a m _B / (mol kg ⁻¹)	$\phi_E^0 \times 10^6 / (\text{m}^3 \text{mol}^{-1} \text{K}^{-1})$				$(\partial \phi_E^0 / \partial T)$
	288.15 K	298.15 K	308.15 K	318.15 K	
Benzylamine					
0.01	0.382	0.411	0.440	0.469	0.0029
0.03	0.332	0.406	0.480	0.555	0.0074
0.05	0.405	0.419	0.433	0.447	0.0013
Benzamide					
0.01	1.382	1.764	2.146	2.528	0.0382
0.03	1.350	1.823	2.296	2.769	0.0473
0.05	1.299	1.823	2.347	2.870	0.0523

Molality of aqueous solution of benzylamine and benzamide is denoted by $^a m_B$. The standard uncertainty in molality as per stated purities is $u(m) = 0.01$. Std. uncertainties in $u(\rho)$ in measurement of density are 0.005 kg.m^{-3} . Std. uncertainty $u(u)$ in sound velocity measurement is 0.05 m.s^{-1} . Std. uncertainty in $u(T)$ in different temperatures are $1 \times 10^{-2} \text{ K}$. Std. uncertainty in pressure $u(P)$ is 0.01 Mpa .

Table 5.20.

Values of ultrasonic speed (u) and apparent molar isentropic compression ($K_{\phi,s}$) of Ionic liquid in aqueous solutions of benzylamine and benzamide at different temperatures and experimental pressure = 0.01 Mpa.

$^a m_A /$ (mol kg ⁻¹)	$u / (\text{ms}^{-1})$				$K_{\phi,s} \times 10^6 (\text{m}^3 \text{mol}^{-1} \text{GPa}^{-1})$			
	288.15 K	298.15 K	308.15 K	318.15 K	288.15 K	298.15 K	308.15 K	318.15 K
[BMPyrr⁺][I⁻] + 0.01 mol kg⁻¹ Benzylamine								
000000	1476.01	1491.89	1508.04	1522.85				
0.00098	1478.32	1494.17	1510.41	1525.34	-26.18	-23.74	-20.57	-18.23
0.00298	1483.02	1498.81	1515.25	1530.41	-25.33	-22.93	-19.73	-17.37
0.00499	1487.73	1503.46	1520.09	1535.49	-24.47	-22.12	-18.89	-16.51
0.00697	1492.37	1508.03	1524.85	1540.49	-23.63	-21.33	-18.06	-15.66
0.00896	1497.04	1512.65	1529.66	1545.53	-22.78	-20.53	-17.23	-14.80
[BMPyrr⁺][I⁻] + 0.05 mol kg⁻¹ Benzylamine								
000000	1480.55	1496.06	1511.36	1527.26				
0.00098	1482.76	1498.30	1513.40	1529.22	-24.27	-21.89	-18.54	-15.37
0.00295	1487.17	1502.79	1517.48	1533.15	-23.22	-20.91	-17.79	-14.71
0.00492	1491.60	1507.29	1521.58	1537.08	-22.18	-19.93	-17.04	-14.04
0.00689	1496.01	1511.78	1525.67	1541.01	-21.13	-18.95	-16.29	-13.38
0.00886	1500.44	1516.27	1529.76	1544.95	-20.09	-17.98	-15.53	-12.72
[BMPyrr⁺][I⁻] + 0.05 mol kg⁻¹ Benzylamine								
000000	1482.16	1498.78	1511.41	1526.58				
0.00098	1484.58	1501.31	1514.09	1529.09	-21.12	-19.16	-17.09	-14.74
0.00294	1489.44	1506.38	1519.47	1534.11	-20.58	-18.63	-16.56	-14.04
0.00492	1494.33	1511.48	1524.88	1539.17	-20.04	-18.09	-16.03	-13.33
0.00689	1499.18	1516.55	1530.26	1544.20	-19.50	-17.56	-15.51	-12.62
0.00885	1504.03	1521.62	1535.63	1549.21	-18.96	-17.03	-14.98	-11.92

[BMPyrr⁺][I⁻] + 0.01 mol kg⁻¹ Benzamide								
000000	1427.87	1438.98	1452.11	1461.74				
0.00098	1430.64	1441.60	1555.97	1537.30	-28.74	-27.25	-25.09	-23.20
0.00298	1514.64	1529.60	1545.16	1560.89	-28.10	-26.39	-24.45	-22.56
0.00499	1539.34	1554.19	1569.37	1584.49	-27.47	-25.53	-23.80	-21.93
0.00697	1563.63	1578.38	1593.19	1607.71	-26.84	-24.68	-23.17	-21.30
0.00896	1588.16	1602.81	1617.24	1631.15	-26.21	-23.83	-22.54	-20.67
[BMPyrr⁺][I⁻] + 0.03 mol kg⁻¹ Benzamide								
000000	1480.92	1497.14	1512.52	1528.35				
0.00098	1493.01	1509.16	1524.41	1540.04	-24.09	-21.43	-18.42	-16.18
0.00298	1517.69	1533.68	1548.66	1563.89	-23.76	-21.12	-17.99	-15.72
0.00499	1542.38	1558.22	1572.93	1587.76	-23.43	-20.82	-17.58	-15.27
0.00697	1566.67	1582.36	1596.80	1611.24	-23.10	-20.52	-17.16	-14.82
0.00896	1591.19	1606.73	1620.91	1634.94	-24.43	-21.73	-18.84	-16.64
[BMPyrr⁺][I⁻] + 0.05 mol kg⁻¹ Benzamide								
000000	1483.15	1500.61	1515.89	1531.14				
0.00098	1494.48	1511.62	1526.71	1541.49	-22.34	-20.16	-18.07	-15.57
0.00298	1517.59	1534.10	1548.79	1562.59	-21.86	-19.57	-17.32	-14.97
0.00499	1540.73	1556.59	1570.89	1583.72	-21.38	-18.98	-16.57	-14.37
0.00697	1563.48	1578.71	1592.62	1604.49	-20.90	-18.39	-15.83	-13.78
0.00896	1586.46	1601.05	1614.57	1625.47	-20.42	-17.80	-15.08	-13.18

Standard uncertainty of molality according to declared purity levels is $u(m) = 0.01 \text{ mol.kg}^{-1}$, $u(p)$ in measurement of density is 0.005 kg.m^{-3} , $u(u)$ in sound velocity measurement is 0.05 m.s^{-1} , in $u(T)$ in different temperatures is $1 \times 10^{-2} \text{ K}$ and in pressure $u(P)$ is 0.01 MPa .

Table 5.21.

Partial molar isentropic compression ($K_{\phi,s}^0$) and experimental slopes (S_K^*) for 1-butyl-1-methylpyrrolidinium iodide in aqueous solutions of benzylamine and benzamide at different temperatures.

$^a m_B /$ (mol kg ⁻¹)	$K_{\phi,s}^0 \times 10^6 / (\text{m}^3 \text{mol}^{-1} \text{GPa}^{-1})$				$S_K^* \times 10^6 / (\text{kg m}^3 \text{mol}^{-2} \text{GPa}^{-1})$			
	288.15 K	298.15 K	308.15 K	318.15 K	288.15 K	298.15 K	308.15 K	318.15 K
IL + Water								
0.00	-31.02 (±0.01)	-28.24 (±0.01)	-25.27 (±0.01)	-21.16 (±0.01)				
Benzylamine								
0.01	-26.60 (±0.01)	-24.13 (±0.01)	-20.98 (±0.01)	-18.65 (±0.01)	46.25 (±0.06)	41.55 (±0.17)	48.55 (±0.06)	48.93 (±0.08)
0.03	-24.79 (±0.01)	-22.38 (±0.01)	-18.92 (±0.01)	-15.71 (±0.01)	50.72 (±0.17)	46.32 (±0.05)	31.35 (±0.07)	37.24 (±0.11)
0.05	-21.39 (±0.05)	-19.43 (±0.01)	-17.36 (±0.01)	-15.10 (±0.01)	23.47 (±0.09)	20.68 (±0.37)	28.16 (±0.04)	38.60 (±0.03)
Benzamide								
0.01	-29.05 (±0.03)	-27.67 (±0.09)	-25.40 (±0.05)	-23.51 (±0.02)	36.66 (±0.06)	48.34 (±0.18)	39.26 (±0.10)	37.04 (±0.05)
0.03	-24.59 (±0.01)	-21.89 (±0.01)	-19.05 (±0.01)	-16.87 (±0.01)	16.35 (±0.17)	12.76 (±0.01)	20.47 (±0.01)	28.22 (±0.01)
0.05	-22.58 (±0.03)	-20.46 (±0.01)	-18.44 (±0.01)	-15.87 (±0.02)	29.95 (±0.01)	26.10 (±0.02)	33.80 (±0.02)	29.44 (±0.04)

^a m_B is the molality of aqueous solution of benzylamine and benzamide. Standard uncertainty of molality according to declared purity levels is $u(m) = 0.01 \text{ mol.kg}^{-1}$, $u(\rho)$ in measurement of density is 0.005 kg.m^{-3} , $u(u)$ in sound velocity measurement is 0.05 m.s^{-1} , in $u(T)$ in different temperatures is $1 \times 10^{-2} \text{ K}$ and in pressure $u(P)$ is 0.01 MPa .

Table 5.22.

Partial molar isentropic compression of transfer ($\Delta K_{\phi,s}^0$) of 1-butyl-1-methyl pyrrolidinium iodide in aqueous solutions of benzylamine and benzamide at temperature from 218.15K to 318.15K and experimental pressure= 0.01 Mpa.

$^a m_B /$ (mol kg ⁻¹)	$\Delta K_{\phi,s}^0 \times 10^6 / (\text{m}^3 \text{mol}^{-1} \text{GPa}^{-1})$			
	288.15 K	298.15 K	308.15 K	318.15 K
Benzylamine				
0.01	4.42	4.11	4.29	2.51
0.03	6.23	5.86	6.35	5.45
0.05	9.63	8.81	7.91	6.06
Benzamide				
0.01	1.91	-0.57	-1.13	-2.35
0.03	6.43	6.35	6.22	4.29
0.05	8.44	7.78	6.83	5.29

Molality of aqueous solution of benzylamine and benzamide is represented by $^a m_B$. Standard uncertainty of molality according to declared purity levels is $u(m) = 0.01 \text{ mol.kg}^{-1}$, $u(\rho)$ in measurement of density is 0.005 kg.m^{-3} , $u(u)$ in sound velocity measurement is 0.05 m.s^{-1} , in $u(T)$ in different temperatures is $1 \times 10^{-2} \text{ K}$ and in pressure $u(P)$ is 0.01 MPa .

Table 5.23.

Pair and triplet interaction coefficients of 1-butyl-1-methyl pyrrolidinium iodide in aqueous solutions of benzylamine and benzamide at different temperatures.

T / (K)	$V_{AB} \times 10^6 /$ (m³ mol⁻² kg)	$V_{ABB} \times 10^6 /$ (m³ mol⁻³ kg²)	$K_{AB} \times 10^6 /$ (m³ mol⁻² kg GPa⁻¹)	$K_{ABB} \times 10^6 /$ (m³ mol⁻³ kg² GPa⁻¹)
Benzylamine				
288.15	-770.97	-622.45	160.50	-896.65
298.15	-230.85	-729.33	159.76	-897.50
308.15	330.21	-476.07	142.90	-1373.55
318.15	993.86	-521.56	138.02	-1033.88
Benzamide				
288.15	-356.28	-908.01	128.28	-573.80
298.15	-218.60	-825.15	104.19	-314.02
308.15	117.22	-873.87	96.36	-221.95
318.15	494.44	-715.11	23.31	102.39

Table 5.24:

Molar conductivity (Λ_m , S.cm²mol⁻¹) 1-butyl-1-methyl pyrrolidinium iodide in aqueous solution of benzylamine and benzamide.

$^a m_A /$ (mol.kg ⁻¹)	Λ_m (S.cm ² mol ⁻¹)			
	T=288.15 K	T=298.15 K	T=308.15 K	T=318.15 K
[BMPyrr⁺][I⁻] + aqueous 0.01 mol kg⁻¹ Benzylamine				
0.000983	52.63	53.51	55.91	56.60
0.002989	48.19	49.79	52.49	53.18
0.004996	41.76	45.37	48.06	50.77
0.006971	37.33	41.96	45.64	48.36
0.008964	35.89	38.54	41.22	45.95
[BMPyrr⁺][I⁻] + aqueous 0.03 mol kg⁻¹ Benzylamine				
0.009829	54.89	56.09	57.79	59.25
0.029489	53.29	54.61	55.18	57.62
0.049115	52.68	53.97	54.56	56.08
0.068800	51.08	52.02	52.95	54.54
0.088511	49.48	50.85	51.13	52.75
[BMPyrr⁺][I⁻] + aqueous 0.05 mol kg⁻¹ Benzylamine				
0.009813	56.55	58.77	60.01	62.01
0.029470	54.76	55.17	57.74	60.20
0.049163	51.97	53.37	55.89	57.38
0.068823	49.18	51.58	53.05	55.57
0.088453	47.39	49.78	51.20	53.76
[BMPyrr⁺][I⁻] + aqueous 0.01 mol kg⁻¹ Benzamide				

0.000983	38.25	62.00	85.45	105.74
0.002989	37.21	60.71	83.99	104.46
0.004997	35.13	58.14	81.08	101.90
0.006971	33.05	55.56	78.17	99.33
0.008965	30.97	52.99	75.26	96.77
[BMPyrr⁺][I⁻] + aqueous 0.03 mol kg⁻¹ Benzamide				
0.000983	42.56	65.12	89.45	108.45
0.002989	41.35	63.66	87.80	107.12
0.004997	38.92	60.73	84.49	104.45
0.006971	36.49	57.80	81.18	101.78
0.008965	34.06	54.87	77.87	99.11
[BMPyrr⁺][I⁻] + aqueous 0.05 mol kg⁻¹ Benzamide				
0.000983	45.12	68.05	90.36	111.28
0.002989	44.12	66.41	88.76	109.98
0.004997	42.11	63.13	85.56	107.38
0.006971	40.10	59.85	82.37	104.79
0.008965	38.09	56.56	79.17	102.19

m_A is the molality of 1-butyl-1-methyl pyrrolidinium iodide in aqueous benzylamine and benzamide solution. Standard uncertainty of molality according to declared purity levels is $u(m) = 0.01 \text{ mol.kg}^{-1}$, $u(\rho)$ in measurement of density is 0.005 kg.m^{-3} , $u(u)$ in sound velocity measurement is 0.05 m.s^{-1} , in $u(T)$ in different temperatures is $1 \times 10^{-2} \text{ K}$ and in pressure $u(P)$ is 0.01 MPa .

Table 5.25:

Limiting molar conductivity (Λ° , S.cm².mol⁻¹) and activation energy (E_A) of 1-butyl-1-methyl pyrrolidinium iodide in aqueous solution of benzylamine and benzamide.

^a m _B (mol kg ⁻¹)	Λ° (S.cm ² .mol ⁻¹)				$E_A \times 10^{-3}$ (kJ.mol ⁻¹)
	288.15 K	298.15 K	308.15 K	318.15 K	
Benzylamine					
0.01	33.03	33.68	34.06	34.84	0.00978
0.03	33.76	34.85	35.58	36.22	0.00705
0.05	34.20	35.71	36.38	37.81	0.00805
Benzamide					
0.01	18.75	21.55	24.52	18.75	0.00578
0.03	19.36	22.61	25.81	19.36	0.00699
0.05	20.88	23.78	26.25	20.88	0.00658

^am_B is molality of aqueous solution benzylamine and benzamide.

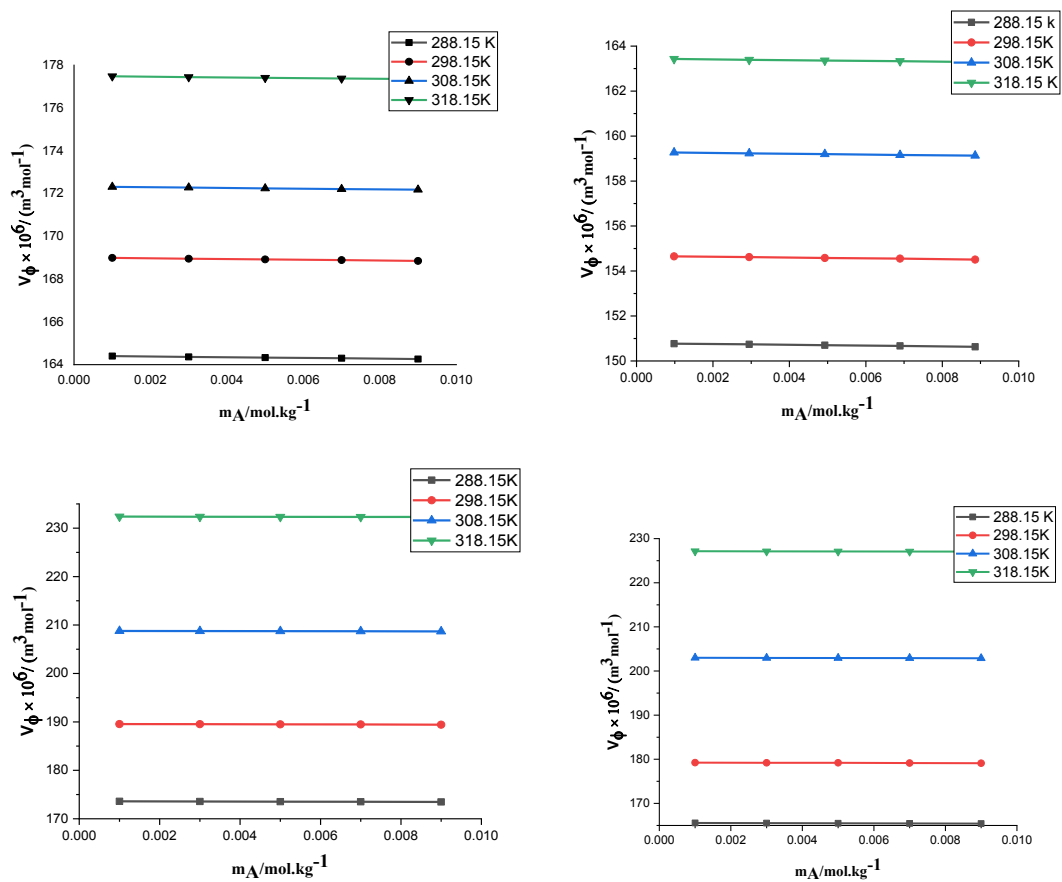
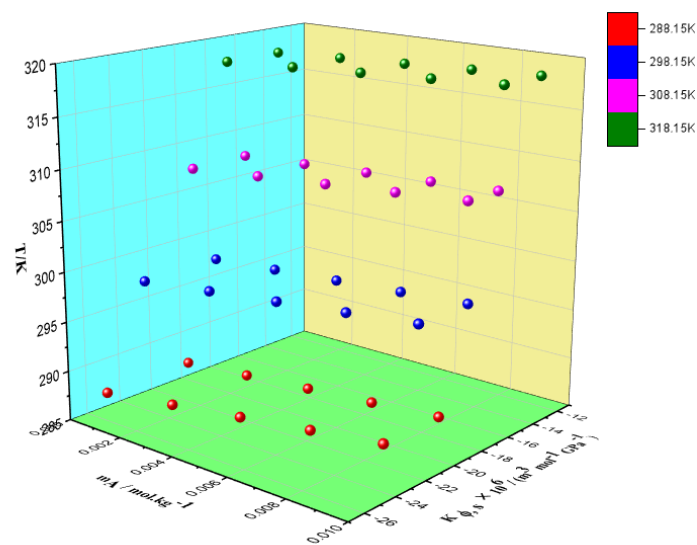
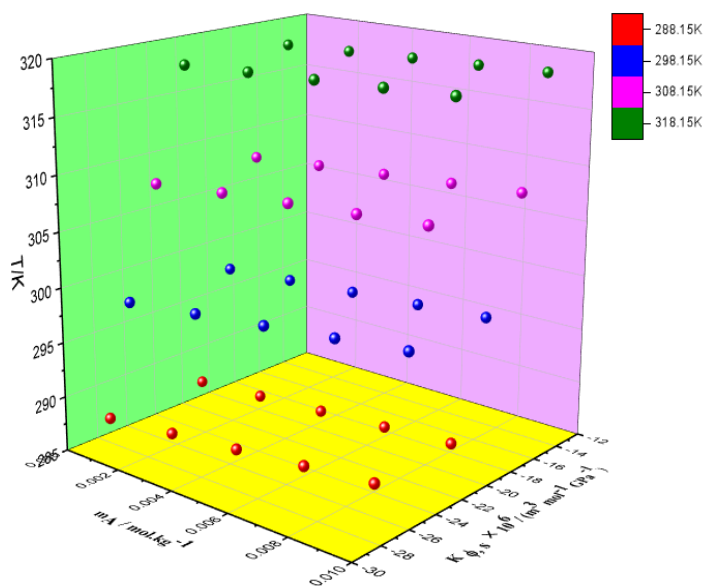


Figure 5.8

Plots of variation of apparent molar volume (V_ϕ) of 1-butyl-1-methyl pyrrolidinium iodide in (a) 0.01 mol kg^{-1} and (b) 0.05 mol kg^{-1} of aqueous solutions of benzylamine ; (c) 0.01 mol kg^{-1} and (d) 0.05 mol kg^{-1} of aqueous solutions of benzamide at T = (288.15, 298.15, 308.15 and 318.15) K



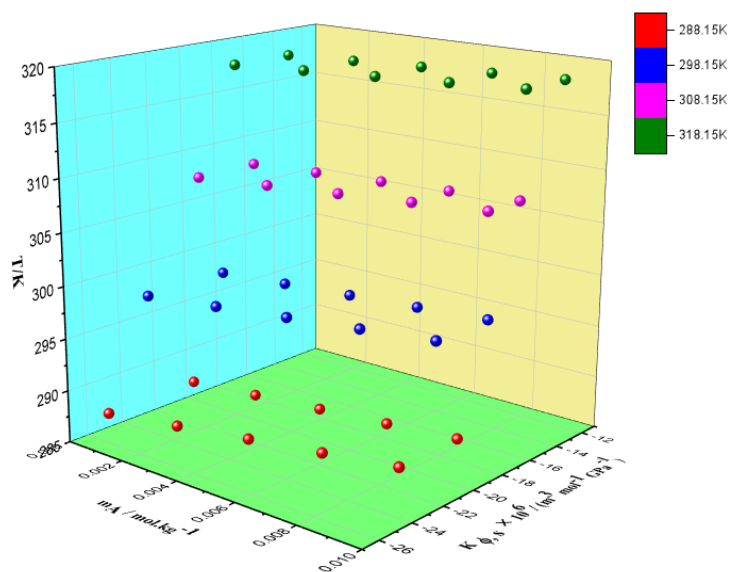
(a)



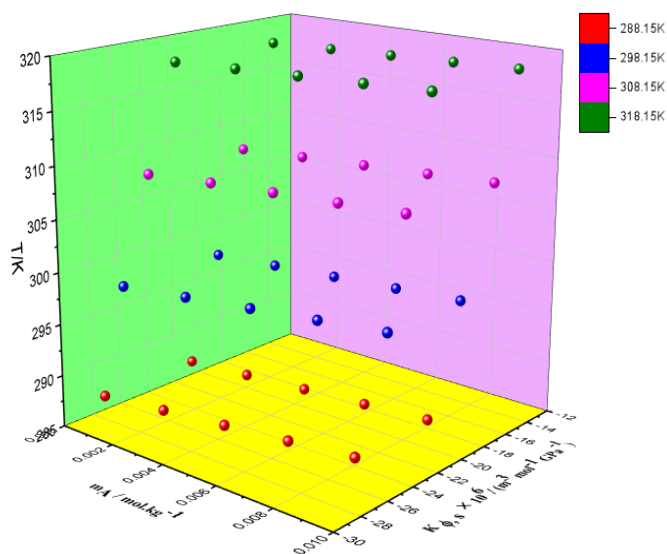
(b)

Figure 5.9

Plot of variation of partial molar volume V_{ϕ}^0 of 1-butyl-1-methyl pyrrolidinium iodide in various concentrations $m = (0.01, 0.03 \text{ and } 0.05) \text{ mol kg}^{-1}$ of (a) aqueous benzylamine; (b) aqueous benzamide at 288.15 K, 298.15 K, 308.15 K and 318.15 K.



(a)



(b)

Figure 5.10

Plot of variation of apparent molar isentropic compression ($K_{\phi,s}$) of 1-butyl-1-methyl pyrrolidinium iodide in (a) 0.01 mol kg⁻¹ and 0.05 mol kg⁻¹ aqueous solutions of benzamide; (b) 0.01 mol kg⁻¹ and 0.05 mol kg⁻¹ aqueous solutions of benzylamine at $T = (288.15, 298.15, 308.15 \text{ and } 318.15) \text{ K}$.

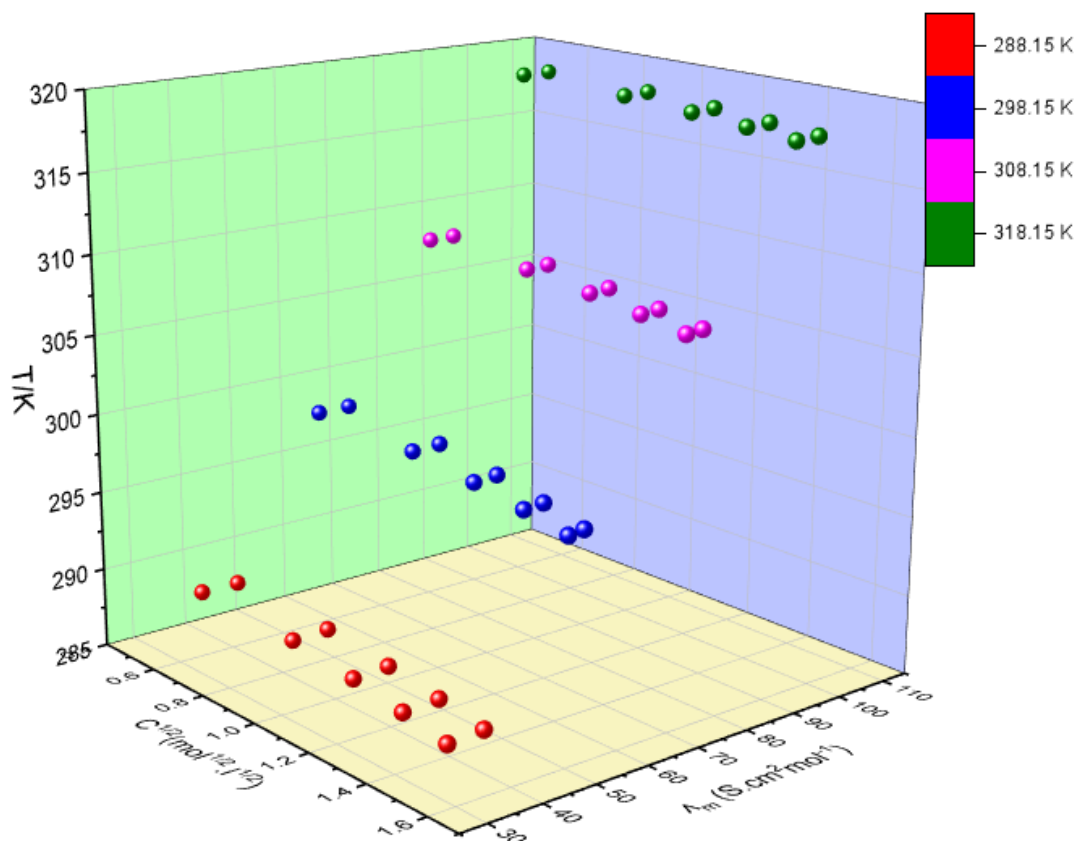


Figure 5.11

Plot of variation of Λ_m against \sqrt{c} for 1-butyl-1-methyl pyrrolidinium iodide in (a) 0.01 mol.kg⁻¹ and 0.05 mol.kg⁻¹ aqueous solutions of benzylamine.

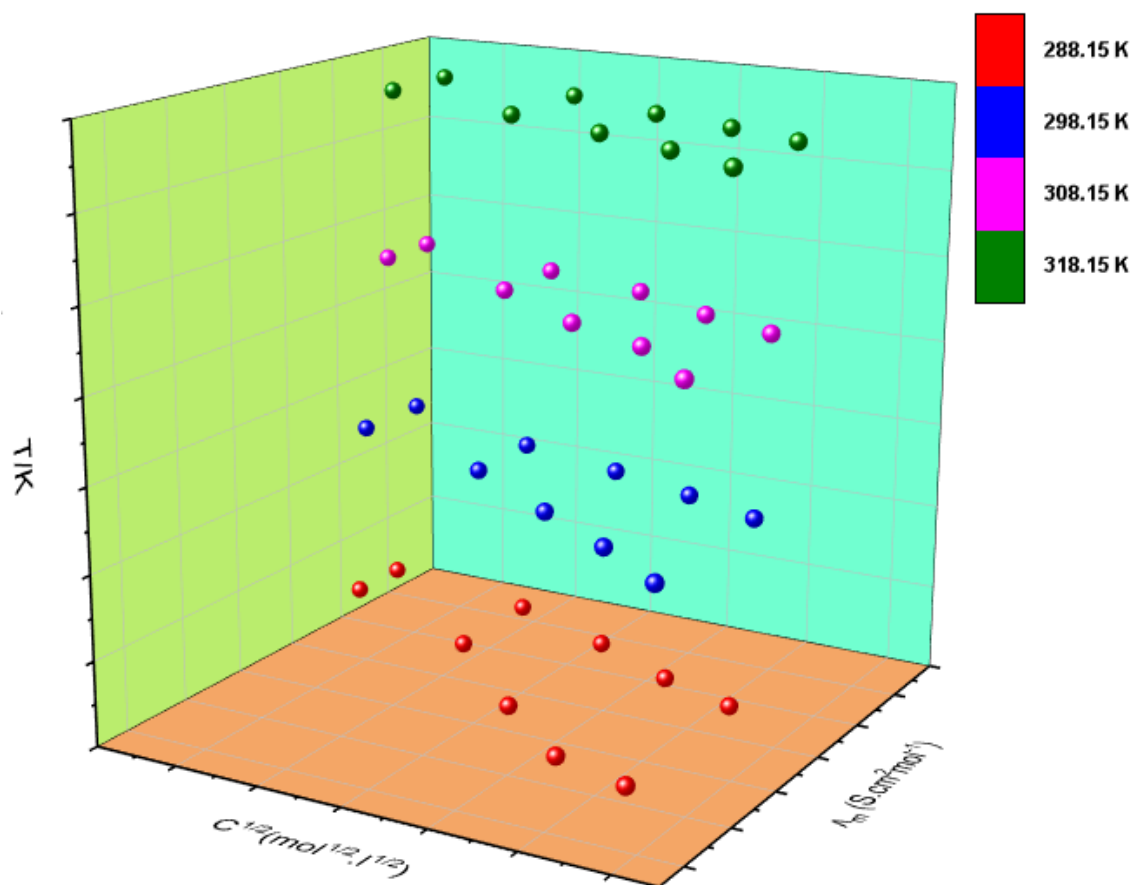


Figure 5.12

Plot of variation of Λ_m against \sqrt{c} for 1-butyl-1-methyl pyrrolidinium iodide in 0.01 mol.kg⁻¹ and 0.05 mol.kg⁻¹ aqueous solutions of benzamide at T = (288.15 K to 318.15 K).

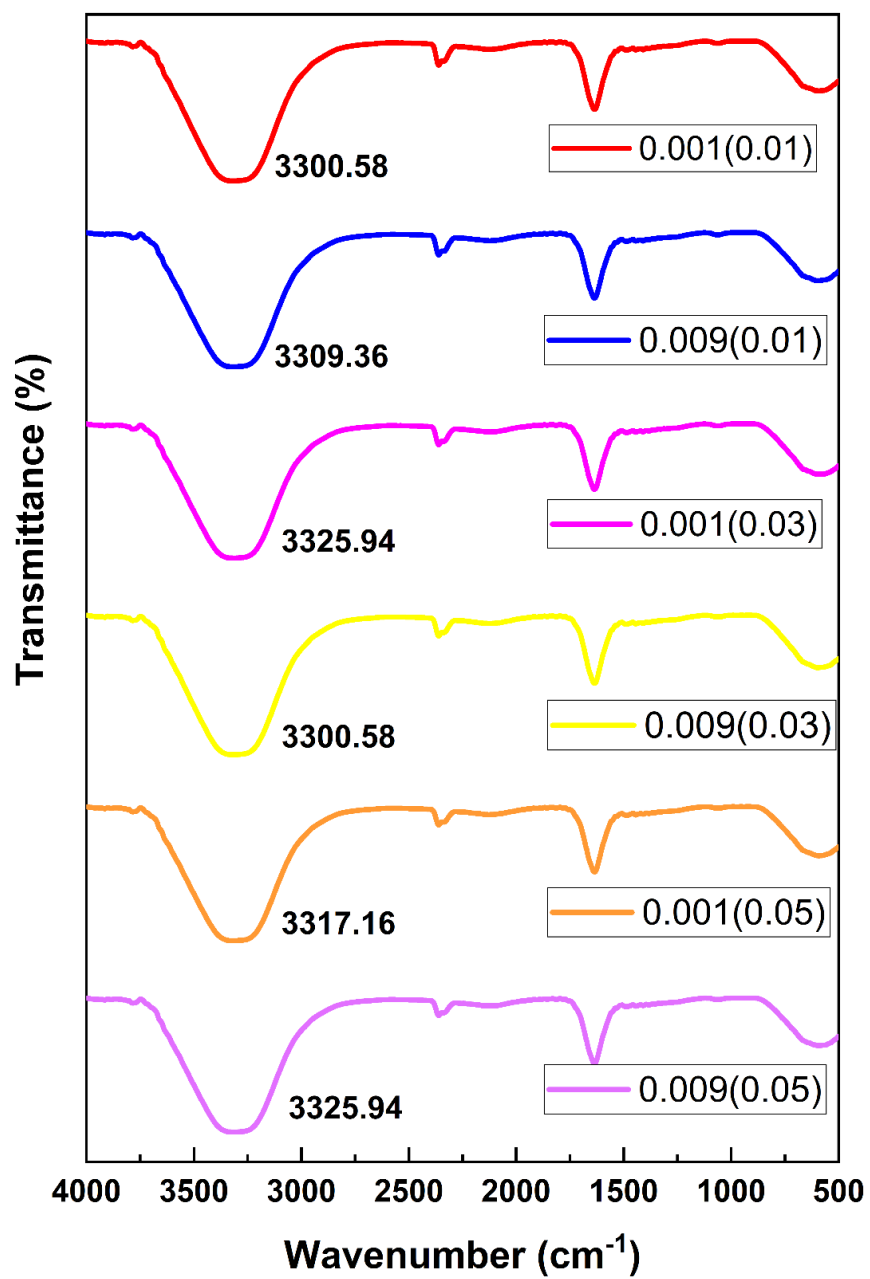


Figure 5.13

Plots of FT-IR spectra for [BMPyr⁺][I⁻] (0.001 and 0.009) mol.kg⁻¹ in aqueous benzylamine.

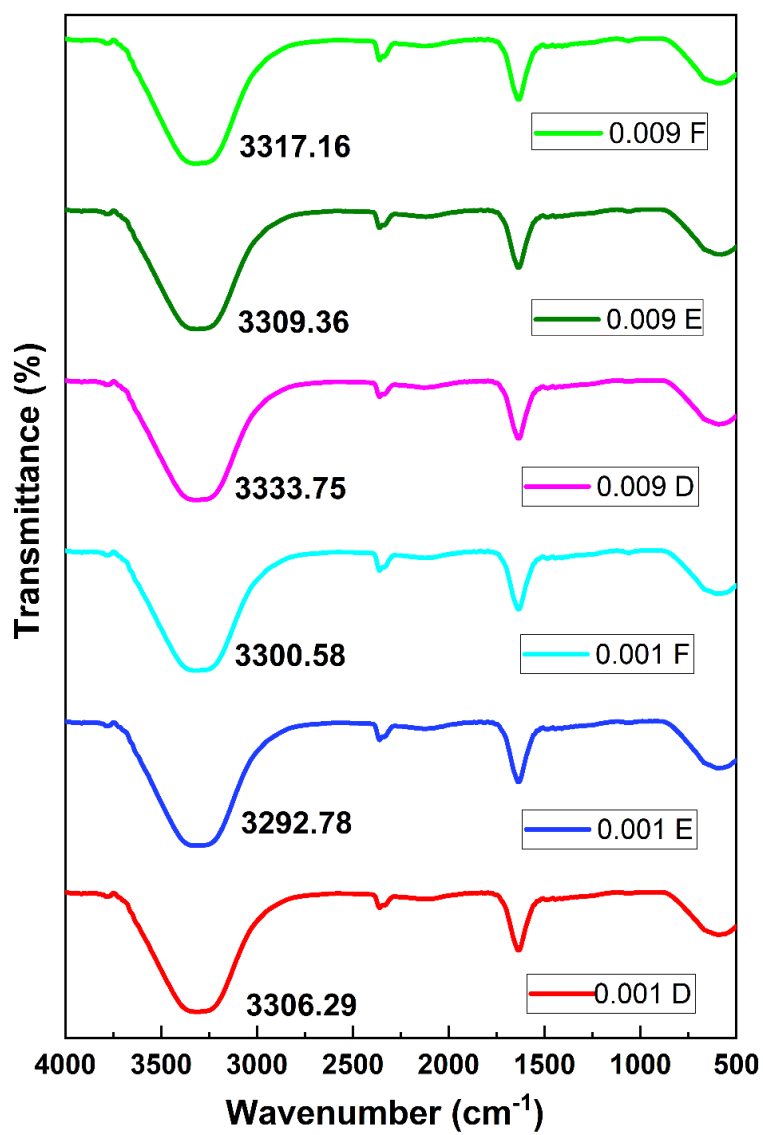


Figure 5.14

Plots of FT-IR spectra for [BMPyr⁺][I⁻] (0.001 and 0.009) mol.kg⁻¹ in aqueous benzamide (0.01 (D), 0.03 (E) and 0.05 (F)) mol.kg⁻¹.

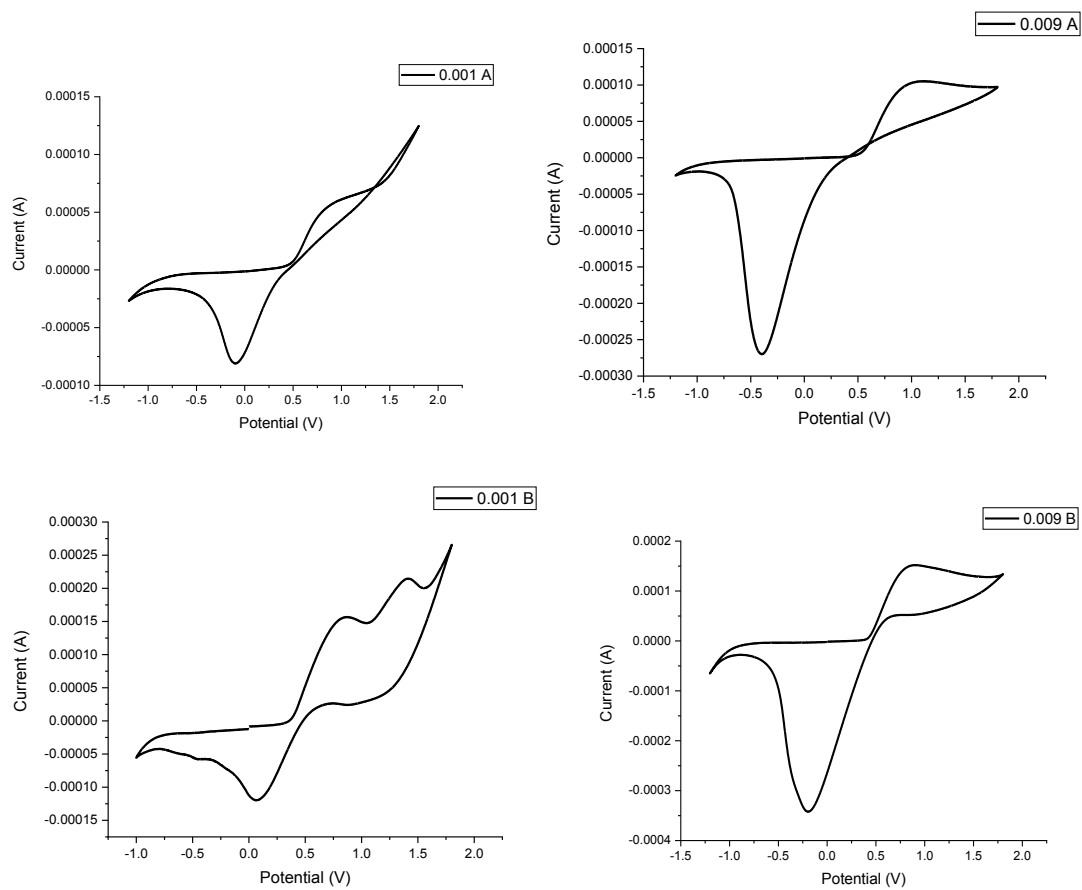


Figure 5.15

Plot of variation of Cyclic Voltammetry of 1-butyl-1-methyl pyrrolidinium iodide (0.01 and 0.05) mol kg⁻¹ of benzylamine.

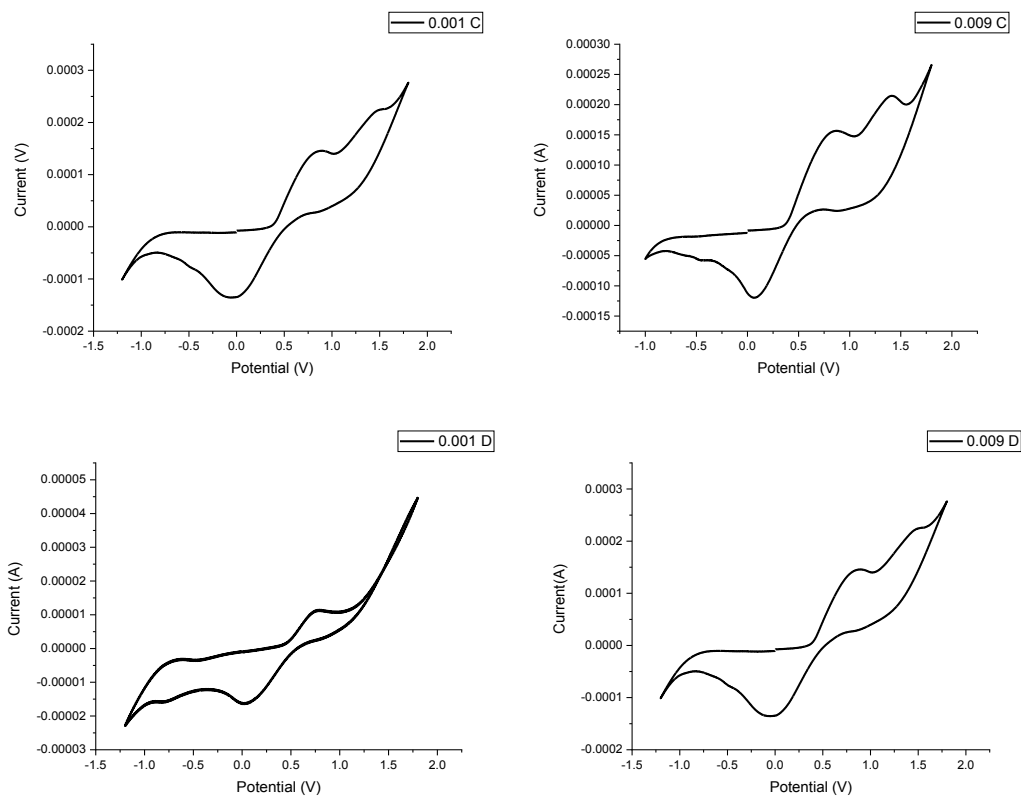


Figure 5.16

Plot of variation of Cyclic Voltammetry of 1-butyl-1-methyl pyrrolidinium iodide in (0.01 and 0.05) mol kg⁻¹ of benzamide.

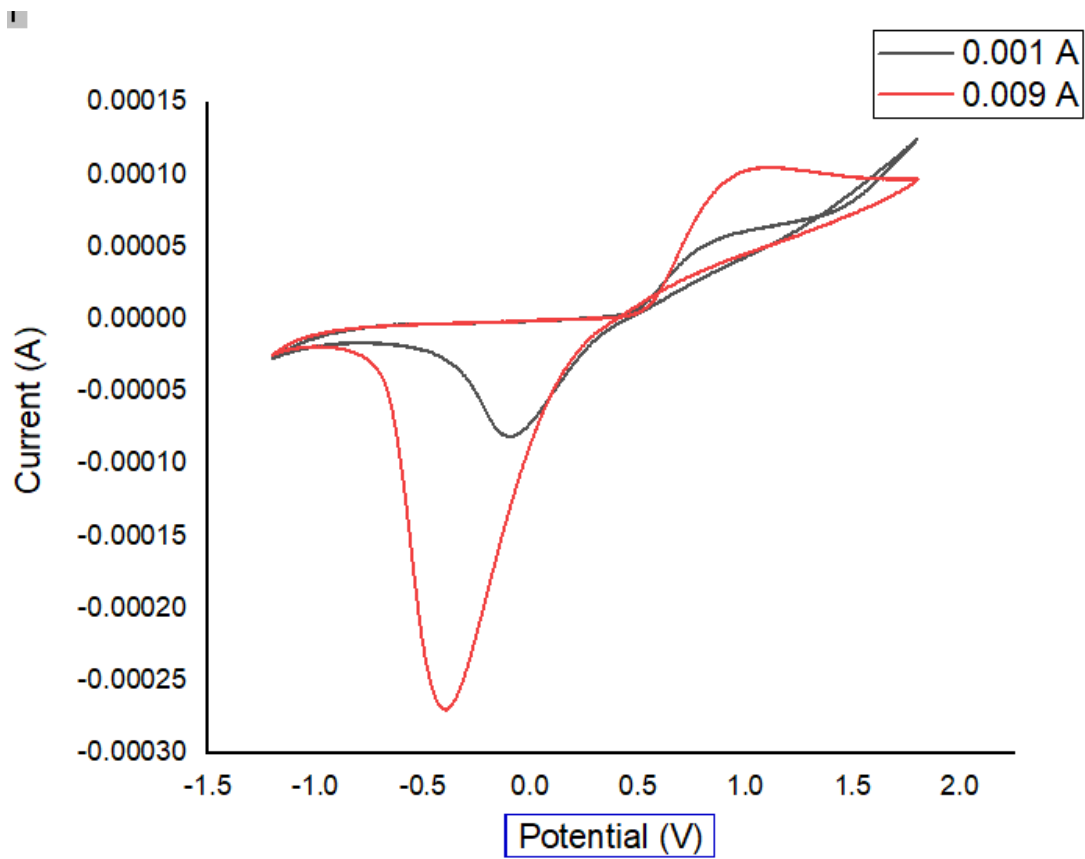


Figure 5.17 (a)

Comparison of CV area of $[\text{BMPyr}^+][\text{I}^-]$ (0.001 and 0.009) mol kg^{-1} in 0.01 (A) of aqueous benzylamine.

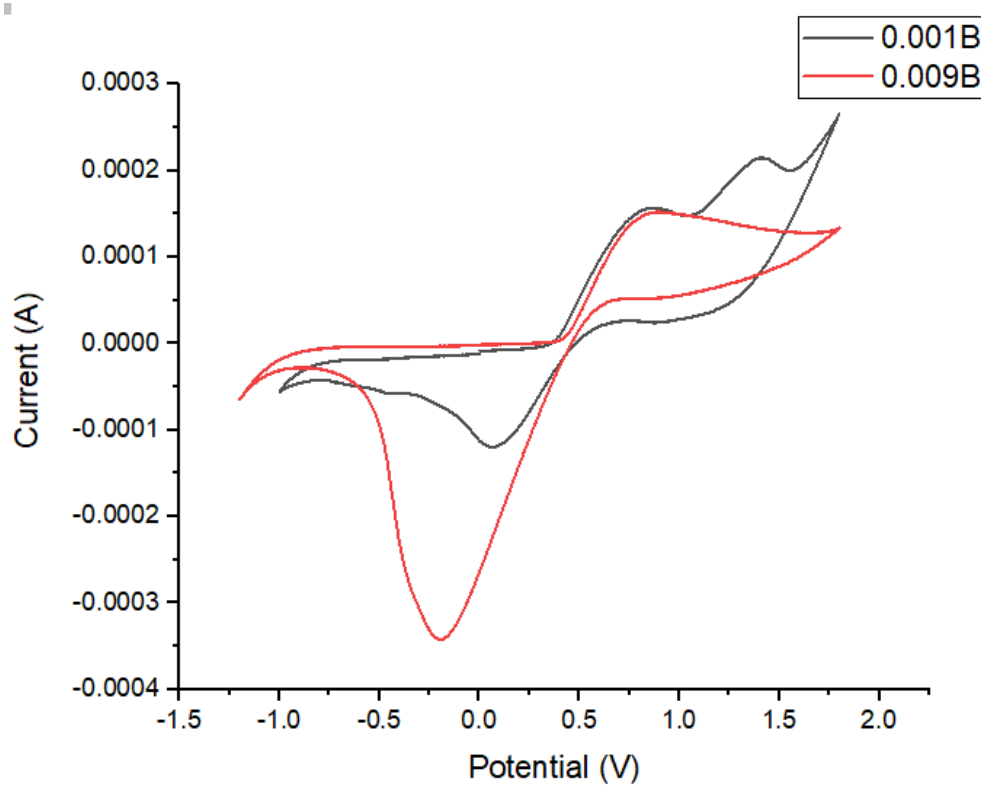


Figure 5.17 (b)

Comparison of CV area of $[\text{BMPyr}^+][\text{I}^-]$ (0.001 and 0.009) mol kg^{-1} in 0.05 (B) of aqueous benzylamine.

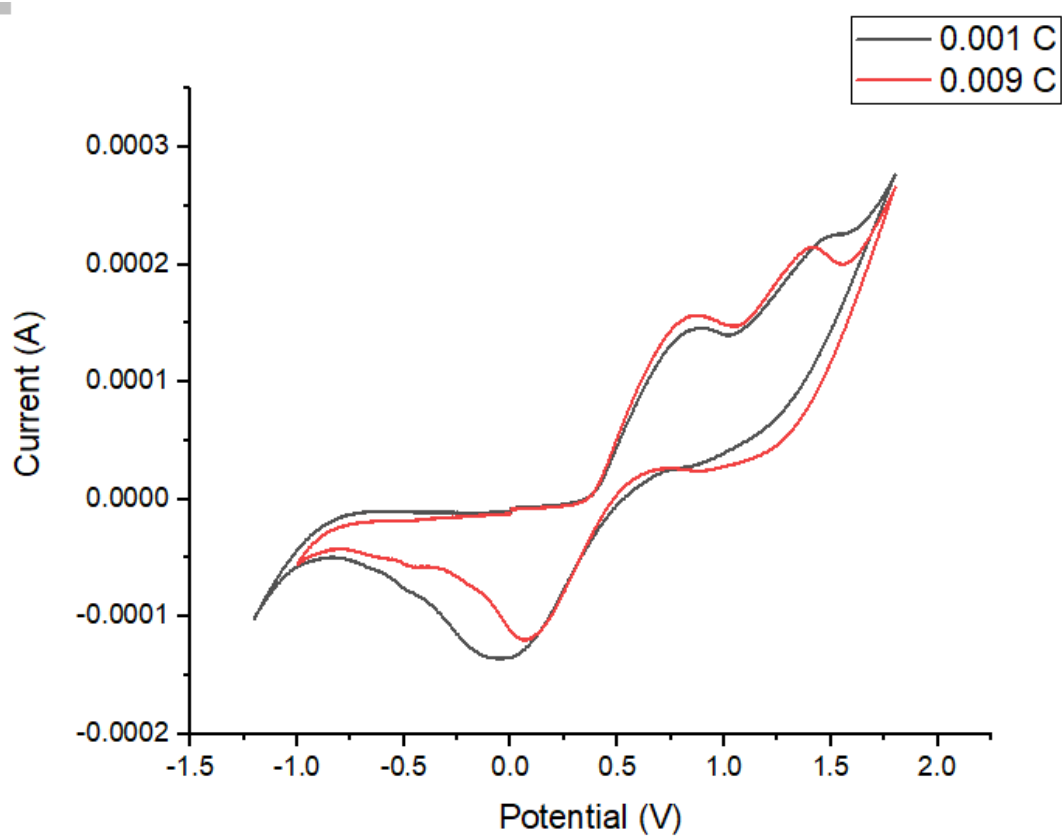


Figure 5.18 (a)

Comparison of CV area of $[\text{BMPyr}^+][\text{I}^-]$ (0.001 and 0.009) mol kg^{-1} in 0.01 (C) of aqueous benzamide.

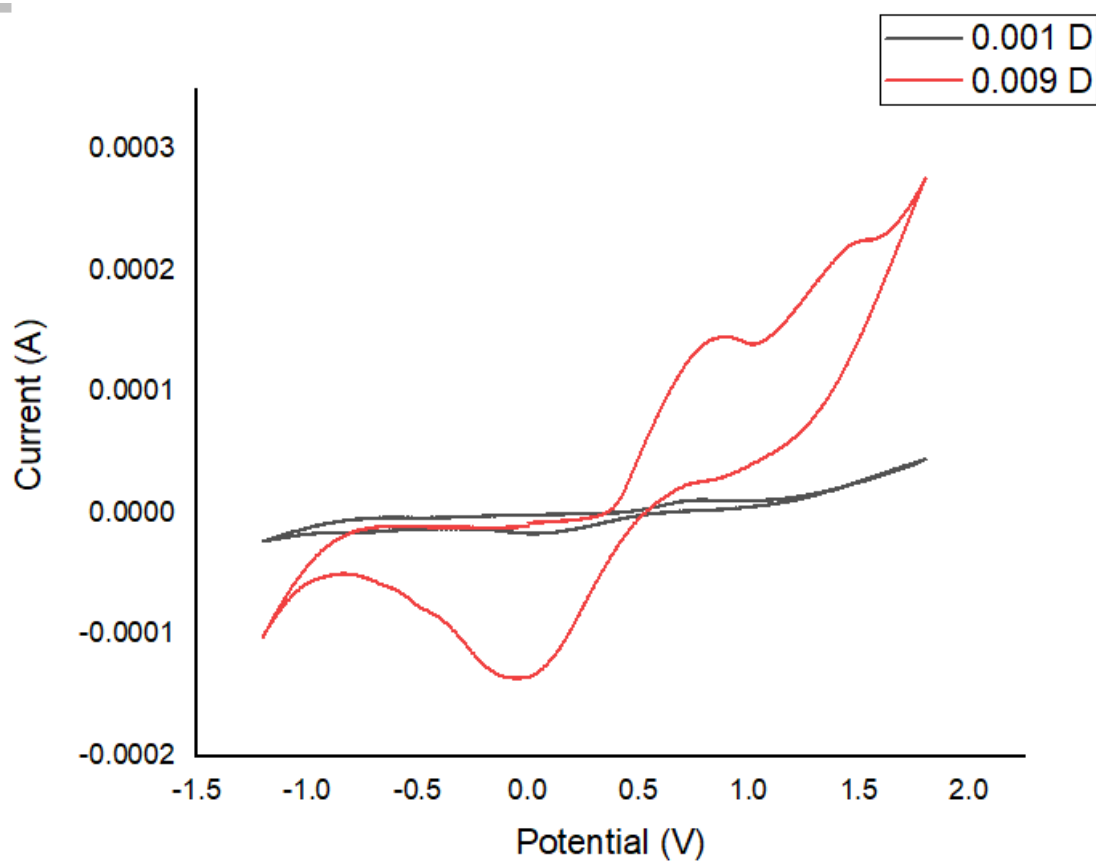


Figure 5.18 (b)

Comparison of CV area of $[\text{BMPyr}^+][\text{I}^-]$ (0.001 and 0.009) mol kg^{-1} in 0.05 (D) of aqueous benzamide.

SECTION-III

Volumetric, acoustic and conductance studies of 1-butyl-1-methyl Pyrrolidinium tetrafluoroborate in binary aqueous benzylamine at various temperatures.

Volumetric, acoustic and conductance studies of 1-butyl-1-methyl Pyrrolidinium tetrafluoroborate in binary aqueous benzylamine at various temperatures.

Density and Sound velocity data

The density as well as sound velocity values of 1-butyl-1-methyl pyrrolidinium tetrafluoroborate are measured in various molal concentrations ranging from (0.01 to 0.05) mol.kg⁻¹ of aqueous solutions of benzylamine at four equidistant temperatures. The data for density and sound velocity is tabulated in Table 5.26. It is clear from the evaluation of density and sound velocity data that values of the density increases as we increase the concentration of ionic liquid from 0.001 mol.kg⁻¹ to 0.009 mol.kg⁻¹ while these values decrease with rising temperature. On the other hand, the sound velocity values hike with the increasing concentration as well as temperature.

Apparent molar volume (V_ϕ) and apparent molar isentropic compression ($K_{\phi,s}$)

Calculation of AMV and apparent molar isentropic compression were done using the measured data for density and sound velocity in the equations (4.13) and (4.23).

AMV values indicates the solute-solvent interactions in the specific system. In the ternary system ([BMPyr⁺][BF₄⁻] aqueous benzylamine), the values of V_ϕ comes out to be positive (tabulated in Table 5.27) confirms the solute-solvent interactions in the investigated system. Fig. 5.19 and Fig. 5.20 represents the values of AMV as a function of molality for (0.01 mol.kg⁻¹ and 0.05 mol.kg⁻¹) at four various temperatures. As we rise the temperature, values of V_ϕ also increases which intensifies the solute-solvent interactions which further pertains to have greater affinity of solute towards solvent at higher temperature.

Equation (4.24), Laplace Newton's equation has been used for the calculation of the isentropic compressibility, κ_s using the measured density and sound velocity data (Galaon et al., 2012).

The values obtained for $K_{\phi,s}$ (Table 5.27) are negative at all concentration and temperatures under consideration and these values becomes less negative as we increase both the temperature and concentration of the IL. For this system, the negative values of $K_{\phi,s}$ specifies the solvation of solute and solvent molecules which results in interactions among solute-solvent.

The molecules of water that are close to the ionic charged centers of the ionic liquid are less compressible in comparison to the molecules of water present in the bulk solution, which enhances the ordering of water molecules. Fig. 5.21 represents the values of $K_{\phi,s}$.

Partial molar volume (V_{ϕ}^o) and partial molar isentropic compression ($K_{\phi,s}^o$)

The AMV and apparent molar isentropic compression at infinite dilution are the partial molar properties that can be used for the confirmation of the presence of solute-solvent interaction.

At constant dilution, the solute-solute interactions become negligible as the solute is completely encircled by the solvent molecules. While the value of V_{ϕ}^o and $K_{\phi,s}^o$ are depicted using the least square fitting method used in equation (4.15) and (4.25).

In the equation, S_V^* and S_K^* are the slopes of the graphs, volumetric and sound velocity coefficients which helps in the prediction of solute-solute interactions while V_{ϕ} and $K_{\phi,s}$ helps in prediction of solute-solvent interactions. The values of V_{ϕ}^o and S_V^* are tabulated in Table 5.28 along with standard errors. The positive value of V_{ϕ}^o at all concentrations and temperature confirms the prevalence of ion-hydrophilic interactions over the ion- hydrophobic and hydrophobic-hydrophobic interactions.

Fig. 5.22 represents the value of V_{ϕ}^o which shows the escalation of values with increasing both temperature and concentration. $K_{\phi,s}^o$ and S_K^* values are represented in Table 5.29 with the standard errors. The values of $K_{\phi,s}^o$ are calculated using the AMV values which also confirms the solute-solvent interactions in this system. The values of $K_{\phi,s}^o$ comes out to be negative for all the concentration which indicated the interactions among solute-solvent (H. Kumar, et al., 2018). As we increase the temperature, these values become less negative signifying the decrease of electrostriction force and because of decreased force the water molecules enter the bulk solution. Therefore, the water molecules are more compressible at the lower concentrations (H. Kaur et al., 2021; P. Kaur et al., 2022).

The negative S_V^* values do not follow any specific trend, but their negative values confirm the poor solute-solute interactions in the system. Interactions among Solute-solute are almost negligible which were also validated by the values of V_{ϕ}^o in comparison to the values of S_V^* .

Partial molar volume of transfer (ΔV_{ϕ}^o) and partial molar isentropic compression of transfer ($\Delta K_{\phi,s}^o$)

The values of ΔV_{ϕ}^o and $\Delta K_{\phi,s}^o$ from water to aqueous benzylamine for 1-butyl-1-methyl pyrrolidinium tetrafluoroborate using the Equation (4.18) and (4.26):

The values of V_{ϕ}^o and $K_{\phi,s}^o$ in water are used in the equations for the calculation of ΔV_{ϕ}^o and $\Delta K_{\phi,s}^o$ and their calculated values are represented in Table 5.30. At all the temperatures and concentration, values of ΔV_{ϕ}^o comes out to be positive, confirming the ion-ion interaction of solute and solvent. Also, the positive values of $\Delta K_{\phi,s}^o$ indicates the structure making tendency of the solute which further intensifies with increasing concentration because of the decreased electrostriction. So, we can state that the water molecule is more compressible in bulk of the solution (A. Kumar et al., 2016).

In the investigated ternary mixture, four types of interactions do exist and these different type of interactions are (a) Hydrophilic- hydrophilic interactions (b) ion- hydrophilic interactions (c) ion- hydrophobic interactions (d) hydrophobic-hydrophobic interactions (K. Lee et al., 2012).

In accordance with co-sphere model, in the specific mixture, hydrophilic -hydrophilic and ion-hydrophilic interaction are dominant over the other two type of interactions. The positive values of ΔV_{ϕ}^o confirms the (a) type of interactions (S. Sharma et al., 2020; V. Sharma et al., 2020).

Dependence of partial molar volume on temperature

AMV shows variation with temperature, and at the infinite dilute variation of V_{ϕ}^o is determined using the polynomial equation (4.19).

a, b and c are the empirical constants which are tabulated in Table 5.31. The values of these constants are positive for a and b and slightly negative of c at 0.01 mol kg⁻¹.

Equation (4.21) is used to calculate the partial molar expansibilities ϕ_E^o which further helps us to determine the different interactions present in the investigated system. For all the concentration, ϕ_E^o values are positive and tabulated in Table 5.32. Positive ϕ_E^o determines the existence of solute-solvent interactions in the specific system.

The structure making or breaking ability of the solute is determined using the equation (4.22) given by Hepler (Hepler, 1969).

$(\partial \phi_E^o / \partial T)_p$ determines the ability of solute to behave as structure maker or breaker. In the system under consideration, positive values of $(\partial \phi_E^o / \partial T)_p$ confirms the structure making tendency.

Pair and triplet interaction coefficients

Friedman and Krishnan modified the theory which was earlier given by McMillan and Mayer to understand the concept of the solute-solvent interactions in the solvation sphere (McMillan & Mayer, 1945; Millero et al., 1978). By fitting the values of ΔV_{ϕ}^o and $\Delta K_{\phi,s}^o$ in equation 4.27 and 4.28 respectively, we can calculate the pair interaction coefficients and triplet interaction coefficients.

The values of pair and triplet coefficients are in Table 5.33. For this system the V_{AB} , V_{ABB} are positive and K_{AB} , K_{ABB} are negative. The positive values of V_{AB} show the pairwise interaction between the amine and IL. Because of the overlap, water molecules leave the hydration co-sphere when non-bonding favorable interactions are present and move into the bulk. The values of V_{AB} are significantly greater than the triplet interaction coefficients V_{ABB} , which explains why pairwise interaction predominates in the mixture of 1-butyl-1-methyl pyrrolidinium tetrafluoroborate and benzylamine.

Conductance studies:

Conductance of 1-butyl-1-methyl pyrrolidinium tetrafluoroborate in aqueous benzylamine at different concentrations (0.01, 0.03 and 0.05)mol.kg⁻¹ were measured using the digital conductivity meter supplied by Labtronics Pvt. Ltd. (India). The conductance of electrolytic solutions determines the character of interactions between solutes-solute, solvent-solvent, or solute-solvent. Ionic conductivities and association constants, two types of thermodynamic and kinetic information, are provided by these studies.

Equation (4.31) was used for the calculation of molar conductivity ($\Lambda_m, S.cm^2.mol^{-1}$) of the ternary solution.

Specific conductivity ($\kappa, \mu S.cm^{-1}$) and molar conductivity ($\Lambda_m, S.cm^2.mol^{-1}$) were measured at four equidistant temperature (288.15 K to 318.15 K) and data for molar conductance is tabulated in Table 5.34. From the obtained data, we can conclude that in case of molar conductivity, it increases with increase in concentration and decreases as we rise the temperature. Higher the temperature, higher the frequency resulting in the breakage of bond due to increase in the

vibrational and translational degrees of freedom resulting in increases mobilities of the ions (P. Kaur et al., 2022; Pathania et al., 2020).

(Fig. 5.11) Plots of Λ_m against \sqrt{c} over the entire composition range within investigated concentration range were found to be straight lines at all temperatures under consideration, which demonstrates the complete dissociation of ionic liquid in the consideration solvent system. The values obtained of molar conductance were used for the calculation of limiting molar conductance using the Onsager relation (Equation 4.32).

(Fig. 5.23 and Fig 24) In the plots, Λ against \sqrt{c} , straight lines give the intercept which is equal to limiting molar conductance and slope is equal to Onsager constant (denoted by S). Table 5.35 tabulates the resultant values of limiting molar conductivity. From the calculated data, it is noticed that the values of Limiting molar conductance increases as we increase the temperature at all concentrations which is due to the mobility of ions. Increase in the temperature results in higher frequency and bond breaking due to which translational and vibrational degrees of freedom increases, thus increases the mobility of ions (Sharma. P., 2021; Z.I. Takai, 2018a). These values obtained helps in interpreting the ion-solvent interactions. Higher the values of limiting molar conductance, greater the ion-solvent interactions. Among all the concentrations, in these ternary mixtures 0.005 mol.kg⁻¹ have the greatest ion-solvent reaction.

Equation 4.33 gives the effect of temperature, where E_A the activation energy and gas constant are denoted by R. It is feasible to calculate E_A from the slope of the straight line generated by the plot of the $\log \Lambda_o$ versus $1/T$. The values of activation energy are tabulated in Table 5.36. We can conclude that solubilization is favorable given that all activation energy values are positive (Shekaari et al., 2019).

Table 5.26.

Value of densities, ρ and speed of sound, u values of ternary mixture of various molalities of 1-butyl-1-methyl pyrrolidinium tetrafluoroborate in aqueous solutions of benzylamine at different temperatures.

$^a m_A /$ (mol.kg ⁻¹)	$\rho \times 10^{-3} / (\text{kg m}^{-3})$				$u / (\text{ms}^{-1})$			
	288.15 K	298.15 K	308.15 K	318.15 K	288.15 K	298.15 K	308.15 K	318.15 K
[BMPyrr⁺][BF₄⁻] + 0.01 mol kg⁻¹ Benzylamine								
000000	0.999221	0.998052	0.996584	0.995016	1469.32	1478.95	1488.98	1496.95
0.00982	0.999473	0.998289	0.996809	0.995227	1470.23	1479.78	1489.68	1497.54
0.02994	0.999992	0.998776	0.997269	0.99565	1472.08	1481.47	1491.11	1498.74
0.04996	1.000509	0.999261	0.997728	0.996090	1473.92	1483.16	1492.53	1499.93
0.06971	1.001019	0.999739	0.998180	0.996514	1475.74	1484.83	1493.93	1501.11
0.08968	1.001533	1.000222	0.998637	0.996944	1477.58	1486.51	1495.35	1502.30
[BMPyrr⁺][BF₄⁻] + 0.03 mol kg⁻¹ Benzylamine								
000000	0.999298	0.997425	0.995622	0.993602	1480.55	1496.06	1511.26	1527.26
0.00982	0.999515	0.997628	0.995812	0.993777	1481.92	1497.41	1512.59	1528.56
0.02948	0.999949	0.998035	0.996194	0.994129	1484.65	1500.10	1515.25	1531.15
0.04911	1.000383	0.998441	0.996574	0.994481	1487.38	1502.80	1517.90	1533.74
0.06880	1.000818	0.998849	0.996956	0.994833	1490.12	1505.50	1520.56	1536.33
0.08851	1.001254	0.999257	0.997339	0.995186	1492.86	1508.20	1523.22	1538.93
[BMPyrr⁺][BF₄⁻] + 0.05 mol kg⁻¹ Benzylamine								

00000	0.999408	0.997451	0.995568	0.993372	1503.42	1507.64	1511.78	1516.21
0.00981	0.999608	0.997639	0.995745	0.993537	1503.65	1507.83	1512.02	1516.47
0.02947	1.000009	0.998016	0.996101	0.993870	1504.11	1508.20	1512.49	1516.98
0.04916	1.000410	0.998394	0.996457	0.994202	1504.57	1508.57	1512.97	1517.50
0.06882	1.000811	0.998772	0.996813	0.994535	1505.04	1508.94	1513.45	1518.01
0.08845	1.001212	0.999149	0.997169	0.994866	1505.50	1509.31	1513.92	1518.53

3m_A is the molality of 1-butyl-1-methyl pyrrolidinium tetrafluoroborate in aqueous benzylamine solutions. Standard uncertainties in molality of benzylamine $u_r(m_{BA})$ and ionic liquid $u_r(m_{IL})$ are $0.0022 \text{ mol}\cdot\text{kg}^{-1}$ and $0.0039 \text{ mol}\cdot\text{kg}^{-1}$ respectively. The respective values of standard uncertainty in density, apparent molar volume, temperature and pressure are $u(\delta\rho) = 0.1 \text{ kg}\cdot\text{m}^{-3}$, $u(\delta V_\phi) = \pm(0.01-0.10) \times 10^{-3} \text{ m}^3\cdot\text{mol}^{-1}$, $u(T) = 0.01 \text{ K}$ and $u(P) = 0.01 \text{ MPa}$.

Table 5.27.

Apparent molar volume, V_ϕ and apparent molar isentropic compression, $K_{\phi,s}$ values of ternary mixtures of various molalities, m of Ionic liquid in benzylamine at different temperatures.

$^a m_A /$ (mol.kg ⁻¹)	$V_\phi \times 10^6 / (\text{m}^3 \text{mol}^{-1})$				$K_{\phi,s} \times 10^6 (\text{m}^3 \text{mol}^{-1} \text{GPa}^{-1})$			
	288.15 K	298.15 K	308.15 K	318.15 K	288.15 K	298.15 K	308.15 K	318.15 K
[BMPyrr⁺][BF₄⁻] + 0.01 mol kg⁻¹ Benzylamine								
0.009826	23.36	25.18	26.76	28.46	-18.49	-15.60	-13.26	-10.82
0.029940	23.26	25.08	26.66	28.37	-18.00	-15.08	-12.74	-10.24
0.049965	23.15	24.98	26.57	28.28	-17.51	-14.56	-12.22	-9.67
0.069714	23.05	24.88	26.47	28.19	-17.03	-14.05	-11.71	-9.11
0.089688	22.95	24.78	26.38	28.11	-16.55	-13.53	-11.19	-8.54
[BMPyrr⁺][BF₄⁻] + 0.03 mol kg⁻¹ Benzylamine								
0.009829	25.05	26.81	27.47	29.38	-21.20	-20.29	19.65	-16.41
0.029489	24.96	26.73	27.39	29.31	-21.03	-19.93	-18.82	-15.58
0.049115	24.87	26.64	27.31	29.23	-20.86	-19.58	-18.00	-14.77
0.068800	24.78	26.56	27.23	29.16	-20.67	-19.14	-17.16	-13.94
0.088511	24.69	26.47	27.15	29.08	-20.00	-18.84	-16.33	-13.12
[BMPyrr⁺][BF₄⁻] + 0.05 mol kg⁻¹ Benzylamine								
0.009813	26.74	27.32	28.79	30.44	-22.86	-20.12	-17.28	-14.71
0.029470	26.66	27.24	28.71	30.37	-22.07	-19.29	-16.57	-14.11
0.049163	26.57	27.17	28.64	30.29	-21.29	-18.45	-15.85	-13.51
0.068823	26.49	27.09	28.56	30.22	-20.50	-17.62	-15.13	-12.90
0.088453	26.41	27.01	28.49	30.15	-19.72	-16.78	-14.41	-12.30

^a m_A is the molality of 1-butyl-1-methyl pyrrolidinium tetrafluoroborate in aqueous benzylamine solutions. Standard uncertainties in molality of benzylamine $u_r(m_{BA})$ and ionic liquid $u_r(m_{IL})$ are 0.0022 mol.kg⁻¹ and 0.0039 mol.kg⁻¹ respectively. The respective values of standard uncertainty in density, apparent molar volume, temperature and pressure are $u(\delta\rho) = 0.1 \text{ kg}\cdot\text{m}^{-3}$, $u(\delta V_\phi) = \pm(0.01-0.10) \times 10^{-3} \text{ m}^3\cdot\text{mol}^{-1}$, $u(T) = 0.01 \text{ K}$ and $u(P) = 0.01 \text{ MPa}$.

Table 5.28.

Values of partial molar volumes, V_{ϕ}^0 and experimental slope, S_v^* of ternary mixtures of Ionic liquid in various molalities of aqueous benzylamine at different temperatures.

$^a m_B$ (mol kg ⁻¹)	$V_{\phi}^0 \times 10^6 / (\text{m}^3 \text{ mol}^{-1})$				$S_v^* \times 10^6 / (\text{m}^3 \text{ kg mol}^{-2})$			
	288.15 K	298.15 K	308.15 K	318.15 K	288.15 K	298.15 K	308.15 K	318.15 K
[BMPyrr⁺][BF₄⁻] + Benzylamine								
0.01	23.41 (±0.0001)	25.22 (±0.0009)	26.80 (±0.0008)	28.50 (±0.0007)	-05.23 (±0.0018)	-04.96 (±0.0016)	-04.74 (±0.0014)	-04.49 (±0.0013)
0.03	25.09 (±0.0007)	27.85 (±0.0006)	28.51 (±0.0006)	30.42 (±0.0005)	-04.57 (±0.0013)	-04.32 (±0.0012)	-04.09 (±0.0011)	-03.82 (±0.0001)
0.05	28.78 (±0.0006)	29.36 (±0.0006)	31.82 (±0.0005)	32.42 (±0.0005)	-04.25 (±0.0011)	-04.04 (±0.0001)	-03.84 (±0.0009)	-03.62 (±0.0008)

^a m_B is molality of aqueous solution of benzylamine

Table 5.29.

Values of limiting apparent molar isentropic compression, $K_{\phi,s}^0$ and experimental slopes, S_K^* of ternary mixtures of Ionic liquid in various molalities, m of aqueous benzylamine at different temperatures.

$a_{m_B} /$ (mol kg ⁻¹)	$K_{\phi,s}^0 \times 10^6 / (\text{m}^3 \text{mol}^{-1} \text{GPa}^{-1})$				$S_K^* \times 10^6 / (\text{kg m}^3 \text{mol}^{-2} \text{GPa}^{-1})$			
	288.15 K	298.15 K	308.15 K	318.15 K	288.15 K	298.15 K	308.15 K	318.15 K
Benzylamine								
0.01	-18.73 (±0.01)	-15.85 (±0.01)	-14.52 (±0.01)	-12.70 (±0.01)	02.75 (±0.06)	01.55 (±0.17)	01.12 (±0.06)	00.83 (±0.08)
0.03	-17.79 (±0.01)	-14.88 (±0.01)	-13.92 (±0.01)	-12.01 (±0.01)	01.62 (±0.17)	01.32 (±0.05)	01.07 (±0.07)	00.74 (±0.11)
0.05	-16.25 (±0.05)	-14.04 (±0.01)	-13.24 (±0.01)	-11.44 (±0.01)	01.07 (±0.19)	0.98 (±0.37)	00.86 (±0.04)	00.49 (±0.03)

^a_{m_B} is the molality of aqueous solution of benzylamine.

Table 5.30.

Values of PMV of transfer, ΔV_{ϕ}^0 and limiting molar isentropic compression of transfer, $\Delta K_{\phi,s}^0$ of ternary mixtures of Ionic liquid in various concentration (molality, $m=0.01, 0.03$ and 0.05) mol.kg^{-1} of aqueous benzylamine.

^a $m_B /$ (mol kg^{-1})	$\Delta V_{\phi}^0 \times 10^6 / (\text{m}^3 \text{mol}^{-1})$				$\Delta K_{\phi,s}^0 \times 10^6 / (\text{m}^3 \text{mol}^{-1} \text{GPa}^{-1})$			
	288.15 K	298.15 K	308.15 K	318.15 K	288.15 K	298.15 K	308.15 K	318.15 K
Benzylamine								
0.01	2.49	2.11	1.81	1.57	6.39	7.27	7.94	8.48
0.03	3.46	3.18	2.78	2.42	7.33	7.74	8.04	8.87
0.05	4.51	4.22	3.85	3.49	8.17	8.58	8.82	9.47

^a m_B is the molality of aqueous solution of benzylamine.

Table 5.31.

Values of empirical parameters (a, b and c) of ternary mixture of Ionic liquid in various molalities, m of aqueous benzylamine at various temperatures.

$^a m_B / (\text{mol kg}^{-1})$	$a \times 10^6 / (\text{mol kg}^{-1})$	$b \times 10^6 / (\text{m}^3 \text{mol}^{-1} \text{K})$	$c \times 10^6 / (\text{m}^3 \text{mol}^{-1} \text{K}^{-2})$	R^2	ARD(σ)
1-butyl-1-methyl pyrrolidinium tetrafluoroborate+ benzylamine					
0.01	25.17	0.1723	-0.0002	0.9989	0.00071
0.03	28.80	0.1635	0.0003	0.9999	0.00066
0.05	31.32	0.1538	0.0011	0.9977	0.00057

$^a m_B$ is molality of aqueous solution of benzylamine.

Table 5.32.

Values of molar expansibilities, ϕ_E^0 of ternary mixture of Ionic liquid in different concentrations of aqueous benzylamine at different temperatures.

^a m _B / (mol kg ⁻¹)	$\phi_E^0 \times 10^6 / (\text{m}^3 \text{mol}^{-1} \text{K}^{-1})$				$(\partial \phi_E^0 / \partial T)$
	288.15 K	298.15 K	308.15 K	318.15 K	
Benzylamine					
0.01	0.177	0.171	0.166	0.160	-0.00055
0.03	0.165	0.172	0.180	0.188	0.00036
0.05	0.151	0.154	0.157	0.160	0.00071

Molality of aqueous solution of benzylamine is denoted by $^a m_B$.

Table 5.33.

Values of pair (V_{AB} and K_{AB}) and triplet interaction coefficients (V_{ABB} and K_{ABB}) of ternary mixtures of Ionic liquid in aqueous benzylamine at different temperatures.

T / (K)	$V_{AB} \times 10^6 /$ (m³ mol⁻² kg)	$K_{AB} \times 10^6 /$ (m³ mol⁻²kgGPa⁻¹)	$V_{ABB} \times 10^6 /$ (m³ mol⁻³ kg²)	$K_{ABB} \times 10^6 /$ (m³ mol⁻³ kg² GPa⁻¹)
Benzylamine				
288.15	36.61	232.80	-783.86	-924.28
298.15	32.51	240.83	-715.84	-2956.18
308.15	28.28	277.46	-658.15	-3280.17
318.15	22.03	317.57	-400.21	-3711.36

Table.5.34.

Specific Conductivity (k , $\mu\text{S.cm}^{-1}$) and molar conductivity (Λ_m , $\text{S.cm}^2\text{mol}^{-1}$) 1-butyl-1-methyl pyrrolidinium tetrafluoroborate in aqueous solution of benzylamine.

^a m_A / (mol.kg^{-1})	Specific Conductivity (k , $\mu\text{S.cm}^{-1}$)				Molar Conductance (Λ_m , $\text{S.cm}^2\text{mol}^{-1}$)			
	288.15	298.15	308.15	318.15	288.15	298.15	308.15	318.15
[BMPyrr⁺][BF₄⁻] + 0.01 mol kg⁻¹ Benzylamine								
0.00982	859.80	773.56	705.00	642.65	49.51	51.30	53.68	49.51
0.02994	1327.30	1233.63	1156.55	1086.94	51.77	53.60	55.95	51.77
0.04996	1792.73	1691.66	1606.09	1529.25	54.04	55.91	58.22	54.04
0.06971	2251.74	2143.36	2049.43	1965.46	56.30	58.21	60.50	56.30
0.08968	2715.98	2600.22	2497.82	2406.64	58.56	60.51	62.77	58.56
[BMPyrr⁺][BF₄⁻] + 0.03 mol kg⁻¹ Benzylamine								
0.00982	1173.65	1059.84	928.17	805.49	53.8	56.08	58.02	60.10
0.02948	1773.74	1659.11	1518.91	1386.07	56.12	58.34	60.48	62.54
0.04911	2372.80	2257.34	2108.62	1965.65	58.44	60.59	62.94	64.98
0.06880	2973.68	2857.39	2700.13	2546.99	60.76	62.85	65.41	67.42
0.08851	3575.35	3458.24	3292.42	3129.10	63.08	65.11	67.86	69.86
[BMPyrr⁺][BF₄⁻] + 0.05 mol kg⁻¹ Benzylamine								
0.00981	1340.55	1212.84	1129.17	998.59	57.33	59.46	61.53	63.48
0.02947	2051.51	1920.35	1809.30	1669.56	59.59	61.70	63.77	65.71
0.04916	2763.79	2629.19	2490.71	2341.79	61.84	63.95	66.02	67.92
0.06882	3474.87	3336.82	3170.95	3012.87	64.09	66.19	68.26	70.14
0.08845	4184.89	4043.41	3850.19	3682.95	66.35	68.43	70.50	72.36

^a m_A is the molality of 1-butyl-1-methyl pyrrolidinium tetrafluoroborate in aqueous benzylamine solutions. Standard uncertainties in molality of benzylamine $u_r(m_{BA})$ and ionic liquid $u_r(m_{IL})$ are $0.0022 \text{ mol.kg}^{-1}$ and $0.0039 \text{ mol.kg}^{-1}$

respectively. The respective values for standard uncertainty in density, apparent molar volume, temperature and pressure are $u(\delta\rho) = 0.1 \text{ kg}\cdot\text{m}^{-3}$, $u(\delta V_\phi) = \pm(0.01-0.10) \times 10^{-3} \text{ m}^3\cdot\text{mol}^{-1}$, $u(T) = 0.01 \text{ K}$ and $u(P) = 0.01 \text{ MPa}$.

Table.5.35.

Limiting molar conductivity (Λ° , $\text{S}\cdot\text{cm}^2\cdot\text{mol}^{-1}$) of 1-butyl-1-methyl pyrrolidinium tetrafluoroborate in aqueous solution of benzylamine .

$^a m_B$ (mol kg ⁻¹)	Λ° (S·cm ² ·mol ⁻¹)			
	288.15 K	298.15 K	308.15 K	318.15 K
Benzylamine				
0.001	23.55	24.33	24.76	25.52
0.003	24.40	25.24	25.77	26.61
0.005	25.26	26.15	26.78	27.70

^a m_B is molality of aqueous solution benzylamine.

Table.5.36.

Activation energy of 1-butyl-1-methyl pyrrolidinium tetrafluoroborate in aqueous benzylamine.

Concentration ^a m _B (mol kg ⁻¹)	Activation Energy $E_A \times 10^{-3}(\text{kJ.mol}^{-1})$		
	0.01	0.03	0.05
Benzylamine			
0.001	0.00614	0.00467	0.00261
0.003	0.00978	0.00875	0.00633
0.005	0.00705	0.01216	0.00983
0.007	0.00657	0.01502	0.01312
0.009	0.00621	0.01745	0.01619

m_a is the molality of 1-butyl-1-methyl pyrrolidinium tetrafluoroborate in aqueous benzylamine solution.

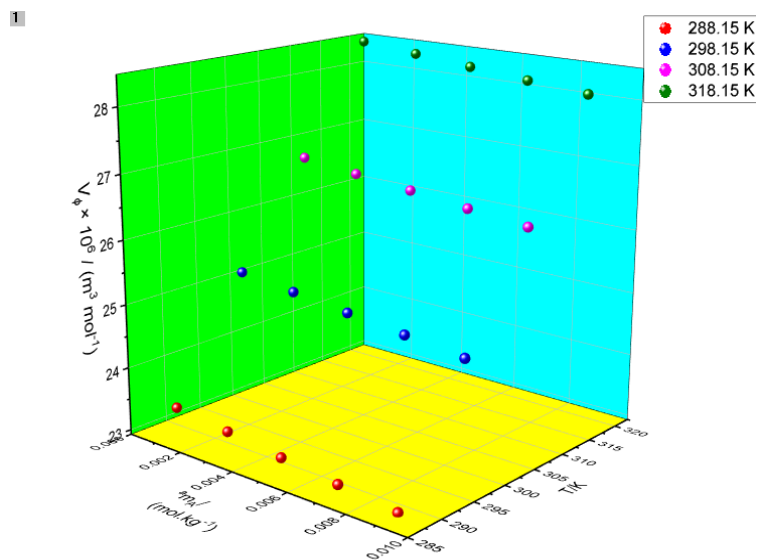


Figure 5.19.

Plot of apparent molar volume (V_ϕ) against molality (m) of 1-butyl-1-methyl pyrrolidinium tetrafluoroborate in 0.01 mol.kg^{-1} aqueous solution of benzylamine at different temperatures.

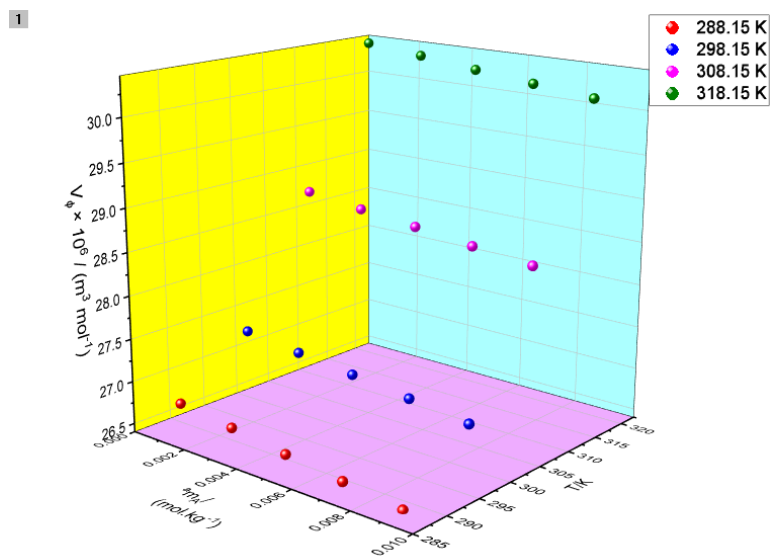


Figure 5.20.

Plot of apparent molar volume (V_ϕ) against molality (m) of 1-butyl-1-methyl pyrrolidinium tetrafluoroborate in 0.05 mol.kg⁻¹ aqueous solution of benzylamine at different temperatures.

1

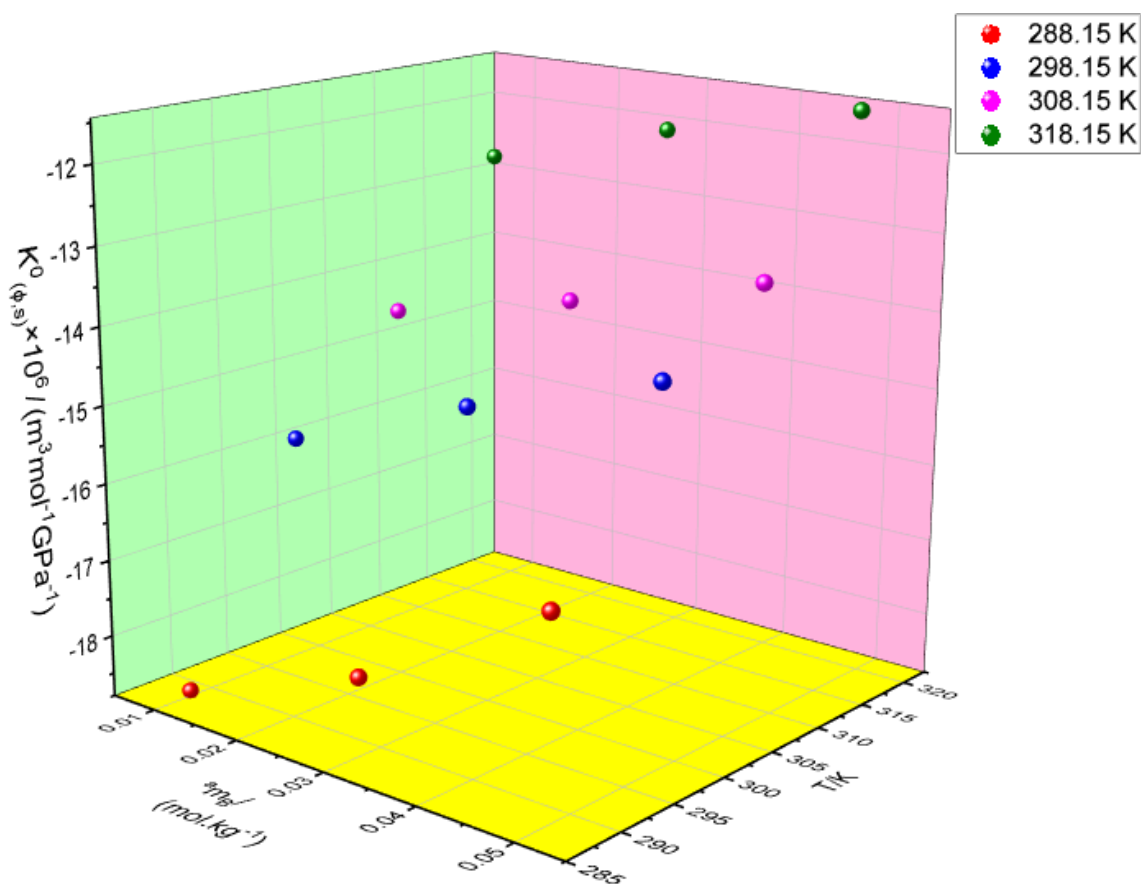


Figure 5.21.

Plot of variation of apparent molar isentropic compression against ($K_{\phi,s}^0$) molality of 1-butyl-1-methyl pyrrolidinium tetrafluoroborate in 0.01 and 0.05 mol.kg⁻¹ of aqueous benzylamine at four equidistant temperatures.

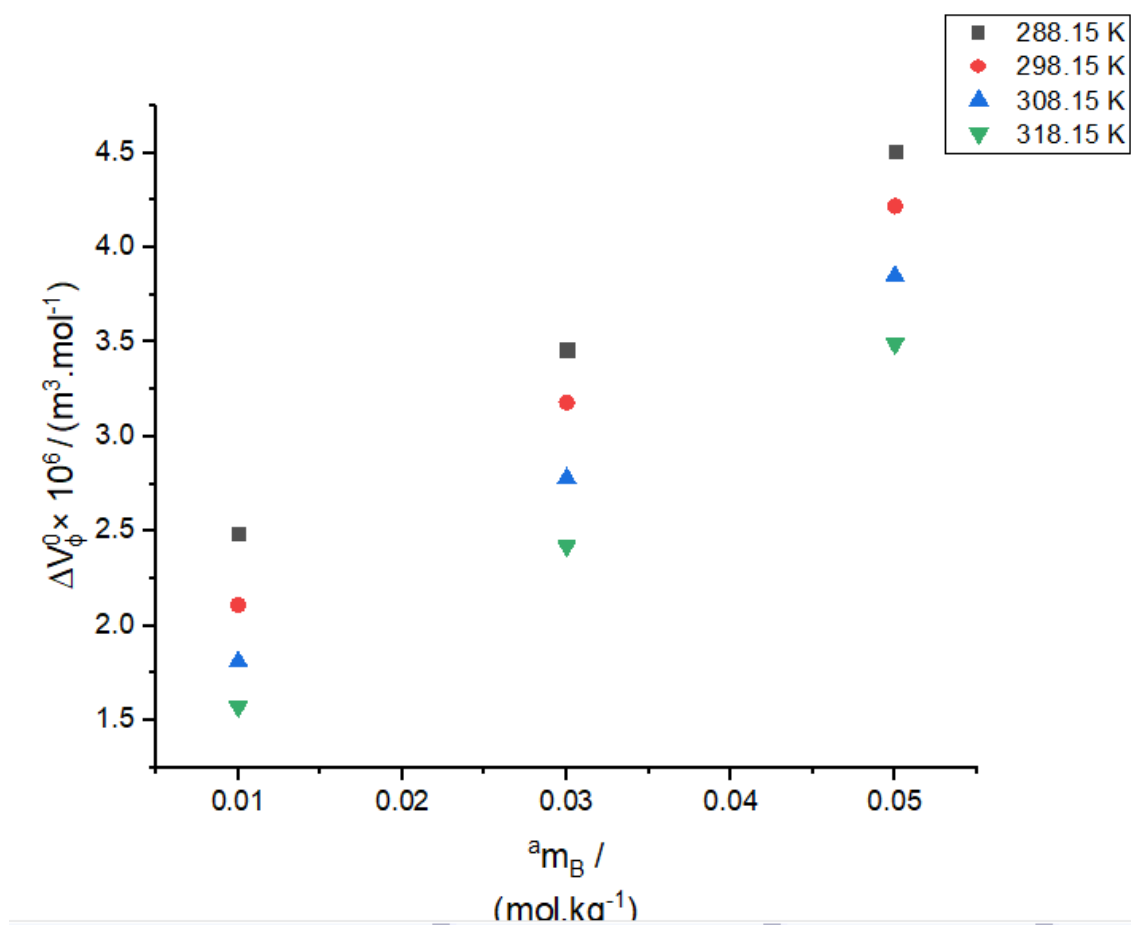


Figure 5.22.

Plot of variation of PMV of 1-butyl-1-methyl pyrrolidinium tetrafluoroborate in aqueous benzylamine at different temperatures (288.15 K to 318.15 K).

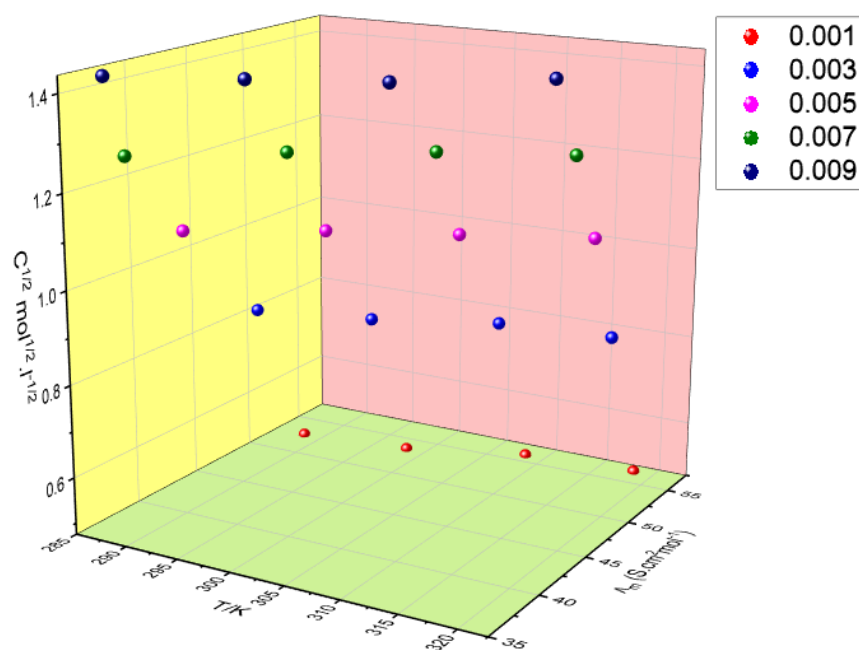


Figure 5.23

Plots showing the variation of Λ_o with \sqrt{C} for 1-butyl-1-methyl pyrrolidinium tetrafluoroborate in 0.01 mol.kg⁻¹ aqueous benzylamine at T = (298.15, 303.15, 308.15 and 313.15) K.

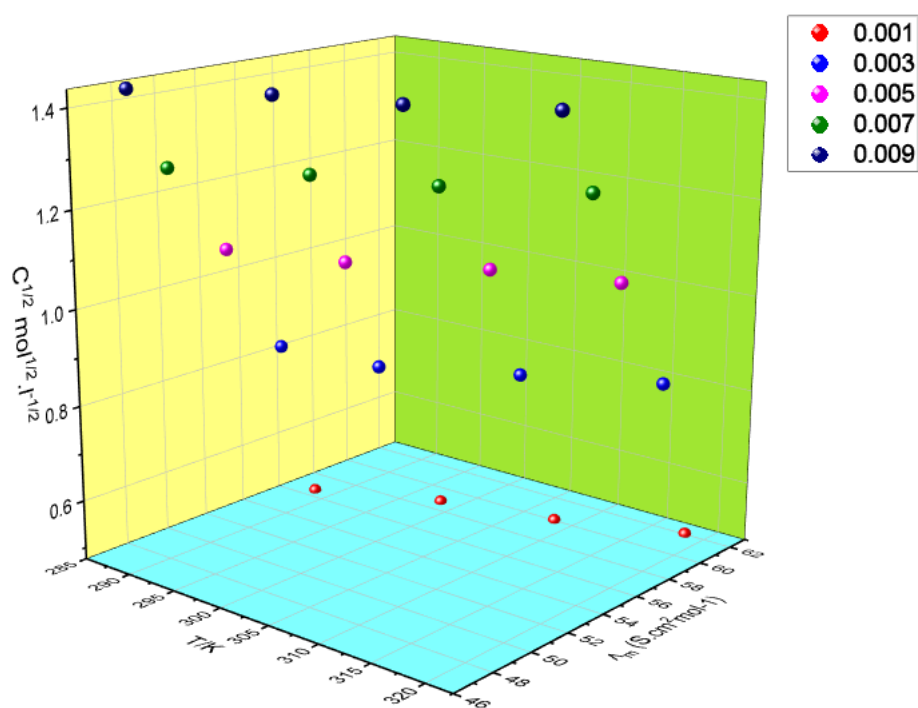


Figure 5.24

Plots showing the variation of Λ_0 with \sqrt{C} for 1-butyl-1-methyl pyrrolidinium tetrafluoroborate in 0.05 mol.kg⁻¹ aqueous benzylamine at T = (298.15, 303.15, 308.15 and 313.15) K.

Chapter 6

SUMMARY AND CONCLUSION

SUMMARY AND CONCLUSION

The thesis titled "**Physicochemical and Conductometric Studies of some Triazolium and pyrrolidinium based Ionic liquids in binary aqueous amine for energy storage applications**" involves synthesis of the ionic liquids (1-butyl-1-methyl pyrrolidinium and 1-ethyl-3-methylimidazolium iodide) followed by their structural elucidation using various spectroscopic techniques, mainly, ^1H -NMR and ^{13}C -NMR. The ternary mixtures (synthesized IL + aqueous benzylamine/benzamide) are next relegated to the calculations of the thermodynamic and acoustic characteristics. Utilizing FT-IR spectral analyses, the conclusions drawn from the thermodynamic parameters are further validated. The values for density and sound velocity were measured, and the results were utilized to compute thermodynamic and acoustic characteristics.

Densities and sound velocity of [DMTI] were measured in 0.01 to 0.05 molkg⁻¹ aqueous solution of aqueous benzamide and benzamide at four equidistant temperatures. The density of the system increases as the concentration increases for IL as well as composition of benzylamine and benzamide and decreases as we raise the temperature. It has been expected that the ternary networks will exhibit several kinds of relationships on behalf of thermophysical parameters derived utilizing the data obtained from density and sound velocity. Solute-solvent associations in the ternary solution are intensified with increasing temperature, as seen by the positive values of V_ϕ and the negative values of $K_{\phi,s}$. On contrary, the interactions among solute and solvent are weakened with the hike in the concentration of aqueous benzamide and benzylamine. Conversely, smaller and negative values of S_V^* confirm the weaker interactions among solute and solute as compared to the interactions among solute-solvent. The values of S_K^* follow no specific trend from which we can conclude that there are various factors affecting the interaction between solute-solute. In the ternary system, ion-hydrophilic synergies prevail over hydrophobic- hydrophobic synergies, indicated by the positive values of V_ϕ^0 which continue to grow with temperature rise and fall with concentration increase. The values of $(\partial\phi_E^0/\partial T)_p$ decides the structure constructor or destroying behavior of the solute in a particular solvent system. In the studied ternary system small and negative values of $(\partial\phi_E^0/\partial T)_p$ have been observed which confirms the structure destroying nature of [DMTI]. The negative data for $\Delta K_{\phi,s}^0$ reflect the tendency of the IL to break down the structure in aqueous solutions of benzamide and benzylamine. And behavior is found in

good agreement with the findings of volumetric studies (V_{ϕ}^0 values). Conductance studies for IL in aqueous solution of benzamide and benzylamine at a temperature range are reported in the present study and the data obtained was further used for the calculation of parameters like specific conductance, molar conductance, limiting molar conductance and activation energy. The results obtained show that the molar concentration of the mixture is directly dependent on temperature and concentration, also in case of benzylamine molar conductivity is greater than that of benzamide. Similarly, the ion-solvent interactions confirmed using the data for limiting molar conductance are dominant in case of IL in aqueous benzylamine and benzamide. In case of benzylamine, activation energy is greater than that of benzamide i.e. the speed of reaction is slower in benzylamine. The FT-IR wavenumber shift indicates some changes in the structure and intermolecular interactions between IL and aqueous amine whenever the content of the combination is changed. Intermolecular H-bonding is responsible for the apparent shift in wavenumber as the ionic liquid, aqueous benzylamine, and benzamide concentrations in the ternary system are varied. In the studied ternary systems, the shift in wavenumber corresponding to –OH group towards lower side confirms the presence of intermolecular interactions in the system.

Further, for 1-butyl-1-methyl pyrrolidinium iodide ([BMPyr⁺][I⁻]) data for density and sound velocity were analyzed in aqueous solutions of benzylamine and benzamide with concentration $m_B = (0.01, 0.03 \text{ and } 0.05) \text{ mol.kg}^{-1}$ at temperatures ($T = 288.15 \text{ K to } 318.15 \text{ K}$). The density of IL increases as we increase the concentration of aqueous amine and decreases with increasing temperature. Partial and apparent molar properties were calculated from the experimental data of density and sound velocity. The positive V_{ϕ} values in the ternary system further intensifies with increase in temperature. Rise in temperature causes a greater thermal movement of the molecules which results in the hike in volume. Positive and large values of V_{ϕ}^0 indicates strong solute-solvent interactions. The decrease in electrostriction with increasing temperature attributes towards the rising V_{ϕ}^0 values with temperature. Additionally, as temperature rises, the mixture's H-bonding decreases, increasing the volume of free solvent available for solvation. As indicated by the positive values V_{ϕ}^0 , the system's hydrophilic interactions are more prevalent than hydrophobic interactions. ΔV_{ϕ}^0 escalates with increase in temperature as increased temperature leads to decrease in electrostriction. Further, observed positive and modest values of $(\partial \phi_E^0 / \partial T)_p$ support the

structure promoting function of [BMPyr⁺][I⁻] in aqueous benzamide and benzylamine solutions. The positive values of ϕ_E^0 can also be attributed to the packing effect phenomenon indicating the important interactions which are prevalent in the studied system. The positive values of ϕ_E^0 at all concentrations and temperatures promotes the solute-solvent interactions in the present system which were also confirmed by the AMV data.

The values of $K_{\phi,s}$ (apparent molar compressibility) are negative at all concentrations and temperatures. These values further rise with a rise in the concentration of IL as well as temperature. Negative values of $K_{\phi,s}$, indicate the lower degree of water molecule compression around the ionic charged groups of IL and these values further decreases, indicating the lowering in structural compressibility of water indicating the lesser ordering of IL on solvents. On the other hand, with rising temperature, again the values of $K_{\phi,s}$ becomes less negative indicating the reduction of electrostriction and promoting the release of some water molecules in the bulk with the hike in temperature. The lower degree of water molecule compression surrounding the ionic-charged groups of IL is shown by the negative value of $K_{\phi,s}$. Strong solute-solvent interactions are signified by negative values of $K_{\phi,s}^0$ while solute-solute interactions are signified by positive values of S_K^* . The positive and small negative values of $\Delta K_{\phi,s}^0$ indicates the structure-making nature of the ionic liquid in aqueous solutions of benzamide and benzylamine. The positive values of V_{AB} except at temperature 288.15K shows the presence of pairwise interactions. The value of the triplet coefficient K_{ABB} is indirectly proportional to the temperature for the first system and directly proportional to the temperature for the second system. From the proposed formalism, we can say that along with pairwise interactions, non-bonding favorable interactions are also present which are due to the overlap of the hydration co-sphere.

Supplementary, conductometric studies are performed for [BMPyr⁺][I⁻] in aqueous benzylamine and benzamide at various temperatures. The value for molar conductivity increases with increasing temperature and decreases with increasing concentration. Onsager equation is then used to determine limiting molar conductance, which increases as we increase the temperature at all concentrations which is due to mobility of ions. Increase in the temperature results in higher frequency and bond breaking due to which translational and vibrational degrees of freedom increases, thus the mobility of ions increases. The values obtained helps in interpreting the ion-solvent interactions. Higher limiting molar conductance, greater the ion-solvent interactions. For

conformation of the results acquired by thermodynamic parameters, FT-IR spectral studies are performed. All vibrations are sensitive, and these vibrations reflect the specific structural characteristics of the system along with the presence of both intra- and intermolecular interactions. The presence of intermolecular interactions is confirmed in the studied ternary system by the change in wavenumber corresponding to the -OH group towards the lower side.

Additionally, for studying electrochemical properties, cyclic voltametric studies are carried out. From the CV data obtained, we can interpret that at higher concentrations, the potential window for ternary system is greater. In both the systems, IL in aqueous benzylamine shows a greater and higher potential window than that of benzamide.

Further, for 1-butyl-1-methyl pyrrolidinium tetrafluoroborate values of density and sound velocity were measured in aqueous solutions of benzylamine with concentration $m_B = (0.01, 0.03 \text{ and } 0.05) \text{ mol.kg}^{-1}$ at temperatures ($T = 288.15 \text{ K to } 318.15 \text{ K}$). The density and sound velocity data values increases with increase in content of IL from $0.001 \text{ mol.kg}^{-1}$ to $0.009 \text{ mol.kg}^{-1}$ while these values decrease as temperature rises. It has been suggested that the positive magnitude of apparent molar volume indicates occurrence of ionic interactions among species present in the system, while the negative magnitude reflects non-ionic interactions. AMV values decrease with increasing concentration of ionic liquid in aqueous solution of benzylamine, while it increases with content of benzylamine. This observation can be revealed that the solute solvent interactions is strengthened with [benzylamine] and weaken with increase in amount of ionic liquid. As we raise the temperature, values of V_ϕ also increases which expose the fact of stronger interactions between solute-solvent molecules at higher temperature. The values obtained for $K_{\phi,s}$ are negative at all concentration and temperatures under consideration and these values become less negative as we increase both the temperature and concentration of the IL. For this system, the negative values of $K_{\phi,s}$ specifies the solvation of solute and solvent molecules which results in stronger affinity among solute-solvent molecules. The decrease of compressibility of the surrounding solvent molecules due to significant electrostrictive pressures causes electrostrictive solvation. S_V^* and S_K^* are the slopes of the graphs, volumetric and sound velocity coefficients which helps in the prediction of solute-solute interactions while V_ϕ and $K_{\phi,s}$ helps in predicting solute-solvent interactions. The positive value of V_ϕ^o at all concentrations and temperature confirms the dominance of ion-hydrophilic interactions over the ion- hydrophobic and hydrophobic-hydrophobic interactions which corroborate the results obtained from apparent molar volume and

apparent molar isentropic compression. The negative S_V^* values do not obey any specific trend. However, their negative values support the system's weak solute-solute interactions. The values of V_ϕ^o as compared to the values of S_V^* also supported the almost nonexistent nature of solute-solute interactions. The values of ΔV_ϕ^o increases with concentration of benzylamine, while decrease with rise in temperature. This confirms the strengthening of ion-ion interactions with concentration. On the other hand, with temperature there is release of water molecule from the loose hydration layer of IL which results in expansion of volume and hence small values of ΔV_ϕ^o . The values of $\Delta K_{\phi,s}^o$ have been found to be positive which becomes higher in magnitude with increase in concentration of benzylamine and temperature. The positive values of $\Delta K_{\phi,s}^o$ indicates the structure making tendency of the solute which further intensifies with increasing concentration because of the decreased electrostriction. However, with rise in temperature the expansion of volume due to release of structured water molecules from the loose hydration layer of ionic liquid make solution compressible and hence higher $\Delta K_{\phi,s}^o$ values. Positive ϕ_E^o determines the prevalence of solute-solvent interactions in the specific system. $(\partial\phi_E^o/\partial T)_p$ determines the ability of solute to behave as structure maker or breaker. In the system under consideration, $(\partial\phi_E^o/\partial T)_p$ values have been found to be positive confirming the structure making tendency which substantiate the results obtained for partial molar isentropic compressibility. For this system the V_{AB} , V_{ABB} are positive and K_{AB} , K_{ABB} are negative. The positive values of V_{AB} show the pairwise interaction between the amine and IL. Because of the overlap, water molecules leave the hydration co-sphere when non-bonding favorable interactions are present and move into the bulk. The values of V_{AB} are significantly greater than the triplet interaction coefficients V_{ABB} , which explains why pair-wise interaction predominates in the mixture of 1-butyl-1-methyl pyrrolidinium tetrafluoroborate and benzylamine.

In addition, Specific conductivity (κ , $\mu S.cm^{-1}$) and molar conductivity (Λ_m , $S.cm^2.mol^{-1}$) were measured at four equidistant temperature (288.15 K to 318.15 K). Molar conductivity increases with increasing concentration and decreases as we raise the temperature. Higher the temperature, higher the frequency resulting in the breakage of bond due to increase in the vibrational and translational degrees of freedom resulting in increases mobilities of the ions and hence higher the magnitude of conductivity. On the other hand, the values of Limiting molar conductance increases as we increase the temperature at all concentrations which is due to the mobility of ions. An

increase in temperature causes bond breakage and higher frequencies, which increase the degrees of freedom for translation and vibration, thus the mobility of ions increases.

SIGNIFICANCE AND SCOPE OF THE STUDY

The field of study of thermophysical and thermodynamic properties is very vast, and a lot of work has already been done and a lot is yet to be explored. The major objective of the study is to enhance the thermal stability and electrochemical stability of the Energy storage devices using the combination of Ionic liquids and amine. Ionic liquids are comparatively “green” as they do not evaporate under the ambient condition. Ionic liquids being green solvent holds great potential from the industrial point of view and also being environment friendly it is the first and foremost priority of today’s innovation. The study also holds great importance for development of new models of Energy Storage Apparatus which will be less toxic and biodegradable using the combined solution of ionic liquids and amine. Where Ionic liquids (ILs) also termed as molten salts are mainly composed of ions and have melting points equal to or below 100° C. On the other hand, Amines are organic compounds. Both of them having great application in the field of energy storage devices.

The energy applications of Ionic liquids have been one of the main research areas for energy storage because of the constant demand of clean and sustainable energy. Due to their unique properties like low volatility, high thermochemical stability, and high conductance, ionic liquids almost meet the needs of the various energy storage appliances. So, for diverse enhancement and improvements in the specific properties of ionic liquids which make them superior of other compounds to be used as electrolytes and electrodes must be explored. One of the main problems faced in case of some batteries now in trend is the explosion. So, this combination of IL and amine has one more advantage regarding this explosion issue. It is very much safe to handle as explosion rates are very low and their flame-retardant nature.

So, while starting our studies on the materials which can be used for Li-ion batteries and are best suited the enforcement was on the material pursuing the properties like the non-volatile nature, low flammability and less toxicity. Considering all these properties the compounds which strikes in our minds were ionic liquids because they fulfil all the demands concerning the safety reasons as well as the stabilities and life cycle of the battery. Applications of ionic liquids as electrolytes in Li-ion batteries seems to utilize their specific set of properties. As ionic liquids have low coordinating properties, so for the Li-sulphur batteries these low coordinating properties are exploited to minimize the dissolution of electroactive material into the electrolytes. It appears that

the absence of electrolyte volatility is a need for Li-oxygen batteries that are exposed to oxygen (air). These two instances utilize specific characteristics of ionic liquids, and other materials don't seem to be as readily adopted. High stability, ionic conductivity, less toxicity and non-volatility has made the ionic liquids not only suitable for energy storage applications but also considered them on third number as the electrolytes (solvents) followed by water and some organic solvents. Properties possessed by the ionic liquids are mainly because of their composition of cations and anions. Vander-Wall forces of attraction, interaction and directionality of the cations and anions are the basic cause of the unique properties of these liquids. On other hand, when it comes to the characteristics of ILs, it is important to keep in mind that not all ILs offer the aforementioned traditional features, which leaves room for the creation of new ILs that are tailored to certain tasks. One of the major factors is to look for a highly improved electrolyte as against the presently used electrolytes having certain limitations. IL based electrolytes are more chemically stable, have useable temperature range, high electrochemical stability window, safety and environmentally friendly as compared to organic electrolytes.

ILs due to their unique properties have the ability to substitute the organic electrolytes in applications where long lifetimes and increased thermal stability are considered as important, such as large-scale stationary storage and in direct combination with renewable energy primary production devices. So basically, one of the greatest importance of our study will be that it will provide a base for a new model of energy storage devices with both high energy and power density, long life cycle and a very less toxic with low rate of explosion. This study will provide a new direction towards a safe approach of energy storage devices by proving the theoretical data for the various and required properties of the ILs for the sustainable and environment friendly energy storage devices.

References

Abbott, A. P., Harris, R. C., & Ryder, K. S. (2007). Application of hole theory to define ionic

- liquids by their transport properties. *Journal of Physical Chemistry B*, 111(18), 4910–4913. <https://doi.org/10.1021/jp0671998>
- Abdullah Aljasmī, Adel S. AlJimaz, Khaled H. A. E. AlKhaldi, and M. S. A. T. (2022). Dependency of Physicochemical Properties of Imidazolium Bis(Trifluoromethylsulfonyl)Imide-Based Ionic Liquids on Temperature and Alkyl Chain. *J. Chem. Eng. Data*, 67(4), 858–868. <https://doi.org/https://doi.org/10.1021/acs.jced.1c00919>
- Albayrak, A. T. (2024). Investigation of the Effect of Temperature on the Physicochemical Properties of NMP-PA Ionic liquid. *JCED*, 69(3), 711–720.
- Aljasmī, A., AlJimaz, A. S., AlKhaldi, K. H., AlTuwaim, M. S., Alhasan, M. F., & Alnajjar, A. (2024). Temperature and Alkyl Chain Dependence of Physicochemical Properties of Pyrrolidinium-and Imidazolium-Based Ionic Liquids. *Journal of Solution Chemistry*, 1–23. <https://doi.org/https://doi.org/10.1007/s10953-023-01358-0>
- Amirchand, K. D., Kaur, S., Banipal, T. S., & Singh, V. (2021). Volumetric and ¹H NMR spectroscopic studies of saccharides-calcium lactate interactions in aqueous solutions. *Journal of Molecular Liquids*, 334, 116077. <https://doi.org/10.1016/j.molliq.2021.116077>
- Ando, M., & Kaoru Ohta, Tateki Ishida, Ryohei Kido, and H. S. (2023). Physical Properties and Low-Frequency Polarizability Anisotropy and Dipole Responses of Phosphonium Bis(fluorosulfonyl)amide Ionic Liquids with Pentyl, Ethoxyethyl, or 2-(Ethylthio)ethyl Group. *Journal of Physical Chemistry B*, 127(2), 542–556. <https://doi.org/https://doi.org/10.1021/acs.jpcc.2c07466>
- Anouti, M., Caillon-Caravanier, M., Dridi, Y., Galiano, H., & Lemordant, D. (2008). Synthesis and characterization of new pyrrolidinium based protic ionic liquids. Good and superionic liquids. *Journal of Physical Chemistry B*, 112(42), 13335–13343. <https://doi.org/10.1021/jp805992b>
- Anouti, M., Porion, P., Brigouleix, C., Galiano, H., & Lemordant, D. (2010). Transport properties in two pyrrolidinium-based protic ionic liquids as determined by conductivity, viscosity and NMR self-diffusion measurements. *Fluid Phase Equilibria*, 299(2), 229–237. <https://doi.org/10.1016/j.fluid.2010.09.035>
- Anvari, S., Hajfarajollah, H., Mokhtarani, B., Enayati, M., Sharifi, A., & Mirzaei, M. (2016). Antibacterial and anti-adhesive properties of ionic liquids with various cationic and anionic heads toward pathogenic bacteria. *Journal of Molecular Liquids*, 221, 685–690. <https://doi.org/10.1016/j.molliq.2016.05.093>
- Aricò, A. S., Bruce, P., Scrosati, B., Tarascon, J.-M., & Schalkwijk, W. Van. (2010). *WSPC-MATERIALS FOR SUSTAINABLE ENERGY-Reprint Volume Book-Trim Size:-11 in x 8.5 in Nanostructured materials for advanced energy conversion and storage devices*. 4(May), 148–159. www.nature.com/naturematerials
- Asha, S., Vijayalakshmi, K. P., & George, B. K. (2019a). Electronic structural studies of pyrrolidinium-based ionic liquids for electrochemical application. *International Journal of Quantum Chemistry*, 119 (17), 1–12. <https://doi.org/10.1002/qua.25972>
- Asha, S., Vijayalakshmi, K. P., & George, B. K. (2019b). Pyrrolidinium-based ionic liquids as electrolytes for lithium batteries: A Computational Study. *International Journal of Quantum Chemistry*, 119(22). <https://doi.org/10.1002/qua.26014>
- Augustyn, V., Come, J., Lowe, M. A., Kim, J. W., Taberna, P. L., Tolbert, S. H., Abruña, H. D., Simon, P., & Dunn, B. (2013). High-rate electrochemical energy storage through Li + intercalation pseudocapacitance. *Nature Materials*, 12(6), 518–522. <https://doi.org/10.1038/nmat3601>
- Austen Angell, C., Ansari, Y., & Zhao, Z. (2012). Ionic Liquids: Past, present and future. *Faraday*

- Discussions*, 154(1), 9–27. <https://doi.org/10.1039/c1fd00112d>
- Bashir, S., Thakur, A., Lgaz, H., Chung, I. M., & Kumar, A. (2020). Corrosion inhibition efficiency of bronopol on aluminium in 0.5 M HCl solution: Insights from experimental and quantum chemical studies. *Surfaces and Interfaces*, 20(May), 100542. <https://doi.org/10.1016/j.surfin.2020.100542>
- Basile, A., Hilder, M., Makhlooghiyazad, F., Pozo-Gonzalo, C., MacFarlane, D. R., Howlett, P. C., & Forsyth, M. (2018). Ionic Liquids and Organic Ionic Plastic Crystals: Advanced Electrolytes for Safer High Performance Sodium Energy Storage Technologies. *Advanced Energy Materials*, 8(17), 1–20. <https://doi.org/10.1002/aenm.201703491>
- Ben Ghanem, O., Mutalib, M. I. A., Léveïque, J. M., Gonfa, G., Kait, C. F., & El-Harbawi, M. (2015). Studies on the Physicochemical Properties of Ionic Liquids Based On 1-Octyl-3-methylimidazolium Amino Acids. *Journal of Chemical and Engineering Data*, 60(6), 1756–1763. <https://doi.org/10.1021/je501162f>
- Bobrova, L. S., Danilov, F. I., & Protsenko, V. S. (2016). Effects of temperature and water content on physicochemical properties of ionic liquids containing $\text{CrCl}_3 \cdot x \text{H}_2\text{O}$ and choline chloride. *Journal of Molecular Liquids*, 223, 48–53. <https://doi.org/10.1016/j.molliq.2016.08.027>
- Borch, R. F. (1969). Nitrilium Salts. A New Method for the Synthesis of Secondary Amines. *Journal of Organic Chemistry*, 34(3), 627–629. <https://doi.org/10.1021/jo01255a031>
- Boruń, A. (2019). Conductance and ionic association of selected imidazolium ionic liquids in various solvents: A review. *Journal of Molecular Liquids*, 276, 214–224. <https://doi.org/10.1016/j.molliq.2018.11.140>
- Bradaric, C. J., Downard, A., Kennedy, C., Robertson, A. J., & Zhou, Y. (2003). Industrial preparation of phosphonium ionic liquids. *Green Chemistry*, 5(2), 143–152. <https://doi.org/10.1039/b209734f>
- Burrell, A. K., Del Sesto, R. E., Baker, S. N., McCleskey, T. M., & Baker, G. A. (2007). The large scale synthesis of pure imidazolium and pyrrolidinium ionic liquids. *Green Chemistry*, 9(5), 449–45. <https://doi.org/10.1039/b615950h>
- Buzzeo, M. C., Klymenko, O. V., Wadhawan, J. D., Hardacre, C., Seddon, K. R., & Compton, R. G. (2003). Voltammetry of oxygen in the room-temperature ionic liquids 1-ethyl-3-methylimidazolium bis((trifluoromethyl)sulfonyl)imide and hexyltriethylammonium bis((trifluoromethyl)sulfonyl)imide: One-electron reduction to form superoxide. Steady-state and transien. *Journal of Physical Chemistry A*, 107(42), 8872–8878. <https://doi.org/10.1021/jp0304834>
- Carla Luzia Borges Reis, Thales Alves Campelo, Cristiane Cunha Frota, Alejandro Pedro Ayala, Lorena Mara Alexandre Silva, Maria Valderez Ponte Rocha, R. S. de S.-A. (2024). Crystallization of isoniazid in choline-based ionic liquids: Physicochemical properties and anti-tuberculosis activity. *Journal of Molecular Liquids*, 394, 123671. <https://doi.org/https://doi.org/10.1016/j.molliq.2023.123671>
- Chaban, V. (2016). Halogenation Thermodynamics of Pyrrolidinium-Based Ionic Liquids. *Journal of Chemical and Engineering Data*, 61(1), 228–233. <https://doi.org/10.1021/acs.jced.5b00505>
- Chakrabarti, M. H., Mjalli, F. S., Alnashef, I. M., Hashim, M. A., Hussain, M. A., Bahadori, L., & Low, C. T. J. (2014). Prospects of applying ionic liquids and deep eutectic solvents for renewable energy storage by means of redox flow batteries. *Renewable and Sustainable Energy Reviews*, 30, 254–270. <https://doi.org/10.1016/j.rser.2013.10.004>
- Chakraborty, N., Kaur, K., Juglan, K. C., & Kumar, H. (2019). Volumetric and Ultrasonic Studies

- on Interactions of Glycols in Aqueous Solutions of Xylitol at Different Temperatures. *Journal of Chemical and Engineering Data*, 65(4), 1435–1446. <https://doi.org/10.1021/acs.jced.9b00869>
- Chau, C. F., Wu, S. H., & Yen, G. C. (2007). The development of regulations for food nanotechnology. *Trends in Food Science and Technology*, 18(5), 269–280. <https://doi.org/10.1016/j.tifs.2007.01.007>
- Che, G., Lakshmi, B. B., Fisher, E. R., & Martin, C. R. (1998). Carbon nanotubule membranes for electrochemical energy storage and production. *Nature*, 393(6683), 346–349. <https://doi.org/10.1038/30694>
- Chen, T., Liu, C., Mu, P., Sun, H., Zhu, Z., Liang, W., & Li, A. (2020). Fatty amines/graphene sponge form-stable phase change material composites with exceptionally high loading rates and energy density for thermal energy storage. *Chemical Engineering Journal*, 382(July 2019). <https://doi.org/10.1016/j.cej.2019.122831>
- Chennuri, B. K., Losetty, V., & Gardas, R. L. (2015). Apparent molar properties of hydroxyethyl ammonium based ionic liquids with water and ethanol at various temperatures. *Journal of Molecular Liquids*, 212, 444–450. <https://doi.org/10.1016/j.molliq.2015.09.050>
- Chhotaray, P. K., Jella, S., & Gardas, R. L. (2014). Physicochemical properties of low viscous lactam based ionic liquids. *Journal of Chemical Thermodynamics*, 74, 255–262. <https://doi.org/10.1016/j.jct.2014.02.009>
- Cho, S. D., Im, J. K., Kim, H. K., Kim, H. S., & Park, H. S. (2012). Functionalization of reduced graphene oxides by redox-active ionic liquids for energy storage. *Chemical Communications*, 48(51), 6381–6383. <https://doi.org/10.1039/c2cc31636f>
- Costa, S. P. F., Azevedo, A. M. O., Pinto, P. C. A. G., & Saraiva, M. L. M. F. S. (2017). Environmental Impact of Ionic Liquids: Recent Advances in (Eco)toxicology and (Bio)degradability. *ChemSusChem*, 10(11), 2321–2347. <https://doi.org/10.1002/cssc.201700261>
- Cui, L., Yu, K., Lv, J., Guo, C., & Zhou, B. (2020). A 3D POMOF based on a {AsW₁₂} cluster and a Ag-MOF with interpenetrating channels for large-capacity aqueous asymmetric supercapacitors and highly selective biosensors for the detection of hydrogen peroxide. *Journal of Materials Chemistry A*, 8(43), 22918–22928. <https://doi.org/10.1039/d0ta08759a>
- Deetlefs, M., Seddon, K. R., & Shara, M. (2006). Predicting physical properties of ionic liquids. *Physical Chemistry Chemical Physics*, 8(5), 642–649. <https://doi.org/10.1039/b513453f>
- Doherty, A. P. (2018). Redox-active ionic liquids for energy harvesting and storage applications. *Current Opinion in Electrochemistry*, 7, 61–65. <https://doi.org/10.1016/j.coelec.2017.10.009>
- Dong, K., Liu, X., Dong, H., Zhang, X., & Zhang, S. (2017). Multiscale Studies on Ionic Liquids. *Chemical Reviews*, 117(10), 6636–6695. <https://doi.org/10.1021/acs.chemrev.6b00776>
- Dubois, D. L. (2014). Development of molecular electrocatalysts for energy storage. *Inorganic Chemistry*, 53(8), 3935–3960. <https://doi.org/10.1021/ic4026969>
- Dukhin, A. S., & Goetz, P. J. (1996). Acoustic spectroscopy for concentrated polydisperse colloids with high density contrast. *Langmuir*, 12(21), 4987–4997. <https://doi.org/10.1021/la951085y>
- Dukhin, A. S., Goetz, P. J., & Hamlet, C. W. (1996). Acoustic spectroscopy for concentrated polydisperse colloids with low density contrast. *Langmuir*, 12(21), 4998–5003. <https://doi.org/10.1021/la951572d>
- Earle, M. J., Esperança, J. M. S. S., Gilea, M. A., Lopes, J. N. C., Rebelo, L. P. N., Magee, J. W., Seddon, K. R., & Widegren, J. A. (2006). The distillation and volatility of ionic liquids. *Nature*, 439(7078), 831–834. <https://doi.org/10.1038/nature04451>
- Eftekhari, A., Liu, Y., & Chen, P. (2016). Different roles of ionic liquids in lithium batteries.

- Journal of Power Sources*, 334, 221–239. <https://doi.org/10.1016/j.jpowsour.2016.10.025>
- Ehsan Kianfar, & Sajjad Mafi. (2020). Ionic Liquids: Properties, Application, and Synthesis. *Fine Chemical Engineering*, 22–31. <https://doi.org/10.37256/fce.212021693>
- Endres, F. (2010). Ionicity in ionic liquids: correlation with ionic structure and physicochemical properties. *Physical Chemistry Chemical Physics*, 12(8), 1648–1648. <https://doi.org/10.1039/c001176m>
- Eriksson, C. G., Bergman, J., Eneroth, P., & Nordström, L. (1984). Formation of imine derivatives between biologically occurring amines and oxo-steroids. *Journal of Steroid Biochemistry*, 21(6), 643–651. [https://doi.org/10.1016/0022-4731\(84\)90025-6](https://doi.org/10.1016/0022-4731(84)90025-6)
- Eshetu, G. G., Armand, M., Scrosati, B., & Passerini, S. (2014). Energy storage materials synthesized from ionic liquids. *Angewandte Chemie - International Edition*, 53(49), 13342–13359. <https://doi.org/10.1002/anie.201405910>
- Fahys, B. R., Herlem, M. P., & Jaume, J. (1994). New electrolytes from concentrated solutions of lithium salts in mixtures of ammonia and amines. *Electrochimica Acta*, 39(16), 2343–2346. [https://doi.org/10.1016/0013-4686\(94\)00211-8](https://doi.org/10.1016/0013-4686(94)00211-8)
- Farhadi, M., & Mohammed, O. (2016). Energy Storage Technologies for High-Power Applications. *IEEE Transactions on Industry Applications*, 52(3), 1953–1962. <https://doi.org/10.1109/TIA.2015.2511096>
- Farres-Antunez, P., Xue, H., & White, A. J. (2018). Thermodynamic analysis and optimisation of a combined liquid air and pumped thermal energy storage cycle. *Journal of Energy Storage*, 18(December 2017), 90–102. <https://doi.org/10.1016/j.est.2018.04.016>
- Faunce, T. A., Lubitz, W., Rutherford, A. W., MacFarlane, D., Moore, G. F., Yang, P., Nocera, D. G., Moore, T. A., Gregory, D. H., Fukuzumi, S., Yoon, K. B., Armstrong, F. A., Wasielewski, M. R., & Styring, S. (2013). Energy and environment policy case for a global project on artificial photosynthesis. *Energy and Environmental Science*, 6(3), 695–698. <https://doi.org/10.1039/c3ee00063j>
- Fekete, A., Malik, A. K., Kumar, A., & Schmitt-Kopplin, P. (2010). Amines in the environment. *Critical Reviews in Analytical Chemistry*, 40(2), 102–121. <https://doi.org/10.1080/10408340903517495>
- Frade, R. F. M., & Afonso, C. A. M. (2010). Impact of ionic liquids in environment and humans: An overview. *Human and Experimental Toxicology*, 29(12), 1038–1054. <https://doi.org/10.1177/09603271110371259>
- Fumino, K., Peppel, T., Geppert-Rybczyńska, M., Zaitsau, D. H., Lehmann, J. K., Verevkin, S. P., Köckerling, M., & Ludwig, R. (2011). The influence of hydrogen bonding on the physical properties of ionic liquids. *Physical Chemistry Chemical Physics*, 13(31), 14064–14075. <https://doi.org/10.1039/c1cp20732f>
- Galán Sánchez, L. M., Espel, J. R., Onink, F., Meindersma, G. W., & De Haan, A. B. (2009). Density, viscosity, and surface tension of synthesis grade imidazolium, pyridinium, and pyrrolidinium based room temperature ionic liquids. *Journal of Chemical and Engineering Data*, 54(10), 2803–2812. <https://doi.org/10.1021/jc800710p>
- Galaon, T., Radulescu, M., David, V., & Medvedovici, A. (2012). Use of an immiscible diluent in ionic liquid / ion pair LC for the assay of an injectable analgesic. *Central European Journal of Chemistry*, 10(4), 1360–1368. <https://doi.org/10.2478/s11532-012-0059-5>
- Galiński, M., Lewandowski, A., & Stepniak, I. (2006). Ionic liquids as electrolytes. *Electrochimica Acta*, 51(26), 5567–5580. <https://doi.org/10.1016/j.electacta.2006.03.016>
- Gao, Y. R., Cao, J. F., Shu, Y., & Wang, J. H. (2021). Research progress of ionic liquids-based gels in energy storage, sensors and antibacterial. *Green Chemical Engineering*, 2(4), 368–

383. <https://doi.org/10.1016/j.gce.2021.07.012>
- Ge, H. H., Zhou, G. D., Liao, Q. Q., Lee, Y. G., & Loo, B. H. (2000). A study of anti-corrosion behavior of octadecylamine-treated iron samples. *Applied Surface Science*, 156(1–4), 39–46. [https://doi.org/10.1016/S0169-4332\(99\)00288-3](https://doi.org/10.1016/S0169-4332(99)00288-3)
- Ghandi, K. (2014). A Review of Ionic Liquids, Their Limits and Applications. *Green and Sustainable Chemistry*, 04(01), 44–53. <https://doi.org/10.4236/gsc.2014.41008>
- Gonçalo A. O. Tiago 1, I. A. S. M. 2, & 2, L. M. D. R. S. M. (2020). *Application of Ionic Liquids in Energy storage devices. November 2010*.
- Govinda, V., Attri, P., Venkatesu, P., & Venkateswarlu, P. (2011). Thermophysical properties of dimethylsulfoxide with ionic liquids at various temperatures. *Fluid Phase Equilibria*, 304(1–2), 35–43. <https://doi.org/10.1016/j.fluid.2011.02.010>
- Govinda, V., Attri, P., Venkatesu, P., & Venkateswarlu, P. (2013). Evaluation of thermophysical properties of ionic liquids with polar solvent: A comparable study of two families of ionic liquids with various ions. *Journal of Physical Chemistry B*, 117(41), 12535–12548. <https://doi.org/10.1021/jp403813g>
- Greaves, T. L., Weerawardena, A., Fong, C., Krodziewska, I., & Drummond, C. J. (2006). Protic ionic liquids: Solvents with tunable phase behavior and physicochemical properties. *Journal of Physical Chemistry B*, 110(45), 22479–22487. <https://doi.org/10.1021/jp0634048>
- Gruzdev, M. S., Shmukler, L. E., Kudryakova, N. O., Kolker, A. M., Sergeeva, Y. A., & Safonova, L. P. (2017). Triethanolamine-based protic ionic liquids with various sulfonic acids: Synthesis and properties. *Journal of Molecular Liquids*, 242, 838–844. <https://doi.org/10.1016/j.molliq.2017.07.078>
- Guerfi, A., Dontigny, M., Charest, P., Petitclerc, M., Lagacé, M., Vijh, A., & Zaghib, K. (2010). Improved electrolytes for Li-ion batteries: Mixtures of ionic liquid and organic electrolyte with enhanced safety and electrochemical performance. *Journal of Power Sources*, 195(3), 845–852. <https://doi.org/10.1016/j.jpowsour.2009.08.056>
- Guo, X., Zhang, L., Ding, Y., Goodenough, J. B., & Yu, G. (2019). Room-temperature liquid metal and alloy systems for energy storage applications. *Energy and Environmental Science*, 12(9), 2605–2619. <https://doi.org/10.1039/c9ee01707k>
- Haddad, B., Brandán, S. A., Assenine, M. A., Paolone, A., Villemin, D., & Bresson, S. (2020). Bidentate cation-anion coordination in the ionic liquid 1-ethyl-3-methylimidazolium hexafluorophosphate supported by vibrational spectra and NBO, AIM and SQMFF calculations. *Journal of Molecular Structure*, 1212, 1–14. <https://doi.org/10.1016/j.molstruc.2020.128104>
- Hall, P. J., & Bain, E. J. (2008). Energy-storage technologies and electricity generation. *Energy Policy*, 36(12), 4352–4355. <https://doi.org/10.1016/j.enpol.2008.09.037>
- Hallett, J. P., & Welton, T. (2011). Room-temperature ionic liquids: Solvents for synthesis and catalysis. 2. *Chemical Reviews*, 111(5), 3508–3576. <https://doi.org/10.1021/cr1003248>
- Hamdy, L. B., Goel, C., Rudd, J. A., Barron, A. R., & Andreoli, E. (2021). The application of amine-based materials for carbon capture and utilisation: An overarching view. *Materials Advances*, 2(18), 5843–5880. <https://doi.org/10.1039/d1ma00360g>
- Mohamed. H, A. Benhammou, Rezk. H, Messaoud. H ,Othmane. A and Saad.M. A (2023). Enhancing hybrid energy storage systems with advanced low-pass filtration and frequency decoupling for optimal power allocation and reliability of cluster of DC-microgrids. *Energy*, 282(1), 128310. <https://doi.org/https://doi.org/10.1016/j.energy.2023.128310>
- Hartmann, D. O., & Pereira, C. S. (2016). Toxicity of Ionic Liquids: Past, Present, and Future. In *Ionic Liquids in Lipid Processing and Analysis: Opportunities and Challenges*. AOCS Press.

- <https://doi.org/10.1016/B978-1-63067-047-4.00013-1>
- Hasnain, S. M. (1998a). Review on sustainable thermal energy storage technologies, part I: Heat storage materials and techniques. *Energy Conversion and Management*, 39(11), 1127–1138.
- Hasnain, S. M. (1998b). Review on sustainable thermal energy storage technologies, part II: Cool thermal storage. *Energy Conversion and Management*, 39(11), 1139–1153. [https://doi.org/10.1016/S0196-8904\(98\)00024-7](https://doi.org/10.1016/S0196-8904(98)00024-7)
- Hepler, L. G. (1969). Thermal expansion and structure in water and aqueous solutions. *Canadian Journal of Chemistry*, 47(24), 4613–4617. <https://doi.org/10.1139/v69-762>
- Hernández, G., Işık, M., Mantione, D., Pendashteh, A., Navalpotro, P., Shanmukaraj, D., Marcilla, R., & Mecerreyes, D. (2017). Redox-active poly(ionic liquid)s as active materials for energy storage applications. *Journal of Materials Chemistry A*, 5(31), 16231–16240. <https://doi.org/10.1039/c6ta10056b>
- Holbrey, J. D., & Rogers, R. D. (2002). *Holbrey2002*. 446–458.
- Ibrahim, H., Ilinca, A., & Perron, J. (2008). Energy storage systems-Characteristics and comparisons. *Renewable and Sustainable Energy Reviews*, 12(5), 1221–1250. <https://doi.org/10.1016/j.rser.2007.01.023>
- Igor Baskin, Alon Epshtein, Y. E.-E. (2022). Benchmarking machine learning methods for modeling physical properties of ionic liquids,. *Journal of Molecular Liquids*, 351, 118616. <https://doi.org/https://doi.org/10.1016/j.molliq.2022.118616>.
- Javed, F., Ullah, F., Zakaria, M. R., & Akil, H. M. (2018). An approach to classification and hi-tech applications of room-temperature ionic liquids (RTILs): A review. *Journal of Molecular Liquids*, 271, 403–420. <https://doi.org/10.1016/j.molliq.2018.09.005>
- Jenkins, H. D. B. (2011). Ionic liquids-an overview. *Science Progress*, 94(3), 265–297. <https://doi.org/10.3184/003685011X13138407794135>
- Zhang. J., Cao.X., Jiao. R., Luo.W., Ma.Y., Chen.Y., Jiyan Li, Sun.H., and A. L. (2023). Multishell Copper Oxide Hollow Spheres Incorporated with Fatty Amines for High Light-To-Thermal Conversion. *Langmuir*, 39(50), 18621–18630. <https://doi.org/https://doi.org/10.1021/acs.langmuir.3c03009>
- Jin, H., O'Hare, B., Dong, J., Arzhantsev, S., Baker, G. A., Wishart, J. F., Benesi, A. J., & Maroncelli, M. (2008). Physical properties of ionic liquids consisting of the 1-butyl-3-methylimidazolium cation with various anions and the bis(trifluoromethylsulfonyl)imide anion with various cations. *Journal of Physical Chemistry B*, 112(1), 81–92. <https://doi.org/10.1021/jp076462h>
- Ávila. J., Martín. D.J., Santos M.S., Zhang. Y., Hua Li, Pádua. A.,and Martin. C. G. (2023). Effect of ion structure on the physicochemical properties and gas absorption of surface active ionic liquidso Title. *Physical Chemistry Chemical Physics*, 25(9), 6808–6816. <https://doi.org/https://doi.org/10.1039/D2CP05145A>
- Johansson, P., Fast, L. E., Matic, A., Appetecchi, G. B., & Passerini, S. (2010). The conductivity of pyrrolidinium and sulfonylimide-based ionic liquids: A combined experimental and computational study. *Journal of Power Sources*, 195(7), 2074–2076. <https://doi.org/10.1016/j.jpowsour.2009.10.029>
- Jónsson, E. (2020a). Ionic liquids as electrolytes for energy storage applications – A modelling perspective. *Energy Storage Materials*, 25(August 2019), 827–835. <https://doi.org/10.1016/j.ensm.2019.08.030>
- Jónsson, E. (2020b). Ionic liquids as electrolytes for energy storage applications – A modelling perspective. *Energy Storage Materials*, 25, 827–835. <https://doi.org/10.1016/j.ensm.2019.08.030>

- Juglan, K. C., Kumar, H., & Chakraborty, N. (2020). Study of thermodynamic and acoustic properties of niacin in aqueous hexylene glycol and propylene glycol at different temperatures. *ACS Omega*, 5(50), 32357–32365. <https://doi.org/10.1021/acsomega.0c04292>
- Yang, J., Shao, P., Zhao, X., Liao, Y. (2023). *Quinone-amine polymer nanospheres with enhanced redox activity for aqueous proton storage*. 650(2), 1811–1820. <https://doi.org/https://doi.org/10.1016/j.jcis.2023.07.106>
- Kaiqi Jiang, Hanming Liu, K. L. (2023). Amine-based thermal energy storage system towards industrial application. *Energy Conversion and Management*, 283, 116954. <https://doi.org/https://doi.org/10.1016/j.enconman.2023.116954>
- Kar, M., Tutusaus, O., MacFarlane, D. R., & Mohtadi, R. (2019). Novel and versatile room temperature ionic liquids for energy storage. *Energy and Environmental Science*, 12(2), 566–571. <https://doi.org/10.1039/c8ee02437e>
- Karu, K., Ruzanov, A., Ers, H., Ivaništšev, V., Lage-Estebanez, I., & de la Vega, J. M. G. (2016). Predictions of physicochemical properties of ionic liquids with DFT. *Computation*, 4(3), 1–14. <https://doi.org/10.3390/computation4030025>
- Karuppasamy, K., Theerthagiri, J., Vikraman, D., Yim, C. J., Hussain, S., Sharma, R., Maiyalagan, T., Qin, J., & Kim, H. S. (2020). Ionic liquid-based electrolytes for energy storage devices: A brief review on their limits and applications. *Polymers*, 12(4), 1–36. <https://doi.org/10.3390/POLYM12040918>
- Karuppasamy, K., Vikraman, D., Hwang, I. T., Kim, H. J., Nicholson, A., Bose, R., & Kim, H. S. (2020). Nonaqueous liquid electrolytes based on novel 1-ethyl-3-methylimidazolium bis (nonafluorobutane-1-sulfonyl imidate) ionic liquid for energy storage devices. *Journal of Materials Research and Technology*, 9(2), 1251–1260. <https://doi.org/10.1016/j.jmrt.2019.11.052>
- Kateryna, Y., Konieczna, K., Marcinkowski, L., and Kumar, A. (2020). Ionic liquids in the microextraction techniques: The influence of ILs structure and properties,. *TrAC Trends in Analytical Chemistry*, 130, 115994. <https://doi.org/https://doi.org/10.1016/j.trac.2020.115994>.
- Kaur, H., Thakur, R. C., & Kumar, H. (2020). Effect of proteinogenic amino acids L-serine/L-threonine on volumetric and acoustic behavior of aqueous 1-butyl-3-propyl imidazolium bromide at T = (288.15, 298.15, 308.15, 318.15) K. *Journal of Chemical Thermodynamics*, 150, 106211. <https://doi.org/10.1016/j.jct.2020.106211>
- Kaur, H., Thakur, R. C., Kumar, H., & Katal, A. (2021). Effect of α -amino acids (glycine, L-alanine, L-valine and L-leucine) on volumetric and acoustic properties of aqueous 1-Butyl-3-propylimidazolium bromide at T = (288.15, 298.15, 308.15, 318.15) K. *Journal of Chemical Thermodynamics*, 158, 106433. <https://doi.org/10.1016/j.jct.2021.106433>
- Kaur, K., Behal, I., Juglan, K. C., & Kumar, H. (2018). Volumetric and ultrasonic studies on interactions of ethylene glycol, diethylene glycol and triethylene glycol in aqueous solutions of glycerol at temperatures T=(293.15 K – 308.15) K. *Journal of Chemical Thermodynamics*, 125, 93–106. <https://doi.org/10.1016/j.jct.2018.05.016>
- Kaur, K., Juglan, K. C., & Kumar, H. (2017). Investigation on Temperature-Dependent Volumetric and Acoustical Properties of Homologous Series of Glycols in Aqueous Sorbitol Solutions. *Journal of Chemical and Engineering Data*, 62(11), 3769–3782. <https://doi.org/10.1021/acs.jced.7b00501>
- Kaur, P., Chakraborty, N., Kumar, H., Singla, M., & Juglan, K. C. (2022). Volumetric and Ultrasonic Studies on Interactions of Hexylene and Propylene Glycols in Aqueous Solutions of Glutaraldehyde at Different Temperatures. *Journal of Solution Chemistry*, 51(10), 1268–

1291. <https://doi.org/10.1007/s10953-022-01192-w>
- Kennedy, E. N. (2009). *A Comparison Of Physical And Electrochemical Properties Of Two Ionic Liquids Containing Different Cations: 1-Butyl-1-Methyl-Pyrrolidinium Beti And 1-Butyl-3-Methyl-Imidazolium Beti*. https://etd.ohiolink.edu/ap/10?0::NO:10:P10_ACCESSION_NUM:wright1253294969#abstract-files
- Khupse, N. D., & Kumar, A. (2010). Ionic liquids: New materials with wide applications. *Indian Journal of Chemistry - Section A Inorganic, Physical, Theoretical and Analytical Chemistry*, 49(5–6), 635–648.
- Kim, E., Han, J., Ryu, S., Choi, Y., & Yoo, J. (2021). Ionic liquid electrolytes for electrochemical energy storage devices. *Materials*, 14(14). <https://doi.org/10.3390/ma14144000>
- Kono, M. (1978). Reliability of palaeointensity methods using alternating field demagnetization and anhysteretic remanence. *Geophysical Journal of the Royal Astronomical Society*, 54(2), 241–261. <https://doi.org/10.1111/j.1365-246X.1978.tb04258.x>
- Kumar, A., Rani, R., Gupta, A., Saini, B., & Bamezai, R. K. (2016). Volumetric and compressibility studies for (L-arginine + D-maltose monohydrate + water) system in the temperature range of (298.15 to 308.15) K. *Physics and Chemistry of Liquids*, 54(5), 602–614. <https://doi.org/10.1080/00319104.2016.1139709>
- Kumar Bhardwaj, R., & Pal, A. (2005). Spectroscopic studies of binary liquid mixtures of alkoxyethanols with substituted and cyclic amides at 298.15 K. *Journal of Molecular Liquids*, 118(1–3), 37–39. <https://doi.org/10.1016/j.molliq.2004.07.007>
- Kumar, H., & Behal, I. (2016). Volumetric, ultrasonic and UV absorption studies on interactions of antibiotic drug chloramphenicol with glycine and its dipeptide in aqueous solutions at T = (288.15–318.15) K. *Journal of Chemical Thermodynamics*, 99, 16–29. <https://doi.org/10.1016/j.jct.2016.03.040>
- Kumar, H., & Chadha, C. (2014). Densities, sound speed, and UV absorption studies of trisodium citrate and tripotassium citrate in aqueous solutions of 1-hexyl-3-methylimidazolium chloride [C6mim][Cl]. *Journal of Chemical and Engineering Data*, 59(12), 4049–4061. <https://doi.org/10.1021/je5006906>
- Kumar, H., Chadha, C., Verma, A., & Singla, M. (2017). Synthesis and study of interactions of ionic liquid 1-methyl-3-pentylimidazolium bromide with amino acids at different temperatures. *Journal of Molecular Liquids*, 242, 560–570. <https://doi.org/10.1016/j.molliq.2017.07.042>
- Kumar, H., & Katal, A. (2018). Temperature dependent physicochemical and spectroscopic (FT-IR) studies of citrate salts (trilithium citrate and triammonium citrate) in aqueous ionic liquid [C4mim][BF4] (1-butyl-3-methyl imidazolium tetrafluoroborate) solutions. *Journal of Molecular Liquids*, 256, 148–162. <https://doi.org/10.1016/j.molliq.2018.02.011>
- Kumar, H., Katal, A., & Sharma, P. K. (2019). Temperature-Dependent Thermodynamic Properties of Amino Acids in Aqueous Imidazolium-Based Ionic Liquid. *Journal of Chemical and Engineering Data*, 65(4), 1473–1487. <https://doi.org/10.1021/acs.jced.9b00902>
- Kumar, H., Kumar, V., Sharma, M., & Behal, I. (2018). Studies on the interactions behaviour of polyhydroxy solutes D(+)-glucose and D(–)-fructose in aqueous triammonium citrate solutions over temperature range T = (288.15–318.15) K. *Journal of Chemical Thermodynamics*, 119, 1–12. <https://doi.org/10.1016/j.jct.2017.12.003>
- Kumar, H., Kumari, S., Behal, I., & Sharma, S. K. (2018). Analysing the molecular interactions of sucrose in aqueous triammonium citrate and trilithium citrate solutions at different temperatures T = (288.15–318.15) K through volumetric and ultrasonic investigations.

- Journal of Chemical Thermodynamics*, 125, 17–31. <https://doi.org/10.1016/j.jct.2018.05.004>
- Kumar, H., Sharma, R., Kumar, V., & AlMasoud, N. (2021). Volumetric and acoustic investigation of L-leucine and N-acetyl L-leucine in the aqueous solution of 1-hexyl-3-methylimidazolium bromide [HMIIm] [br] at different temperatures. *Journal of Chemical Thermodynamics*, 158, 106452. <https://doi.org/10.1016/j.jct.2021.106452>
- Kumar, H., Sharma, R., & Singla, M. (2021). Studies on volumetric and acoustic behavior of L-alanine and L-leucine in aqueous 1-dodecyl-3-methylimidazolium bromide ionic liquid solutions at different temperatures. *Journal of Molecular Liquids*, 342, 117022. <https://doi.org/10.1016/j.molliq.2021.117022>
- Kumar, H., Sheetal, & Behal, I. (2017). Study of interactions of D(+)-glucose and D(-)-fructose with trilithium citrate in aqueous medium through volumetric and ultrasonic properties over the temperature range $T = (288.15\text{--}318.15)$ K. *Journal of Chemical Thermodynamics*, 106, 59–70. <https://doi.org/10.1016/j.jct.2016.11.010>
- Kumar, H., Sheetal, Behal, I., & Sharma, S. (2017). Temperature dependence of the volumetric and acoustic behaviour of aqueous mixtures of monosaccharides and trilithium citrate. *Journal of Chemical Thermodynamics*, 113, 52–63. <https://doi.org/10.1016/j.jct.2017.05.032>
- Kumar, H., Sheetal, & Sharma, S. K. (2016). Volumetric and Acoustic Behavior of D(+)-glucose and D(-)-fructose in Aqueous Trisodium Citrate Solutions at Different Temperatures. *Journal of Solution Chemistry*, 45(1), 1–27. <https://doi.org/10.1007/s10953-015-0427-9>
- Kumar, H., Singla, M., & Jindal, R. (2013). Interactions of glycine, L-alanine and L-valine with aqueous solutions of trisodium citrate at different temperatures: A volumetric and acoustic approach. *Journal of Chemical Thermodynamics*, 67, 170–180. <https://doi.org/10.1016/j.jct.2013.08.010>
- Kumar, H., Singla, M., & Jindal, R. (2014). Solvation behavior of some amino acid compounds in aqueous solutions of trilithium citrate at different temperatures. *Journal of Molecular Liquids*, 197, 301–314. <https://doi.org/10.1016/j.molliq.2014.05.016>
- Kumar, H., Verma, A., & Chadha, C. (2017). Synthesis and thermodynamics studies of ionic liquid 1-methyl-3-pentylimidazolium bromide ([C5mim][Br]) with amino acids (L-cysteine and N-acetyl-L-cysteine) at different temperatures. *Journal of Chemical Thermodynamics*, 111, 238–249. <https://doi.org/10.1016/j.jct.2017.03.040>
- Kumari, M., Maurya, J. K., Singh, U. K., Khan, A. B., Ali, M., Singh, P., & Patel, R. (2014). Spectroscopic and docking studies on the interaction between pyrrolidinium based ionic liquid and bovine serum albumin. *Spectrochimica Acta - Part A: Molecular and Biomolecular Spectroscopy*, 124, 349–356. <https://doi.org/10.1016/j.saa.2014.01.012>
- Kuravi, S., Trahan, J., Goswami, D. Y., Rahman, M. M., & Stefanakos, E. K. (2013). Thermal energy storage technologies and systems for concentrating solar power plants. *Progress in Energy and Combustion Science*, 39(4), 285–319. <https://doi.org/10.1016/j.pecs.2013.02.001>
- Kwong, K. V., Meissner, R. E. ., Ahmed, S., & Wendt, C. J. (1991). Application of amines for treating flue gas from coal-fired power plants. *Environmental Progress*, 10(3), 211–215. <https://doi.org/10.1002/ep.670100321>
- Lee, K., Kim, H., & Hong, J. (2012). N-Heterocyclic Carbene Catalyzed Oxidative Macrolactonization: Total Synthesis of (+)-Dactylolide. *Angewandte Chemie*, 124(23), 5833–5836. <https://doi.org/10.1002/ange.201201653>
- Lee, M. J., Hwang, S. M., & Kuo, Y. C. (1993). Densities and Viscosities of Binary Solutions Containing Butylamine, benzylamine, and Water. *Journal of Chemical and Engineering Data*, 38(4), 577–579. <https://doi.org/10.1021/je00012a026>
- Li, F., Jiang, T., Zhai, J., Shen, B., & Zeng, H. (2018). Exploring novel bismuth-based materials

- for energy storage applications. *Journal of Materials Chemistry C*, 6(30), 7975–7981. <https://doi.org/10.1039/c8tc02801j>
- Li, Y., Feng, X., Ren, D., Ouyang, M., Lu, L., & Han, X. (2019). Thermal Runaway Triggered by Plated Lithium on the Anode after Fast Charging. *ACS Applied Materials and Interfaces*, 11(50), 46839–46850. <https://doi.org/10.1021/acsami.9b16589>
- Lierde, A. Van, Meyer, F. De, Berwaer, V., Adams, J. L., & Metcalfla, B. W. (1988). *Jm00402a018*. 15 mL, 1355–1359.
- Liu, C., Li, F., Lai-Peng, M., & Cheng, H. M. (2010). Advanced materials for energy storage. *Advanced Materials*, 22(8), 28–62. <https://doi.org/10.1002/adma.200903328>
- Liu, H., & Yu, H. (2019). Ionic liquids for electrochemical energy storage devices applications. *Journal of Materials Science and Technology*, 35(4), 674–686. <https://doi.org/10.1016/j.jmst.2018.10.007>
- Lu, Y. C., Gasteiger, H. A., Parent, M. C., Chiloyan, V., & Shao-Horn, Y. (2010). The influence of catalysts on discharge and charge voltages of rechargeable Li-oxygen batteries. *Electrochemical and Solid-State Letters*, 13(6), 4–7. <https://doi.org/10.1149/1.3363047>
- Luntz, A. C., & McCloskey, B. D. (2014). Nonaqueous Li-air batteries: A status report. *Chemical Reviews*, 114(23), 11721–11750. <https://doi.org/10.1021/cr500054y>
- Macfarlane, D., & Kar, M. (2017). *CO*. 1–26.
- Macfarlane, D. R., Tachikawa, N., Forsyth, M., Pringle, J. M., Howlett, P. C., Elliott, G. D., Davis, J. H., Watanabe, M., Simon, P., & Angell, C. A. (2014). Energy applications of ionic liquids. *Energy and Environmental Science*, 7(1), 232–250. <https://doi.org/10.1039/c3ee42099j>
- Marsh, K. N., Boxall, J. A., & Lichtenthaler, R. (2004). Room temperature ionic liquids and their mixtures - A review. *Fluid Phase Equilibria*, 219(1), 93–98. <https://doi.org/10.1016/j.fluid.2004.02.003>
- Martins, V. L., & Torresi, R. M. (2018). Ionic liquids in electrochemical energy storage. *Current Opinion in Electrochemistry*, 9, 26–32. <https://doi.org/10.1016/j.coelec.2018.03.005>
- Mashtalir, O., Lukatskaya, M. R., Zhao, M. Q., Barsoum, M. W., & Gogotsi, Y. (2015). Amine-assisted delamination of Nb₂C MXene for li-ion energy storage devices. *Advanced Materials*, 27(23), 3501–3506. <https://doi.org/10.1002/adma.201500604>
- McMillan, W. G., & Mayer, J. E. (1945). The statistical thermodynamics of multicomponent systems. *The Journal of Chemical Physics*, 13(7), 276–305. <https://doi.org/10.1063/1.1724036>
- Miao, L., Song, Z., Zhu, D., Li, L., Gan, L., & Liu, M. (2021). Ionic Liquids for Supercapacitive Energy Storage: A Mini-Review. *Energy and Fuels*, 35(10), 8443–8455. <https://doi.org/10.1021/acs.energyfuels.1c00321>
- Millero, F. J., Surdo, A. Lo, & Shin, C. (1978). The apparent molal volumes and adiabatic compressibilities of aqueous amino acids at 25°C. *Journal of Physical Chemistry*, 82(7), 784–792. <https://doi.org/10.1021/j100496a007>
- Naseem, B., Khan, M., & Jamal, M. A. (2016). Acoustical studies of pharmaceutical excipients in binary solvent mixtures. *Journal of Molecular Liquids*, 220(87), 581–591. <https://doi.org/10.1016/j.molliq.2016.04.091>
- Nasirpour, N., Mohammadpourfard, M., & Zeinali Heris, S. (2020). Ionic liquids: Promising compounds for sustainable chemical processes and applications. *Chemical Engineering Research and Design*, 160, 264–300. <https://doi.org/10.1016/j.cherd.2020.06.006>
- Nazir, H., Batool, M., Bolivar Osorio, F. J., Isaza-Ruiz, M., Xu, X., Vignarooban, K., Phelan, P., Inamuddin, & Kannan, A. M. (2019). Recent developments in phase change materials for energy storage applications: A review. *International Journal of Heat and Mass Transfer*, 129,

- 491–523. <https://doi.org/10.1016/j.ijheatmasstransfer.2018.09.126>
- Neale, A. R., Murphy, S., Goodrich, P., Hardacre, C., & Jacquemin, J. (2017). Thermophysical and Electrochemical Properties of Ethereal Functionalised Cyclic Alkylammonium-based Ionic Liquids as Potential Electrolytes for Electrochemical Applications. *ChemPhysChem*, 18(15), 2040–2057. <https://doi.org/10.1002/cphc.201700246>
- Neale, A. R., Schütter, C., Wilde, P., Goodrich, P., Hardacre, C., Passerini, S., Balducci, A., & Jacquemin, J. (2017). Physical-Chemical Characterization of Binary Mixtures of 1-Butyl-1-methylpyrrolidinium Bis{(trifluoromethyl)sulfonyl}imide and Aliphatic Nitrile Solvents as Potential Electrolytes for Electrochemical Energy Storage Applications. *Journal of Chemical and Engineering Data*, 62(1), 376–390. <https://doi.org/10.1021/acs.jced.6b00718>
- Nicotera, I., Oliviero, C., Henderson, W. A., Appetecchi, G. B., & Passerini, S. (2005). NMR investigation of ionic liquid-LiX mixtures: Pyrrolidinium cations and TFSI anions. *Journal of Physical Chemistry B*, 109(48), 22814–22819. <https://doi.org/10.1021/jp053799f>
- Nidhi, & Kaur, H. (2022). Advancement in field of Energy storage applications by using Ionic Liquids. *Journal of Physics: Conference Series*, 2267(1). <https://doi.org/10.1088/1742-6596/2267/1/012043>
- Nidhi, Thakur, R. C., Kumar, A., Sharma, P. K., Pathania, V., & Garg, A. (2024). Effect of triazolium-based ionic liquid (1, 4-dimethyl-4H-1, 2, 4-triazolium iodide) on volumetric and ultrasonic properties of binary aqueous solutions of benzamide/benzylamine: experimental and computational study. *Physics and Chemistry of Liquids*, 1-19. <https://doi.org/10.1080/00319104.2024.2382143>
- Pal, A., Kumar, H., Maan, R., & Sharma, H. K. (2014). Solute-solvent interactions of alkyl acetoacetates in aqueous {1-butyl-3-methylimidazolium bromide [bmim][Br]} ionic liquid solutions in the temperature interval (288.15–308.15) K. *Thermochimica Acta*, 577, 79–86. <https://doi.org/10.1016/j.tca.2013.12.015>
- Pal, A., Kumar, H., Maan, R., & Sharma, H. K. (2015). Densities and speeds of sound of glycine, l-alanine, and l-valine in aqueous 1-ethyl-3-methylimidazolium chloride solutions at different temperatures. *Journal of Chemical and Engineering Data*, 60(5), 1217–1226. <https://doi.org/10.1021/je500324a>
- Pal, A., & Kumar, S. (2005). Volumetric and ultrasonic studies of some amino acids in binary aqueous solutions of MgCl₂•6H₂O at 298.15 K. *Journal of Molecular Liquids*, 121(2–3), 148–155. <https://doi.org/10.1016/j.molliq.2004.12.003>
- Parveen, G., Bashir, S., Thakur, A., Saha, S. K., Banerjee, P., & Kumar, A. (2019). Experimental and computational studies of imidazolium based ionic liquid 1-methyl- 3-propylimidazolium iodide on mild steel corrosion in acidic solution. *Materials Research Express*, 7(1). <https://doi.org/10.1088/2053-1591/ab5c6a>
- Pathania, V., Sharma, S., Vermani, S. K., Vermani, B. K., & Grover, N. (2020). Ultrasonic Velocity and Isentropic Compressibility Studies of Monoalkylammonium Salts in Binary Mixtures of Acetonitrile and N,N-Dimethylacetamide at Variable Temperature and Atmospheric Pressure. *Journal of Solution Chemistry*, 49(6), 798–813. <https://doi.org/10.1007/s10953-020-00991-3>
- Pathania, V., Sharma, S., Vermani, S. K., Vermani, B. K., & Grover, N. (2021). Physicochemical Study of Solvation Behavior of n-Butylammonium Perchlorate in Binary Mixtures of Acetonitrile and Dimethylsulfoxide at Various Temperatures. *Journal of Solution Chemistry*, 50(9), 1204–1235. <https://doi.org/10.1007/s10953-021-01113-3>
- Pathania, V., Sharma, S., Vermani, S. K., Vermani, B. K., Grover, N., & Kaur, M. (2021). Viscometric Study of n-Hexylammonium and n-Octylammonium perchlorates in Binary

- Non-Aqueous Solvents Probed by a Physicochemical Approach in the Temperature Ranging 298 - 328K at Atmospheric Pressure. *Oriental Journal Of Chemistry*, 37(3), 656–662. <https://doi.org/10.13005/ojc/370319>
- Patil, R. A., Talebi, M., Xu, C., Bhawal, S. S., & Armstrong, D. W. (2016). Synthesis of Thermally Stable Geminal Dicationic Ionic Liquids and Related Ionic Compounds: An Examination of Physicochemical Properties by Structural Modification. *Chemistry of Materials*, 28(12), 4315–4323. <https://doi.org/10.1021/acs.chemmater.6b01247>
- Paul, A., Mandal, P. K., & Samanta, A. (2005). On the optical properties of the imidazolium ionic liquids. *Journal of Physical Chemistry B*, 109(18), 9148–9153. <https://doi.org/10.1021/jp0503967>
- Pereiro, A. B., Legido, J. L., & Rodríguez, A. (2007). Physical properties of ionic liquids based on 1-alkyl-3-methylimidazolium cation and hexafluorophosphate as anion and temperature dependence. *Journal of Chemical Thermodynamics*, 39(8), 1168–1175. <https://doi.org/10.1016/j.jct.2006.12.005>
- Plechko, N. V., & Seddon, K. R. (2008). Applications of ionic liquids in the chemical industry. *Chemical Society Reviews*, 37(1), 123–150. <https://doi.org/10.1039/b006677j>
- Pont, A. L., Marcilla, R., De Meatza, I., Grande, H., & Mecerreyes, D. (2009). Pyrrolidinium-based polymeric ionic liquids as mechanically and electrochemically stable polymer electrolytes. *Journal of Power Sources*, 188(2), 558–563. <https://doi.org/10.1016/j.jpowsour.2008.11.115>
- Poole, C. F., & Atapattu, S. N. (2021). Determination of physicochemical properties of ionic liquids by gas chromatography. *Journal of Chromatography A*, 1644, 461964. <https://doi.org/10.1016/j.chroma.2021.461964>
- Powell, D., & Whittaker-Brooks, L. (2022). Concepts and principles of self-n-doping in perylene diimide chromophores for applications in biochemistry, energy harvesting, energy storage, and catalysis. *Materials Horizons*, 9(8), 2026–2052. <https://doi.org/10.1039/d2mh00279e>
- Prathibha Pillai, A. M. (2020). A comprehensive micro scale study of poly-ionic liquid for application in enhanced oil recovery: Synthesis, characterization and evaluation of physicochemical properties. *Journal of Molecular Liquids*, 302, 112553. <https://doi.org/10.1016/j.molliq.2020.112553>
- Qiao, Z., Wang, Z., Zhang, C., Yuan, S., Zhu, Y., & Wang, J. (2012a). A New Fragment Contribution-Corresponding States Method for Physicochemical Properties Prediction of Ionic Liquids. *AIChE Journal*, 59(4), 215–228. <https://doi.org/10.1002/aic>
- Qiao, Z., Wang, Z., Zhang, C., Yuan, S., Zhu, Y., & Wang, J. (2012b). Group Contribution Methods for the Prediction of Thermophysical and Transport Properties of Ionic Liquids. *AIChE Journal*, 59(4), 215–228. <https://doi.org/10.1002/aic>
- Radousky, H. B., & Liang, H. (2012). Energy harvesting: An integrated view of materials, devices and applications. *Nanotechnology*, 23(50). <https://doi.org/10.1088/0957-4484/23/50/502001>
- Ribeiro, A. P. C., Vieira, S. I. C., França, J. M., Queirós, C. S., Langa, E., Lourenço, M. J. V., Murshed, S. M. S., & Castro, C. A. N. De. (2009). Thermal Properties of Ionic Liquids and Ionanofluids. *Ionic Liquids: Theory, Properties, New Approaches*.
- Riyazuddeen, & Afrin, S. (2012). Effect of nacl and nano3 on the partial molar volumes and partial molar isentropic compressibilities of some amino acids at several different temperatures (298.15–328.15) K. *Journal of Solution Chemistry*, 41(7), 1144–1155. <https://doi.org/10.1007/s10953-012-9860-1>
- Roberts, M. E., Wheeler, D. R., McKenzie, B. B., & Bunker, B. C. (2009). High specific capacitance conducting polymer supercapacitor electrodes based on

- poly(tris(thiophenylphenyl)amine). *Journal of Materials Chemistry*, 19(38), 6977–6979. <https://doi.org/10.1039/b916666a>
- Rocha, M. A. A., Van Den Bruinhorst, A., Schröer, W., Rathke, B., & Kroon, M. C. (2016). Physicochemical properties of fatty acid based ionic liquids. *Journal of Chemical Thermodynamics*, 100, 156–164. <https://doi.org/10.1016/j.jct.2016.04.021>
- Romero, C. M., Estes, M. A., & Trujillo, G. P. (2018). Partial Molar Volumes, Partial Molar Compressibilities, and Viscosities of α,ω -Amino Acids in Water and in Aqueous Solutions of Sodium Chloride over a Temperature Range of 293.2–333.2 K. *Journal of Chemical and Engineering Data*, 63(11), 4012–4019. <https://doi.org/10.1021/acs.jced.8b00236>
- Roy, M. N., Dakua, V. K., & Sinha, B. (2007). Partial molar volumes, viscosity B-coefficients, and adiabatic compressibilities of sodium molybdate in aqueous 1,3-dioxolane mixtures from 303.15 to 323.15 K. *International Journal of Thermophysics*, 28(4), 1275–1284. <https://doi.org/10.1007/s10765-007-0220-0>
- Safa, M., Chamaani, A., Chawla, N., & El-Zahab, B. (2016). Polymeric Ionic Liquid Gel Electrolyte for Room Temperature Lithium Battery Applications. *Electrochimica Acta*, 213, 587–593. <https://doi.org/10.1016/j.electacta.2016.07.118>
- Sagbas, S., & Sahiner, N. (2018). Carbon dots: Preparation, properties, and application. In *Nanocarbon and its Composites: Preparation, Properties and Applications*. Elsevier Ltd. <https://doi.org/10.1016/B978-0-08-102509-3.00022-5>
- Sarkar, J., & Bhattacharyya, S. (2012). Application of graphene and graphene-based materials in clean energy-related devices Minghui. *Archives of Thermodynamics*, 33(4), 23–40. <https://doi.org/10.1002/er>
- Schmidt, O., Hawkes, A., Gambhir, A., & Staffell, I. (2017). The future cost of electrical energy storage based on experience rates. *Nature Energy*, 2(8), 1–8. <https://doi.org/10.1038/NENERGY.2017.110>
- Schon, T. B., McAllister, B. T., Li, P. F., & Seferos, D. S. (2016). The rise of organic electrode materials for energy storage. *Chemical Society Reviews*, 45(22), 6345–6404. <https://doi.org/10.1039/c6cs00173d>
- Seddon, K. R., Stark, A., & Torres, M. J. (2000). Influence of chloride, water, and organic solvents on the physical properties of ionic liquids. *Pure and Applied Chemistry*, 72(12), 2275–2287. <https://doi.org/10.1351/pac200072122275>
- Shah, F. U., Gnezdilov, O. I., Gusain, R., & Filippov, A. (2017). Transport and Association of Ions in Lithium Battery Electrolytes Based on Glycol Ether Mixed with Halogen-Free Orthoborate Ionic Liquid. *Scientific Reports*, 7(1), 1–13. <https://doi.org/10.1038/s41598-017-16597-7>
- Sharma, P. S., Payagala, T., Wanigasekara, E., Wijeratne, A. B., Huang, J., & Armstrong, D. W. (2008). Trigonal Tricationic Ionic Liquids : Molecular Engineering of Trications to Control Physicochemical Properties Simple modification of traditional ionic liquids (ILs) by varying their cations and anions can produce ILs with variable and tunable physicoch. *Communications*, 17, 4182–4184.
- Sharma, S. K., Singh, G., Kumar, H., & Kataria, R. (2016). Solvation behavior of some amino acids in aqueous solutions of non-steroidal anti-inflammatory drug sodium ibuprofen at different temperatures analysed by volumetric and acoustic methods. *Journal of Chemical Thermodynamics*, 98, 214–230. <https://doi.org/10.1016/j.jct.2016.03.016>
- Sharma, S., Singh, M., Sharma, S., Singh, J., Sharma, A. K., & Sharma, M. (2020). Molecular interactions of L-Histidine in aqueous ionic liquid [C4mim][BF4] solution at different temperatures: Volumetric, acoustic and viscometric approach. *Journal of Molecular Liquids*, 303, 112596. <https://doi.org/10.1016/j.molliq.2020.112596>

- Sharma, V., Yañez, O., Alegría-Arcos, M., Kumar, A., Thakur, R. C., & Cantero-López, P. (2020). A physicochemical and conformational study of co-solvent effect on the molecular interactions between similarly charged protein surfactant (BSA-SDBS) system. *Journal of Chemical Thermodynamics*, 142, 106022. <https://doi.org/10.1016/j.jct.2019.106022>
- Shekaari, H., Zafarani-Moattar, M. T., & Mirheydari, S. N. (2015). Density, Viscosity, Speed of Sound, and Refractive Index of a Ternary Solution of Aspirin, 1-Butyl-3-methylimidazolium Bromide, and Acetonitrile at Different Temperatures T = (288.15 to 318.15) K. *Journal of Chemical and Engineering Data*, 60(6), 1572–1583. <https://doi.org/10.1021/je5008372>
- Shekaari, H., Zafarani-Moattar, M. T., Mirheydari, S. N., & Faraji, S. (2019). Thermophysical Properties of 1-Hexyl-3-methylimidazolium Salicylate as an Active Pharmaceutical Ingredient Ionic Liquid (API-IL) in Aqueous Solutions of Glycine and L-Alanine. *Journal of Chemical and Engineering Data*, 64(1), 124–134. <https://doi.org/10.1021/acs.jced.8b00644>
- Shi, Y., Noelle, D. J., Wang, M., Le, A. V., Yoon, H., Zhang, M., Meng, Y. S., & Qiao, Y. (2016). Role of Amines in Thermal-Runaway-Mitigating Lithium-Ion Battery. *ACS Applied Materials and Interfaces*, 8(45), 30956–30963. <https://doi.org/10.1021/acsami.6b10501>
- Shukla, S. K., & Mikkola, J. P. (2020). Use of Ionic Liquids in Protein and DNA Chemistry. *Frontiers in Chemistry*, 8(December), 1–23. <https://doi.org/10.3389/fchem.2020.598662>
- Singh, R., Bhattacharya, B., Gupta, M., Rahul, Khan, Z. H., Tomar, S. K., Singh, V., & Singh, P. K. (2017). Electrical and structural properties of ionic liquid doped polymer gel electrolyte for dual energy storage devices. *International Journal of Hydrogen Energy*, 42(21), 14602–14607. <https://doi.org/10.1016/j.ijhydene.2017.04.126>
- Singh, S., Bahadur, I., Redhi, G. G., Ramjugernath, D., & Ebenso, E. E. (2014). Density and speed of sound measurements of imidazolium-based ionic liquids with acetonitrile at various temperatures. *Journal of Molecular Liquids*, 200(PB), 160–167. <https://doi.org/10.1016/j.molliq.2014.10.017>
- Singh, V., Banipal, P. K., Banipal, T. S., & Gardas, R. L. (2015). Volumetric Properties of Disaccharides in Aqueous Solutions of Benzyltrimethylammonium Acetate as a Function of Temperature. *Journal of Chemical and Engineering Data*, 60(6), 1764–1775. <https://doi.org/10.1021/je501169y>
- Song, Z., & Zhou, H. (2013). Towards sustainable and versatile energy storage devices: An overview of organic electrode materials. *Energy and Environmental Science*, 6(8), 2280–2301. <https://doi.org/10.1039/c3ee40709h>
- Steinmann, W. D. (2017). Thermo-mechanical concepts for bulk energy storage. *Renewable and Sustainable Energy Reviews*, 75(October), 205–219. <https://doi.org/10.1016/j.rser.2016.10.065>
- Stettner, T., & Balducci, A. (2021). Protic ionic liquids in energy storage devices: past, present and future perspective. *Energy Storage Materials*, 40, 402–414. <https://doi.org/10.1016/j.ensm.2021.04.036>
- Stettner, T., Dugas, R., Ponrouch, A., & Balducci, A. (2020). Ionic Liquid-Based Electrolytes for Calcium-Based Energy Storage Systems. *Journal of The Electrochemical Society*, 167(10), 100544. <https://doi.org/10.1149/1945-7111/ab9c89>
- Stettner, T., Gehrke, S., Ray, P., Kirchner, B., & Balducci, A. (2019). Water in Protic Ionic Liquids: Properties and Use of a New Class of Electrolytes for Energy-Storage Devices. *ChemSusChem*, 12(16), 3827–3836. <https://doi.org/10.1002/cssc.201901283>
- Stettner, T., Huang, P., Goktas, M., Adelhelm, P., & Balducci, A. (2018). Mixtures of glyme and aprotic-protic ionic liquids as electrolytes for energy storage devices. *Journal of Chemical Physics*, 148(19). <https://doi.org/10.1063/1.5013117>

- Studies, C. (2022). *Physicochemical and Conductometric Studies of some Triazolium and*.
- Tawalbeh, M., Khan, H. A., Al-Othman, A., Almomani, F., & Ajith, S. (2023). A comprehensive review on the recent advances in materials for thermal energy storage applications. *International Journal of Thermofluids*, 18(March), 100326. <https://doi.org/10.1016/j.ijft.2023.100326>
- Taylor, A. W., Qiu, F., Hu, J., Licence, P., & Walsh, D. A. (2008). Heterogeneous electron transfer kinetics at the ionic liquid/metal interface studied using cyclic voltammetry and scanning electrochemical microscopy. *Journal of Physical Chemistry B*, 112(42), 13292–13299. <https://doi.org/10.1021/jp8024717>
- Thakur, A., Juglan, K. C., Kumar, H., & Kaur, K. (2020). Apparent molar properties of glycols in methanol solutions of propyl 4-hydroxybenzoate (propylparaben) at T = (293.15 to 308.15) K: an acoustic and volumetric approach. *Physics and Chemistry of Liquids*, 58(6), 803–819. <https://doi.org/10.1080/00319104.2019.1660980>
- Thangavel, R., Kannan, A. G., Ponraj, R., Thangavel, V., Kim, D. W., & Lee, Y. S. (2018). High-energy green supercapacitor driven by ionic liquid electrolytes as an ultra-high stable next-generation energy storage device. *Journal of Power Sources*, 383(January), 102–109. <https://doi.org/10.1016/j.jpowsour.2018.02.037>
- Tingting Chen, Tingting Chen, Xiaorong Wu, Y. X. (2022). Effects of the structure on physicochemical properties and CO₂ absorption of hydroxypyridine anion-based protic ionic liquids. *Journal of Molecular Liquids*, 362, 119743. <https://doi.org/https://doi.org/10.1016/j.molliq.2022.119743>.
- Tokuda, H., Hayamizu, K., Ishii, K., Susan, M. A. B. H., & Watanabe, M. (2004). Physicochemical properties and structures of room temperature ionic liquids. 1. Variation of anionic species. *Journal of Physical Chemistry B*, 108(42), 16593–16600. <https://doi.org/10.1021/jp047480r>
- Tokuda, H., Tsuzuki, S., Susan, M. A. B. H., Hayamizu, K., & Watanabe, M. (2006). How ionic are room-temperature ionic liquids? An indicator of the physicochemical properties. *Journal of Physical Chemistry B*, 110(39), 19593–19600. <https://doi.org/10.1021/jp064159v>
- Truong, Q. D., Devaraju, M. K., & Honma, I. (2014). benzylamine-directed growth of olivine-type LiMPO₄ nanoplates by a supercritical ethanol process for lithium-ion batteries. *Journal of Materials Chemistry A*, 2(41), 17400–17407. <https://doi.org/10.1039/c4ta03566f>
- Tsuda, T., Stafford, G. R., & Hussey, C. L. (2017). Review—Electrochemical Surface Finishing and Energy Storage Technology with Room-Temperature Haloaluminate Ionic Liquids and Mixtures. *Journal of The Electrochemical Society*, 164(8), H5007–H5017. <https://doi.org/10.1149/2.0021708jes>
- Tsunashima, K., Sakai, Y., & Matsumiya, M. (2014). Physical and electrochemical properties of phosphonium ionic liquids derived from trimethylphosphine. *Electrochemistry Communications*, 39, 30–33. <https://doi.org/10.1016/j.elecom.2013.12.008>
- Vancov, T., Alston, A. S., Brown, T., & McIntosh, S. (2012). Use of ionic liquids in converting lignocellulosic material to biofuels. *Renewable Energy*, 45, 1–6. <https://doi.org/10.1016/j.renene.2012.02.033>
- Vatamanu, J., Hu, Z., Bedrov, D., Perez, C., & Gogotsi, Y. (2013). Increasing energy storage in electrochemical capacitors with ionic liquid electrolytes and nanostructured carbon electrodes. *Journal of Physical Chemistry Letters*, 4(17), 2829–2837. <https://doi.org/10.1021/jz401472c>
- Vatamanu, J., Vatamanu, M., & Bedrov, D. (2015). Non-Faradaic Energy Storage by Room Temperature Ionic Liquids in Nanoporous Electrodes. *ACS Nano*, 9(6), 5999–6017. <https://doi.org/10.1021/acsnano.5b00945>

- Wang, B., Liu, X., Liu, H., Wu, D., Wang, H., Jiang, J., Wang, X., Hu, P. A., Liu, Y., & Zhu, D. (2003). Controllable preparation of patterns of aligned carbon nanotubes on metals and metal-coated silicon substrates. *Journal of Materials Chemistry*, 13(5), 1124–1126. <https://doi.org/10.1039/b301061a>
- Watanabe, M., Thomas, M. L., Zhang, S., Ueno, K., Yasuda, T., & Dokko, K. (2017). Application of Ionic Liquids to Energy Storage and Conversion Materials and Devices. *Chemical Reviews*, 117(10), 7190–7239. <https://doi.org/10.1021/acs.chemrev.6b00504>
- Wojnarowska, Z., & Paluch, M. (2015). Recent progress on dielectric properties of protic ionic liquids. *Journal of Physics Condensed Matter*, 27(7), 73202. <https://doi.org/10.1088/0953-8984/27/7/073202>
- Wu, W., Bai, Y., Huang, H., Ding, Z., & Deng, L. (2019). Charging and discharging characteristics of absorption thermal energy storage using ionic-liquid-based working fluids. *Energy*, 189, 116126. <https://doi.org/10.1016/j.energy.2019.116126>
- Wu, W., You, T., & Leung, M. (2020). Screening of novel water/ionic liquid working fluids for absorption thermal energy storage in cooling systems. *International Journal of Energy Research*, 44(12), 9367–9381. <https://doi.org/10.1002/er.4939>
- Xiaoyin Cao, Lijuan Yang, Lijuan Yan, Zhaoqi Zhu, Hanxue Sun, Weidong Liang, Jiyan Li, A. L. (2023). ZnO nanorods loading with fatty amine as composite PCMs device for efficient light-to-thermal and electro-to-thermal conversion. *Journal of Colloid and Interface Science*, 629, 307–315. <https://doi.org/https://doi.org/10.1016/j.jcis.2022.09.032>
- Xu, C., Yang, G., Wu, D., Yao, M., Xing, C., Zhang, J., Zhang, H., Li, F., Feng, Y., Qi, S., Zhuo, M., & Ma, J. (2021). Roadmap on Ionic Liquid Electrolytes for Energy Storage Devices. *Chemistry - An Asian Journal*, 16(6), 549–562. <https://doi.org/10.1002/asia.202001414>
- Xue, L., Tucker, T. G., & Angell, C. A. (2015). Ionic Liquid Redox Catholyte for High Energy Efficiency, Low-Cost Energy Storage. *Advanced Energy Materials*, 5(12), 1–8. <https://doi.org/10.1002/aenm.201500271>
- Yahia, M., Mei, S., Mathew, A. P., & Yuan, J. (2019). Linear Main-Chain 1,2,4-Triazolium Poly(ionic liquid)s: Single-Step Synthesis and Stabilization of Cellulose Nanocrystals. *ACS Macro Letters*, 8(10), 1372–1377. <https://doi.org/10.1021/acsmacrolett.9b00542>
- Yan, R., Antonietti, M., & Oschatz, M. (2018). Toward the Experimental Understanding of the Energy Storage Mechanism and Ion Dynamics in Ionic Liquid Based Supercapacitors. *Advanced Energy Materials*, 8(18), 1–12. <https://doi.org/10.1002/aenm.201800026>
- Yang, G., Song, Y., Wang, Q., Zhang, L., & Deng, L. (2020). Review of ionic liquids containing, polymer/inorganic hybrid electrolytes for lithium metal batteries. *Materials and Design*, 190, 108563. <https://doi.org/10.1016/j.matdes.2020.108563>
- Yang, Z., Liu, J., Li, Y., Zhang, G., Xing, G., & Chen, L. (2021). Arylamine-Linked 2D Covalent Organic Frameworks for Efficient Pseudocapacitive Energy Storage. *Angewandte Chemie*, 133(38), 20922–20927. <https://doi.org/10.1002/ange.202108684>
- Yim, T., Hyun, Y. L., Kim, H. J., Mun, J., Kim, S., Oh, S. M., & Young, G. K. (2007). Synthesis and properties of pyrrolidinium and piperidinium bis(trifluoromethanesulfonyl)imide ionic liquids with allyl substituents. *Bulletin of the Korean Chemical Society*, 28(9), 1567–1572. <https://doi.org/10.5012/bkcs.2007.28.9.1567>
- Yimei Tang, Kuan Yang, Siyu Zhao, Qingqing Chen, Lan Qin, and B. Q. (2023). Evaluation of Solubility, Physicochemical Properties, and Cytotoxicity of Naproxen-Based Ionic Liquids. *ACS Omega*, 8(9), 8332–8340. <https://doi.org/https://doi.org/10.1021/acsomega.2c07044>
- Yohannes, A., Li, J., & Yao, S. (2020). Various metal organic frameworks combined with imidazolium, quinolinum and benzothiazolium ionic liquids for removal of three antibiotics

- from water. *Journal of Molecular Liquids*, 318, 114304. <https://doi.org/10.1016/j.molliq.2020.114304>
- Yu, L., & Chen, G. Z. (2019). Ionic liquid-based electrolytes for supercapacitor and supercapattery. *Frontiers in Chemistry*, 7(APR). <https://doi.org/10.3389/fchem.2019.00272>
- Z.I.Takai. (2018a). Ournal of. *Asian Journal of Chemistry*, 30(18), 2424–2430.
- Z.I.Takai. (2018b). Study of Molecular Interactions of Ternary L-Arginine-Water-1-Ethyl-3-Methylimidazolium Chloride Solutions. *Asian Journal of Chemistry*, 30(18), 2424–2430.
- Zhang, E., Fulik, N., Paasch, S., Borchardt, L., Kaskel, S., & Brunner, E. (2019). Ionic liquid - Electrode materials interactions studied by NMR spectroscopy, cyclic voltammetry, and impedance spectroscopy. *Energy Storage Materials*, 19(January), 432–438. <https://doi.org/10.1016/j.ensm.2019.03.015>
- Zhang, Q., Liu, S., Li, Z., Li, J., Chen, Z., Wang, R., Lu, L., & Deng, Y. (2009). Novel cyclic sulfonium-based ionic liquids: Synthesis, characterization, and physicochemical properties. *Chemistry - A European Journal*, 15(3), 765–778. <https://doi.org/10.1002/chem.200800610>
- Zhang, Y., Zhou, G., Lin, K., Zhang, Q., & Di, H. (2007). Application of latent heat thermal energy storage in buildings: State-of-the-art and outlook. *Building and Environment*, 42(6), 2197–2209. <https://doi.org/10.1016/j.buildenv.2006.07.023>
- Zhao, D., Liu, M., Zhang, J., Li, J., & Ren, P. (2013). Synthesis, characterization, and properties of imidazole dicationic ionic liquids and their application in esterification. *Chemical Engineering Journal*, 221, 99–104. <https://doi.org/10.1016/j.cej.2013.01.077>
- Zheng, W., Mohammed, A., Hines, L. G., Xiao, D., Martinez, O. J., Bartsch, R. A., Simon, S. L., Russina, O., Triolo, A., & Quitevis, E. L. (2011). Effect of cation symmetry on the morphology and physicochemical properties of imidazolium ionic liquids. *Journal of Physical Chemistry B*, 115(20), 6572–6584. <https://doi.org/10.1021/jp1115614>
- Zhou, L., & Liu, C. (2009). Enthalpies of transfer of amino acids from water to aqueous solutions of N-methylacetamide and N,N-dimethylacetamide at T = 298.15 K. *Thermochimica Acta*, 482(1–2), 72–74. <https://doi.org/10.1016/j.tca.2008.10.011>
- Zhu, J., Yang, D., Yin, Z., Yan, Q., & Zhang, H. (2014). Graphene and graphene-based materials for energy storage applications. *Small*, 10(17), 3480–3498. <https://doi.org/10.1002/smll.201303202>
- Zu, C. X., & Li, H. (2011). Thermodynamic analysis on energy densities of batteries. *Energy and Environmental Science*, 4(8), 2614–2624. <https://doi.org/10.1039/c0ee00777c>

LIST OF PUBLICATIONS

Research Articles:

1. Paper with Title “Effect of additive (1-butyl-1-methyl pyrrolidinium tetrafluoroborate) on volumetric, acoustic and conductance properties of aqueous solutions of benzylamine at T = (288.15, 298.15, 308.15, 318.15) K.” has been published in *Asian Journal of Chemistry*.
2. Paper with Title “Investigating the physicochemical properties and interactions behavior of lithium perchlorate in ternary solutions of ethaline DES and bio-

additives” has been **Published** in **Journal Biomass Conversion and Biorefinery**. (Co-author)

3. Paper with Title “**Understanding Influence of Triazolium–based Ionic Liquid (1, 4-Dimethyl- 4H-1, 2, 4-triazolium iodide) on the volumetric and ultrasonic properties of binary aqueous solutions of benzamide / benzylamine at four equidistant temperatures**” has been **Published** in **Physics and Chemistry of Liquids**.
4. Paper with Title “**Effect of Pyrrolidinium-based Ionic Liquid (1-butyl-1-methyl pyrrolidinium iodide) on the volumetric, acoustic and electrochemical properties of binary aqueous solutions of benzylamine and benzamide at different equidistant temperatures (288.15 K to 318.15K).**” has been communicated in **Chemistry Africa**.
5. Paper with Title “**Comparative analysis of thermodynamic, volumetric and conductometric studies of 1-butyl-1-methyl pyrrolidinium iodide in aqueous solutions of acetamide at four equidistant temperatures (T= 288.15K to 318.15K)**” is under revision in **Journal of Molecular Structure**.
6. Paper with Title “**Thermodynamic, acoustic, and electrochemical investigation of 1-ethyl-3-methyl imidazolium iodide in binary aqueous solutions of acetamide at different temperatures (T= 288.15K to 318.15K)**” is communicated in **Journal of Chemical Thermodynamics and Thermal Analysis**.

Conference Papers:

7. Conference Paper with title “**Advancement in field of Energy storage applications by using Ionic Liquids**” has been presented in RAFAS and **published** in **Journal of Physics**.
8. Conference Paper with title “**Effect of Temperature on conductance studies of 1,4-Dimethyl-4H-1,2,4- pyrrolidinium iodide in binary aqueous solutions of benzylamine**”

and benzamide.” has been presented orally in ICMET-2021 and is **published** in AIP.

9. Conference Paper with title “**Recent progress in the application of electrochemically rechargeable metal-air batteries: A focus review.**” has been presented orally in ICMET-2021 and is **published** in AIP.

10. Conference Paper with title “**Study of interaction behavior of aliphatic amino acids (glycine and L-alanine) in Choline -based ionic liquid (Cholinium butanoate)**” has been **published** as conference proceeding in AIP (Co-author).

11. Conference Paper with title “**An Overview of hydrogels and their potential applications in drug delivery**” has been **published** as conference proceeding in AIP (Co-author).

Book Chapter:

12. Book chapter with title “**Microbial Carotenoids in nutrition and baby foods**” has been **communicated** in Elsevier Book.

13. Book Chapter with title “**Potential of Ionic Liquids in Green Energy Resources**” has been **published** in “Green Energy Systems”.

14. Book Chapter with title **“3D printed conducting polymers for supercapacitors”** has been **communicated** in “3D Printed Conducting Polymers: Fundamentals, Advances, and challenges.”
15. Book Chapter with title **“Nano delivery Food Systems”** is **In Press** in “Nanotechnology approaches to the advancements of Innovations in food technology”.
16. Book Chapter with title **“Application of fullerene-based materials in fabrication of photovoltaic devices”** for the Book“ Advanced Nanomaterials for Solution-Processed Flexible Optoelectronic Devices: Processing to Applications” has been accepted.
17. Book Chapter with title **“Solution processed advanced materials as hole transporting layer for application in optoelectronic devices”** in “Advanced Nanomaterials for Solution-Processed Flexible Optoelectronic Devices: Processing to Applications” has been accepted.

Conferences attended:

18. **Recent Advances in Fundamental and Applied Sciences" (RAFAS 2021)** held on June 25-26, 2021, organized by School of Chemical Engineering and Physical Sciences, Lovely Faculty of Technology and Sciences, Lovely Professional University, Punjab.
19. **International Conference on Materials for Emerging Technologies (ICMET-21)** held on February 18-19, 2022, organized by Department of Research Impact and Outcome, Division of Research and Development, Lovely Professional University, Punjab.

20. **Recent Advances in Fundamental and Applied Sciences” (RAFAS 2023)** held on March 24-25, 2023, organized by School of Chemical Engineering and Physical Sciences, Lovely Faculty of Technology and Sciences, Lovely Professional University, Punjab.
21. **International Conference on Recent Advances on Green and Sustainable Developments (ICRAGSD-2023)** which will be organized on 6th-8th September 2023 at Akal University, Talwandi Sabo, Bathinda.
22. **National Conference on Environmental Sustainability and Conservation** on 9th February 2024 at Banwari Lal Jindal Suiwala College, Tosham (Bhiwani).
23. **Recent Advances in Fundamental and Applied Sciences” (RAFAS 2024)** held on April 19-20, 2024, organized by School of Chemical Engineering and Physical Sciences, Lovely Faculty of Technology and Sciences, Lovely Professional University, Punjab.

Webinars attended :

24. TEQIP-III sponsored webinar **“BIOENERGY:TRANSITION AND TECHNOLOGY”** held on July 03, 2020.
25. National Webinar series on **Practicing Chemdraw , Origin and Mendeley Tools in Research**, Laxman Singh Mahar Government Post Graduate College, Pithoragarh, August 8 -10, 2020.
26. Awareness Program to Introduce Giloy in Routine Life for The Promotion of Health” held on 26th March 2022, organized under the funded project entitled *“National Campaign on Amrita for Life (Tinospora cordifolia)”* at Lovely Professional University, Punjab.

Workshops attended :

27. Workshop on **Molecular Spectroscopy and Thermal Analysis for Innovation and Industrial Applications**, Lovely Professional University, Phagwara, Punjab, December 5-6, 2020.
28. **Three-day Innovation Ambassador Training Program** organized by MHRD’s Innovation cell, Lovely professional University in January 2020.

29. One day International Level Workshop on **Cyber Security and FPGA: The Future Technology** held on 7 July 2020 organized by Chitkara University Research and Innovation Network (CURIN), Chitkara University, Punjab.
30. Workshop for **Cultivation, Collection, and Preparations of Household Formulations of Giloy** held on 19th March 2022, organized under the funded project entitled “*National Campaign on Amrita for Life (Tinospora cordifolia)*” at Lovely Professional University, Punjab.

Revised Thesis.docx

ORIGINALITY REPORT

5%

SIMILARITY INDEX

3%

INTERNET SOURCES

4%

PUBLICATIONS

1%

STUDENT PAPERS

PRIMARY SOURCES

1

asianpubs.org

Internet Source

2%

2

pubs.aip.org

Internet Source

1%

3

www.researchgate.net

Internet Source

<1%

4

Harpreet Kaur, R.C. Thakur, Harsh Kumar. "Effect of proteinogenic amino acids L-serine/L-threonine on volumetric and acoustic behavior of aqueous 1-butyl-3-propyl imidazolium bromide at T=(288.15, 298.15, 308.15, 318.15)K", The Journal of Chemical Thermodynamics, 2020

Publication

<1%

5

Harpreet Kaur, Ramesh Chand Thakur, Harsh Kumar, Arjuna Katal. "Effect of α -amino acids (glycine, L-alanine, L-valine and L-leucine) on volumetric and acoustic properties of aqueous 1-Butyl-3-propylimidazolium bromide at T=(288.15, 298.15, 308.15, 318.15)

<1%



Effect of triazolium-based ionic liquid (1, 4-dimethyl- 4H-1, 2, 4-triazolium iodide) on volumetric and ultrasonic properties of binary aqueous solutions of benzamide/benzylamine: experimental and computational study

Nidhi^a, Ramesh Chand Thakur^b, Ashish Kumar^c, Praveen Kumar Sharma^a, Vivek Pathania^d and Ankita Garg^d

^aDepartment of Chemistry, Lovely Professional University, Phagwara, Punjab, India; ^bDepartment of Chemistry, Himachal Pradesh University, Shimla, Himachal Pradesh, India; ^cDepartment of Science and Technology, Government of Bihar, NCE, Bihar Engineering University, Patna, India; ^dDepartment of Chemistry, D.A.V. College Chandigarh, Chandigarh, India

ABSTRACT

In the current investigation, effect of triazolium-based ionic liquid 1, 4-Dimethyl- 4 H-1,2,4-triazolium iodide (DMTI) on volumetric and ultrasonic properties of binary aqueous solutions of benzamide/benzylamine is analysed at four equidistant temperatures and atmospheric pressure. Molecular interactions of DMTI in binary aqueous solutions of benzylamine/benzamide are also interpreted using density (ρ) and speed of sound (u) data along with FT-IR measurements. Different volumetric and ultrasonic parameters were also computed by employing the experimental values of density (ρ) and speed of sound (u), and are further used to elucidate various kinds of interactions in the ternary system. Volumetric and acoustic transfer parameters were further used for the computation of interaction coefficients (pair and triplet). To analyse the outcomes of the estimated parameters, spectroscopic and density-functional theory (DFT) investigations have also been carried out.

ARTICLE HISTORY

Received 6 March 2024
Accepted 16 July 2024


KEYWORDS

Apparent molar volume (AMV); benzylamine; benzamide; acoustic parameters; molecular interactions; DFT

1. Introduction

Nowadays, focus of solution chemistry research has been put on a novel family of solvents known as ionic liquids (ILs), which are much safer and eco-friendly as compared to conventional solvents. ILs made of ions belong to one of the most well-known class of solvents in recent research and are termed as ionic melts, liquid salts, fused salts, fluids and greener solvents [1–5]. These are novel and promising materials with a variety of advantageous features such as extremely low vapour pressure, higher ion density, higher thermochemical stability, good ionic conductance, a large electrochemical window, negligible volatility, extremely low melting point, tunable polarity, solvent miscibility and aqua phobic properties, which can be altered by modifying both cations and anions [6,7]. The need for sustainable solvents that can effectively substitute the current conventional solvents, which are harming the environment and creating various health risks. ILs have shown to be potential substitutes and are currently attracting a lot of interest as potentially safe solvents for their use in several applications, which include fuel cells, rechargeable batteries, supercapacitors, dye-sensitive solar cells, as a biocatalyst and green solvents. ILs have also

CONTACT Ramesh Chand Thakur ✉ drthakurchem@gmail.com Department of Chemistry, Himachal Pradesh University, Summer Hill, Shimla, Himachal Pradesh 171005, India; Ashish Kumar ✉ drashishchemlpu@gmail.com Department of Science and Technology, Government of Bihar, NCE, Bihar Engineering University, Patna, India

 Supplemental data for this article can be accessed online at <https://doi.org/10.1080/00319104.2024.2382143>

© 2024 Informa UK Limited, trading as Taylor & Francis Group



Effect of Additive (1-Butyl-1-methyl Pyrrolidinium Tetrafluoroborate) on Volumetric, Acoustic and Conductance Properties of Binary Aqueous Solutions of Benzylamine at T = (288.15, 298.15, 308.15, 318.15) K

NIDHI^{1,*}, RAMESH CHAND THAKUR^{2,*}, ASHISH KUMAR^{3,*}, PRAVEEN KUMAR SHARMA^{1,4} and KULDEEP SINGH^{4,4}

¹Department of Chemistry, Lovely Professional University, Phagwara-144411, India

²Department of Chemistry, Himachal Pradesh University, Summer Hill Shimla-171005, India

³Nalanda College of Engineering, Bihar Engineering University, Department of Science, Technology and Technical Education, Government of Bihar, Patna-803108, India

⁴Department of Chemistry, MCM DAV College, Kangra-176001, India

*Corresponding author: E-mail: drthakurchem@gmail.com; drashishchemlpu@gmail.com

Received: 21 April 2024;

Accepted: 24 May 2024;

Published online: 29 June 2024;

AJC-21682

Effect of additive, 1-butyl-1-methyl pyrrolidinium tetrafluoroborate [BmPyr⁺][BF₄⁻] on the volumetric, acoustic and conductance properties of binary aqueous solution of benzylamine has been analyzed at equidistant temperature range using different techniques. Using density and speed of sound data, volumetric and acoustic parameters like apparent and partial molar volumes (V_ϕ and V_ϕ^0), apparent and partial molar isentropic compressions ($K_{\phi,S}$ and $K_{\phi,S}^0$), partial molar volume of transfer and partial molar isentropic compression of transfer (ΔV_ϕ^0 and $\Delta K_{\phi,S}^0$) have been calculated. Conductance parameters like molar conductance (Λ_m), limiting molar conductance (Λ_m^0) and activation energy are also calculated using conductance data. All these parameters were used to analyze various types of interactions present in the system. Furthermore, density functional theory (DFT) calculations were conducted for comprehensive understanding of structural variations of ion pairs affecting their physical properties. The hydrogen bond formation in the mixture components was examined by using IR spectrum. Both DFT and Hartree-Fock (HF) methods were used to analyze the results. In addition, the DFT/B3LYP-D3 calculations were also carried out to gather data on the molecular geometry, interactions and other molecular characteristics of the ionic liquid under study.

Keywords: 1-Butyl-1-methylpyrrolidinium tetrafluoroborate, Benzylamine, Partial molar volume, Solute-solvent interaction, DFT.

INTRODUCTION

Today's scientific advances are the product of scientists' attempts to find, synthesize or develop new materials that can be the result of the integration, fusion and penetration of several domains. It is a matter of fact that synthesis of new materials such as nanomaterials, gemini surfactants, ionic liquids, etc. are the resultant of such efforts of scientific community. These innovations lead to the investigation of new areas and development axes for the developed fields. Ionic liquids have emerged as a result of this backdrop, offering up new fields for chemical technological improvement. Ionic liquids are known as an emerging form of compounds which gained high surge of attention in 21st century [1]. The discovery of these liquids, which are typically referred as organic salts having characteristics like a wide voltage/electrochemical window, negligible vapour pressure,

good solvation, low inflammability, high thermal stability, liquid state at a wide range of temperatures, high electrochemical stability, great solubility towards organic compounds and high conductivity. The aforesaid distinctiveness has been found to be the most fascinating areas of recent research in case of ionic liquids. Ionic liquids are basically comprised of combinations of nitrogen containing organic cations like pyridinium, imidazolium, ammonium, pyrrolidinium, phosphonium derivatives, sulphonium, alkylammonium and bulky soft anions, such as bis[(trifluoromethyl)sulfonyl]imide, tetrafluoroborate [BF₄⁻], hexafluorophosphate [PF₆⁻] anion and [(CFSO₂)₂N], halide ions and tetrachloroaluminate (AlCl₄⁻) [2,3].

The physico-chemical characteristics of the ionic liquids can be easily modified by modifying the structure of the component ions in a variety of cationic and anionic forms. The right anion-cation combination in ionic liquids can control a variety



Effect of Pyrrolidinium Based Ionic Liquid on Thermo Physical and Electrochemical Properties of Binary Aqueous Solutions of Benzylamine and Benzamide at Different Equidistant Temperatures (288.15 K to 318.15 K)

Nidhi¹ · Ramesh Chand Thakur² · Ashish Kumar³ · Praveen Kumar Sharma¹ · Akshay Sharma² · Renuka Sharma² · Nancy George¹ · Jandeep Singh¹

Received: 9 May 2024 / Accepted: 19 October 2024
© The Tunisian Chemical Society and Springer Nature Switzerland AG 2024

Abstract

Effect of pyrrolidinium-based ionic liquid (IL) (1-butyl-1-methyl pyrrolidinium iodide) on the volumetric, acoustic and electrochemical properties of aqua solutions of benzylamine and benzamide has been analyzed at equidistant temperature range (288.15 K to 318.15 K) using different techniques. Density (ρ) and sound speed (u) for five different molal compositions (0.001 mol kg⁻¹ to 0.009 mol kg⁻¹) of the IL has been measured in binary aqua solutions of benzyl amine and benzamide. Using the measured density and sound velocity data, volumetric and acoustic quantities viz., AMV (apparent molar volume, V_ϕ), PMV (partial molar volumes, V_ϕ^0), standard partial molar volume of transfer (ΔV_ϕ^0), partial molar isentropic compression ($K_{\phi,s}^0$), apparent molar isentropic compression ($K_{\phi,s}$), and partial molar isentropic compression of transfer ($K_{\phi,s}^0$) have been calculated. Transfer parameters were also determined and further used for the computation of pair and triplet interaction coefficients. The ion–solvent interactions have also been analyzed from conductance studies. Cyclic Voltammetry (CV) studies were further performed to investigate the electrochemical properties of the ternary mixtures for exploring their applications in different energy storage devices. The experimental results were also used to predict the structural behavior of the IL in aqueous benzylamine/benzamide solutions. Additionally, FTIR (Fourier Transformation Infrared Spectroscopy) and DFT (Density Functional Theory) techniques using (B3LYP)/6-311G++ (d, p) basis set of hybrid density functional theory was applied to the optimized geometrical structure of the ionic liquid using the Gaussian 09 program.

Keywords Ionic liquid (IL) · 1-Butyl-1-methyl pyrrolidinium iodide [BMPyr⁺] [I] · Benzylamine · Benzamide · Volumetric properties · Acoustic properties

1 Introduction

In conformity with the green chemistry ideology, the design, development, optimization, and manufacturing of state-of-the-art technologies has become significant in the present scenario [1]. The idea of ionic liquids (ILs) was first coined by Paul Walden in 1914 which was in the form of molten salt at room temperature. Ethyl ammonium nitrate [EtNH₃] [NO₃], the first reported ionic liquid, was obtained by removing water through distillation from the mixture of concentrated nitric acid and ethylamine to obtain pure salt [2]. These are molten salts which are made up of ions, mainly a weakly coordinated inorganic/organic anion and a large asymmetric organic cation [3, 4]. Hexafluorophosphate, tetrafluoroborate, halide,

✉ Ramesh Chand Thakur
drthakurchem@gmail.com

✉ Ashish Kumar
drashishchemlpu@gmail.com

¹ Department of Chemistry, Lovely Professional University, Phagwara 144411, Punjab, India

² Department of Chemistry, Himachal Pradesh University, Summer Hill, Shimla 171005, Himachal Pradesh, India

³ NCE, Department of Science and Technology, Government of Bihar, Patna, India



Investigating the physicochemical properties and interactions behavior of lithium perchlorate in ternary solutions of ethaline DES and bio-additives

Akshay Sharma¹ · Renuka Sharma¹ · Ramesh Thakur¹ · Nidhi²

Received: 6 April 2024 / Revised: 17 May 2024 / Accepted: 24 May 2024
© The Author(s), under exclusive licence to Springer-Verlag GmbH Germany, part of Springer Nature 2024

Abstract

Deep eutectic solvents (DES) are becoming popular in energy storage applications, especially as electrolytes because of their favorable properties like low toxicity, great biodegradability, high thermal stability, and availability. To design, optimize, and develop new lithium-ion battery electrolytes, it is important to understand the physicochemical properties and molecular interactions of these green solvents. In this respect, the density (ρ) and sound speed (u) at four distinct temperatures were measured and at different concentrations of lithium perchlorate (LiClO_4) solutions of the ethaline DESs along with dextrose and L-tyrosine as additives. In the whole concentration range, using density and speed of sound, physical parameters like apparent and partial molar volumes (V_ϕ and V_ϕ^0), apparent and partial molar isentropic compressions ($K_{\phi,S}$ and $K_{\phi,S}^0$), and limiting molar expansibilities (ϕ_E^0) were calculated and results indicate that solvent-solvent interactions are dominant over solute-solute interactions with the rise in temperature and potentially enhancing ion solvation. Also, Hepler's constant and other metrics demonstrate the structure breaker behavior of the studied systems. Cyclic voltammetry (CV) studies were also conducted to predict the electrochemical working stability of the studied systems. FTIR studies were also done to further analyze the interactions.

Keywords Deep eutectic solvent (DES) · Partial molar volume · Electrochemical window · Solute-solvent interaction

1 Introduction

The escalating energy demands of the ever-growing global population, coupled with concerns surrounding fossil fuel depletion and the consequences of global warming, necessitate collaborative endeavors aimed at creating techniques

for storing electrical energy that are environment-friendly [1–3]. One promising avenue for large-scale energy storage is hydrogen (H_2). H_2 offers a clean energy carrier with a high energy density by weight. However, efficient and safe storage of hydrogen remains a significant challenge. Several materials are being explored for hydrogen storage, including lithium-nitrogen-hydrogen (Li-N-H) systems [4], lithium borohydrides (LiBH_x) [5], and metal tetrahydrides (TMH_4) [6]. Understanding the structural stability, hydrogen storage capacity, and electronic properties of these materials is critical for their development [7–10]. Currently, lithium-ion batteries stand as the forefront storage devices, but they grapple with various challenges, including issues related to the availability and toxicity of active materials, elevated materials costs, brief life cycles, and concerns about electrolyte safety at high current rates [11]. Addressing the latter predicament mandates the substitution of hazardous and volatile organic solvents [12] with materials that are safer, more economical, and sustainable. While extensive research has been dedicated to ionic liquids (ILs) as alternative electrolyte media [13–15], deep eutectic solvents (DESs) are emerging as

Highlights

- Thermophysical study of lithium perchlorate ethaline DES, and the additives.
- Dominance of solute-solvent interactions among the additives and DES.
- LiClO_4 act as structure breaker in both the additives.
- FT-IR, CV studies to validate structural and electrochemical properties respectively.

✉ Ramesh Thakur
drthakurchem@gmail.com

¹ Department of Chemistry, Himachal Pradesh University, Summer Hill, Shimla 171005, Himachal Pradesh, India

² Department of Chemistry, Lovely Professional University, Phagwara 144411, Punjab, India

Effect of Temperature on Conductance Studies of 1,4-Dimethyl-4H-1,2,4-Triazolium Iodide in Binary Aqueous Solutions of Benzylamine and Benzamide

Nidhi¹, Harpreet Kaur¹, Ramesh Chand Thakur^{2,a)}, Ashish Kumar^{1,b)}

¹ Department of Chemistry, Lovely Professional University, Phagwara, 144411, Punjab, India.

² Department of Chemistry, Himachal Pradesh University, Summer Hill Shimla, 171005, Himachal Pradesh, India

Corresponding author: ^{a)}drthakurchem@gmail.com

^{b)}drashishchempu@gmail.com

Abstract. The Present study reports a conductometric investigation of 1,4-Dimethyl-4H-1,2,4-triazolium iodide in binary aqueous solutions of benzylamine and benzamide respectively. Effect of temperature is also analyzed for different ternary systems (1,4-dimethyl-4H-1,2,4-triazolium iodide + water + benzylamine) and (1,4-dimethyl-4H-1,2,4-triazolium iodide + water + benzamide) at various concentrations. Conductance parameters like molar conductance (Λ_m), limiting molar conductance (Λ_m^∞), and activation energy have also been calculated using the conductance data. From the parameters calculated, the existence of ion-solvent and ion-ion interactions in the considered systems have also been examined.

Keywords: Conductance, limiting Molar Conductance (LMC), 1,4-dimethyl-4H-1,2,4-triazolium iodide, benzamide.

INTRODUCTION

Ionic Liquids (ILs) are acknowledged with great attention because of the specific set of characteristics. Basically these are defined as molten salts with a wide degree of variations and lower M.P (<100°C) [1]. They possess specific characteristics providing them their tunable character making them suitable specially for energy storage devices. The composition of different cations and anions led to different types including high thermal stability, chemical stability, ionic conductivity, non-flammability, negligible vapor pressure [2]. IL's are comprised of cations (organic) such as ammonium, imidazolium, sulfonium, pyrrolidinium, and pyridinium [3-9], joined by organic or inorganic anions like tetrafluoroborate, dicyanamide, bis(fluorosulfonyl) imide, and hexafluorophosphate [10-13]. Different types of Ionic Liquid formed are triazolium based-Ionic Liquid, pyrrolidinium based-Ionic Liquid, piperdinium based-Ionic Liquid, imidazolium based-Ionic Liquid, ammonium based-Ionic Liquid and sulfonium based-Ionic Liquid [14-15].

Triazolium based-IL have shown great applications in many fields including synthesis of solvents, capillary electrophoresis and energy storage devices due to their versatile nature with extremely low vapour pressure, non flammability, high thermal potential and chemical stability. IL also possess great properties as antimicrobial and antifungal substances [16-17]. Also these are proven to be useful because of their anti-corrosion behavior [18-22]. Benzamide and Benzylamine have a great purpose in purification, production of amino acids, drug industries and also considered as a great purpose in energy storage applications [23-25].

Physicochemical properties of the ternary system Benzylamine + 1,4-dimethyl- 4H-1,2,4-triazolium iodide + water and Benzamide + 1,4-dimethyl- 4H-1,2,4-triazolium iodide + water explains the structure of the solutions and different interactions occurring in the solutions. Conductance studies also entails the information regarding interactions like proton solvent, ion-solvent, proton anion interactions and the structure of the solvent.

Recent Progress in the Application of Electrochemically Rechargeable Metal-air Batteries: A Focus Review

Nidhi¹, Abhinay Thakur¹, Ishrat Fatma¹, Humira Assad¹, Shveta Sharma¹, Richika Ganjoo¹, Savas Kaya², Ashish Kumar^{1,3,a)}, Ramesh Chand Thakur^{4,b)}

¹Department of Chemistry, Faculty of Technology and Science, Lovely Professional University, Phagwara, Punjab, India

²Department of Chemistry, Faculty of Science, Cumhuriyet University, Sivas, Turkey

³Nalanda College of Engineering, Department of Science and Technology, Chandi, Government of Bihar, India

⁴Department of Chemistry, Himachal Pradesh University, Summer Hill Shimla, 171005, Himachal Pradesh, India.

^{a)}Corresponding author: drashishchemlpu@gmail.com,

^{b)}drthakurchem@gmail.com

Abstract. The metal-air battery has become the primary power source since its invention in 1840 by Smee. Maiche demonstrated functional primary Zn-air batteries utilizing a porous platinized carbon cathode in 1878, which was the outcome of several outstanding scientist's and engineers' studies and endeavors. Owing to its high density, very low self-discharge, extremely lengthy lifetime, long cycling performances, and easy maintenance, metal-air batteries are effective energy storage systems for multifunctional electronic devices, electrical power grids, and electrified transportation such as EVs. Considering the fact that this topic is quickly growing and recruiting a significant number of researchers, the construction of next-generation metal-air batteries still face significant obstacles. A number of novel chemistries have been developed, resulting in improved energy density, long-term storage capacity, stability, and sustainability. The goal of this review is to initiate the basics and current advances in the field of metal-air batteries, as well as the fundamentals behind their functionality along with its components.

Keywords: Metal-air batteries; Li-air; Zn-air; Electrolyte; Membrane; Organic electrode

INTRODUCTION

The necessity for energy has risen dramatically as the global economy continues to grow. Regrettably, non-renewable energy supplies including oil, coal and natural gas are constrained on the planet. As a result, the creation of new energy gadgets is vital for a stable civilization[1–3]. Supercapacitors, biofuel batteries and metal-air batteries (MABs) are among the most intriguing technologies for storing energy. MABs are the most efficient of the several power storage methods now available. MAB is an electrochemical cell comprising an air +ve electrode, a metal -ve electrode and an electrolyte[4–7]. The positive electrode's active substance is oxygen in the air, which has a number of advantages in the battery. Since the active element, oxygen (O₂), is extremely lightweight and has a high redox potential, it has a significant specific capacity (3.35 Ah g⁻¹) (1.23 V vs. RHE). All across the world, O₂ in the environment is freely available and environmentally acceptable. Because the air flows from outside the cell, the MAB is effectively free of capacity for the +ve electrode active element and may confine the -ve electrode active material as often as possible as shown in Fig.1. Negative electrode active materials are commonly base metals with high reducing power[8–14]. Due to the inexhaustible characteristic of oxygen, the MAB may generate electricity till the negative metal is completely depleted. This advantageous characteristic has long been recognized, and it has practical uses in the form of long-lasting sources of energy, particularly primary batteries. Despite the fact that MABs contain an air electrode comparable to the fuel cell, they are primarily a storage cell/battery, whereas fuel cells are primarily the energy stations without energy retention capability. MABs have recently attracted a lot of attention due to their potential to operate in the open air. MABs are made up of an air cathode and metal anodes. The MAB cathode utilizes O₂ from the air, resulting in a significant weight decrease in the battery that has unrivaled benefits for a variety of applications.

Proceedings of the International Conference on Materials for Emerging Technologies
AIP Conf. Proc. 2800, 020047-1–020047-8; <https://doi.org/10.1063/5.0162874>
Published by AIP Publishing. 978-0-7354-4631-1/\$30.00

020047-1

09 September 2023 04:48:33

Advancement in field of Energy storage applications by using Ionic Liquids

Nidhi* and Harpreet Kaur

Department of Chemistry, Lovely Professional University, Phagwara, 144411, Punjab, India.

Email: nidhi86593@gmail.com

Abstract:

Now-a-days the storage and power demands are increasing at a very rapid speed and system has evolved in the form of batteries and other storage devices which lacks some safety measures as well as electrochemical stability factors. As a class of novel media, Ionic liquids pursuing a specific set of properties had made them suitable for a number of energy related applications and modifications in their properties. So to overcome the challenges faced by the storage device, substitution of electrolytes of these devices by Ionic liquid mainly known as green solvents, has proven out to be a promising field by enhancing their properties.

This article throws a light on the advancement and development of energy storage applications by the material used i.e., Ionic liquids providing a stable and friendly electrolyte system along with the modified storage system with increased thermochemical and other stability factors.

Key Words:

Ionic Liquids, Energy Storage Devices, Electrochemical potential, Electrolytes, Electrochemical and Thermal Stability.

Highlights:

- An overview on the use of Ionic Liquids as a novel electrolyte in energy storage devices to enhance the capacitance as well as efficiency.
- Ionic Liquids can serve as multipurpose material with a lot of applications in energy field.
- Explanation of specific characteristics of Ionic liquid along with their application part in ESDs.
- Discussion of latest advancement in field of different kind of batteries using Ionic Liquids.
- Throws a light on the problems faced during composition of ESDs which further led to some shortcomings in their performance and ways to overcome these.

1. Introduction:

Energy storage devices are mainly used for storing electric energy as and when required and in this era of advanced technology, these devices are considered as the key element in the modern energy supply chain. Energy storage requirements are widely increasing, and these are mainly driven by many type of applications and a single technology cannot meet all the required demands [1]. This insufficient capability of energy storage devices proves out to be an obstacle in almost every field whether its green, chemical, transport or electronics.

The solution to this problem lies in the fabrication and designing materials used for making smart and efficient devices and some of the insufficient capabilities can be overcome by making changes in their



Content from this work may be used under the terms of the [Creative Commons Attribution 3.0 licence](https://creativecommons.org/licenses/by/3.0/). Any further distribution of this work must maintain attribution to the author(s) and the title of the work, journal citation and DOI.

Published under licence by IOP Publishing Ltd

1



LOVELY
PROFESSIONAL
UNIVERSITY

Transforming Education Transforming India



Certificate No. 329218



Certificate of Presentation

This is to certify that **Dr./Mr./Ms. Nidhi** of **Lovely Professional University, Phagwara** has given **Oral** presentation on **Thermodynamic, acoustic and electrochemical investigation of 1-ethyl-3-methyl imidazolium iodide in binary aqueous solutions of acetamide at different temperatures** in the **5th International Conference on Recent Advances in Fundamental and Applied Sciences (RAFAS-2024)** held from 19th to 20th April 2024, organized by School of Chemical Engineering and Physical Sciences, Lovely Faculty of Technology and Sciences, at Lovely Professional University, Punjab.

Date of Issue : 20-05-2024

Place : Phagwara (Punjab), India

Prepared by

(Administrative Officer-Records)

Organizing Secretary
(RAFAS-2024)

Head of Faculty
Lovely Professional University

DIVISION OF RESEARCH AND DEVELOPMENT

[Under the Aegis of Lovely Professional University, Jalandhar-Delhi G.T. Road, Phagwara (Punjab)]

Certificate No.240445

Certificate of Participation

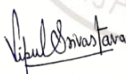
This is to certify that **Ms.Nidhi** of **Lovely Professional University, Phagwara, Punjab, India** has presented paper on **Effect of temperature on conductance studies of 1,4-Dimethyl-4H-1,2,4-triazolium iodide in binary aqueous solutions of Benzylamine and Benzamide.** in the **International Conference on Materials for Emerging Technologies (ICMET-21)** held on February 18-19, 2022, organized by Department of Research Impact and Outcome, Division of Research and Development, Lovely Professional University, Punjab.

Date of Issue: 16-03-2022

Place: Phagwara (Punjab), India



Prepared by
(Administrative Officer-Records)



Dr. Vipul Srivastava
Convener
(ICMET-21)



Dr. Manish Vyas
Organizing Secretary
(ICMET-21)



Dr. Chander Prakash
Co-Chairperson
(ICMET-21)



Certificate of Participation

This is to certify that Prof./Dr./Mr./Ms. Ms. Nidhi
of Lovely Professional University
has given poster presentation on Advancement in field of Energy storage applications by using Ionic Liquids
in the International Conference on "Recent Advances in Fundamental and Applied Sciences" (RAFAS 2021) held on
June 25-26, 2021, organized by School of Chemical Engineering and Physical Sciences, Lovely Faculty of Technology
and Sciences, Lovely Professional University, Punjab.

Date of Issue : 15-07-2021
Place of Issue: Phagwara (India)



Prepared by
(Administrative Officer-Records)



Organizing Secretary
(RAFAS 2021)



Convener
(RAFAS 2021)



**International Conference on
Recent Advances on Green and Sustainable Developments (ICRAGSD-2023)
6th -8th September, 2023**

Organised by:

Green Chemistry Network Centre Chapter, Akal University, Talwandi Sabo, Bathinda, Punjab, India

In collaboration with

Green Chemistry Network Centre (DU), Indian Chemical Society (Kolkata)
Eternal University (Baru Sahib), Synthetic Communications (Taylor and Francis)
De Gruyter (Germany), DRDO (New Delhi)

This conference is a part of the Centennial Jubilee Year Celebration (Shatabdi Mahotsav) of the Indian Chemical Society (Kolkata)



Presenter's photograph

Certificate of Presentation

This is to certify that *Ms. Nidhi, Department of Chemistry, Lovely Professional University, Phagwara, 144411, Punjab, India* has successfully delivered an oral presentation on the below mentioned topic under Category 2 (only for research scholars).

Oral Presentation Title: *A comparison of the thermodynamic, volumetric, viscometric, and conductometric parameters of 1-butyl-1-methyl pyrrolidinium iodide in aqueous solutions of acetamide at four equidistant temperatures (T= 288.15K to 318.15K)*

Dr. Bubun Banerjee
Convener, ICRAGSD

Prof. Rakesh K. Sharma
Coordinator, GCN8

Prof. Ganapati D. Yadav
President, ICS

Prof. Sukhjeet Singh Dhindsa
Registrar, AUTS